



Sándor Nagy
INTRODUCTION TO NUCLEAR SCIENCE
(for the non-physicist)



For Évika

ln e

LIBRARY OF NAGY'S E-BOOKS

ELTE, KI, Budapest, 2010

© Nagy Sándor



Contents

INTRODUCTORY STUFF	4
ACKNOWLEDGEMENTS	5
1. RADIOCHEMISTRY AND NUCLEAR CHEMISTRY (RC&NC)	6
1.1. RC&NC AS AN INTERDISCIPLINARY FIELD OF SCIENCE	6
1.2. THE BEGINNINGS OF RC&NC AND THE TIMELINE OF NUCLEAR SCIENCE	7
1.3. RC&NC—OUTLOOK	10
2. NUCLIDES AND NUCLEI—ISOTOPES, ISOBARS, ISOTONES, AND ISOMERS	13
2.1. THE BUILDING BLOCKS OF ATOMS AND NUCLEI	14
2.2. NUCLIDES—ATOMIC SPECIES DETERMINED BY THEIR NUCLEI	15
2.3. NUCLIDIC NOTATION WITH EXAMPLES	17
3. MASS AND ENERGY—BASIC QUANTITIES AND UNITS	20
3.1. THE ELECTRON VOLT—THE ENERGY UNIT IN NUCLEAR SCIENCE	20
3.2. ENERGY AND TEMPERATURE	20
3.3. THE NUCLIDIC MASS AND THE UNIFIED ATOMIC MASS UNIT	21
3.4. QUANTITIES CHARACTERIZING STABILITY AND INSTABILITY	23
3.4.1. <i>The Q-value and the criterion for spontaneity</i>	23
3.4.2. <i>The Binding Energy of the Nucleus and the B/A Value</i>	25
3.4.3. <i>The Mass Excess</i>	27
3.4.4. <i>Nucleon Separation Energies</i>	29
4. PARTICLES AND FORCES—THE STANDARD MODEL IN A NUTSHELL	31
4.1. THE ORIGIN OF NUCLEAR FORCE	31
4.2. CLASSIFICATION OF PARTICLES AND FORCES	32
4.3. THE COLOR CHARGE	36
5. CHARACTERIZATION OF THE ATOMIC NUCLEUS	38
5.1. NUCLEAR RADIUS AND MASS DENSITY	38
5.2. NUCLEAR SPIN, ELECTRIC AND MAGNETIC PROPERTIES OF NUCLEI	40
5.3. THE ONE-NUCLEON SHELL MODEL OF THE NUCLEUS	47
6. TOPOLOGY OF THE VALLEY/CONTINENT OF STABILITY	51
6.1. SYSTEMATICS OF STABLE ELEMENTS AND NUCLIDES	51
6.2. DEPENDENCE OF THE AVERAGE BINDING ENERGY PER NUCLEON ON THE MASS NUMBER	55
6.3. THE WEIZSÄCKER FORMULA AND THE LIQUID DROP MODEL	57
7. INTRODUCTION TO NUCLEAR REACTIONS	63
7.1. TYPES OF NUCLEAR REACTIONS	63
7.2. REACTIONS INDUCED BY NEUTRONS AND POSITIVE IONS	65
7.2.1. <i>Geometrical Cross Section of the Nucleus</i>	65
7.2.2. <i>The Nucleus as Felt by a Neutron and a Proton</i>	66
7.2.3. <i>Reaction Cross Section Systematics</i>	66
8. RADIOACTIVITY-RELATED CONCEPTS	70
8.1. CHARACTERIZATION OF THE MAIN DECAY MODES AND RADIATIONS	70
8.2. RADIOACTIVE DECAY VS. CHEMICAL AND NUCLEAR REACTIONS	73
8.3. CHARACTERIZATION OF RADIOACTIVE SAMPLES—DECAY RATE AND COUNT RATE	75
8.4. HALF-LIFE, MEAN LIFE, DECAY CONSTANT AND THE EXPONENTIAL LAW OF DECAY	76
8.5. DECAY CHAIN, EQUILIBRIUM, BRANCHING, AND DECAY SCHEMES	77
8.6. RADIONUCLIDES ON EARTH	79
9. TOWARDS GREATER STABILITY—RADIOACTIVE DECAY	81
9.1. RADIOACTIVE DECAY AND THE CHART OF NUCLIDES	81
9.2. INVESTIGATION OF THE SPONTANEITY OF BETA AND ALPHA DECAY	83
9.3. GAMMA DECAY	90

9.4.	FISSION	92
9.5.	EXOTIC AND RARE DECAY MODES	97
10.	KINETICS OF RADIOACTIVE DECAY AND ACTIVATION.....	99
10.1.	RADIOACTIVE DECAY AND GROWTH	99
10.2.	DECAY FOLLOWING ACTIVATION	104
10.3.	PARALLEL DECAY PROCESSES	105
11.	AFTEREFFECTS OF RADIOACTIVE DECAY AND NUCLEAR REACTIONS	106
11.1.	RECOIL	106
11.2.	INNER BREMSSTRAHLUNG, X-RAYS AND AUGER EFFECT	110
12.	INTERACTION OF NUCLEAR RADIATIONS WITH MATTER	112
12.1.	DOSIMETRIC CONCEPTS	113
12.2.	INTERACTIONS OF ALPHA RADIATION (HEAVY IONS)	115
12.3.	INTERACTIONS OF BETA RADIATION (LIGHT IONIZING PARTICLES)	118
12.4.	INTERACTIONS OF GAMMA RADIATION (HIGH-ENERGY PHOTONS)	128
12.5.	INTERACTIONS OF NEUTRONS	134
13.	NUCLEOSYNTHESIS.....	136
13.1.	CHEMICAL PUZZLE—BINDING ENERGIES VS. ABUNDANCES OF ELEMENTS AND ISOTOPES	136
13.2.	NUCLEOSYNTHETIC PROCESSES AND RELATED CONCEPTS.....	137
APPENDIX		142
14.	SPECIAL RELATIVITY ASIDE—SUMMARY OF EQUATIONS AND NOTATIONS.....	142
15.	MASSLESS PARTICLES—CASES OF EXTREMELY RELATIVISTIC BEHAVIOR.....	143
16.	SCATTERING OF ‘PHOTON-LIKE’ PARTICLES ON FREE ‘MASSIVE’ PARTICLES	143
17.	CALCULATION OF RECOIL ENERGY	146
18.	HALF-LIFE FROM LEVEL WIDTH.....	147
SUGGESTED READING.....		148
INTERNET SOURCES		150
GLOSSARY.....		151
INDEX.....		153

Introductory Stuff

This electronic material is the further developed and integrated version of my works **Radiochemistry and Nuclear Chemistry**¹ and **Subatomic Particles, Nuclear Structure and Stability**².

I originally wrote the above works for [UNESCO-EOLSS](#)—an electronic encyclopedia (Encyclopedia of Life Supporting Systems)—in my capacity as the ‘Honorary Theme Editor’ (HTE) of the theme [RADIOCHEMISTRY AND NUCLEAR CHEMISTRY](#), for which they served as the introductory and closing chapters (or ‘topics’ using the terminology of EOLSS). These chapters/topics were meant to summarize the ‘nuclear background’ for the non-physicist to an extent that I thought was necessary for the understanding of the rest of the topics elaborated by a team of international experts including a few scientists from Hungary.

As an HTE I did my best to make the two original chapters as self-sufficient as possible and this made some overlapping unavoidable. Although I considerably developed the original material later, I kept the two chapters apart for some time. Even now after merging them there are some redundancies in the text. Some of them are intentional because I wanted to save the reader from leafing back and forth in the printed version following the references. The rest of the repetitions come by mistake or due to my mental laziness. So if you have a *dejà vu* feeling while you read, it is not necessarily because there is a ‘*glitch in the Matrix*’.

The present material is basically meant to serve as a study aid for International/Hungarian students enrolled at Eötvös Loránd University (ELTE) to get credit for completing ‘**Basics of Nuclear Chemistry**’ (**A magkémia alapjai**), a compulsory course in our Eurobachelor-labeled BSc Chemistry Program. However the topics covered are not specific to chemistry except for the first chapter (which defines radiochemistry *and* nuclear chemistry as an interdisciplinary field of science). Therefore I sincerely believe that this material can be used not only by chemistry majors but other students as well except for physics majors who study this field much more thoroughly.

The editing of the text will probably not impress everybody. The main idea that I kept in mind when I arranged the material was that the ‘trickier’ parts should only appear when it is absolutely necessary. The ‘trickiest’ parts are placed in the APPENDIX as numbered chapters. These are meant for very motivated students only.

The composition of the APPENDIX is rather diverse in nature. After the **numbered sections** that are related to the rest of the text, but can be left unread, the **bibliography** follows together with a few important **internet sources**. I have also placed in the appendix a **glossary** which may or may not be a good idea considering that the appendix ends with a very detailed **index** which comes in handy if you prefer to study from the print-out. If you prefer to read the Acrobat file on the screen, you can not only see the color of the figures (cheaper), but you can also make use of the external links and the internal cross references (helping you to jump directly to legends of figures, headers of tables and to equations).

¹ Sándor Nagy, (2007), RADIOCHEMISTRY AND NUCLEAR CHEMISTRY, in Radiochemistry and Nuclear Chemistry, [Ed. Sándor Nagy], in Encyclopedia of Life Support Systems (EOLSS), Developed under the Auspices of the UNESCO, Eolss Publishers, Oxford, UK, [<http://www.eolss.net>]

² Sándor Nagy, (2007), SUBATOMIC PARTICLES, NUCLEAR STRUCTURE AND STABILITY, in Radiochemistry and Nuclear Chemistry, [Ed. Sándor Nagy], in Encyclopedia of Life Support Systems (EOLSS), Developed under the Auspices of the UNESCO, Eolss Publishers, Oxford, UK, [<http://www.eolss.net>]

If you are interested in the Hungarian equivalents of the technical terms found in this module you might want to download the [nuclear dictionary](#) that I prepared as an Excel file. The expressions found there reflect IUPAC opinion, and therefore the dictionary may help to spread a common and unambiguous vocabulary in this field of science.

Acknowledgements

The author expresses his gratitude to Prof. Attila Vértes, Member of the Hungarian Academy of Sciences, and his colleague, Dr. Károly Süvegh, for reviewing the original of this teaching material and making valuable suggestions. The author is also obliged to Dr. Joseph Magill of the Institute for Transuranium Elements (ITU), Karlsruhe, Germany, for getting the opportunity to draw ideas and inspiration from his excellent publications listed in the Bibliography as is to some other authors listed there (Choppin, Cuninghame, Friedlander, Leo, and, again, Vértes) whose books helped his development at various stages of his professional life. He is also thankful to Chris Bester, an ERASMUS student from [Jersey, UK](#), for checking the English.

Törökbálint, January 11, 2009.

Sándor Nagy

1. Radiochemistry and Nuclear Chemistry (RC&NC)

1.1. RC&NC as an interdisciplinary field of science

The ‘official’ definitions of [radiochemistry](#) (RC) and [nuclear chemistry](#) (NC) in the ‘[IUPAC Gold Book](#)’ read as follows:

- Radiochemistry: ‘That part of chemistry which deals with radioactive materials. It includes the production of radionuclides and their compounds by processing irradiated materials or naturally occurring radioactive materials, the application of chemical techniques to nuclear studies, and the application of radioactivity to the investigation of chemical, biochemical or biomedical problems.’
- Nuclear chemistry: ‘The part of chemistry which deals with the study of nuclei and nuclear reactions using chemical methods.’

However there is a wide interdisciplinary area between chemistry and nuclear science/technology which is not always easy to unambiguously divide into the above categories. Therefore I prefer to consider *radiochemistry and nuclear chemistry* as a single technical term (RC&NC) covering the whole area that can be characterized by either of the following criteria:

- nuclear science with relevance to chemistry
- chemistry with relevance to nuclear science.

There are workers in the field of what I call RC&NC who define themselves either as *radiochemists* or as *nuclear chemists*. However, a considerable part of the core of knowledge of these areas is common, and they are interlaced to a degree where it is practically not worth the trouble trying to disentangle them here. The term *radionuclear chemistry* also occurs in the literature, which speaks for itself.

Historically, in the early years of RC&NC, the term RC was used for the whole field. Later on, in the 1930s, the term NC was introduced for the chemical aspects of the study, production, properties and reactions of atomic nuclei. Several decades later, either of these terms was also applied to all kinds of nuclear instrumental methods used as tools in chemical research, such as Mössbauer spectroscopy. By now a kind of ‘fusion’ has taken place between the once distinct meanings and for many people active in these fields RC and NC have become practically synonyms.

Note that some of the nuclear methods of chemical structure investigation, e.g. *NMR*, are often not considered as being part of either RC or NC. With NMR this is partly so because the resonance energies involved are negligible, and partly because it has become a widely used independent method in its own right whose nuclear origins have been ‘forgotten’ for various reasons. (It is probably no accident, e.g., that the adjective ‘nuclear’ has been dropped out from the acronym of one of the best diagnostic methods, MRI.) On the other hand, some of the methods connected with X-rays, e.g. *XRFS*, are often included. So when outlining RC&NC, high-energy radiations (nuclear or other) can be useful practical markers. Accordingly, books on RC&NC always contain chapters on non-radioactive radiation sources such as *synchrotrons*. *Isotopic chemistry* (radioactive or not) is usually considered as part of the topics included. *Radiation chemistry* may or may not be included.

The ambiguity concerning the borderline between RC and NC can also be observed when browsing through books titled ‘Radiochemistry’, ‘[Handbook of Nuclear Chemistry](#)’, ‘Nuclear and Radiochemistry’ or the like. The contents are very similar or practically the same. As a

matter of fact, the introductory chapters (dealing with subatomic particles, properties of nuclei, stability/instability, decay modes, interactions of radiations with matter, detection of radiations etc.) are in common with most fields of nuclear science although the depth of treatment may be different.

1.2. *The Beginnings of RC&NC and the Timeline of Nuclear Science*

The history of RC&NC cannot be separated from that of the rest of nuclear science (and related fields). This is so, because

- chemistry is much older than nuclear science (chemists held their [first international meeting](#) in Karlsruhe as early as 1860 on fundamental issues like the definition of atoms³ and molecules);
- chemists got involved in the research of radioactivity as soon as it was discovered in 1896.

The role of chemistry in nuclear science (and related fields) can be seen in Figure 1 showing that there were 10 such years in the 105-year history of Nobel Prizes when the chemistry award was associated with this field. The achievements awarded cover the period from the very beginnings till about 1946. The last Nobel Prize in chemistry was awarded in this field in 1960.

The beginning of the nuclear epoch of humankind is marked by the 1896 discovery of the radioactivity of [uranium](#) by Antoine Henri [Becquerel](#) (1852-1908), representing the third generation of a family of French physicists, who won a 1903 shared [Nobel Prize](#) in physics ‘for the discovery of spontaneous radioactivity’.

³ Being a chemist myself, I find it remarkable that Ernst [Mach](#) (1838-1916)—the great Austrian philosopher, physicist and mathematician who made an impression on Albert [Einstein](#) (with what Einstein called Mach’s Principle) and did pioneering work in the study of supersonic flow (hence the Mach number, M, used as a unit for measuring supersonic speeds)—in 1913 still stubbornly denied even the existence of atoms (not to mention atomic nuclei) saying: ‘*I can accept the theory of relativity as little as I can accept the existence of atoms and other such dogmas*’. When someone mentioned atoms in Mach’s presence, his stereotype question was supposed to be this: ‘*Habens’ schon eins gesehen?*’—‘Have you ever seen one?’

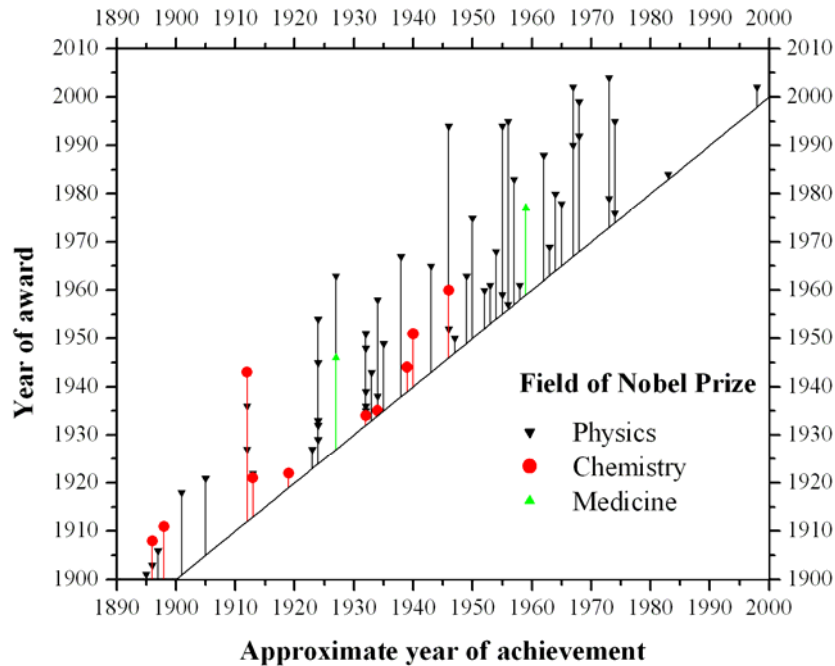


Figure 1: Nobel Prizes related to the development of nuclear science and subatomic concepts. The length of each drop-line shows the delay between award and achievement. Note that some achievements had been awarded almost promptly, whereas the longest delay was almost half a century. (The drop-lines of the first few points are meaningless, as the Nobel Prize was first given in 1901.)

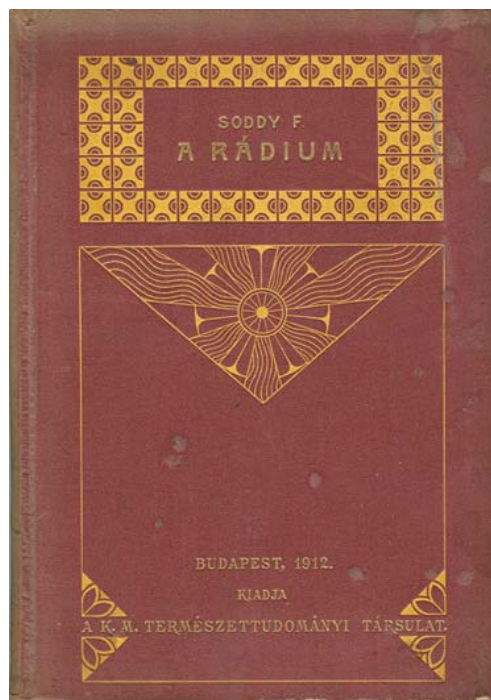


Figure 2: Radioactivity and radium itself arouse worldwide interest both among scientists and the public. [Soddy](#)'s 1908 book on radium was also published in Hungarian in 1912 by the Royal Hungarian Society of Sciences to serve 'the Hungarian public interested in the development of science'. Note that according to the preface of the above edition, the first Hungarian book on the very same topic appeared as early as 1905 written by the physicist Győző Zemplén, the older brother of the chemist [Géza Zemplén](#) who earned a special place in the pantheon of Hungarian science.

Some put the year of birth of nuclear science one year earlier, to 1895, when the German physicist Wilhelm Conrad [Röntgen](#) (1845-1923) discovered his famous *X-rays*, X-Strahlen in German, a technical term coined by him. The expression X-ray, with X to remind of the traditional symbol *x* for unknown algebraic quantities, is an appropriate name indeed for a ‘mysterious’ radiation that penetrates materials impenetrable to ordinary light. It is worth mentioning, however, that in some languages this same high-energy electromagnetic radiation bears its discoverer’s name and is called the equivalent of roentgen-rays, Röntgen-rays or similar (e.g. **röntgensugárzás** in Hungarian). Röntgen also developed [X-ray photography](#), revolutionizing medical diagnosis. He won the 1901 [Nobel Prize](#) in physics (which was also the first such prize given to anybody) for his discovery. His work also gave inspiration to Becquerel and [Rutherford](#) for their experiments on radioactivity.

Whichever date we accept as official year of birth of nuclear science in general (or nuclear and particle physics in particular), the year of birth of RC (and so that of RC&NC) is certainly at the latest 1898 when [Marie Curie](#), née Maria Skłodowska (1867-1934), a Polish-born French chemist, together with her husband [Pierre Curie](#) (1859-1906), a French physicist, (who also studied the radioactivity of [thorium](#)) discovered [polonium](#) (and somewhat later [radium](#), see Figure 2) using the first [radiochemical methods](#) ever. The Curies were also the ones who shared the 1903 [Nobel Prize](#) with Becquerel. (In 1911, Madame Curie also won a second [Nobel Prize](#), this time in chemistry, for ‘her services to the advancement of chemistry by the discovery of the elements radium and polonium, by the isolation of radium and the study of the nature and compounds of this remarkable element’.)

Considering the [timeline of discoveries](#), one can easily understand why the year of birth of RC has been emphasized above. Namely, it would be rather anachronistic to talk about NC before the birth of the concept of the *atomic nucleus* itself, which dates from more than a decade later, 1911, when the New Zealand-born British physicist Ernest Rutherford (1871-1937) concluded that the vast majority of the mass of an atom must be concentrated in a tiny part of its volume, and this tiny but massive volume, referred to as the atomic nucleus, must be positively charged. His nuclear atom model replaced the Kelvin-Thomson ‘[plum pudding model](#)’ according to which the atom should be pictured as a positively charged spherical mass in which *Z* electrons are embedded like raisins in a cake. The short-lived Kelvin-Thomson model was postulated in 1903 by [Lord Kelvin](#), also known Sir William Thomson, (1824-1907), a Scottish-Irish mathematical physicist and engineer, and further developed by [Joseph John Thomson](#) (1856-1940), an English physicist, who studied the conduction of electricity by gases, discovered the electron (the first subatomic as well as truly elementary/fundamental particle) and determined its [specific charge](#) (charge to mass ratio), an important achievement that brought him a [Nobel Prize](#) in physics in 1906.

Although Rutherford’s nuclear atom model changed the picture of chemists about the atom profoundly, he won his 1908 [Nobel Prize](#) in chemistry for an even more bizarre idea that contradicted the most sacred dogma of the chemists of his time, namely, that the atoms of the chemical elements are ultimate and unchangeable parts of matter. Around 1902-1903, together with the British chemist Frederick Soddy (1877-1956), he came to the heretical conclusion that *thorium and uranium became different elements through radioactive decay*. Rutherford was well aware how daring this conclusion was⁴. Against all expectations, however, chemists turned out to be open-minded enough to acknowledge him, a physicist, as one of their kin by giving him the chemistry Nobel Prize.

⁴ To prove this, here is a dialog as Soddy recalled it later:

*‘Rutherford, this is transmutation: the thorium is disintegrating and transmuting itself into argon gas.’
‘For Mike’s sake, Soddy, don’t call it transmutation! They’ll have our heads off as alchemists!’*

By way of compensation maybe, physicists repaid this debt by giving 1/4 of the 2002 [Nobel Prize](#) in physics to a chemist, [Raymond Davis Jr.](#) (1914-2006), the discoverer of the *solar neutrino problem*, ‘for pioneering contributions to astrophysics, in particular for the detection of cosmic neutrinos’.

As these examples show, the roles of chemists and physicists got rather mixed up in nuclear and particle science in full accordance with the interdisciplinarity of the fields and the complexity of the problems to be solved. We can also see that although the last nuclear-related Nobel Prize in chemistry was awarded almost half a century ago, the last Nobel Prize to a radionuclear chemist was given much later, in 2002, although for an achievement that dates back to 1967.

Besides Nobel Prizes, the appreciation for the achievements of the forerunners of nuclear science has been expressed in several other ways:

- Elements 96, 104 and 111 bear the names of Curie ([curium](#), Cm), Rutherford ([rutherfordium](#), Rf), and Röntgen ([roentgenium](#), Rg), respectively.
- The pre-SI unit of *radiation exposure to photons* also bears Röntgen’s name (*roentgen*, R).
- Both ‘successful’ units of *activity* (*disintegration rate*, *decay rate*) had been named after the pioneers of radioactivity. The first activity unit, the *curie* (Ci), was introduced in 1930. Although not an SI unit, it is still widely used especially in medicinal applications (see Table 1). Since 1975, the official SI unit of activity is the *becquerel* (Bq) getting increasingly accepted by nuclear scientists. (A third and short-lived activity unit—the *rutherford*, meaning 10^6 decays per second—was also suggested in the 1930s in Rutherford’s honor, but it has never become widely accepted.)

For further information on the development of subatomic concepts etc. see the introductory part of the chapter 2 as well as the [detailed timeline](#) which is meant to be self-contained as much as possible.

1.3. RC&NC—Outlook

The last decades of the 20th century did not favor nuclear science in general and RC&NC in particular. Even before the 1986 Chernobyl accident that made the public suspicious about anything related to ‘radioactive’, ‘isotope’, or even ‘nuclear’, chemical research took a turn from the ‘nuclear’ direction as is clear from the Nobel Prize ‘statistics’ in Figure 1.

The shift of the focus of scientific interest can also be seen from the 2005 impact factors (IF) of periodicals. The list contains 6033 entries with non-zero IF starting with a medical journal on cancer research (IF 49.794) and ending with an engineering periodical (IF 0.04). The first publication that would have been labeled as nuclear several decades ago is dedicated to NMR (place 201, IF 6.462). The first ‘really’ nuclear periodical on the list is NUCL PHYS B (place 255, IF 5.522). And—with ANNU REV BIOCHEM (place 4, IF 33.456)—this does not mean at all that chemistry as such is a deserted area, but the shift of the main interest towards life sciences is obvious.

Stricter regulations of nuclear industry following Chernobyl (making nuclear energy production more expensive) and the cutback of funds for research have been combined with bad timing too. Having finished with ‘easily’ achievable goals, research has gradually moved towards more challenging problems which called for increasingly sophisticated physical and engineering solutions and, of course, for more money. This kind of time evolution is illustrated by Figure 3 in the case of one particular field: the exploration of the

valley/continent of stability on the map of the Chart of Nuclides.

There is also a tendency in research to move towards Large Science from Small Science in some fields, especially when huge accelerators are needed to the work. Large Science and multinational cooperation is also called for to make the dream of fusion reactors a reality, which has been ‘just a few decades away’ for several decades now. Physicists did most of what they were supposed to do—now comes the turn of engineering, materials science, and chemistry.

Chemists who can communicate with nuclear/reactor physicists or physicists/engineers understanding chemistry will be needed for at least four to five decades to take care of the nuclear fuel cycle of fission reactors and to do everything that has to be done with spent nuclear fuel, nuclear waste, etc. (And, of course, I could have substituted the word ‘chemist’ for ‘biologist’, ‘medical expert’ or ‘environmental expert’

With international terrorism getting more aggressive, special knowledge of radionuclear chemists is also needed in forensic science (nuclear forensic).

Knowledge of both chemistry and nuclear science will always be needed in nuclear medicine applications, preparation of labeled compounds, and a variety of industrial and medical applications of radiations, as well as in environmental protection.

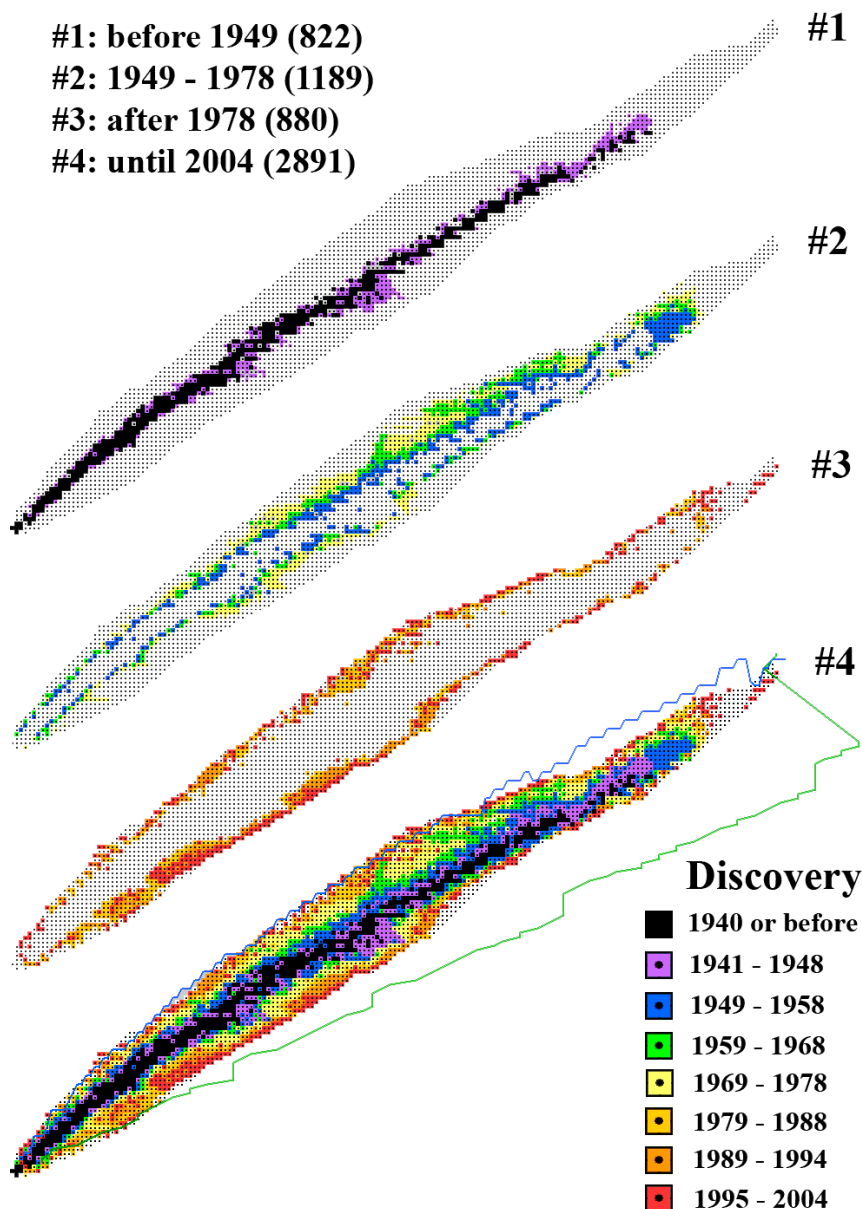


Figure 3: Charts of Nuclides colored according to the year of discovery (created by using *Nucleus-Win* http://amdc.in2p3.fr/web/nubdisp_en.html, a free software, produced by AMDC at CSNSM-Orsay). Graphs #1 through #3 show a clear trend as regards the aims/results of teams of nuclear chemists and physicist. Period #1 is the epoch of the exploration of the stable isotopes of known elements and later on that of the radionuclides in the immediate vicinity of stability. The first part of studies started in 1913 right after Soddy’s isotope hypothesis was born and before the concept of nuclide as we understand it today could have been phrased. (Note that the existence of the neutron was only proved in 1932 by Chadwick.) There are two remarkable protrusions in the direction of higher neutron numbers up the steeper sides of the valley representing the typical mass number ranges of the two chunks ²³⁵U is broken to when fissioned by thermal neutrons ($A = 90-100$ and $A = 135-150$). Note also that the vicinity of uranium had also been well researched by the end of the period. On the other hand, period #3 including the present is that of the exploration of the frontiers of nuclear existence and includes the discovery of artificial elements produced in very small amounts (a few atoms at a time) and with very large effort.

2. Nuclides and Nuclei—Isotopes, Isobars, Isotones, and Isomers

While studying naturally occurring [decay series](#) (see Figure 51), radiochemists were baffled because some of the members of the series could not be separated by chemical methods, although their radioactive properties (decay mode, half-life) were markedly different.

By 1907 ‘the doctrine of the complete chemical non-separability’ of these members (an expression borrowed from Soddy’s [Nobel lecture](#) given in 1921) had become an accepted fact among the workers in this field. [Let us note that the Hungarian chemist George ‘György’ [Hevesy](#) (1885-1966) made good use of this fact by inventing the radioactive tracer technique in the meantime (see Figure 4), thus earning the 1943 chemistry [Nobel Prize](#).] To give an explanation for ‘non-separability’, as early as 1913 (i.e. six years before Rutherford discovered the *proton* as the constituent of the nucleus, thus taking the first large step towards identifying the atomic number of elements used by chemists for ‘ages’ with something fundamental), Soddy introduced the concept of *isotopy* from the Greek words ‘isos’ (ἴσος: equal, same) and ‘topos’ (τόπος: place). His idea was that in spite of internal differences, different atomic species—*isotopes*—may occupy the same place on the [periodic table](#), thus representing the same element. Note that isotopes are not really *inseparable* after all as it turns out from the very existence of isotope separation, a process based on isotope effects, which is of crucial importance for nuclear energy production for instance (isotope enrichment of uranium).

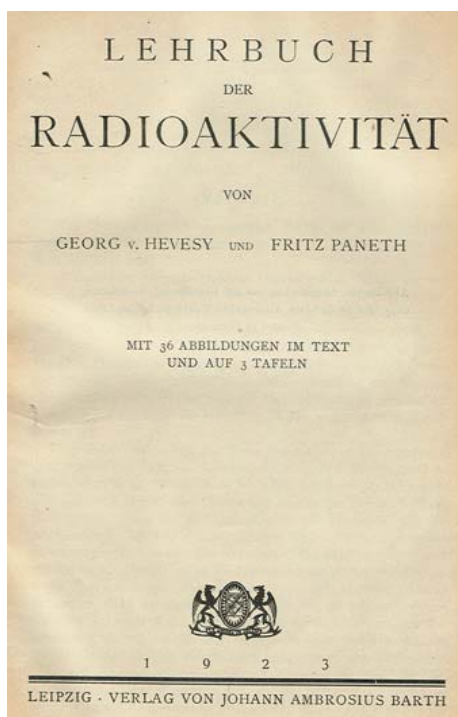


Figure 4: The ‘Textbook of Radioactivity’ by Hevesy and Paneth, a German book from 1923. Radioactive ‘indicators’—now called radioactive tracers—are also discussed on two and a half pages. In this book, according to the general custom, the different isotopes of the elements were identified by special names. For instance, the names/symbols of the isotopes of element 86 now called radon ([Rn](#))—then called Emanation (Em)—were derived from the parent element. These were as follows: Actinium Emanation (Ac Em, later Action, An), Thorium Emanation (Th Em, later Thoron, Tn), and Radium Emanation (Ra Em, later Radon, Rn). These are nowadays identified as ^{119}Rn , ^{220}Rn , and ^{222}Rn , respectively. Watch out, however, because there are some conservative areas in nuclear science, where the old isotope names thoron (meaning ^{220}Rn) and radon (meaning ^{222}Rn) are still being used.

Proof for the existence of isotopes as atomic species with different atomic masses was given within a year by J.J. Thomson via deflecting neon ions in electromagnetic fields. It turned out that natural Ne atoms could be divided in two classes which we now refer to as ^{20}Ne and ^{22}Ne . (The third stable isotope, ^{21}Ne —making up only 0.27% of neon—escaped detection then.) This also showed that ‘isotopy’ is not specific to radioactivity.

The deeper physical interpretation of isotopes followed about two decades later, after the discovery of the *neutron* in 1932 by the British physicist [James Chadwick](#) (1891-1974) who won the 1935 physics [Nobel Prize](#) for this achievement. According to this interpretation, the different isotopes of an element represent different classes of atoms/nuclei of that element, each containing the same number of protons (Z), but different number of neutrons (N).

Over the next decade or so, however, the term ‘isotope’ had become overused/misused to the point where laypersons started to understand it as ‘*a dangerous type of atom that is radioactive*’. To straighten out things, the American physicist [Truman P. Kohman](#) introduced the concept of *nuclide* in 1947. However, a fat half century was not quite enough for this useful term to replace the term isotope everywhere it ought to. As a matter of fact even those who use it interpret its meaning differently. Therefore I devote this chapter to clarifying these terms and to introducing some closely related concepts.

2.1. The Building Blocks of Atoms and Nuclei

Figure 5 shows the artistic representation of [the structure of an ‘ordinary’ helium atom](#) based on the Standard Model of particles and interactions summarized in chapter 4. The *nucleus* of this particular atomic species is distinguished from other nuclei that it contains two *protons* (p) and two *neutrons* (n), i.e. altogether four *nucleons* (N).

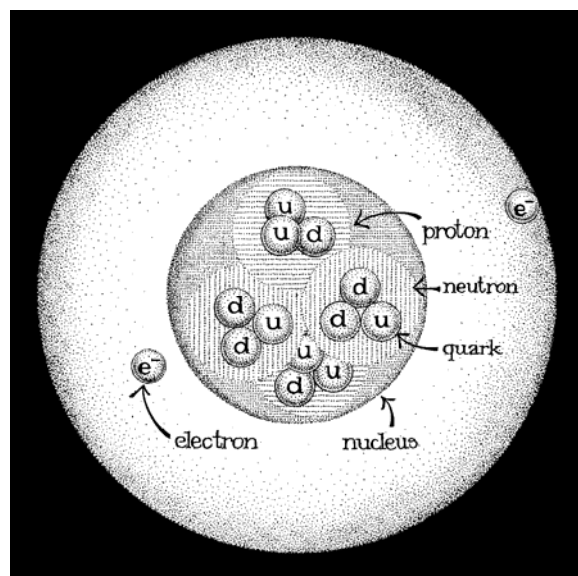


Figure 5: Naïve representation of the structure of a helium atom by ‘Iscsu’ (pencil name of graphic artist István Molnár) based on the Standard Model (SM). Note that for better visibility, [the actual dimensions of the particles, the nucleus, and the atom](#) are by far not in proportion with each other. If a nucleon (neutron or proton) were 1 cm across, then the ^4He nucleus would be 1.6 cm, but the atom itself would have a diameter of 1 km. It means that the atom is way undersized in the picture compared to its nucleus. The quarks and electrons, on the other hand, are fundamental particles according to the SM without any internal structure, i.e. point-like. Anyway, their size would be certainly not larger than 10^{-10} μm , if the picture were proportional in every detail.

In general, a nucleus contains A *nucleons* (N: p and n together) out of which Z are protons and

the rest are neutrons:

$$N = A - Z, \quad (1)$$

where the integer N is simply called the *neutron number* of the nucleus.

The integer A is often referred to as the *nucleon number* for obvious reasons, but it is most often called the *mass number*. The latter name is justified because protons and neutrons have very nearly the same mass (see Table 1 showing that the difference is merely ~ 2.5 electron masses, making the neutron $\sim 0.14\%$ heavier than the proton) and therefore the nuclear mass m_N is approximately proportional to the number of nucleons:

$$m_N \propto A = Z + N. \quad (2)$$

Comment on notation: As the capital letter ‘N’ has been used with three different meanings in the last few paragraphs, It should be emphasized here that whenever it occurs as a subscript in regular (upright) style like here (${}_N$), it will always refer to the nucleus. Where the subscript is in *italic* (slanted) style (${}_N$), it normally refers to the neutron number. Apart from this, depending on the context, N can also mean the number of atoms.

Since electrons are much lighter than nucleons ($m_e \approx 0.05\%$ of m_n or m_p), the mass of the neutral atom ‘built’ from the given nucleus and Z electrons will also be approximately proportional to A , and therefore the term mass number is also rightly applied to atoms.

The integer Z is known in chemistry as the *atomic number* (of the given element). It is also referred to as the *proton number* of the nucleus). Since the electric charge of the nucleus is eZ , where e is the charge of the proton called the *elementary charge* (Table 1), Z is also referred to as the *charge number* of the nucleus. As the electric charge of the electron (e^-) is equal to $-e$, a neutral atom contains exactly Z extra-nuclear/orbital electrons. So Z also indicates the *electron number* of a neutral atom.

The nucleus built from protons and neutrons can exist in different energy states the lowest of which is called its *ground state*. (The structure of the nucleus is briefly discussed in chapter 5.) *Excited-state* nuclei—same as excited atoms—seek higher stability and usually return to the ground state very quickly (typically in 10^{-17} – 10^{-10} s) by emitting electromagnetic radiation (called γ -rays in this case).

2.2. Nuclides—Atomic Species Determined by their Nuclei

The latest ‘official’ [IUPAC recommendation](#) as of 2007 (published in 1987) contains the following instructions as to the proper use of the terms *nuclide*, *isotope*, *isobar* and *isotone*:

- A species of atoms identical as regards atomic number (proton number) and mass number (nucleon number) should be indicated by the word ‘nuclide’, not by the word ‘isotope’. Different nuclides having the same mass number are called ‘isobaric nuclides’ or ‘isobars’. Different nuclides having the same atomic number are called ‘isotopic nuclides’ or ‘isotopes’. (Since nuclides with the same number of **p**rotons are ‘isotop**e**s’, nuclides with the same number of **n**eutrons have sometimes been designated as ‘isoton**e**s’.)

The ‘[IUPAC Gold Book](#)’ defines a *nuclide* as follows:

- A species of atom, characterized by its mass number, atomic number and nuclear energy state, provided that the mean life in that state is long enough to be observable.

Note that according to either definition, *nuclides are atoms* and not nuclei. And this is well worth knowing, because in texts written by physicists, the term nuclide—contrary to IUPAP

recommendation—is often used in the sense ‘nuclear species’⁵, which makes a huge difference when it comes to mass–energy calculations considering that the mass–energy equivalent of a single electron is about $500\,000\text{ eV} \Leftrightarrow 49\text{ GJ mol}^{-1}$ according to Table 1.

The IUPAC definition is also explicit in stating that symbols like ^{119}Sn and $^{119\text{m}}\text{Sn}$ represent different nuclides. The superscript ‘m’ in the second case, namely, indicates that the nucleus is in an excited state, whose half-life is so long that for some practical purpose (i.e. observability) it can be considered as *metastable* (hence the notation). As a matter of fact, the half-life of this particular *nuclear isomer* (as relatively long-lived nuclear excited states are also referred to) is 293 days, i.e. almost a year. And this is a lot of time, considering that de-excitation normally occurs within a tiny fraction of a second.

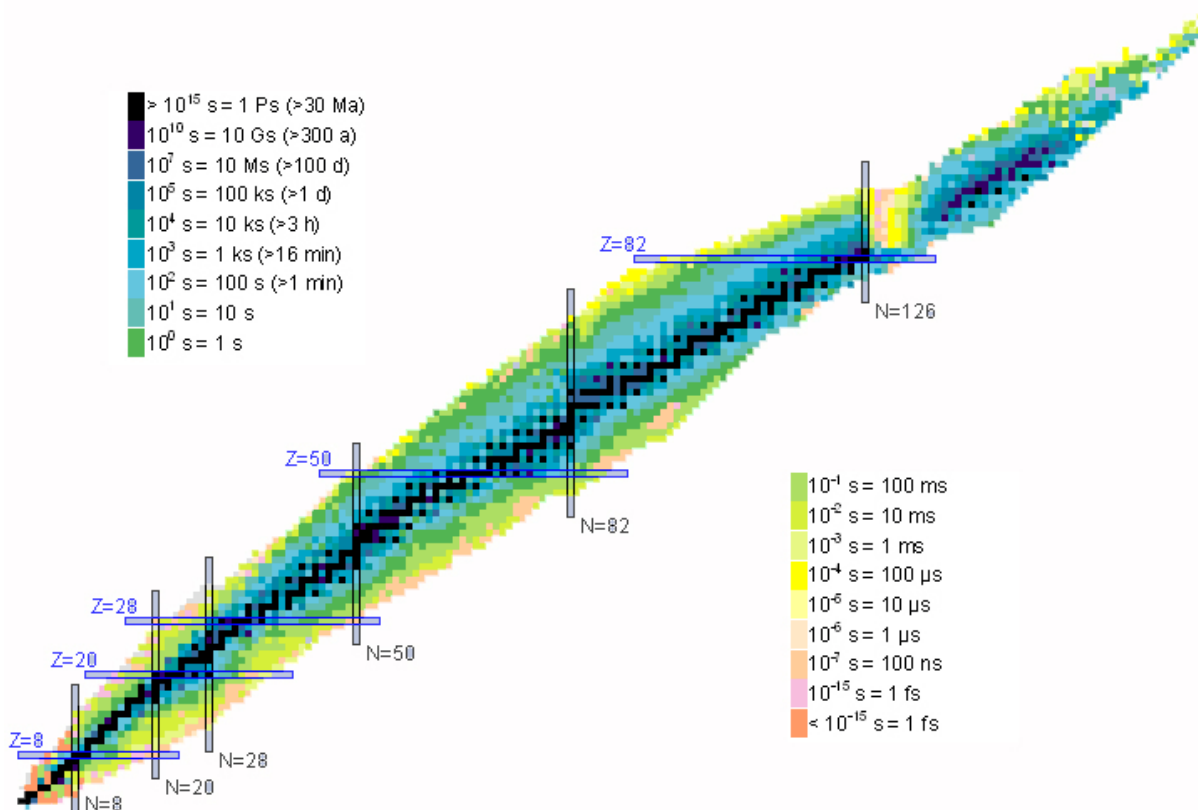


Figure 6: Chart of Nuclides colored according to half-life (information extracted from the *Chart of Nuclides database, National Nuclear Data Center, <http://www.nndc.bnl.gov/chart>*). Framed columns/rows indicate ‘nuclear magic numbers’ for N (horizontal axis) and Z (vertical axis). Magic nuclei occupy the same distinguished position among nuclei, as noble gases among elements. Both groups are characterized by closed shell structures—one for protons and/or neutrons, the other for electrons. The ‘continent of stability’ (one of the metaphors used in this context) ends shortly above the intersection of the magic lines $Z = 82$ and $N = 126$. The heaviest stable nuclide is $^{209}\text{Bi}_{126}$, the only stable isotope of bismuth. After a narrow reef of instability, the island/peninsula of relative stability follows, consisting of comparatively long-lived nuclides in the vicinity of Th and U. Then the whole continent/island drops below the sea level of instability marked by $T_{1/2} < 1\text{ fs}$. The unexplored areas—as usual with maps—are left white. Note that Th and U are not absolutely stable either, but they are very long-lived and therefore escaped extinction over the last 4.5 billion years since the Earth exists.

⁵ In 2007 I made a successful attempt to edit the entry [Nuclide](#) in [Wikipedia](#) to change ‘nuclear species’ to ‘atomic’, but [my corrections](#) only survived three weeks. Then someone [changed back](#) everything. However, I find Wikipedia a surprisingly reliable source of information in my field—in spite of the fact that anybody can change it as s/he wishes.

Note also that the definition given by IUPAC is rather vague because the qualifier ‘long enough’ is anything but exact. Setting the lowest limit of half-life for nuclear isomers to the rather conservative value of $T_{1/2} = 1 \mu\text{s}$ adds about 500 atomic/nuclear species to the number of known ground-state nuclides/nuclei. (As of 2007 the ‘NuDat 2’ data base contained the data of 3166 known nuclei and a total number of nuclear levels in the order of 146 thousand.)

Nuclide charts (see for instance Figure 6) reserve only one box for one combination of Z and A (actually Z and N) and therefore the nuclear isomers/metastable states share the box of the ground-state nuclide just as different isotopes share the same place on the periodic table of elements. If the nucleus has more than one nuclear isomer, the respective subscripts are usually ‘m’, ‘n’, etc., in increasing order of energy. Alternatively, the notation can also be m1, m2, etc.

2.3. Nuclidic Notation with Examples

Ground-state nuclides in general can be denoted in one of the following ways:

$${}^A_Z\text{X}_N, {}^A_Z\text{X}, {}_Z\text{X}_N, \quad (3)$$

where X is a general placeholder for any *chemical symbol* (He, for instance), which therefore does not carry any information about the value of Z . If the chemical symbol (implying Z) is given explicitly, it is enough to specify A , i.e. one can choose to write ${}^4\text{He}$ instead of ${}^4_2\text{He}_2$, ${}^4_2\text{He}$, or ${}_2\text{He}_2$. Note that in special applications the general placeholders can also be Y, P, F, and D, which are not to be mixed up with the concrete symbols denoting yttrium, phosphorus, fluorine, and deuterium (i.e. ${}^2\text{H}$), respectively.

Apart from the above IUPAC-supported possibilities, the notation AZ also occurs in the literature, especially in papers on super-heavy elements (SHEs). Thus all of the following symbols

$${}^{235}_{92}\text{X}_{143}, {}^{235}_{92}\text{X}, {}_{92}\text{X}_{143}, {}^{235}92, {}^{235}\text{U} \quad (4)$$

stand for the same *nuclide* called uranium-235 or U-235—that particular *isotope of the element uranium*, which is the most well-known fuel in existing nuclear reactors.

Note that a right subscript can only be used, if a left subscript is used, too. The reason is that the right subscript can be easily misunderstood (e.g. when writing up stoichiometric formulas of molecules such as H_2 or H_2O). It is also not supported by IUPAC (but widely adopted in the literature) the use of the notation D for *deuterium* (${}^2\text{H}$) and T for *tritium* (${}^3\text{H}$) in order to distinguish them from H for *protium* (${}^1\text{H}$). According to IUPAC, the symbol H in itself is to denote all conceivable isotopes of *hydrogen* regardless of their mass numbers and stability.

We will reserve the right superscript for the characterization of the electronic state of the atom. As an illustration, consider the following symbols:

$${}^A_m\text{X}_N, {}^A_*\text{X}_N, {}^A\text{X}_N, {}^A\text{X}_N^*, {}^A\text{X}_N^{2-}. \quad (5)$$

Species ${}^A_m\text{X}_N$ is the nuclear isomer of the ground-state nuclide ${}^A\text{X}_N$. Symbol ${}^A_*\text{X}_N$ means that the nucleus of nuclide ${}^A\text{X}_N$ is in excited state. However, it is not considered as a separate nuclide (i.e. a nuclear isomer), because its lifetime is too short. (The alternative notations ${}^A_e\text{X}_N$ and ${}^A_g\text{X}_N$ are also used in the literature to distinguish between excited and ground state nuclei.) Symbol ${}^A\text{X}_N^*$ denotes an excited electronic state of nuclide ${}^A\text{X}_N$. And, finally,

symbol ${}^A_Z X_N^{2-}$ stands for a -2 ion of nuclide ${}^A_Z X_N$ with an excess of two orbital electrons as compared to the neutral atom.

To give an example of the proper use of the above terminology, let us consider the following five *nuclides* (and *not isotopes*): ${}^1_1\text{H}_0$, ${}^2_1\text{H}_1$, ${}^3_1\text{H}_2$, ${}^3_2\text{He}_1$, ${}^4_2\text{He}_2$ (or, which is the same, ${}^1\text{H}$, ${}^2\text{H}$, ${}^3\text{H}$, ${}^3\text{He}$, ${}^4\text{He}$).

- One can identify ${}^1_1\text{H}_0$, ${}^2_1\text{H}_1$, and ${}^3_1\text{H}_2$ as the *isotopes* of hydrogen ($Z = 1$), forming a group of three *isotopic nuclides*. The nuclides ${}^3_2\text{He}_1$ and ${}^4_2\text{He}_2$ are the *isotopes* of helium ($Z = 2$), forming a group of two *isotopic nuclides*.
- ${}^3_1\text{H}_2$ and ${}^3_2\text{He}_1$ form a group of two *isobaric nuclides* ($A = 3$). Note that each isobar represents a different element as different *isobars* always do (see Figure 7).
- ${}^2_1\text{H}_1$ and ${}^3_2\text{He}_1$ are *isotonic nuclides* ($N = 1$). ${}^3_1\text{H}_2$ and ${}^4_2\text{He}_2$ also form a group of two *isotones* ($N = 2$). Note that an element—as always—is only represented once in an isotonic group of nuclides (see Figure 7).

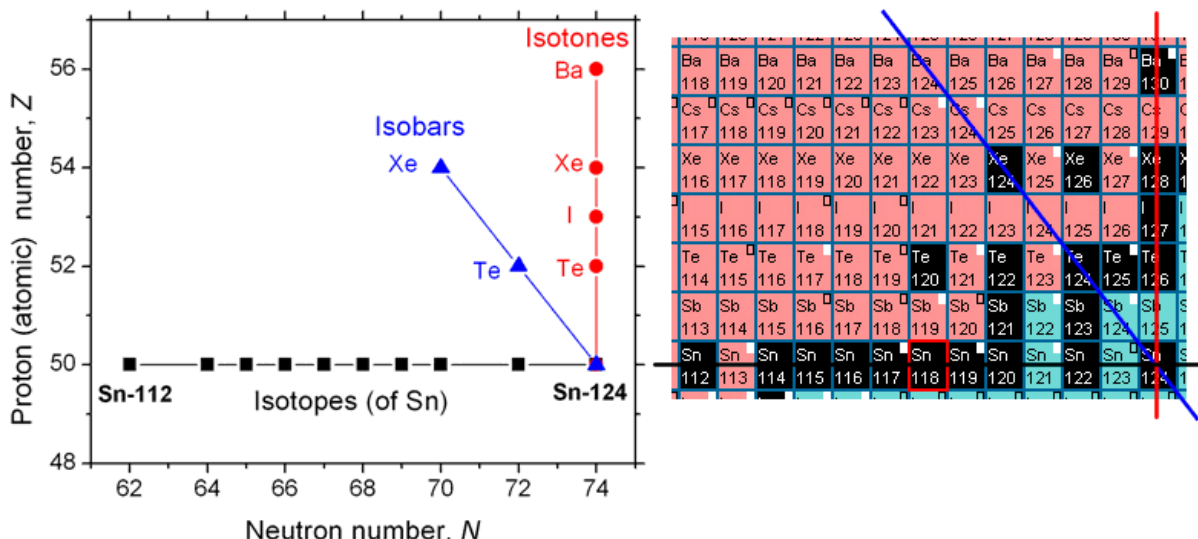
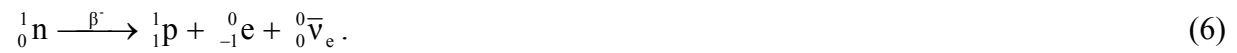


Figure 7: Representation of isotopes, isotones and isobars on the (N, Z) plane (Segrè plot) most frequently used for visualizing nuclides in nuclide charts. The left panel shows all the stable and primordial nuclides that are isotopic, isotonic and isobaric with the nuclide ${}^{124}\text{Sn}$. The right panel shows for comparison the corresponding portion of the screen picture of an electronic nuclide chart from the CD-ROM supplied with the book *Radioactivity–Radionuclides–Radiation (Universal Nuclide Chart, Copyright European Communities, 2005)*. Black cells in this particular case indicate stable and primordial nuclides, colored cells radionuclides undergoing different types of decay. (Each cell may contain different nuclear isomers same as a single cell of the periodic table usually represents a collection of isotopes of the corresponding element.) The symbols (■, ▲, ●) on the left panel correspond to the black cells of stable/primordial nuclides connected by lines on the right panel.

It is also customary to apply the ‘nuclidic notation’ to nuclei as well as to common particles such as the neutron (${}^1_0\text{n}$) and the electron (${}^0_{-1}\text{e}$). In the latter case the left subscript is the indicator of the electric charge only. As a matter of fact, the neutron can even be considered as a nuclide, namely, the most stable (actually the only existing⁶) isotope of the [0th element on the periodic system](#) containing no proton. The notation is also used for electron neutrinos such

⁶ Note that out of the three conceivable binary bound systems—nn, np, and pp—only np (i.e., the deuteron $d = {}^2\text{H}^+$) exists.

as the *electron antineutrino* (${}^0_0\bar{\nu}_e$) formed in *beta minus decay*. Thus, the β^- decay of the neutron is sometimes written as follows (see also Figure 8):



Note that the subscripts (as well as the superscripts) are balanced, i.e., they result in the same sum on both sides of the arrow. This is the manifestation of conservation laws that must be satisfied by nuclear processes like radioactive decay.

3. Mass and Energy—Basic Quantities and Units

This section is devoted to the memory of [Aaldert H. Wapstra](#) (1922-2006), who died at an age of 84 when the original of this work was just about finalized. Professor Wapstra was awarded the [SUNAMCO](#) Medal in 2004 ‘for his role in the Atomic Mass Evaluations from their inception to the present’ by the International Commission on Symbols, Units, Nomenclature, Atomic Masses and Fundamental Constants. Chemists might want to know that he was one of the scientists who prepared the introduction of the unified atomic mass unit (u), the basis for atomic weight calculations since 1960-61.

3.1. The Electron Volt—the Energy Unit in Nuclear Science

The preferred energy unit in nuclear science is the *electron volt* eV (see the SI value in Table 1). Its physical interpretation is rather straightforward: 1 eV is the kinetic energy acquired by an electron when accelerated by a potential difference of 1 V in a vacuum. IUPAC also supports the use of SI prefixes with eV, so keV (kiloelectron volt) means 1000 eV, MeV (megaelectron volt) means one million eV and GeV (gigaelectron volt) means one billion eV, etc.

In order to bring this unit closer to chemists, it is worth giving its molar equivalent too by multiplying it with the *Avogadro number* (Table 1). The approximate correspondence (\Leftrightarrow) is as follows (see Table 1 for the accurate value of the ‘conversion factor’):

$$1 \text{ eV} \Leftrightarrow 100 \text{ kJ mol}^{-1}, \quad (7)$$

which is of the order of the activation energy of chemical reactions. Considering this, the energies typical of RC&NC ($\sim 1 \text{ MeV} = 1\,000\,000 \text{ eV}$) can initiate tens of thousands of elementary chemical processes. Energies typical of particle physics are even higher ($\sim 1 \text{ GeV} = 1\,000\,000\,000 \text{ eV}$ and up).

3.2. Energy and Temperature

When talking about *thermal energies*, what we mean is that the kinetic energy of the particles (e.g. *thermal neutrons*) is typical of gas atoms/molecules doing thermal motion at room temperature. Note that the air molecules in our lungs move with an average kinetic energy of $(3/2)kT \approx 0.04 \text{ eV} = 40 \text{ meV}$, where k is the *Boltzmann constant* (Table 1) and T is the thermodynamic temperature. At 25°C (i.e. at standard room temperature) the average kinetic energy is a little lower, about 38.5 meV .

The *thermalization* of radiation particles means that they slow down in a material to thermal energies by collisions or by other mechanisms. The beginning of the thermalization phase is usually taken as $\sim 1 \text{ eV}$, when the kinetic energy of the particles (e.g. neutrons) is in the order of the binding energy of valence electrons.

The *temperature equivalent* of 1 eV is usually given through the formula $E_{\text{kin}} = kT$ representing the kinetic energy of a gas atom/molecule moving at the most probable speed at the given temperature. (Note that the most probable kinetic energy is only $kT/2$ and, as mentioned above, the average kinetic energy is $3kT/2$.) For the accurate correspondence between energy and temperature see Table 1. The approximate correspondence is as follows:

$$1 \text{ eV} \Leftrightarrow 10\,000 \text{ K} = 10 \text{ kK}. \quad (8)$$

At 25°C the value of kT is about 25.7 meV.

Table 1: Physical constants and units mentioned in the text. Following IUPAC recommendations, their symbols are in *italics* and in normal style, respectively. ‘Corresponds to’ (denoted by the symbol \Leftrightarrow in the text) means a value given in a unit whose use is only justified through the proportionality between different physical quantities. Energy and mass are connected by the proportionality $E_0 = m c^2$, energy and temperature by $E_{\text{kin}} = k T$.

Physical constant or unit		Value		
Name	Symbol	in SI unit	in other unit	corresponds to
elementary charge	e	$1.60217653 \times 10^{-19}$ C		
Avogadro number	N_A	6.0221415×10^{23} mol ⁻¹		
electron volt	eV	$1.60217653 \times 10^{-19}$ J		96.485 kJ mol ⁻¹ 11.60451 kK
gigaelectron volt	GeV	$1.60217653 \times 10^{-10}$ J		1.073544 u
Boltzmann constant	k	1.380650×10^{-23} J K ⁻¹	8.61734×10^{-5} eV K ⁻¹	
speed of light in empty space	c	2.99792458×10^8 m s ⁻¹		
unified atomic mass unit (\approx amu, a.m.u.)	u	$1.6605387 \times 10^{-27}$ kg	m_u 1 Da	931.49401 MeV
electron mass	m_e	9.109382×10^{-31} kg	$5.48579911 \times 10^{-4}$ u	510.9989 keV 0.5109989 MeV 49.3037 GJ mol ⁻¹
proton mass	m_p	$1.6726216 \times 10^{-27}$ kg	1.0072764669 u $1836.152668 m_e$	938.2720 MeV 0.938272 GeV
neutron mass	m_n	$1.6749272 \times 10^{-27}$ kg	1.0086649158 u $1838.683655 m_e$	939.5654 MeV 0.9395654 GeV
neutrino mass	m_ν		$< 4 \times 10^{-6} m_e$	< 2 eV
becquerel	Bq	1 s ⁻¹	1 dps	
curie	Ci	3.7×10^{10} Bq		
Planck constant	h	$6.6260688 \times 10^{-34}$ J s	$4.1356673 \times 10^{-15}$ eV s	
reduced Planck constant, Dirac constant	\hbar	$1.0545716 \times 10^{-34}$ J s	$6.5821189 \times 10^{-16}$ eV s	
barn	b	10^{-28} m ² = 100 fm ²		
angstrom	Å	0.1 nm		
parsec	pc	30.857×10^{12} km		
light year		9 460 730 472 581 km	0.3066 pc	
day	d	86 400 s		
year	a	3.1556952×10^7 s	365.2425 d	

Note that kelvin is a favored ‘energy unit’ in the field of thermonuclear reactions and in cosmology. The above correspondence also explains why atoms recoiled by α decay and thus receiving a kinetic energy of, say, 100 keV (\Leftrightarrow 1 GK \approx 1 000 000 000 °C) are referred to as *hot atoms* in hot-atom chemistry.

3.3. The Nuclidic Mass and the Unified Atomic Mass Unit

Following IUPAC recommendations, the mass of an atom will be denoted by m_a . The masses of subatomic particles will be denoted by symbols like m_p , m_e , etc. (p for proton, e for electron, etc). Although it is not an IUPAC/IUPAP recommendation, following some

established examples, I will denote the mass of the nucleus by m_N . (For instance, the nuclear magneton is denoted by μ_N everywhere in the literature.)

The *nuclidic mass* is defined by IUPAC as ‘the rest mass of a nuclide in atomic mass units’. In other words, the nuclidic mass is the relative atomic mass of a specific nuclide rather than the weighted average of the relative atomic masses (nuclidic masses) of the naturally occurring isotopes of a given element. Accordingly, we will use the following formula⁷ for the calculation of the nuclidic mass M :

$${}^A_Z M = \frac{m_a({}^A_Z X)}{m_u} = m_a({}^A_Z X) / u \equiv A_r({}^A_Z X), \quad (9)$$

where m_u is the *atomic mass constant* that is equal to the *unified atomic mass unit* u also called *dalton* (Da) defined as one twelfth of the mass of a carbon-12 atom in its nuclear and electronic ground state:

$$1 \text{ u} = 1 \text{ Da} = m_u = \frac{m_a({}^{12}\text{C})}{12} = 1.660\,538\,7 \times 10^{-27} \text{ kg} \Leftrightarrow 931.494 \text{ MeV}. \quad (10)$$

The correspondence (\Leftrightarrow) between mass and energy comes from the formula

$$E_0 = m c^2, \quad (11)$$

[see Eq. (163) in chapter 14 on special relativity] where E_0 is the *rest energy*, m is the mass, and c is the speed of light in a vacuum (see Table 1).

Comments:

1. Note that the unit ‘u’ only became accepted both by IUPAP and IUPAC in 1961. (Physicists started to use it already in 1960.) Before that the unit ‘amu’ was used in physics and chemistry but it meant [not quite the same thing](#) in these fields of science. Therefore, in terms of energy, 1 u is ~ 40 keV higher than 1 amu used to be in chemistry and ~ 296 keV higher than 1 amu used to be in physics. Because of the ambiguity the use of ‘amu’ should better be avoided.
2. The unit dalton is mostly used in biochemistry and molecular biology, but also occurs in books on RC&NC. Otherwise it works just as well as u.
3. The atomic mass constant is not considered a unit by SI as its typography reveals (it is written in *italic*). However it works just as well.

Table 1 shows the presently (2006) most accurate values of masses and rest energies for the electron, proton, and neutron. The approximate values below are only given for comparison:

$$m_e \approx 0.000\,548 \text{ u} \Leftrightarrow 0.511 \text{ MeV} \approx \frac{1}{2} \text{ MeV}, \quad (12)$$

$$m_p \approx 1.007\,276 \text{ u} = 1836.2 m_e \Leftrightarrow 938.272 \text{ MeV} \approx 1 \text{ GeV}, \quad (13)$$

$$m_n \approx 1.008\,665 \text{ u} = 1838.7 m_e \Leftrightarrow 939.565 \text{ MeV} \approx 1 \text{ GeV}. \quad (14)$$

We can conclude therefore that

- nucleons are much heavier than the electron;

⁷ Note that the actual unit of M thus defined is actually 1. In other words it is just a pure number. However, it yields the correct mass of one atom of the given nuclide as soon as it is multiplied by the unit u, i.e., $m_a = M u$.

- nucleons are only about 1% heavier than 1 u;
- the neutron is only about 2.5 electron-mass units heavier than the proton (see also Figure 8);
- the electron is relatively light, but its energy equivalent—half a MeV—is a lot and thus
- the energy equivalent of an ion is significantly different from that of a neutral atom;
- atomic/nuclidic masses need to be known to many significant figures to yield accurate enough rest energies.

The mass of a single atom of a given nuclide can be expressed as follows:

$$m_a({}_Z^A\text{X}) = {}_Z^A M \text{ u} \Leftrightarrow {}_Z^A M \times 931.494 \text{ MeV} . \quad (15)$$

For convenience's sake we will also use the term nuclidic mass for the neutron ${}_0^1\text{n}$ defined as follows:

$${}_0^1 M = m_n / \text{u} . \quad (16)$$

Moreover, we will also use the notation M for any particle in the following sense:

$$M = m / \text{u} , \quad (17)$$

where m is the mass of the particle. (No matter how tempting is the use of the name 'nuclidic mass'⁸ in the latter case, I will try to avoid it.)

The *relative atomic mass* $A_r({}_Z\text{X})$ of the element ${}_Z\text{X}$ (also called the *atomic weight*)—defined by IUPAC as 'the ratio of the average mass of the atom to the unified atomic mass unit'—is readily calculated for any element from the nuclidic masses of its isotopes:

$$A_r \equiv A_r({}_Z\text{X}) = \sum_A a_A A_r({}_Z^A\text{X}) \equiv \sum_A a_A {}_Z^A M , \quad (18)$$

where a_A is the natural *isotopic abundance* (atomic fraction) of the isotope ${}_Z^A\text{X}$ among the atoms of the element ${}_Z\text{X}$. The biennially revised atomic weight values of elements recommended by IUPAC are called *standard atomic weights*. Periodic tables, as a rule, show the approximate values of these.

3.4. Quantities Characterizing Stability and Instability

3.4.1. The Q -value and the criterion for spontaneity

The most widely applicable quantity as regards the energetics of nuclear transformations (radioactive decay, nuclear reaction) is the Q -value illustrated by Figure 8 in the special case of the β decay of the neutron. The illustration on the top reflects the spirit of the Standard Model of particles and interactions summarized in chapter 4.

Instead of giving a verbal definition for Q at once, let us first consider a general process without detailing the particles/nuclides that are involved:

$$\text{reactants} \rightarrow \text{products} \text{ or more briefly: } A \rightarrow \Omega . \quad (19)$$

⁸ Note that IUPAC may not agree with this type of the generalization of the concept 'nuclidic mass'. However I once read a sentence something like this and I liked it: 'One mole of moles means 6×10^{23} burrowing animals of the species *Talpa europaea*.' However so many moles—taking as an average 100 g/mole—would weigh about 6×10^{22} kg, so they would hardly be able to burrow in our Earth which only weighs 100 times more, i.e. 6×10^{24} kg, including its hot Fe/Ni core.

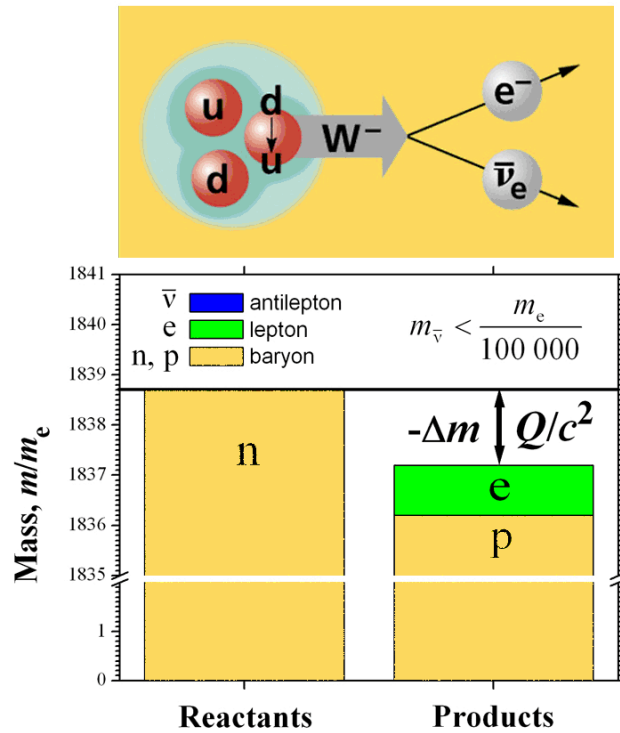


Figure 8: Spontaneous processes, like the β^- decay of the free neutron, can only take place if the rest energy (mass) of the system decreases. The change of the rest energy determines the Q -value of the process. Q is considered positive if the rest energy decreases. The Q -value (782 keV in the present case) is spent on the kinetic energy of the particles produced. Due to momentum conservation the share of the lighter particles from Q will be larger than that of the heavier ones. Because of this, the major part of Q is divided between the electron (β^- particle) and the antineutrino (see also Figures 31-58). Note that the vertical axis is broken between $2 m_e$ and $1835 m_e$. Therefore the apparent proportions of the columns do not reflect the fact that only a tiny part ($< 0.1\%$) of the neutron mass m_n is converted to kinetic energy, which is still about 75 GJ mol^{-1} . The picture above the plot shows how the decay of a neutron (udd) to a proton (uud) is interpreted by the SM in terms of the transformation of a d quark to a u quark via a mediating W^- boson. The properties of the W^- boson, a mediator of the weak force, are summarized in Table 4. (The [motif](http://ParticleAdventure.org) has been taken from *The Standard Model of Fundamental Particles and Interactions Chart*, copyright 1999 by the Contemporary Physics Education Project, <http://ParticleAdventure.org>.)

The energy balance holds for the total energy E [see Eq. (170) in chapter 14] consisting of two terms, namely, the rest energy expressed by Eq. (11) and the (relativistic) kinetic energy E_{kin} :

$$E = E_0 + E_{\text{kin}} = m c^2 + E_{\text{kin}} . \quad (20)$$

The energy balance is simply:

$$\sum_A E = \sum_\Omega E . \quad (21)$$

After substituting Eq. (20) and rearrangement, we can introduce the energy quantity:

$$Q = \sum_A m c^2 - \sum_\Omega m c^2 = \sum_\Omega E_{\text{kin}} - \sum_A E_{\text{kin}} = \Delta E_{\text{kin}} , \quad (22)$$

which is referred to as the Q -value of the process.

As we see, the Q -value is calculated by subtracting the rest energies of all products (Ω) from those of the reactants (A).

On the other hand, Q is also equal to the difference of the kinetic energies taken in the reversed order, i.e. kinetic energy of the products (Ω) minus that of the reactants (A). Therefore, **the Q -value is positive if and only if the kinetic energy of the products is higher than that of the reactants.**

Spontaneous processes (which need no external ‘help’ to take place) must be exoergic (exothermic), meaning that they must produce more kinetic energy than they consume. According to the above comment this demands that their Q -value be positive. Thus the **necessary condition for spontaneity** is:

$$Q > 0. \quad (23)$$

If the masses (m or M) involved are available with high enough accuracy, then the Q -value can be calculated using either of the following formulas:

$$Q = \left(\sum_A m - \sum_\Omega m \right) \times 931.494 \frac{\text{MeV}}{u} = \left(\sum_A M - \sum_\Omega M \right) \times 931.494 \text{ MeV}. \quad (24)$$

Note that the mass differences in the above equation are not taken in the conventional order. With conventional notation (i.e. $\Delta M = \sum_\Omega M - \sum_A M$) therefore we should add a negative sign to ΔM :

$$Q = (-\Delta M) \times 931.494 \text{ MeV}. \quad (25)$$

Note that Figure 8 also demonstrates the conservation of several quantities besides that of the total energy indicated by the horizontal solid line on top of the bar representing the mass (rest energy) of the neutron:

- Electric charge. The charges of p and e being oppositely equal cancel, while the rest are neutral.
- Lepton charge/number. L is +1 for the electron (see section 4.2) and -1 for the antineutrino. The baryons have no lepton charge, i.e. their lepton number is 0.
- Baryon charge/number. B is +1 for both nucleons and 0 for the leptons.

The above conservations represent further restrictions on possible processes. That is, condition $Q > 0$ is indeed only a necessary criterion and not a sufficient one. The above conservations are always satisfied in radioactive decay. More specifically, the conservation of the baryon number takes on the form of the *conservation of the nucleon number* in all types of radioactive decay.

3.4.2. The Binding Energy of the Nucleus and the B/A Value

Another important energy quantity is the *binding energy of the nucleus* (E_N) that constitutes the major part of the *total binding energy of the atom* (E_a) of a particular nuclide ${}^A_Z X$:

$${}^A_Z E_a = {}^A_Z E_N + {}_Z E_{Ze}, \quad (26)$$

which also includes the total binding energy E_{Ze} of the Z orbital electrons. (The value of E_{Ze} is practically independent of the mass number, i.e. the *isotope effect* can be neglected, and therefore the left superscript can be omitted.) As such, the atomic binding energy E_a is the Q -value of the fictitious process in which the neutral atom ${}^A_Z X_N$ is formed from its components (i.e. N neutrons, Z protons, and Z electrons for the present purpose).

We can write up several equations related to the processes implied above, each representing a

formation reaction with its Q -value added to the right side to make it balanced for mass. The equations below are completed with a short comment on the energy term in question:

$$Z \text{ p} + N \text{ n} + Z \text{ e}^- = {}^A_Z\text{X} + {}^A_Z E_a \quad \text{total binding energy of the neutral atom } {}^A_Z\text{X}, \quad (27)$$

$$Z \text{ p} + N \text{ n} = {}^A_Z\text{X}^{Z+} + {}^A_Z E_N \quad \text{actual binding energy of the nucleus } {}^A_Z\text{X}^{Z+}, \quad (28)$$

$${}^A_Z\text{X}^{Z+} + Z \text{ e}^- = {}^A_Z\text{X} + {}_Z E_{Ze} \quad \text{total binding energy of the } Z \text{ orbital electrons in } {}^A_Z\text{X}, \quad (29)$$

$$\text{p} + \text{e}^- = {}^1_1\text{H} + {}_1 E_{1e} \quad \text{binding energy of the single orbital electron in } {}^1_1\text{H}, \quad (30)$$

$$Z {}^1_1\text{H} + N {}^1_0\text{n} = {}^A_Z\text{X} + {}^A_Z B \quad \text{so-called binding energy of the nucleus } {}^A_Z\text{X}^{Z+}. \quad (31)$$

The last equation introduces a new energy quantity B characterizing the formation of the nuclide from Z hydrogen atoms and N neutrons. Using Eqs. (9), (16), and (24) we can calculate B as follows:

$${}^A_Z B = (Z {}^1_1 M + N {}^1_0 M - {}^A_Z M) \times 931.494 \text{ MeV} \Leftrightarrow (Z {}^1_1 M + N {}^1_0 M - {}^A_Z M) \text{ u}. \quad (32)$$

By tradition B (often denoted as E_B or BE) is called the nuclear binding energy (or the binding energy of the nucleus), although it must be clear that it is not quite the same as E_N , namely:

$${}^A_Z B = {}^A_Z E_N + ({}_Z E_{Ze} - Z \times {}_1 E_{1e}) \geq {}^A_Z E_N, \quad (33)$$

as one can easily algebra it out from the above formation equations [(28) + (29) - $Z \times$ (30) - (31)]. (To verify the inequality, too, one should also consider that the binding energy of the innermost electron shells steeply increases with the atomic number.) However, following the old tradition—and also because the relative difference due to electrons is rather small—further on I too will refer to B as the binding energy (of the nucleus). Note, however, that in some extreme cases a little difference matters a lot and therefore sometimes it is the binding energy of the electron that settles the question whether the nucleus can decay in a given mode or not. This is the case, e.g., with electron capture [EC, see Eq. (93)] and with bound beta decay (β_b , see Figure 50).

The binding energy B is kind of an ‘extensive’ property of the nucleus, i.e. it ‘automatically’ gets larger as Z and N (or, actually, the number A of interacting nucleons) increases, thus hiding what really important is, namely, how the ‘average’ nucleon is bonded to the rest of the nucleus. It is customary therefore to use the quantity called the *average binding energy per nucleon* instead, which is defined as follows:

$$B/A = \frac{{}^A_Z B}{A} = \frac{{}^A_Z E_N}{A} + \frac{{}_Z E_{Ze} - Z \times {}_1 E_{1e}}{A} \approx \frac{{}^A_Z E_N}{A}. \quad (34)$$

Note that the binding energy per nucleon averages at ~ 8 300 keV for stable nuclides. On the other hand, the term from the binding energies of orbital electrons is a mere ~ 1.5 keV even for bismuth, which means that the error of the approximate formula stays below 0.02%. This seems to be acceptable for a chemist.

Figure 9 shows the 3D representation of the average binding energy per nucleon for stable nuclides as the function of Z and N . The points of the graph have been calculated from actual nuclidic mass data using Eqs. (32)-(34). Note that the general tendency can also be explained in rather simple terms using a clone of the Weizsäcker equation (53), the original of which was created in 1935 as the first step towards the liquid drop model.

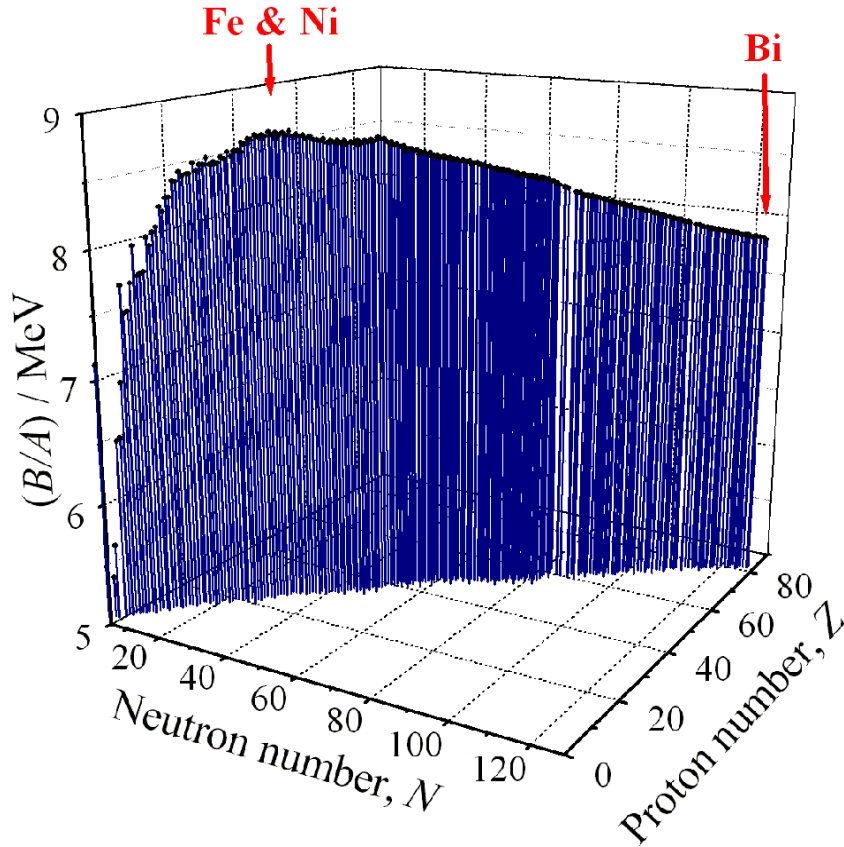


Figure 9: The average binding energy per nucleon calculated from the nuclidic masses of the 266 most stable nuclides. The drop lines mark out from the (N, Z) plane the black zigzag of stable nuclides seen in Figure 6. Continuing the ‘continent of stability’ metaphor started there, B/A gives the altitude of the mountain ridge along the continent showing iron and nickel as the most stable elements on the whole periodic table (see the upper panel in Figure 10). Bismuth is also marked as the heaviest stable element represented in nature by a single stable isotope.

3.4.3. The Mass Excess

Sometimes, instead of the nuclidic mass, the *mass excess* (Δ) is presented in databases. The mass excess of the nuclide ${}^A_Z\text{X}$ is:

$${}^A_Z\Delta = ({}^A_ZM - A)\text{u} \Leftrightarrow ({}^A_ZM - A) \times 931.494 \text{ MeV}. \quad (35)$$

The mass excess values give a very good idea about the relative stabilities of isobaric nuclides—lower Δ means higher stability in this particular case (see the lower panel in Figure 10). Besides u, often used units for Δ values are μu (10^{-6} u), mu (10^{-3} u), keV, and MeV.

It follows from Eq. (32) that the binding energy B is readily calculated from the mass excess values:

$${}^A_ZB = (Z {}^1_1\Delta + N {}^1_0\Delta - {}^A_Z\Delta) \times 931.494 \frac{\text{MeV}}{\text{u}} \Leftrightarrow Z {}^1_1\Delta + N {}^1_0\Delta - {}^A_Z\Delta. \quad (36)$$

Since A_ZB and ${}^A_Z\Delta$ have opposite signs in the above equation, the curves in Figure 10 are approximately mirror images of each other.

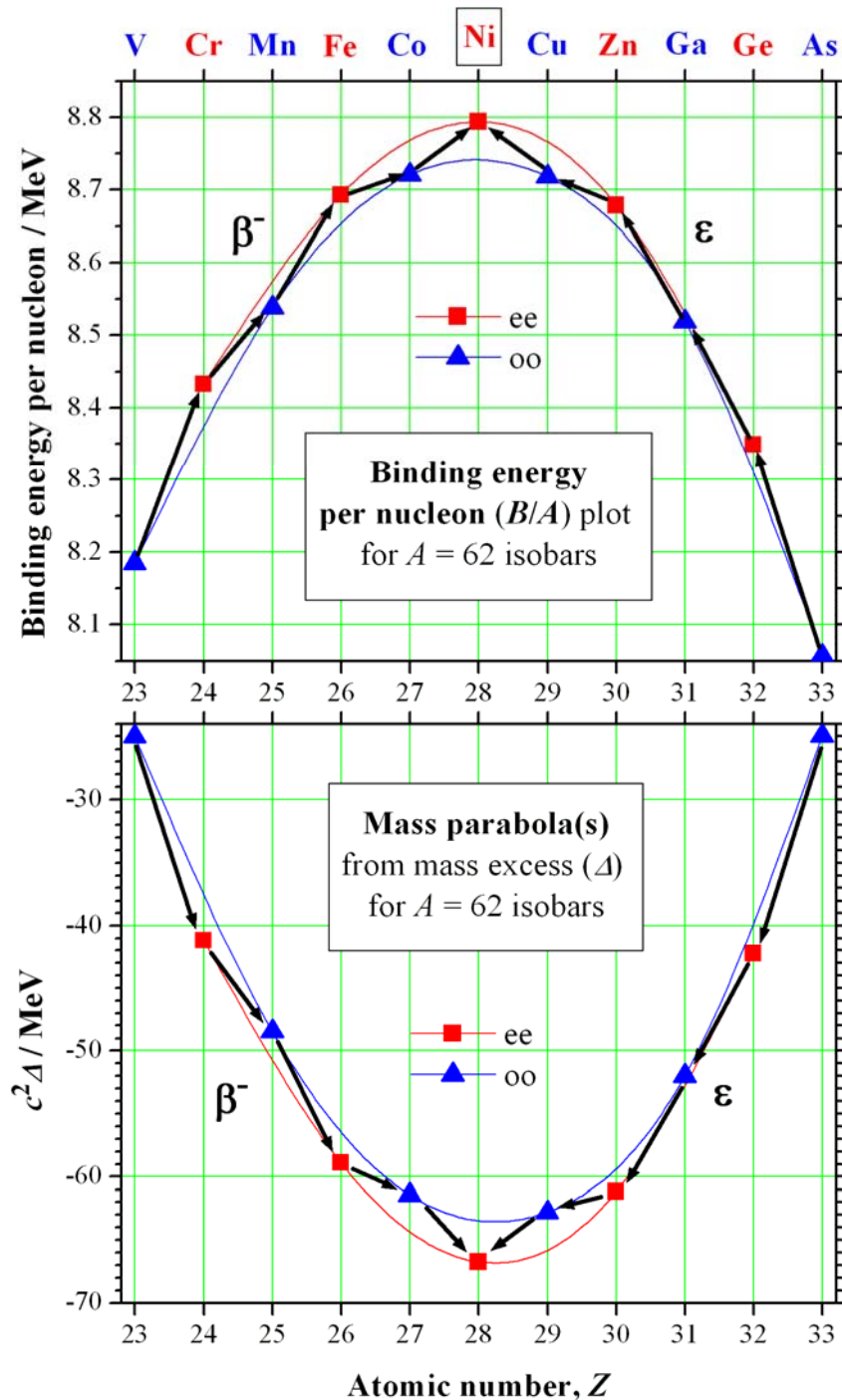


Figure 10: Energy plots for the isobars of ^{62}Ni , the most stable of the existing nuclides, preceding even ^{56}Fe which is most often credited with being number one. Note that both plots feature ^{62}Ni as the winner of the race for stability among the isobaric nuclides with $A = 62$, although the graphs are not exact mirror images of each other. More or less ragged upside-down parabolas like the one on the upper panel characterize the rocky slopes of the mountain of stability whose ridge is shown in Figure 9. The equally ragged mass parabola on the lower panel gives an idea of how the isobaric cross sections of the valley of stability look like. This metaphoric description of the energy surfaces used for representing the stability of nuclides over the (N, Z) plane was introduced by [Seaborg](#), the eponym of seaborgium [Sg](#), while talking about the ‘sea of instability’ that surrounds the ‘peninsula of stability’.

Finally, it should be mentioned the term *mass defect* or *mass deficit* the use of which I will avoid further on. However I cannot ignore it completely, because it is still often used in the

literature, alas, in various senses.

- Mass defect is sometimes mixed up with mass excess, i.e. it is identified either with $(-\Delta)$ or with Δ .
- A more reasonable definition for the mass defect is Q/c^2 in general (i.e. the mass equivalent of the Q -value of a process, especially a spontaneous one, when the mass decreases and therefore the mass defect so defined turns out positive). For instance, the $(-\Delta m)$ value in Figure 8 can be considered as mass defect in this general sense.
- Mass defect is also used in the restricted sense meaning the Q/c^2 value related to the formation of the nucleus from nucleons according to Eq. (28). In that case it is equal to the mass difference $(Z m_p + N m_n - m_N)$.

3.4.4. Nucleon Separation Energies

Sometimes it is more appropriate to use the *nucleon separation energy* in order to compare a group of nuclides for stability. As there are two types of nucleon, there are also two types of separation energy related to the following separation processes:



The *neutron* separation energy S_n and the *proton* separation energy S_p are defined as follows:

$${}^A_Z S_n = \left(-{}^A_Z M + {}^{A-1}_Z M + {}^1_0 M \right) \times 931.494 \text{ MeV}, \quad (39)$$

$${}^A_Z S_p = \left(-{}^A_Z M + {}^{A-1}_{Z-1} M + {}^1_1 M \right) \times 931.494 \text{ MeV}. \quad (40)$$

In other words, the larger the nucleon separation energy, the harder it is to separate the given nucleon from the rest of the nucleus. So it is also a type of measure of the ‘per-nucleon-stability’ of the nucleus, but—in contrast to the average binding energy per nucleon B/A —it is not an average value.

In a way this concept is similar to that of the *first ionization potential/energy* of elements known from chemistry. Remember that noble gases, due to their closed electronic shells, have much higher ionization potentials than their neighbors on the periodic table. This helps to accept the interpretation of the higher peaks or edges on the color graphs in Figure 11 as the sign of closed nucleon shells at certain ‘magic’ numbers of neutrons/protons. The disjointedness of the color and black graphs (with the latter lying below the color one) is explained both by the *pairing term* of the Weizsäcker equation (53) and by the shell model (see in sections 5.3 and 6.3).

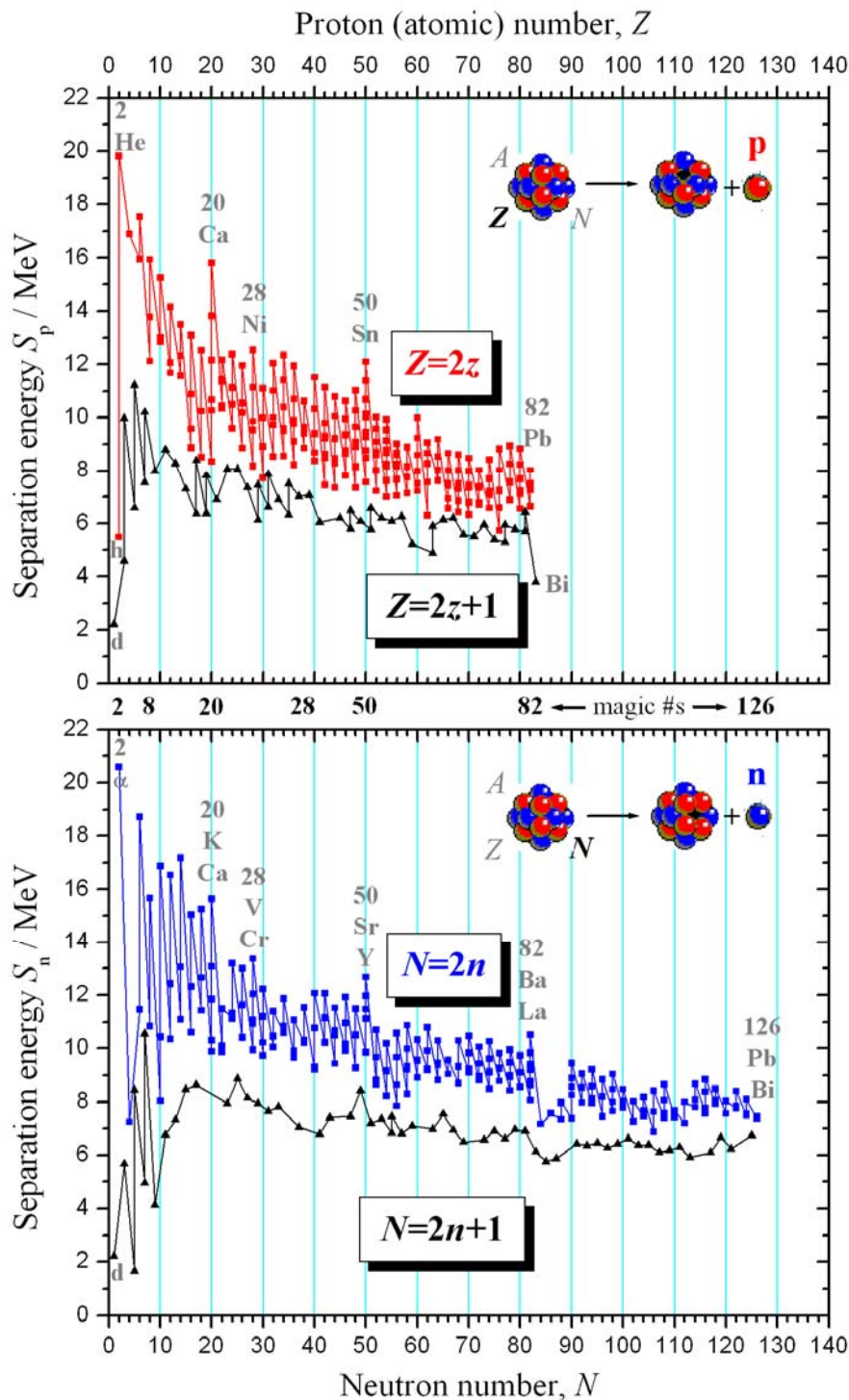


Figure 11: Separation energies for protons (upper panel) and neutrons (lower panel) calculated for 256 of the most stable nuclides (with the obvious exception of ^1H), most of which are also represented in Figure 9. Note that an unpaired proton/neutron (black \blacktriangle curves representing odd numbers of like nucleons) can be separated from the nucleus much more easily than one that is paired off (color \blacksquare curves). The conspicuous peaks on the color curves at $Z = N = 2, 20, 50,$ and 82 show that protons and neutrons have the same nuclear magic numbers. Closed shells characterized by such proton/neutron numbers are particularly stable making the separation of a nucleon especially difficult.

4. Particles and Forces—the Standard Model in a Nutshell

After the discovery of the nucleons and with the aid of increasingly powerful accelerators, experimental physicists kept busily discovering new particles every week until it became clear that all of these particles could not be elementary. Enrico Fermi's comment on this was supposed to be: *'Had I foreseen that, I would have gone into botany!'* The solution to the problem came with the classification scheme of hadrons by the aid of the *quark concept* established by M. Gell-Mann in 1964 ([Nobel Prize](#) in physics, 1969). His ideas were based on the *symmetry principles* recognized by E.P. Wigner ([Nobel Prize](#) in physics, 1963) as early as 1927 (see the site [Development of Subatomic Concepts, Nuclear Science and Technology—A Timeline](#) which I update from time to time).

The brief summary of particle physics background I give in this chapter is based on the theory called the Standard Model. For more detail see the free site of the Contemporary Physics Education Project at <http://www2.slac.stanford.edu/vvc/theory.html>. For personal use or for teaching purposes one can also load down a very informative 2006 poster and its printable parts from the site http://www.cpepweb.org/cpep_sm_large.html.

4.1. The Origin of Nuclear Force

Figure 5 presented in section 2.1 shows the artistic representation of the structure of a ${}^4\text{He}$ atom based on the Standard Model. The *nuclear force* that holds the nucleus together is only a residual of the *strong force* or [color force which acts inside the nucleons between quarks](#) and is mediated by gluons (not represented in the figure). The color force is never completely compensated at every point of the 'surface' of a nucleon. Thus, if observed from close enough, the nucleon is not 'neutral' as regards the *color charge*, and the locally uncompensated color charge makes it 'sticky' thus attracting other nucleons nearby. The nuclear force that binds the nucleons to each other—being just a residual of color force—has a very *short range* in the order of the size of a nucleon (see Table 5).

Chemical analogy. The 'force' binding electrically neutral atoms together to form molecules can also be regarded as the residual of the electric force that is neutralized within atomic scale. And so is the attractive London force (dispersion force) between nonpolar molecules which is explained by fluctuations in the instantaneous distribution of the electrons. In contrast to the Coulomb force whose range is infinite, the interatomic/intermolecular 'residual electric' forces are also short-range forces. In the case of molecules, the bonding electrons moving between the atoms can also be regarded as 'force carriers', thus playing the same role as the (virtual) pions between neighboring nucleons (see the last row, shaded in yellow, in Table 4). The nuclear force acting between nucleons has another similarity with the bond between two atoms forming a molecule, namely, with decreasing internucleonic distance (at about 0.5 fm) the nuclear force becomes repulsive. That is, nucleons—same as atoms (or molecules)—cannot be easily squeezed into each other. Such behavior is the basis of the 'incompressibility' of liquids.

The recognition of this kind of similarity between internucleonic and interatomic forces led to the creation of the *liquid drop model* of the atomic nucleus, which had been successfully used for the explanation of many nuclear properties.

4.2. Classification of Particles and Forces

Tables 2 through 6 show some properties of a few particles, which are only representatives of the several hundred whose existence is proven by experiment. The data have been compiled from the Particle Data Group site <http://pdg.lbl.gov/> (Particle Listings 2006). Data in Table 5 are mostly from the Standard Model Chart (<http://particleadventure.org/frameless/chart.html>, copyright 1999 by the Contemporary Physics Education Project).

Particles and their *antiparticles* have the same mass, and certain additive parameters assigned to them called generalized ‘charges’ (including *electric charge*, *strangeness*, *bottomness*, *topness*, *charm*, *baryon number*, *lepton number*, etc.) change to the opposite. Thus, the positron e^+ , the antiparticle of the ordinary electron e (which is also called negatron e^- in this context), has positive electric charge. (Since the electron/negatron is a lepton having an assigned value of lepton number $L = +1$, its antiparticle, the positron, has $L = -1$. Since leptons are not baryons, the baryon number of e^- and e^+ is $B = 0$.) Similarly, the antiparticle of π^+ is π^- and vice versa. There are some ‘absolutely neutral’ particles, such as π^0 , which are identical with their antiparticles. Particles meeting their antiparticles may *annihilate* with each other, which means that the whole rest energy (mass) of the ensemble gets converted to ‘pure’ energy, i.e. to photons, according to the equation $E_0 = m c^2$ (see the mass concept described in chapter 14). Unless they bump into each other with high energy, e.g., in the [proton-antiproton collider Tevatron](#), when they tend to produce further particles. On the other hand, if a particle is stable (e.g. the electron), so is its antiparticle (e.g. the positron) when left alone. Their apparent instability is just the consequence of the fact that—surrounded by ordinary matter—they are never left alone for very long and therefore [annihilation](#) takes place.

Subatomic particles—once all of them referred to as elementary—are classified according to different criteria.

One important aspect of classification is whether the *spin quantum number of the particle* (s) is a *half-integer* (i.e. $1/2, 3/2, 5/2\dots$) as with *fermions*, or an *integer* (i.e. $0, 1, 2\dots$) as with *bosons*. This may seem just a trifle, but has important implications. [In particle physics lingo, s is simply referred to as *spin*, because it gives the maximum observable projection of the spin vector \mathbf{s} in units of \hbar , where \hbar is the reduced Planck constant (or Dirac constant), i.e. the Planck constant h divided by 2π .]

Fermions—similarly to their well-known representative, the electron—are all subject to the *Pauli exclusion principle*, whereas bosons (such as the photon) are not.

The names themselves are mnemonics of statistics. Fermions obey *Fermi–Dirac statistics* (connected with the problem of placing n undistinguishable objects in N labeled boxes with storage capacity limited to one object only), whereas bosons obey *Bose–Einstein statistics* (placing n undistinguishable objects in N labeled boxes with unlimited storage capacity).

Another important aspect is *complexity*. According to this, those particles that are considered nowadays as the ultimate building blocks of matter are called [fundamental particles](#) or, alternatively, [elementary particles](#). These are thought of as lacking any internal structure and therefore point-like. Even [the mass of them](#) is sometimes far from being easily interpreted by anybody except particle physicists. (This is particularly true for [quarks](#).)

The known elementary particles are divided in three classes. Two of them (the leptons and the quarks) are [elementary fermions](#) with spin $1/2$, whereas the elementary force carriers are bosons with spin $0, 1, 2, \dots$

Table 2: Leptons are the class of elementary fermions ($s = 1/2$) that are not affected by strong/color force (see Table 5). The upper limit for the mass of electron neutrino (actually antineutrino) also sets an upper limit for the mass of the lightest neutrino independent of flavor. Note that the antiparticle of the electron (i.e. the positron) remained undiscovered till 1932.

Gener- ation (flavor)	Lepton		Rest energy ($E_0 = m c^2$), mass (m)			Charge	Found in year
	Symbol	Name	E_0/MeV	m/m_e	m/u	q/e	
1 st	ν_e	electron neutrino	$<0.000\ 002$	$<4 \times 10^{-6}$	$<2 \times 10^{-9}$	0	1956
	e	electron	0.511	1	5.486×10^{-4}	-1	1897
2 nd	ν_μ	muon neutrino	<0.19	<0.37	$<2 \times 10^{-4}$	0	1962
	μ	muon	106	207	0.11343	-1	1937
3 rd	ν_τ	tau neutrino	<18.2	<35.6	<0.02	0	2000
	τ	tau lepton	1777	3477	1.908	-1	1974

Leptons, one of the classes of fundamental particles consisting of six known members only (as well as their antiparticles which makes them 12 altogether), are listed in Table 2. Their name, coming from Greek ($\lambda\epsilon\pi\tau\acute{o}\varsigma = \text{leptós} \approx \text{delicate, slender, thin}$), is obviously associated with the lightness of electron, the best and longest known representative of the group.

Leptons, in spite of their name, are not all really light. The tau lepton of the 3rd generation, e.g., is several thousand times heavier than the electron, the ‘prototype’ of the group. In fact, the τ is almost as heavy as a whole hydrogen molecule, H_2 .

The electron is the only ‘absolutely stable’ member of this group in every sense. It is proven that [its mean life](#) is at least 4.6×10^{26} years, which is about 30 million billion times longer than the age of the Universe.

It was believed until some time ago that special lepton numbers— L_1 , L_2 , and L_3 —assigned to the different generations/flavors/families of them are themselves individually conserved. While this still seems to be true for charged leptons, the neutral ones have been shown to violate this kind of conservation (neutrino oscillation). However, the total lepton number $L = L_1 + L_2 + L_3$ is conserved in any process.

In the case of neutrinos stability is a delicate question, because the representatives of the generations (i.e. different ‘flavors’, ν_e , ν_μ , ν_τ) can change into each other with some probability (*change of flavor*, [neutrino oscillation](#)). On the other hand, neutrino oscillation is considered as a proof that all neutrinos cannot be mass-less particles.

Neutrinos are also special in that they have definite (i.e. *intrinsic*) *helicity/handedness*. Antineutrinos are all ‘right-handed’ (having positive helicity), which means that their spins all point in their direction of propagation. Neutrinos, ‘on the other hand’, are all left-handed (having negative helicity), i.e., their spins show backwards as they move. Helicity also determines the [parity](#) of neutrinos. Therefore parity is also intrinsic property in this case. The [helicity of charged leptons is not an intrinsic property](#), because their handedness depends on the frame of reference.

Table 3: Quarks (q) are the class of elementary fermions ($s = 1/2$) that are affected not only by strong/color force, but also by the rest of the fundamental forces (see Table 5). They are also the [constituents of composite particles](#) that give the ‘bulk’ of the matter in and around us. The nucleons (N), e.g., are built from the two 1st generation quarks u and d. Note that the names of quarks are the symbols themselves according to IUPAP. What most people think are the names of quarks are actually mnemonics for the symbols. The interpretation of the masses is not at all straightforward, e.g., the shown masses of u and d are only tiny fractions of the nucleons they build up.

Gener- ation (flavor)	Quark		Rest energy ($E_0 = m c^2$), mass (m)			Charge	Found in year
	Name & symbol	Mne- monic	E_0/MeV	m/m_e	m/u	q/e	
1 st	u	up	2	4	0.002	+2/3	1970
	d	down	5	10	0.005	-1/3	
2 nd	c	charm	1020	2450	1.3	+2/3	1976
	s	strange	90	190	0.1	-1/3	1964
3 rd	t	top (truth)	175 000	337 000	185	+2/3	1995
	b	bottom (beauty)	4500	8200	4.5	-1/3	1977

[Quarks](#), a group of six also (as well as their antiparticles which makes them 12 altogether), are listed in Table 3. The name itself comes from literature, namely from James Joyce’s cultic book ‘Finnegans Wake’ (<http://www.trentu.ca/faculty/jjoyce/fw-383.htm>), where a rhyme starting with the following lines can be read:

– Three quarks for Muster Mark!
Sure he hasn’t got much of a bark
And sure any he has it’s all beside the mark.

Note that Gell-Mann originally hypothesized only three quarks (u, d, s).

The distinctive feature of quarks is *confinement* meaning that they cannot be separated from each other and can only exist in twos or threes forming hadrons. Strangely enough for a chemist, the electric charge of quarks is 1/3 or 2/3 of e , the elementary charge (which does not appear to be elementary after all).

Table 4: Bosons are particles with integer spin ($s = 0, 1, \dots$). Un-shaded rows show elementary bosons (gauge bosons) which propagate the fundamental forces (Table 5) integrated into the Standard Model (SM). The yellowed row shows [pions](#) (π), which were hypothesized by Yukawa (1935) to mediate what is now called the residual strong force (nuclear force) which binds the nucleons (N) together. Pions are just a sample of the numerous types of mesons composed of one quark and an antiquark.

Force mediated	Boson		Rest energy ($E_0 = m c^2$), mass (m)			Charge	Found in year
	Symbol	Name	E_0/MeV	m/m_e	m/u	q/e	
Electro- magnetic	γ	photon	0	0	0	0	1905
Weak	W ⁻	W bosons	80 400	157 000	86	-1	1983
	W ⁺					+1	
	Z ⁰	Z boson				91 188	
Strong (color)	g	gluon	0	0	0	0	1970
Strong residual (nuclear)	π^\pm	pion	139.6	273.1	0.150	± 1	1947
	π^0		135.0	264.1	0.145	0	1950

Table 5: Characteristics of the [fundamental forces](#) as well as of nuclear force. Weak force, in spite of its name, on short distance is much stronger than gravitational force. Its range, however, is very short, even shorter than that of the nuclear force. Its range is short because it is mediated by very massive particles (see Table 4). Note, e.g., that either ‘weight-class’ of the carriers is heavier than a whole molecule of benzene, C₆H₆, which only weighs ~78 u. The column of the gravitational force is shaded gray to remind of its Janus-faced nature: under terrestrial conditions it has no effect whatsoever on nuclear processes, whereas on much larger scale it becomes a decisive factor in [nucleosynthesis](#). Also, it is not integrated into the SM. The last yellowed column with the properties of nuclear force corresponds to the yellowed row in Table 4. The cells filled with a pattern of slanting lines are not applicable to the given force.

Force: Characteristics	Gravitational	Electroweak		Strong	
		Electro-magnetic	Weak	Fundamental (color)	Residual (nuclear)
Acting on	mass-energy	electric charge	flavor ch.	color charge	residual color
Particles feeling it	all of them	electrically charged	leptons, q	q, g	hadrons
Known carriers		γ	W ⁺ , W ⁻ , Z ⁰	g	mesons
Range of force	∞	∞	~0.001 fm	∞	~1 fm
Dependence on distance <i>d</i>	decreasing ($\propto d^{-2}$)	decreasing ($\propto d^{-2}$)	steeply decreasing	increasing	steeply decreasing
Relative strength					
u–u at 0.001 fm	10 ⁻⁴¹	1	0.8	25	
u–u at 0.01 fm	10 ⁻⁴¹	1	0.0001	60	
p–p at 1 fm	10 ⁻³⁶	1	0.0000001		20

Elementary bosons, five of which are known to exist in all (*gauge bosons*), are *carriers of fundamental forces* (see Table 5). The photon (γ), their most familiar representative to a chemist, is the mediator of the electromagnetic force. They are listed together with some composite bosons (pions) in Table 4.

Hadrons are composite particles built directly from quarks. The name comes [from Greek](#) (ἄδρός = hadrós ≈ thick, bulky). They have two types: *baryons* (from Greek βαρύς = barýs ≈ heavy) and *mesons* (from Greek μέσος = mésos ≈ average, medium).

Mesons, consisting of an even number of fermions (i.e. one quark and one antiquark, $q\bar{q}$) are bosons. (Note that $1/2 \pm 1/2$ is always an integer, namely either 0 or 1.) None of the mesons are stable. Even the charged pions (π^\pm)—hypothesized (as the mediators of the nuclear force between nucleons) by H. Yukawa ([Nobel Prize](#) in physics, 1949) 12 years before their actual discovery by C.F. Powell ([Nobel Prize](#) in physics, 1950) et al.—have a mere 18 ns for half-life. Some of the properties of pions are shown in the last row of Table 4. Their quark composition is as follows: π^+ ($u\bar{d}$), π^- ($\bar{u}d$), π^0 (mixed state from $u\bar{u}$ and $d\bar{d}$). The meson π^0 is its own antiparticle.

Table 6: Baryons, the ‘heavier’ types of hadrons, are fermions. Only four examples are shown of the many that have been discovered: the nucleons ($s = 1/2$), because of their importance to chemists, as well as their antiparticles.

Baryon		Quark content	Rest energy ($E_0 = m c^2$), mass (m)			Charge	Found in year
Symbol	Name		E_0/MeV	m/m_e	m/u	q/e	
p	proton	u u d	938.3	1836.2	1.0073	+1	1919
\bar{p}	anti-proton	$\bar{u} \bar{u} \bar{d}$				-1	1955
n	neutron	u d d	939.6	1838.7	1.0087	0	1932
\bar{n}	anti-neutron	$\bar{u} \bar{d} \bar{d}$				0	1957

Baryons, consisting of an odd number of fermions (i.e. three quarks, qqq), are also fermions themselves. (Note that $1/2 \pm 1/2 \pm 1/2$ cannot be an integer.) The antiparticles of baryons (antibaryons) are built from three antiquarks ($\bar{q} \bar{q} \bar{q}$). Some examples of the huge variety of baryons are shown in Table 6.

Two of the baryons—the proton and the neutron—are known to every chemist as the building units of the atomic nucleus, called therefore together as *nucleons* N. The nucleons and their antiparticles—as their quark contents reveal—are different particles.

The proton is absolutely stable (and so is its antiparticle \bar{p}). More strictly speaking: the [mean life of the proton](#) is certainly no shorter than 2.1×10^{29} a, which is more than ten-billion-billion times longer than the age of the Universe. This figure allows less than two protons to ‘disappear’ annually in 1 m^3 of water including the protons bound in the nucleus of oxygen. The disappearance means that the free proton—being the lightest of the baryons—could only decay by changing from baryon to a lighter particle. However, apart from the photon, only some of the leptons (namely, the electron/positron and the neutrinos) are the only stable particles that are lighter than the proton. Thus the stability of the proton is directly connected with the conservation of the baryon number.

The free neutron, on the other hand, is an unstable particle with a half-life of only just a little longer than 10 min ($T_{1/2} = 614 \text{ s}$). This and the fact that there are a lot of stable nuclei in and around us containing neutrons helps to remember that the whole (e.g. the nucleus) is always more than just a simple collection of its parts (i.e. the $N + Z$ nucleons).

4.3. The Color Charge

The *color charge* of particles is a quantum-state descriptor (kind of a quantum number).

As regards its ‘function’ and ‘algebra’, color charge shows some resemblance to ordinary electric charge:

- Electric charge (the two kinds of which are traditionally called positive and negative) functions as a ‘grip’ for Coulomb force, just as the color charge provides a ‘hold’ for color force.
- The simple algebra of the additive electric charges can result in an electrically neutral state (plus and minus can add up to zero). The color-neutral state—called *colorless* or *white*—can be ‘mixed out’ according to the ‘color algebra’ shown in Figure 12.

As a quantum-state descriptor, color charge plays a similar role as the spin of fermions (which obey the Pauli exclusion principle). Elementary fermions like leptons and quarks can only have two different quantum states as regards their spin. By tradition, the two states are expressed verbally as ‘up’ and ‘down’, but ‘left’ and ‘right’ or ‘plus’ and ‘minus’ would have been just as good choices. In order to classify hadrons that were known by the early 1960s,

Gell-Mann assumed that the heavier types called baryons consist of a combination of three of the quarks whose existence he originally postulated (u, d, s). To make his model nice and symmetric, Gell-Mann was forced to predict the existence of the *omega minus baryon* (Ω^-) that was supposed to be composed of three s quarks (see Table 3). To satisfy the Pauli principle (demanding that the three identical fermions should be in different states), a new quantum-state descriptor was needed for not just two but three different states. This is the *color charge* (introduced by O.W. Greenberg in 1964), and the names of the different states became known as *red*, *green* and *blue*. The color metaphor also provides a useful mnemonic that helps to remember how composite particles are built up. For instance, the *confinement of quarks* can now be phrased that only colorless/white quark combinations can be observed as opposed to color ones (e.g. free quarks). The rest can be ‘figured out’ from Figure 12, showing also the basics of **RGB** color mixing.

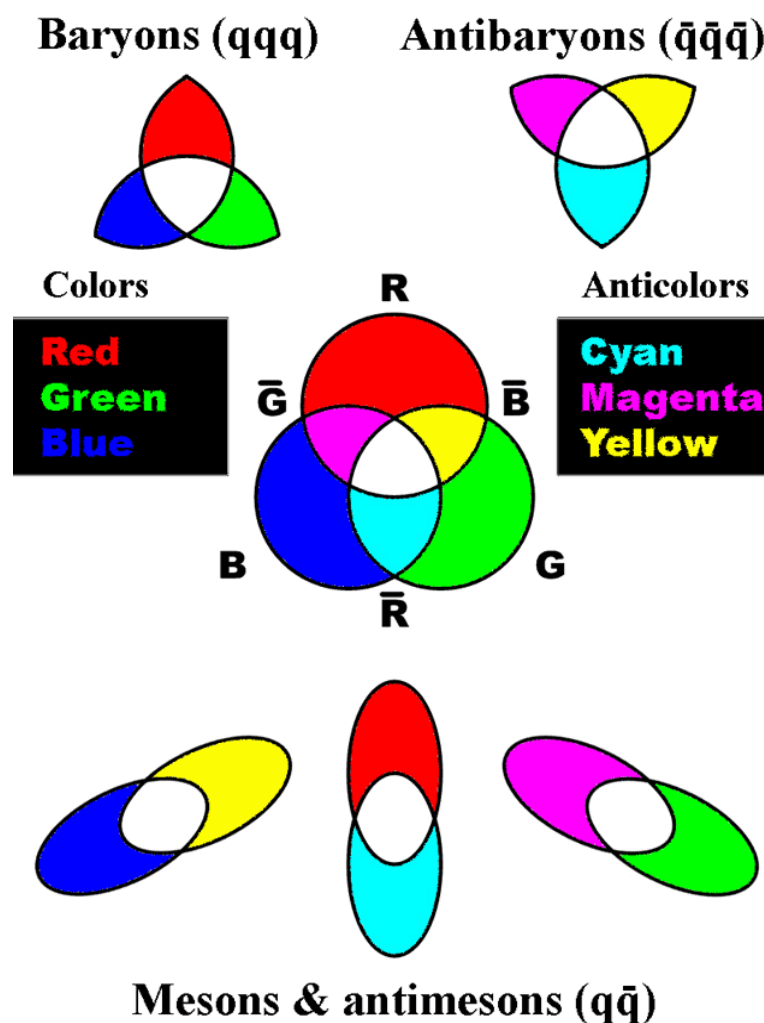


Figure 12: Colors and anticolors—the [color of quarks](#) and antiquarks. Mnemonic aid to the composition of different types of hadrons (baryons and mesons). Anticolors can be imagined as the complementary colors of pure **RGB** colors (**CMY** colors). Thus a colorless/white (i.e. observable) state can be obtained by mixing either all three RGB colors (\rightarrow baryons) or anticolors (\rightarrow antibaryons), or by mixing an RGB color with its CMY anticolor (\rightarrow mesons). Actually the color mixing shown here does not cover the whole ‘color algebra’ of what is known as QCD (quantum chromodynamics), but the metaphor helps to get the ‘picture’.

5. Characterization of the Atomic Nucleus

5.1. Nuclear Radius and Mass Density

For approximate calculations, the nucleus can be pictured as a solid sphere of uniform mass and charge distribution.

Nevertheless, at a closer look, the actual charge density of the nucleus is not quite homogeneous as shown by the shaded diagram in Figure 13. In comparison with a solid-sphere nuclear model (see the stepwise function reflecting a uniform charge distribution), the charge distribution is smeared within a more or less constant range called the *skin of the nucleus*. The nuclear mass distribution is not quite uniform either and, what is more interesting, it also differs from the nuclear charge distribution. Consequently, the distribution of the protons and the neutrons must also be different in the nucleus. However, for our purpose the simple solid-sphere model will do with the comment that due to the constant *skin thickness* ($d_N \approx 1$ fm) heavy nuclei are somewhat more compact than light nuclei.

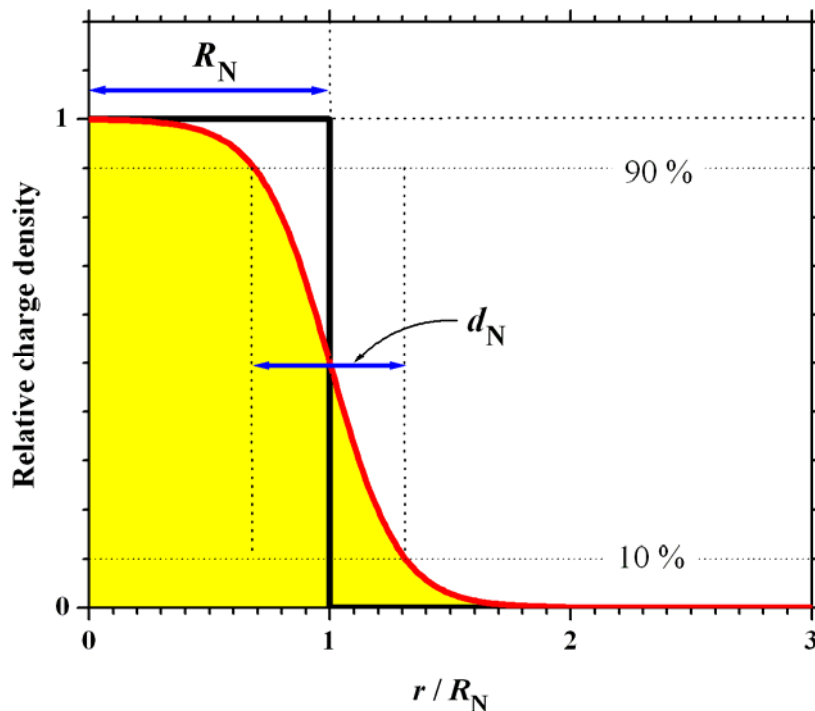


Figure 13: The electric-charge density within a nucleus of radius R_N . The parameter d_N is called the skin thickness of the nucleus.

There is a well researched relationship between the radius R_N of the nucleus and its mass number/nucleon number A :

$$R_N \approx r_0 A^{1/3} \propto A^{1/3}, \quad (41)$$

where the proportionality constant is on the order of $r_0 \approx (1.2 \dots 1.4) \times 10^{-15} \text{ m} \approx 1.3 \text{ fm}$.

The above relationship works surprisingly well except for *halo nuclei* (which are much less compact according to Figure 14). The above formula has been checked with various methods including the scattering of electrically charged particles, i.e. basically in the same way as the famous [\$\alpha\$ -scattering](#) experiments were performed that led Rutherford to discover the nucleus

itself. Note, however, that purely electric methods like electron scattering (which are not sensitive to nuclear force) give characteristically lower r_0 values than experiments performed with nucleon-containing particles (high-energy neutrons, for instance). The straightforward interpretation of the difference is that the skin of the nucleus (see Figure 13) ‘contains’ more neutrons than protons. This conclusion, however, is in contradiction with the naïve expectation that it would be energetically more favorable if the skin were enriched in protons because Coulomb expulsion could be lower. The shell model helps to explain this peculiarity. Neutrons, as the atomic number increases, outnumber protons and therefore occupy higher shell levels (see Figure 20) which extend farther from the center of the nucleus than lower shells. [Halo nuclei](#) (of which [He-6](#) is the simplest) can be regarded as extreme examples of this.

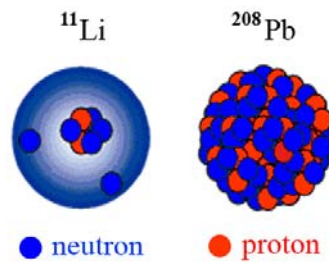


Figure 14: Schematic comparison of the size of the [halo nucleus](#) ^{11}Li to the ‘normal’ nucleus ^{208}Pb . The nucleus of ^{11}Li , being [near the neutron dripline](#) (see also Figure 38), consists of a compact ^9Li core surrounded by a halo consisting of two loosely bound neutrons. Normal nuclei, on the other hand, can be pictured as conglomerates of nucleons/balls in close contact with each other.

If the nucleus is imagined as a sphere (which—for most nuclei—is just as good an approximation as in the case of planets), we must conclude that the *surface area of the nucleus* ($4R_N^2\pi$) is proportional to the square of its radius:

$$S_N \propto R_N^2 \propto A^{2/3}. \quad (42)$$

Finally, the *volume of the nucleus* ($4R_N^3\pi/3$) is proportional to the cube of its radius:

$$V_N \propto R_N^3 \propto A. \quad (43)$$

On the other hand, the *mass of the nucleus* is also proportional to the mass number:

$$m_N \propto A. \quad (44)$$

The last two equations lead us to an interesting conclusion, namely, that the *density of nuclear material* has the characteristic feature of condensed phases such as liquids, i.e. the density is independent of the size:

$$\rho_N = \frac{m_N}{V_N} = \text{constant}. \quad (45)$$

Well, this density is rather high: 1 cm^3 of nuclear matter—the stuff [neutron stars](#)’ bulk is made of—weighs about 20 billion kilograms! (Neutron stars can be thought of as massive but [tiny stars](#) or, alternatively, as huge nuclei stabilized by gravity consisting only of neutrons.)

Thus the nucleus can be imagined as a tiny but dense drop of liquid in which Z protons are dissolved representing a total electric charge of Ze . Note that the volume of the droplet only depends on the number of the ‘molecules’ A , but is independent of its composition expressed

by the ratio of Z and N . This means that the nucleons (protons as well as neutrons) can be pictured as tiny balls of equal size, which are in close contact with each other like the molecules in a liquid, building up together a larger unit called the atomic nucleus. The average volume occupied by one nucleon in the nucleus is just about 6 fm^3 (or, more accurately, $\sim 5.9 \text{ fm}^3/A$).

This simple picture is basically the sketch of what is called the *liquid drop model* of the atomic nucleus. The model has been used with success to explain the process of nuclear fission, when the nucleus splits in two parts of commensurable (but usually unequal) size.

5.2. Nuclear Spin, Electric and Magnetic Properties of Nuclei

[I.I. Rabi](#), winner of the 1944 [Nobel Prize in physics](#), was supposed to say this: ‘*Spin is a very slippery thing.*’ This comment certainly holds for *nuclear spin*, which is not really spin in the strict sense. The term nuclear spin (whose quantum number is usually denoted by I in chemistry) actually means the total angular momentum of the nucleus that includes both the orbital angular momentum and the spin momentum of the nucleons. (In non-spherical nuclei the total angular momentum may also contain a component connected with the collective spinning motion of the core of the nucleus around a certain axis.)

The reason for naming the resultant angular momentum nuclear spin is historical. It is a heritage from the pre-shell-model era (i.e. from before 1949), when the nucleus was still considered an ‘elementary particle’ in a sense, having an ‘intrinsic’ angular momentum whose origin was not quite understood.

As with orbital electrons, the observable orbital angular momentum of nucleons is always an integer in units of \hbar , whereas the spin component is always half integer (because nucleons are fermions just like electrons). Therefore the total angular momentum (quantum number) of the nucleus (I) is an integer if the number of nucleons (A) is an even number and it is a half integer if A is odd. Moreover, for even- Z & even- N types of even- A nuclei $I = 0$ in the ground state. This is explained by the tendency of like nucleons to pair off, which means that protons from the same level tend to form pairs of opposite angular momentum projection (and so do neutrons). As a result, for even-even nuclei, the angular momenta cancel and the nuclear spin I becomes zero.

Nuclear spin values found in the literature or in nuclear databases and tables (e.g. <http://www.nndc.bnl.gov/amdc/nubase/nubtab03.asc>) typically contain values like this: 0^{+9} , $1/2^{+}$, $1/2^{-}$, 1^{+} , 1^{-} , $3/2^{+}$, $3/2^{-}$, etc. The numbers indicate the value of I and the $+/-$ represent the ‘value’ of *parity* (+ for ‘even’ and - for ‘odd’), a rather abstract quantum mechanical quantity that cannot be explained in simple terms. ([Parity](#) is connected with the spatial symmetry of the wave function. *Even/+ parity* means that the function is *symmetrical as regards spatial inversion*, i.e., it does not change if all of the spatial coordinates change sign. Note that one-variable even functions like $f(x) = x^2$ or x^4 possess this property. *Odd/- parity* means that the function is *antisymmetric as regards spatial inversion*, i.e., it changes its sign if all of the spatial coordinates change sign. Note that one-variable odd functions like $f(x) = x$ or x^3 possess this property. See also the respective entries in [Hyperphysics](#), starting with ‘[Parity](#)’) However, it is an important quantity as it is *almost always* conserved in nuclear processes. Its importance is also expressed by the fact that the 1927 interpretation of parity conservation brought E.P Wigner a [Nobel Prize](#) in 1963. The ‘almost always’ part seems to be even more important,

⁹ Note that there is no such thing as 0^{-} .

because the 1956 experimental design leading to the 1957 discovery of the violation of parity conservation in weak interaction resulted in a prompt [Nobel Prize](#) for T.D. Lee and C.L. Yang.

Most well-behaved [nuclei are spheroids](#), i.e. more or less spherical. Apart from *superdeformed nuclei* and those of exotic shape (which occur in all kinds of form resembling cucumbers, pears or even bananas, undergoing all kinds of [vibrations](#)), the deviation from spherical shape of nuclei does not exceed much that of the planets (see Figure 16). They are in general rotational ellipsoids—either slightly *prolate* (elongated like an American football) or *oblate* (like M&M’s chocolate candies or glass pebbles) or completely *spherical* (like a ping-pong ball) as shown in Figure 15.

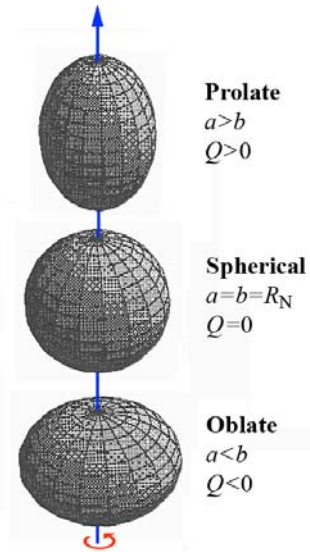


Figure 15: Classification of simple nuclei by shape. The notation is explained in the text following Eq. (46). Most nuclei fall into these three categories, even the actual distortion is less than indicated. If the nuclear spin is $I = 0$ or $1/2$, the nucleus has $Q = 0$ for quadrupole moment. Superdeformed nuclei ($a:b \approx 2:1$) may rotate around an axis that encloses an angle with the symmetry axis indicated by the blue arrow. (Note that the curved red arrow is only to remind of the rotational symmetry of the ellipsoids and not of actual rotation.)

Since all ellipsoids are centrally symmetrical, such nuclei do not have a *static electric dipole moment*. However, they may possess an *electric quadrupole moment* which can interact with the *electric field gradient* (EFG) caused by asymmetric distribution of orbital electrons and ligands around the nucleus, thus causing hyperfine splitting in the nuclear levels depending on the orientation of the nucleus relative to the principal axis of EFG.

The electric quadrupole moment of a nucleus having the shape of a rotational ellipsoid (see Figure 15) is given by the following formula:

$$Q = \frac{2Z}{5} (a^2 - b^2) \approx \frac{4ZR_N}{5} (a - b) \approx \frac{4ZR_N^2}{5} \varepsilon, \quad (46)$$

where a and b are the polar and equatorial radii; $R_N \approx (a + b)/2$ is the average radius of the nucleus given by Eq. (41); $\varepsilon = (a - b)/a \approx (a - b)/R_N$ is the *ellipticity*, a parameter used e.g. for the characterization of the elliptic distortion of planets; and Z is the atomic number (i.e. the charge number) of the nucleus.

As the formula reveals, the quadrupole splitting makes a convenient measure of the deviation from spherical shape: for prolate nuclei ($a > b$) we have $Q > 0$, for oblate nuclei ($a < b$) $Q < 0$,

and for spherical nuclei ($a = b = R_N$) $Q = 0$. Note that nuclei with $I = 0$ or $1/2$ have no quadrupole moment. As mentioned before, nuclei with $I = 0$ also have even (+) parity.

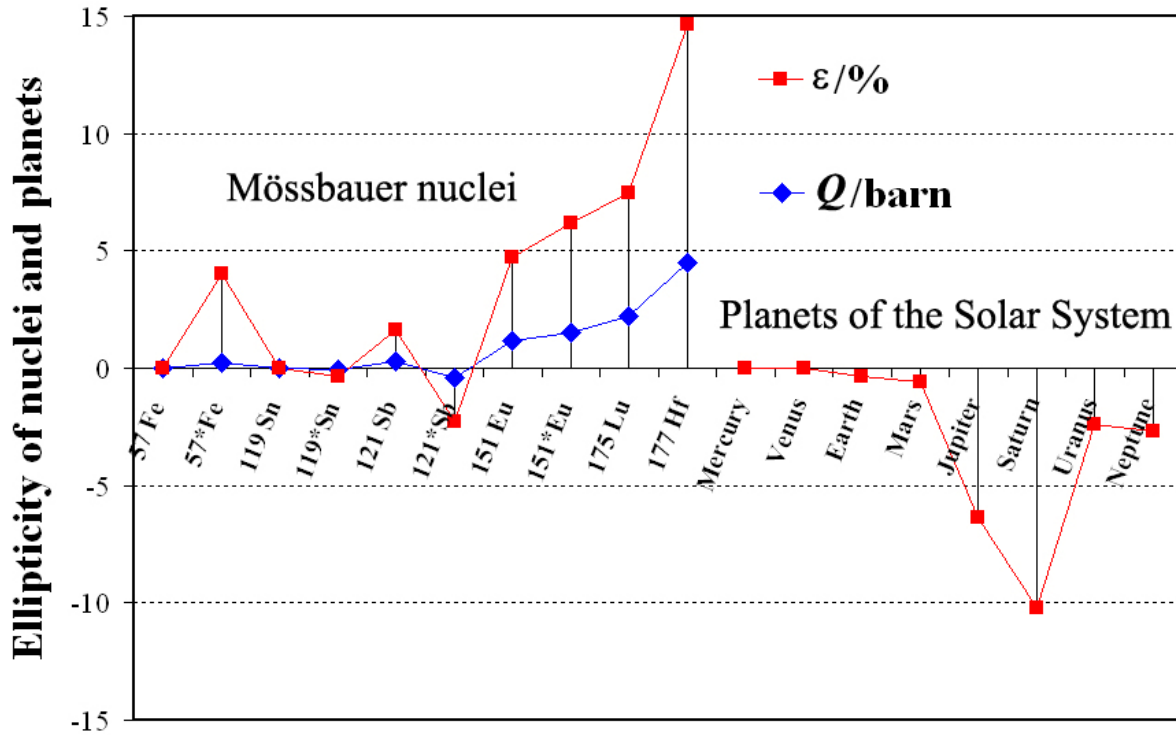


Figure 16: Comparison of the ellipticity ϵ (■) of some Mössbauer nuclei with that of planets. Note that the magnitude of the distortion of nuclei is about the same as that of the planets; however the latter are either spherical or oblate, whereas most nuclei in the given set of examples are prolate. For the nuclei the quadrupole moment Q (◆) is also presented. Note that for a given value of Q , the actual geometrical deformation expressed by ϵ is much larger for light nuclei than for heavy ones. The reason can be easily figured out from Eq. (46).

Nuclei, supposing that they actually had a uniform mass and charge density within their volume and 0 outside (see the stepwise function in Figure 13), would exert an electric potential shown in Figure 17 which repels positive particles like positrons (or protons). For nucleons the nuclear potential also contains an attractive component which is not felt by leptons.

Positrons (top panel in Figure 17), being leptons and therefore blind to nuclear force (see Table 5), only experience the electric repulsion of the nuclear charge. (Electrons would experience the same strength of attraction.) If the initial energy of a positron projectile were lower than indicated by the dotted horizontal line, its kinetic energy E_k would drop to zero before it could reach the nucleus. Note that the potential curve follows that of the point-charge potential (dotted curve) down to the surface of the nucleus and then it increases much less steeply. The potential reaches its maximum (\sim a few MeV) in the very center of the nucleus at a value which is only 50% higher than the potential at the surface of the nucleus. Note that if the nucleus were smaller (with Z remaining the same), the Coulomb potential of the nucleus would shift higher up along the point-charge curve, which gives a key to how nuclear radii can be determined by [charged-particle scattering experiments](#).

Neutrons (middle panel in Figure 17), being neutral, are blind to Coulomb force (electric force). However, since they are hadrons, from close enough they feel the attraction of the

residual strong force (nuclear force) exerted by the nucleus as shown here by a *Woods–Saxon potential* (or, more accurately, by its real component). Note that neutrons feel no barrier whatsoever, so they can reach the nucleus with energies approaching to zero (e.g. thermal energies in the order of a few tens of meV or lower).

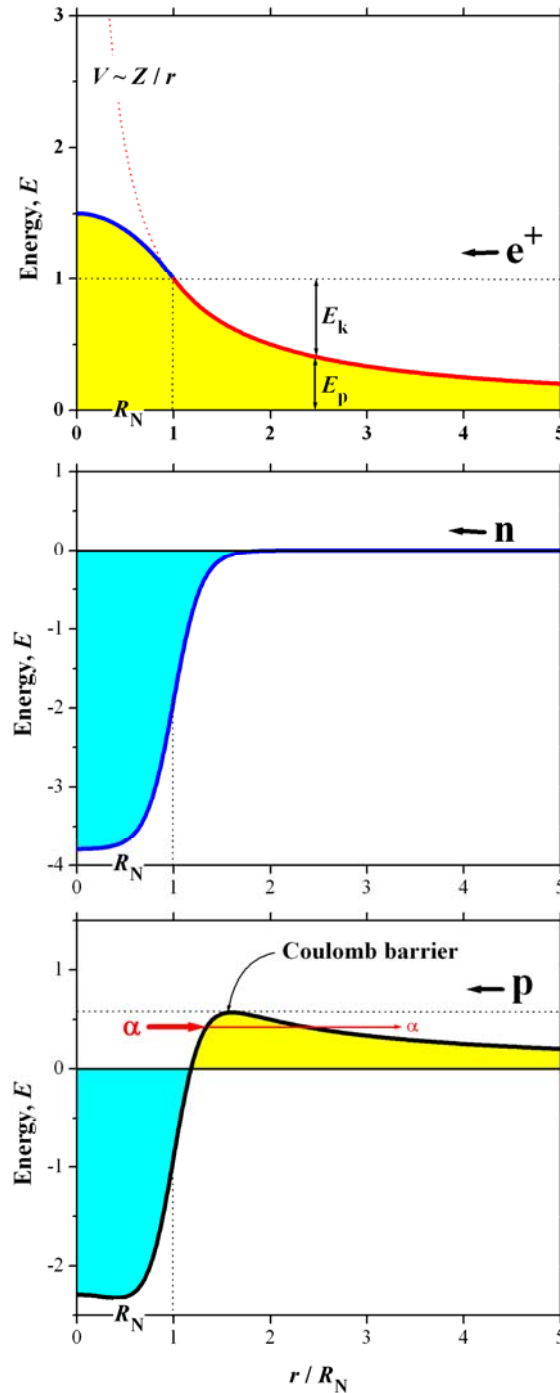


Figure 17: Schematic potential curves for different subatomic particles in the field of the nucleus. The vertical axis is in arbitrary unit: E_k is kinetic energy, E_p is potential energy. R_N is the nuclear radius and r is the distance from the center of the nucleus chosen as the origin. See the text for further explanation. Here (focusing on nuclear reactions and α -decay) only the lower panels are explained showing the schematic ‘view’ of the nucleus ‘seen through the eyes’ of a neutron and a proton. The neutron, being a neutral particle, can approach the nucleus with as little energy as it wants. Even thermal neutrons have no problem with getting in close contact with the nucleus. The proton, on the

other hand, being a positive particle, has to conquer the Coulomb barrier surrounding the nucleus which can take an initial kinetic energy in the order of a few MeV. On the potential energy curve $E > 0$ (yellow fill) means repulsion for the approaching particle. At infinity the potential energy is zero for both types of nucleons, which means neither attraction, nor repulsion.

Protons (bottom panel in Figure 17), being sensitive to both forces, experience the superposition (sum) of both potential curves. This creates the *Coulomb barrier* that works both ways for charged nuclear particles.

Alpha decay, for instance, is only possible due to quantum mechanical *tunneling*, which means that a particle of lower than enough kinetic energy still can penetrate through a not very ‘thick’ potential wall with finite probability.

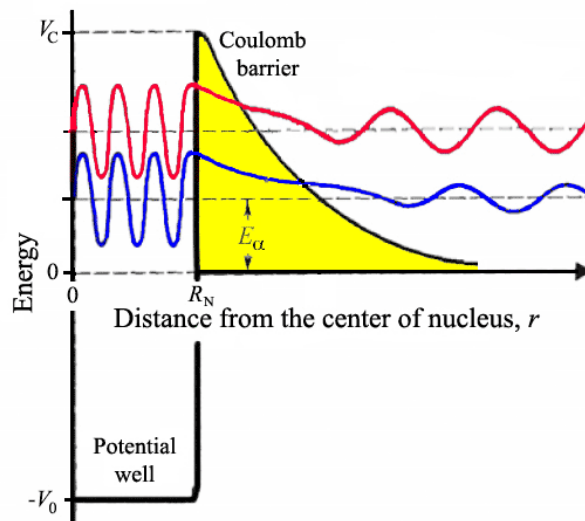


Figure 18: An alpha particle (blue wave) tunneling through the Coulomb barrier of a nucleus. Note that if the kinetic energy of the particle were higher, its wave function (red wave) would be less damped by the barrier. Remember also that the probability density of the particle is proportional to the square of the wave amplitude and therefore a little drop/increase in amplitude means a lot of change in probability and therefore in decay constant as well (see also the bottom panel in Figure 17).

The probability of potential-wall penetration sensitively depends on the wall thickness, which explains why higher-energy branches of α decay are much stronger than lower-energy ones. This is obviously due to the fact that the Coulomb barrier becomes thinner as the α energy gets higher (see Figure 18). It also explains the strong energy dependence of α -decay constants as expressed by the *Geiger–Nuttall rule*¹⁰:

$$\log\{\lambda\} = a \log\{E_\alpha\} + b, \quad (47)$$

where $a > 0$ and $b > 0$ are constants for different classes of α emitters, and $\{\lambda\}$ is the numerical value of the (partial) decay constant λ of the decay (branch) producing α particles of (kinetic) energy E_α .

Comment. Note that the logarithm only makes sense if its argument is a pure number. Therefore I have followed above the [IUPAP symbolism](#) for expressing a **physical**

¹⁰ In its original form the rule expressed a linear relationship between the logarithms of λ and R , the range of α radiation. However, the latter was found to be approximately proportional to the 1.5th power of α energy, and therefore the law is nowadays cited in the form given in Eq. (47). Also, $\log\{\lambda\}$ vs. $\log\{E\}$ (or $\log\{T_{1/2}\}$ vs. $\log\{E\}$) types of plots are referred to as Geiger–Nuttall plots.

quantity X as the product of a **numerical value** $\{X\}$ and a **unit** $[X]$ in which X is given:

$$X = \{X\} \times [X]. \quad (48)$$

The linearity of $\log \{\lambda\}$ vs. $\log \{E\}$ plots implies linearity of the $\log \{\tau\}$ ($= -\log \{\lambda\}$) vs. $\log \{E\}$ plots and $\log \{T_{1/2}\}$ vs. $\log \{Q_\alpha\}$ plots as well, only the slopes are of the opposite sign ($a < 0$). The latter is well demonstrated by Figure 19 showing an incredibly strong energy dependence of α half-lives in the four major decay series.

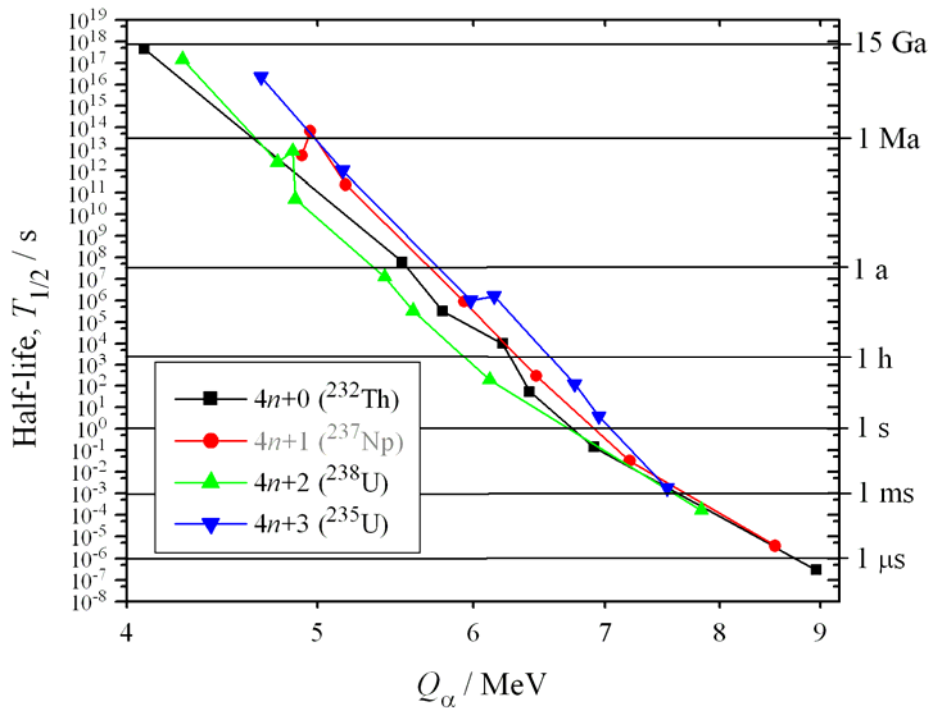


Figure 19: Modern Geiger–Nuttall plot for the α -decaying nuclides of the four major decay chains including the three naturally occurring ones (starting from ^{232}Th , ^{238}U , and ^{235}U) once studied by the eponyms of this type of log–log presentation. The label of the fourth series (starting from ^{237}Np) is in gray color to indicate that this series has been wiped out from Earth due to its relatively short half-life. Note that the α half-lives sweep the range from less than a microsecond (see the labels along the right vertical axis) to 15 billion years (the estimated age of our Universe), which means a scale of ~ 24 decimal or ~ 80 binary orders of magnitude. The Q -values ($\sim E_\alpha$), on the other hand, only drop from 9 MeV to about 4 MeV, a range just about a little wider than 1 binary order of magnitude (i.e. a range covered by a factor of 2).

Returning back to Figure 18, it should be noted that for the α particle (He^{2+}) the Coulomb barrier would be actually about twice higher than for the proton (H^+) due to its larger charge. (From this fact one might erroneously conclude that proton decay is much more common than α decay, which is far from the truth.) Note also that for a proton (baryon) the nucleus ‘looks’ larger than for the positron (lepton).

According to classic electrodynamics, an orbiting particle having electric charge will also have a *magnetic (dipole) moment* (the same physical property that makes the needle of a compass a useful object) the magnitude of which is proportional to the charge and the angular momentum of the particle. The direction (sign) of this magnetic moment (corresponding to the direction of the ‘red end’ of the needle) is either parallel or antiparallel to the orbiting axis, depending on whether the orbiting charge is positive (e.g. proton) or negative (e.g. electron).

Neutral bodies (e.g. neutrons) are not supposed to have a magnetic moment due to orbiting.

G.E. Uhlenbeck and S.A. Goudsmit who introduced the spin as a quantum-state descriptor in 1926 proposed a similar proportionality between the intrinsic magnetic moment of the electron and its spin (an intrinsic angular momentum that can be thought of as one originating from spinning motion). To make their theory fit the experimental facts, they were forced to postulate that the magnetic moment arising from a given magnitude of angular momentum is twice larger for spinning than for orbiting.

With this well-proven theory in the background, Table 7 compares the expected and actually measured *intrinsic magnetic moments* μ_e , μ_p , and μ_n of the electron, proton, and neutron using appropriate units, i.e. the *Bohr magneton* (μ_B) for the electron and the *nuclear magneton* (μ_N) for the nucleons:

$$\mu_B = \frac{e\hbar}{2c m_e} ; \quad \mu_N = \frac{e\hbar}{2c m_p} . \quad (49)$$

Table 7: Comparison of intrinsic magnetic moments of some subatomic particles. The experimental data have been taken from ‘Particle Listings 2006’ at the site of the Particle Data Group (<http://pdg.lbl.gov>).

Subatomic particle	Electron	Proton	Neutron
Magnetic moment unit	Bohr magneton, μ_B	nuclear magneton, μ_N	
<i>Expected</i> intrinsic magnetic moment	-1	1	0
<i>Measured</i> intrinsic magnetic moment	-1.0011659208	2.792847351	-1.9130427

Looking at Table 7 we come to the following conclusions:

- The electron, a really elementary particle, behaves almost as expected. The difference is only $\sim 0.1\%$.
- The neutron, surprisingly enough, behaves as if it were a **negative** particle having almost twice as high a charge than the electron.
- The proton’s magnetic moment is about that much higher than expected ($1.8 = 2.8 - 1$) as the neutron’s is lower ($-1.9 = -1.9 - 0$).

This curious magnetic behavior of the nucleons was observed much earlier (p: 1933, n: 1939) than the quark hypothesis was set up, puzzling physicists. The quark hypothesis helped the pieces of the puzzle to snap into position. The proton is supposed to be built up from two positive and one negative quarks (uud), and the neutron from one positive and two negative ones (udd). The three point-like quarks are bound to each other by color force which confines their unceasing motion to a volume of space that we experience as the size of the nucleon they form. Of course, the charge distribution produced by the three moving quarks is not necessarily averaged out to a uniform distribution which would make the neutron’s charge zero everywhere. Apparently, the [internal structure of the neutron](#) (produced by the moving quarks) is such that it behaves as if a negatively charged particle were spinning, although the net charge (as observed from a larger distance) is zero.

Before closing this section, I call the reader’s attention to an important practical consequence of Eq. (49):

$$\frac{\mu_B}{\mu_N} = \frac{m_p}{m_e} \approx 1836. \quad (50)$$

When it comes to explaining the macroscopic magnetic properties of materials such as *diamagnetism*, *paramagnetism* or *ferromagnetism*, only the electrons are considered and the question always is whether or not their spins are canceled by pairing or not. Although the same question could be asked in the case of the nucleons as well, the answer would make no difference at all except for the most sophisticated applications such as *nuclear magnetic resonance (NMR)* spectroscopy. Nucleon/nuclear spins do not affect the macroscopic magnetic properties, because—all things considered, including both Table 7 and Eq. (50)—the ‘conversion factor’ that converts their spin moments to magnetic moments is only ~0.1% of that of the electron.

5.3. The One-Nucleon Shell Model of the Nucleus

The *nuclear magic numbers* (2, 8, 20, 28, 50, 82, and 126) marked as horizontal and vertical bands in Figure 6 might remind a chemist of the ‘Mendeleev-type’ magic numbers 2, 10, 18, 36, 54, and 86, which are, of course, the electron numbers characterizing the closed-shell configurations of noble gases.

Magic nuclei having a magic number either for Z or N , especially *doubly magic nuclei* for which both Z and N are magic numbers (see the upper panel in Figure 24), show a couple of distinguishing features including exceptional stability. They also serve as ‘centers of attraction’ for nuclides whose N or Z is just one unit above or below a magic number. Such ‘off-magic’ nuclides usually decay to magic nuclides very quickly. Note that this behavior is similar to that of alkali metals and halogens which also strive for reaching the ‘magic’ shell structure of the neighboring noble gas by forming positive or negative ions, respectively.

It is a sensible conclusion that there must be some kind of a quantum mechanical model for the nucleus that explains such behaviors. This idea first occurred to J.H.D. Jensen and M.G. Mayer when they established the *shell model* of the atomic nucleus in 1949, which brought them a [Nobel Prize](#) in 1963. The fact that the magic numbers work for protons and neutrons separately is also reflected by the model, namely, protons and neutrons occupy their own separate level systems (see Figure 20). The other fact, namely that the magic numbers are the same for protons and neutrons¹¹, is an indication of their similarity in some important respect.

¹¹ The only exception is $Z = 114$ where a closed proton shell is expected by those hunting for super heavy elements. (By the way, using the term SHE for superheavies reflects a rather male chauvinist attitude inappropriate for a scientist. Remember that formerly, unpleasant things like hurricanes used to be labeled by female names, too, which was a shame. See also: [P. Howard: The Blonde Hurricane :-\)](#)

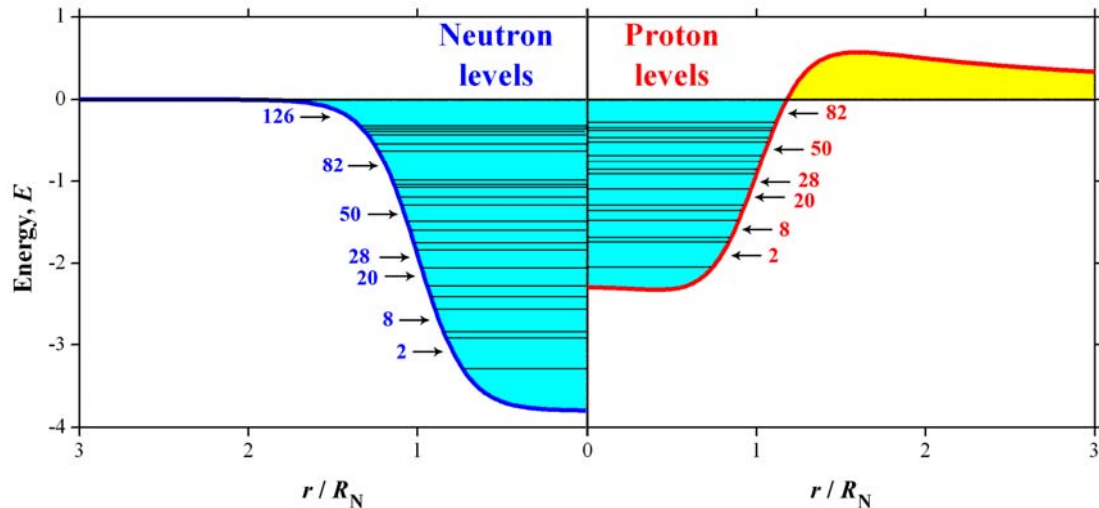


Figure 20: Schematic representation of how the shell model explains the unequal number of neutrons (N) and protons (Z) for heavy elements like lead. Due to the increase of Coulomb potential, the levels of protons are gradually shifted upwards relative to those of the neutrons as the atomic number increases. The numbers marking the wider gaps between the levels are nuclear magic numbers each representing the number of neutrons/protons occupying the levels below the respective arrow. The nuclide ^{208}Pb ($_{82}\text{Pb}_{126}$) happens to be doubly magic.

This successful nuclear model is analogous in many ways to the quantum mechanical model of the atoms/orbital electrons. It involves orbital and spin momenta, energy levels, Pauli exclusion principle and all. The electrons in the atomic model and the protons in the nuclear model correspond to each other. So do electrons and neutrons, too, but not electrons and nucleons in general. (In other words, protons are arranged in proton shells, neutrons are arranged in neutron shells separately, and there is no such thing as ‘nucleon shell’ for protons and neutrons together.) The field holding the respective particles together is the central Coulomb field of the positively charged nucleus in the first case and the attractive nuclear force acting between the core of the nucleus and the nucleon (irrespective of type) in the second.

Being aware of the analogy between the nuclear shell model and the quantum mechanical model of the atom, it might come as a surprise to chemists that there is a *tendency for like nucleons to pair off*. This preference can be concluded from facts like those reflected by Figures 21 and 22, for instance. (See for further evidences on pairing in the next paragraphs discussing Figure 23.) The source of the surprise is *Hund’s rule*, the qualitative message of which is that orbital electrons avoid pairing whenever possible. The difference is caused by the following facts:

- The nuclear force (residual strong force) has a very short range on the order of 1 fm, while the repulsive Coulomb force acting between two electrons or two protons has an infinite range, i.e., charged particles ‘feel’ the other’s presence from a large distance, although the strength of the force (repulsion in the given case) quickly decreases with the distance ($\propto d^{-2}$).
- Within its range the attractive nuclear force is about 20 times stronger between two protons than the repulsive Coulomb force (see Table 5). Electrons, being leptons, are not attracted to each other by nuclear force at any distance. They only experience a steep increase of the Coulomb repulsion as they approach each other.
- Unpaired electrons and unpaired protons/neutrons tend to be farther away from each

other on average than paired ones which share the same orbital.

Therefore even the protons are better off if they form pairs because they can get closer, where nuclear force can overcompensate the Coulomb force, which has a long (actually infinite) range.

The pairs of like nucleons are formed in such a way that their angular momenta cancel. Therefore the resultant angular momentum of the nucleus (i.e. the nuclear spin I) will always be determined by the unpaired proton (at most 1) and/or the unpaired neutron (at most 1). Therefore the nuclear spin for even- Z & even- N combinations is always zero.

The pairing of nucleons can be pictured depending on what type of coupling is assumed between the angular momenta of the individual nucleons or the vector components of these. Coupling also determines the magic numbers that can be predicted using the related nuclear model. Since spin-orbit coupling (j - j coupling) can give an explanation for the magic numbers of heavy nuclei as well, we will only discuss this briefly.

With spin-orbit coupling it is assumed that the nucleon level belonging to the orbital angular quantum number l splits to two sublevels depending on whether the spin is parallel ($j = l + 1/2$) or antiparallel ($j = l - 1/2$) to the orbital momentum. The energy difference between the two j sublevels is determined the quantum number l —the larger the angular momentum, the larger the energy difference ΔE :

$$|\Delta E| \propto (2l + 1). \quad (51)$$

According to experience, the above proportionality is such that the combination ($j = l + 1/2$) has the lower energy. Of course ($j = l \pm 1/2$) can only be a half integer, since l is an integer. The multiplicity/degeneracy of these sublevels is $(2j + 1)$, which is always an even number, because twice of the half integer j can only be an odd number. The quantum numbers that determine the projections of the angular momentum \mathbf{j} are: $j, j-1, \dots, -j+1, -j$. Since the spin is already included in the value of j -be, each projection can only characterize one single nucleon (rather than two). In this special case pairing means that the nucleon with projection $+|m|$ yields a resultant angular momentum 0 with the nucleon of projection $-|m|$. Since the multiplicity of each sublevel is even, all nucleons on any particular level can pair off provided that their number is even.

In the case of spin-orbit coupling the individual levels (or rather sublevels) are denoted according to the following scheme:

$$\nu L_j, \quad (52)$$

where $\nu = 1, 2, 3, \dots$ is the radial quantum number¹²; and the letter symbol L identifies the concrete value of the orbital angular momentum quantum number ($l = 0, 1, 2, 3, \dots$) in the same way as with atomic orbitals (i.e.: s, p, d, f, ...). Therefore the notations for the 1d sublevels are $1d_{3/2}$ ($j = 2 - 1/2 = 3/2$) and $1d_{5/2}$ ($j = 2 + 1/2 = 5/2$). It follows from the above that the latter level is the lower and therefore it is supposed to fill up before the former one.

¹² For the principal quantum number n we have $n = \nu + l$. Thus the radial quantum number is not an upper boundary for l and therefore the symbol $1p_{1/2}$ makes sense in this context.

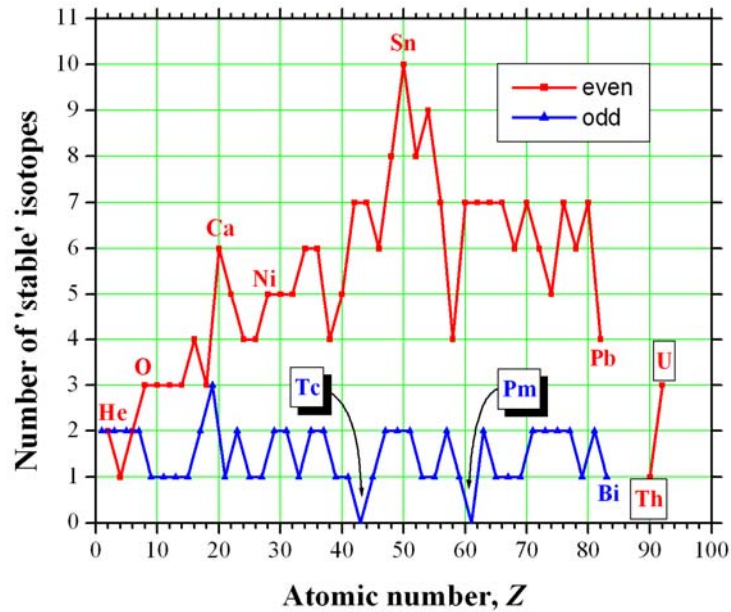


Figure 21: Comparison of the number of stable/primordial isotopes of different elements. As a rule, even- Z elements (red graph) have significantly more such isotopes than odd- Z ones (blue graph). The symbols of magic- Z elements— ${}_{2}\text{He}$, ${}_{8}\text{O}$, ${}_{20}\text{Ca}$, ${}_{28}\text{Ni}$, ${}_{50}\text{Sn}$, and ${}_{82}\text{Pb}$ —are also displayed. One of them—tin—has as many as ten stable isotopes. The heaviest stable even- Z element is lead, whose most abundant stable isotopes— ${}^{208}\text{Pb}$ (a doubly magic nuclide), ${}^{207}\text{Pb}$, and ${}^{206}\text{Pb}$ —are the last members of the three naturally occurring decay series starting from the primordial nuclides ${}^{232}\text{Th}$, ${}^{235}\text{U}$, and ${}^{238}\text{U}$, respectively. (The frames around the symbols U and Th are to remind that uranium and thorium—both belonging to the even- Z group—have no stable isotope at all.) The heaviest stable odd- Z element bismuth is represented by a single magic- N isotope ${}^{209}\text{Bi}$, the last member of the now extinct fourth major decay chain starting from ${}^{237}\text{Np}$ (see Figure 51). Two of the medium-weight odd- Z elements—technetium Tc and promethium Pm —have only relatively short-lived isotopes and therefore had disappeared from the Earth a long time ago.

6. Topology of the Valley/Continent of Stability

6.1. Systematics of Stable Elements and Nuclides

It is no surprise for a chemist that using spectroscopic methods for studying the light that reaches us from outer space can help determine the cosmic abundances of the various elements. The method is not new either.

It was in 1868, when the French astronomer P.-J.-C. Janssen (1824-1907)—having made use of a total solar eclipse—performed the first spectroscopic study of the [Sun's chromosphere](#), which led to the discovery of [helium](#). The name of the element was coined from the Greek word 'hélios' (ἥλιος: meaning sun). It is indeed a proper verbal memorial to an achievement that preceded by almost three decades W. Ramsay's 1895 discovery of the helium on Earth.

The chronological order of the discoveries is completely logical. Helium is very rare on Earth, because due to the low atomic mass of ${}^4\text{He}$, atmospheric helium atoms doing thermal motion will sooner or later gain the 11.2 km/s *escape velocity* and leave the gravitational trap of Earth for good. On the other hand, having been produced in great quantities shortly after the Big Bang, helium is the second most abundant element in the Universe according to Figure 22. Helium is also abundant in the Sun because it cannot conquer the Sun's huge gravitation—neither can [hydrogen](#) which is still lighter than helium. Also, He is continuously produced there as a [net result of 'hydrogen burning'](#), a series of fusion reactions energizing the Sun and thus supporting most forms of life on Earth via visible light, the fuel of photosynthesis. (As a notable exception I should mention that in 2006 a research group [reported](#) discovery of bacteria 2.8 km underground at Mponeng Gold Mine, South Africa. These bacteria are related to [Desulfotomaculum](#) and derive energy from the radioactivity of rocks rather than from sunlight. The life of these sulfate reducers depends on the hydrogen produced by the radiolysis of water.) In other words, these bacteria are still energized by the ancient supernova the debris of which had been collected by the young Solar System some 4.5 billion years ago. In that they are similar to the nuclear reactors working today or even more so to the so-called atomic batteries or [RTGs](#) (radioisotopic thermoelectric generators) which supply satellites with electric energy directly produced from the heat released by the radioactive decay of a suitable fuel (e.g. ${}^{238}\text{Pu}$).

By studying Figure 22 we can arrive to the obvious conclusion that for some reason the atoms of even- Z elements outnumber those of the odd- Z elements. In nuclear terms this means that for at least one type of nucleons (the proton), it is more favorable to form pairs (in other words: to pair off) than to be left alone. (The data¹³ for the plots in h Figure 22 have been taken from the page http://www.kayelaby.npl.co.uk/chemistry/3_1/3_1_3.html.)

¹³ Note that there are different sets of abundance data on the web which are different in details. However, the general trends are the same supporting the conclusions drawn from the above figure.

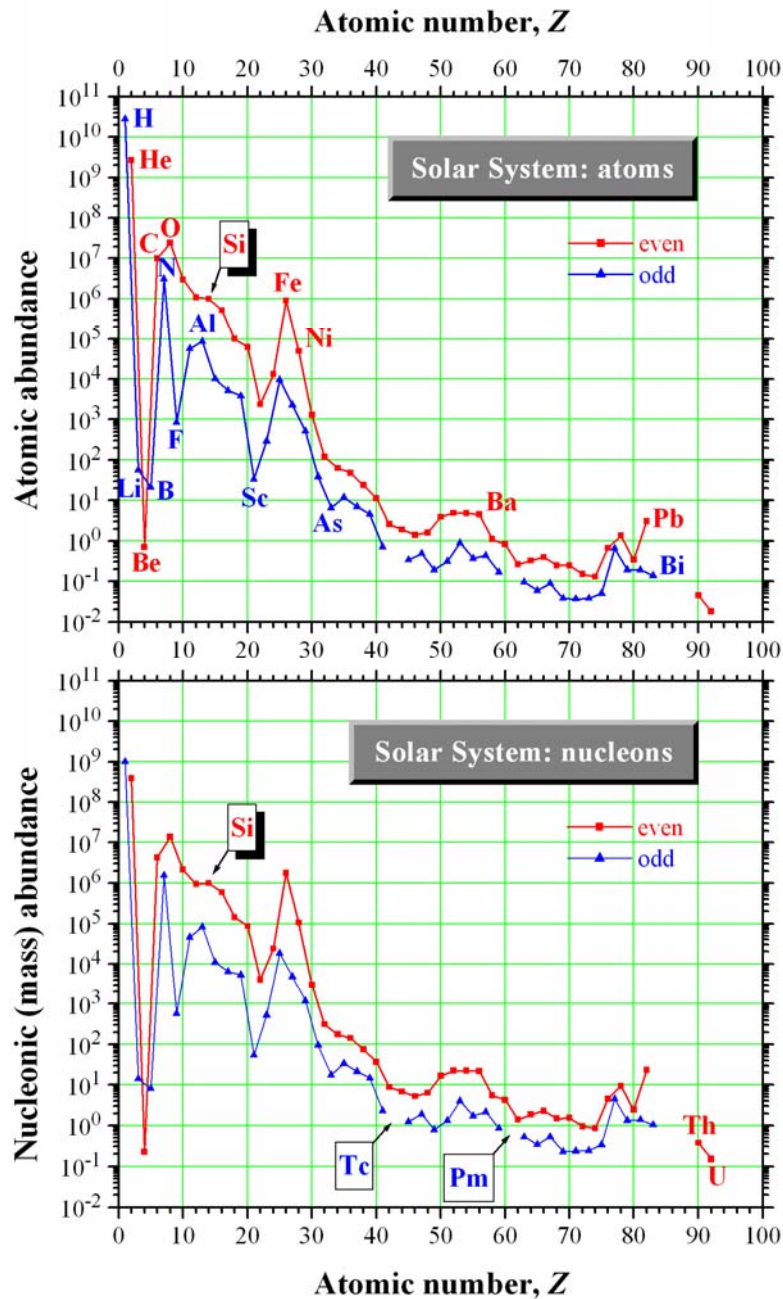


Figure 22: Atomic and nucleonic/mass abundances of elements in the Solar System (SS). (For isobar abundances in the SS see Figure 76.) The label **Si** is to indicate the omnipresent [silicon](#) as a reference meaning that the ‘homogeneous samples’ considered contain among others either 10^6 Si atoms (upper panel) or 10^6 nucleons bound in $10^6/28$ ^{28}Si nuclei (lower panel). The solar abundances are very similar, except that lithium (**Li**) is about 150 times less common in the Sun because it has been destroyed there by thermonuclear reactions. The upper panel shows hydrogen atoms to be by far the most abundant in the SS. The lower panel proves an even more shocking predominance of hydrogen, namely, that the vast majority of nucleons exist as free protons, the nuclei of ^1H . Note that even- Z elements are often ~ 10 times more abundant than their odd- Z neighbors. This is a special manifestation of the tendency of like nucleons (in this case: protons) to pair off. (See for further evidence in Figure 23.) The heaviest stable element, [bismuth](#) (Bi), is an odd- Z element, but its only stable isotope has a magic neutron number ($_{83}\text{Bi}_{126}$). **Th** and **U** are unstable but long-lived, called primordial. The ‘missing links’ **Tc** and **Pm** are also odd- Z elements. Note also the remarkably high relative abundance of [iron](#) (Fe), around which the binding energy per nucleon reaches its maximum for nuclei.

Figure 23 shows basically the same stable/primordial nuclides that form the dark reptile-skin

pattern zigzagging along the chart of nuclides in Figure 6.

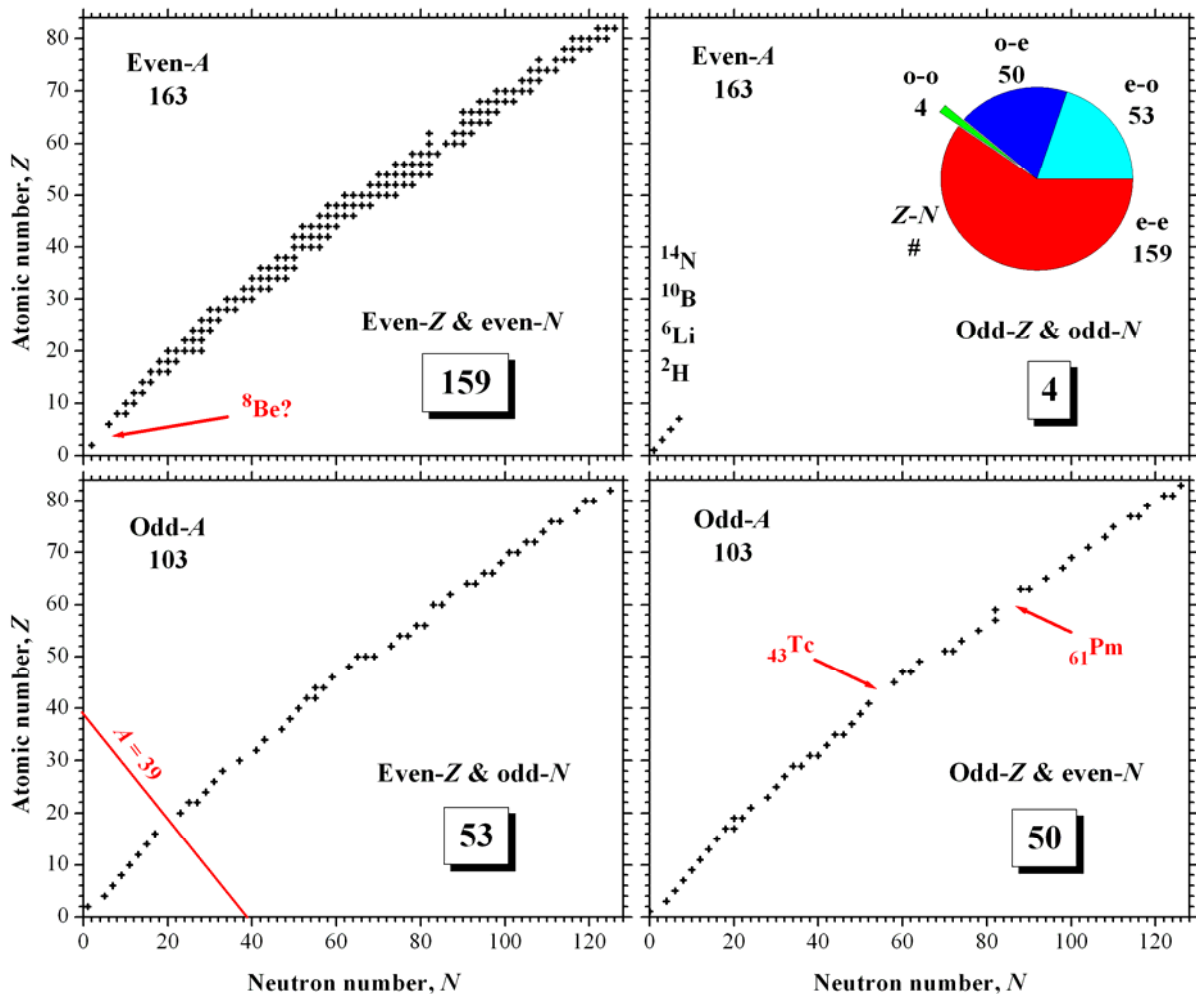


Figure 23. Classification of the 266 most stable nuclides out of which 228 are known as absolutely stable and 38 practically stable undergoing only 2β decay, a very slow process, with typical half-lives millions of times longer than the age of the Universe. The numbers in the panels—163 and 103 as well as 159, 4, 53, and 50—indicate the numbers of ‘stable’ nuclides in the respective classes and subclasses as specified. The pie diagram compares the ‘sizes’ of the four disjoint subclasses shown in the Z - N plots. The comparison reveals a clear tendency for like nucleons to pair off. Odd-odd combinations are extremely scarce: only four stable nuclides exist, all of which are light. (Note that ${}^{14}\text{N}$, the most common component of air and an essential ingredient of DNA and all proteins, is one of those four, which is a very fortunate fact as regards terrestrial life.) On the other hand, even-even nuclides abound. Even-odd and odd-even combinations are in between and about equal in number.

The nuclides in Figure 23 are divided in two main classes. The upper panels show nuclides having an even number for mass number A . The lower panels show only odd- A nuclides. The main classes are again divided in two disjoint subclasses each. The upper panels represent the alternative possibilities for A to become an even number. Since $A = Z + N$, either both Z and N should be even or both should be odd. The lower panels represent the alternative possibilities for A to be an odd number: either Z is even and N is odd or the other way around.

Common sense tells us that, if the odds were even (so to say), the two classes and the four sub-classes should contain about the same number of nuclides. Well, there are 163 even- A and 103 odd- A nuclides. It is hard to judge whether or not this is a significant asymmetry in favor of the even- A side (see the pie diagram in the lower panel of Figure 26). The distribution of

the nuclides over the four sub-classes, however, speaks for itself. The odd-odd combination seems to be a serious disadvantage and the even-even combination looks like a great advantage. The even-odd and odd-even combinations are somewhere in between and as far as the numbers can tell us neither of the two seems to be any better than the other. One can even risk concluding that it is indifferent as regards the stability of the nucleus which type of the nucleons is odd in number. This also implies that—in spite of the difference in electric charge—protons and neutrons are in a sense very much alike¹⁴.

One can translate the above observation to a **game of cards** with very simple rules:

- There are two decks of cards (deck p and deck n).
- The cards of each deck are numbered (Z and N , respectively).
- Draw one card from each deck (you get a concrete combination of Z & N).
- Add up the numbers on the two cards just drawn ($A = Z + N$).
- If the sum is an odd number (odd A), you will neither win nor lose, i.e. your net gain/loss is 0.
- If the sum is even, then
 - for an even-even combination (even Z & even N) you get a bonus $|E_p|$,
 - for an odd-odd combination (odd Z & odd N) you pay the same penalty $|E_p|$.

Later on we will see that these rules of game are built in the last (pairing) term of the Weizsäcker equation (53) which gives a straightforward explanation for lots of things about nuclides including Figure 23.

As we have seen in Figure 22, even- Z elements are more abundant in the Universe than odd- Z elements. According to Figure 21, the number of their stable isotopes is also larger. Figure 23 proves that this is especially true for the even- N type isotopes, as shown by quite a number of groups of nuclides lined up horizontally in the upper left panel. (Note also that some even- N nuclides have several even- Z isotones lined up vertically.)

The bottom diagrams show noticeably ‘narrower’ bands of data points than the upper left graph. This is partly so because odd- Z elements have only a few stable isotopes and odd- N nuclides have only a few stable isotones.

A less conspicuous (however equally important) reason for the difference is that odd- A isobaric groups never consist of more than one single nuclide, while even- A isobaric groups may contain 1, 2 or even 3 members, a curiosity that is explained by Eq. (59) derived from the Weizsäcker equation (53). (Isobars line up parallel with the slanting red line shown for $A = 39$ in the lower left plot. The isobaric line is drawn across the ‘gap’ which indicates that there are no stable nuclides at all for $N = 19$ and 21 .) Also, the two ‘extinct’ medium-weight elements, Tc and Pm, are the odd- Z type.

¹⁴ This similarity serves as a basis for the approach which considers the proton and the neutron as different states of the same particle (i.e. the nucleon) which are determined by the two possible ‘projections’ (p: $T_z = 1/2$; n: $T_z = -1/2$) of the **isospin** ($T = 1/2$), a quantum number designed after the spin. Also called isobaric spin, the isospin is an additive quantum number. Therefore, for the isospin of a nucleus we can write: $T_z = (Z - N)/2$.

6.2. Dependence of the Average Binding Energy per Nucleon on the Mass Number

Figure 24 shows the average binding energy per nucleon B/A as the function of A for stable nuclides in two types of representation.

The upper panel shows the whole range of mass number A covered by stable nuclides from ${}^1\text{H}$ to ${}^{209}\text{Bi}$. The drop lines indicate magic values of Z (black) and N (blue). *Doubly magic* nuclides, when both Z and N are magic, are indicated by red star. Magic elements, when Z is magic, are also marked on the top of the curve. Note that Ca has two doubly-magic isotopes: ${}_{20}\text{Ca}_{20}$ and ${}_{20}\text{Ca}_{28}$. The chemical symbols written across bands of drop lines are to show that the respective elements have magic- N isotopes there. Non-magic nuclides are connected by a solid line.

The lower panel shows the same range of A but in two parts for better resolution.

The main graph shows the binding energy per nucleon from $A = 20$ to 209. Note that the values for even- A nuclides (red dots) show considerable scattering around the solid line of the odd- A nuclides. This behavior will be explained later in connection with the Weizsäcker equation (53). The local behavior of the curve is obviously connected with the magic numbers copied from the upper panel. The absolute maximum is at the elements near to iron or, more precisely, around Cr, Fe, and Ni. The existence of the maximum has an important role in the evolution of the chemical elements in the Universe.

The inset covers the range from $A = 1$ to 20 in major steps of 4. The ‘ α nuclides’ marked by the drop lines are more stable than their neighbors with one remarkable exception, namely, there is no stable nuclide at all for $A = 8$. The possible candidates—the respective isotopes of ${}^2\text{He}$ ($T_{1/2} = 119$ ms), ${}^3\text{Li}$ ($T_{1/2} = 840$ ms), ${}^4\text{Be}$ ($T_{1/2} < 1$ fs), ${}^5\text{B}$ ($T_{1/2} = 770$ ms)—are all short-lived radionuclides. Surprisingly enough, the most logical candidate— ${}^8\text{Be}$ —is the shortest-lived of all, a very important fact concerning stellar nucleosynthesis. (This is the reason that the initial step of ‘helium burning’, the energy producing process in some stars, is the [triple alpha process](#), which skips the production of the unstable ${}^8\text{Be}$, leading directly to the nucleosynthesis of ${}^{12}\text{C}$, the single most important nuclide for terrestrial life.) As far as the binding energy is concerned, ${}^8\text{Be}$ is more stable than any of its isobars (see Figure 25). However, this cannot save its nucleus from falling apart again to two α particles as soon as it is formed from them by collision.

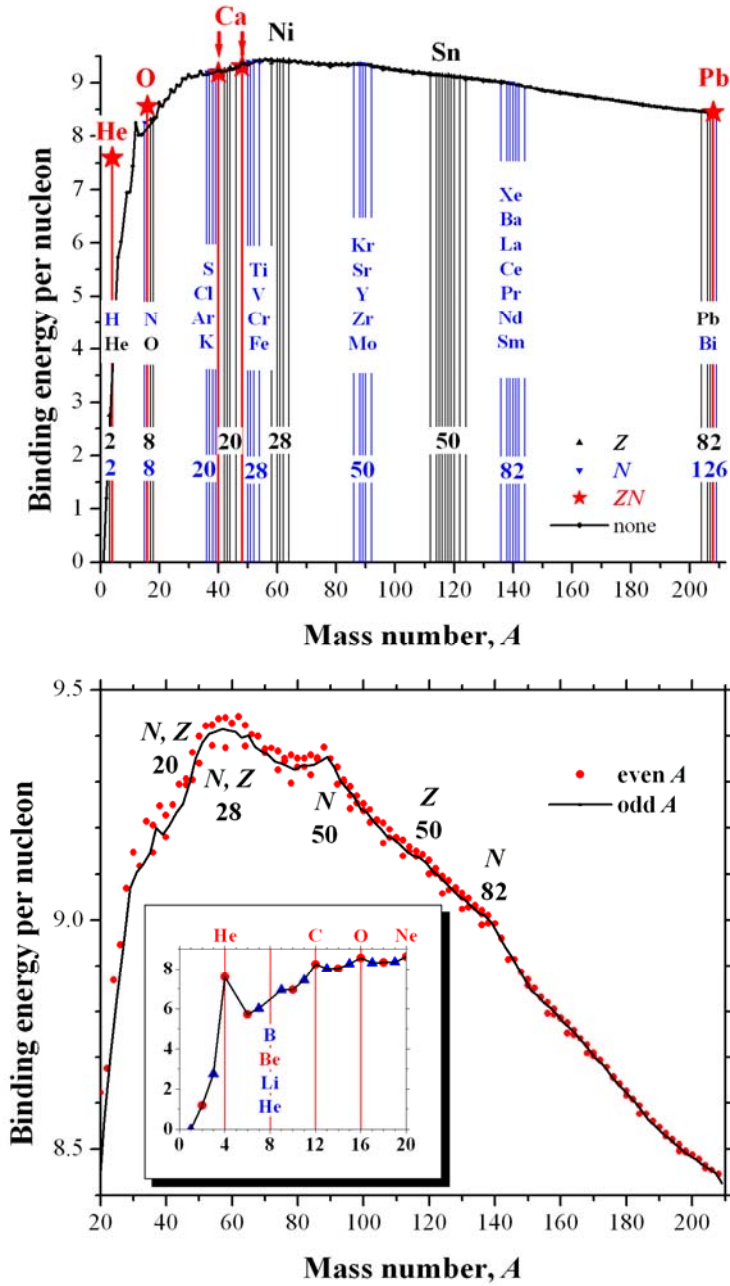


Figure 24: The average binding energy per nucleon (or rather its mass equivalent) calculated from the nuclidic masses of the 266 most stable nuclides (unit: μ corresponding to about one MeV). The drop lines in the upper panel indicate magic values of Z (black) and N (blue). Doubly magic nuclides are indicated by red star. The lower panel shows the same range of A but in two parts for better resolution. The inset covers the range from $A = 1$ to 20 in major steps of 4 to call attention to ‘ α nuclides’ also marked by drop lines. The main graph shows the binding energy from $A = 20$ to 209. See the text for more detail.

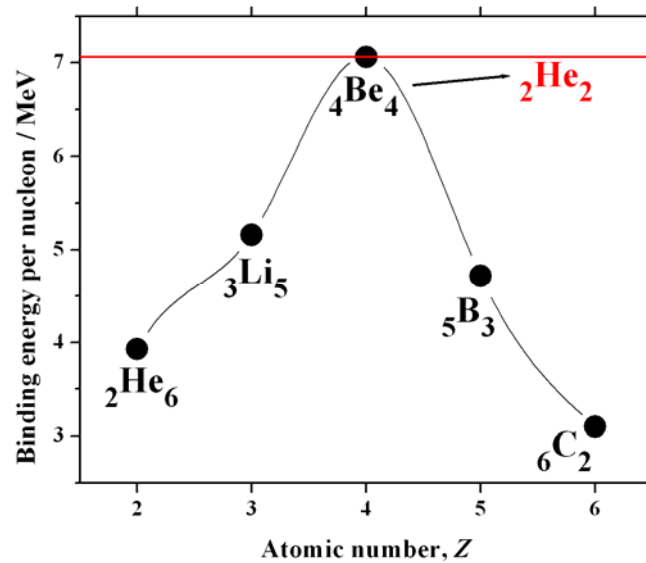


Figure 25: The average binding energy per nucleon for ${}^8\text{Be}$ and its isobaric nuclides (symbol ● connected by curve). It is obvious that ${}^8\text{Be}$ should be the most stable of all five isobars. The horizontal red line represents the respective value for ${}^4\text{He}$. The line goes right through the symbol of ${}^8\text{Be}$, indicating that the binding energies must be nearly equal. Closer inspection of the data reveals that B/A is about 0.16% higher for the nucleus of ${}^4\text{He}$, which is enough for erasing ${}^8\text{Be}$ from the list of stable nuclides due to the ‘femto-decay’ ${}^8\text{Be} \rightarrow 2\,{}^4\text{He}$.

6.3. The Weizsäcker Formula and the Liquid Drop Model

In 1935, C.F. Weizsäcker took the first large step towards the liquid drop model that was born in 1937.

When writing up the semi empirical formula (53) for the binding energy E_N of the nucleus, his starting point was G. Gamow’s 1929 recognition that the atomic nucleus resembles a drop of liquid in many ways. To translate it to chemistry, the nucleus can be considered as a droplet of ‘nuclear solution’ in which the positive protons (i.e. the ‘solute’) are ‘diluted’ with neutrons (the ‘solvent’) in order to bring them farther away from each other to curb the Coulomb force that would otherwise ‘tear apart’ the droplet as the number of protons gets larger. This simple metaphor—without any calculation—can help to understand at least one characteristic of Figure 26, namely, why the ridge of stability gets departed from the $Z = N$ line typical of light elements towards the direction marked by the condition $Z < N$ as the atomic number increases.

As mentioned before, the *binding energy* E_N of the nucleus (if neglecting the binding energy of orbital electrons) is nearly equal to the binding energy E_a of an atom and the energy quantity B , which is also called binding energy. Since mass data for the calculation of the latter are readily available in free data bases via the internet, I will interpret B accordingly:

$$B \approx E_a \approx E_N = E_V - E_S - E_C - E_A + E_P. \quad (53)$$

The first two terms in the above formula (called the [Weizsäcker equation](#))—i.e., the *volume term* E_V and the *surface term* E_S —will be trivial to anybody who is familiar with the concept of surface tension or has a ready answer for the question why liquid droplets tend to be spherical in free fall. The *Coulomb term* E_C accounts for the electric repulsion between protons. The *asymmetry term* E_A gives a penalty for any deviation from the $Z = N$ line in Figure 26. This makes sense considering that for small values of Z , the proton number and the

neutron number tend to be the same. On the other hand, the asymmetry term is also a necessity because without it the Coulomb term would force the formula to predict stable nuclei consisting only of neutrons, which—except for [neutron stars](#)—is clearly in contradiction with the facts. Finally, the *pairing term* E_P gives a bonus (i.e., B increases), a penalty (B decreases) or nothing (B remains unaffected) according to the rules of the game of cards described in connection with Figure 23.

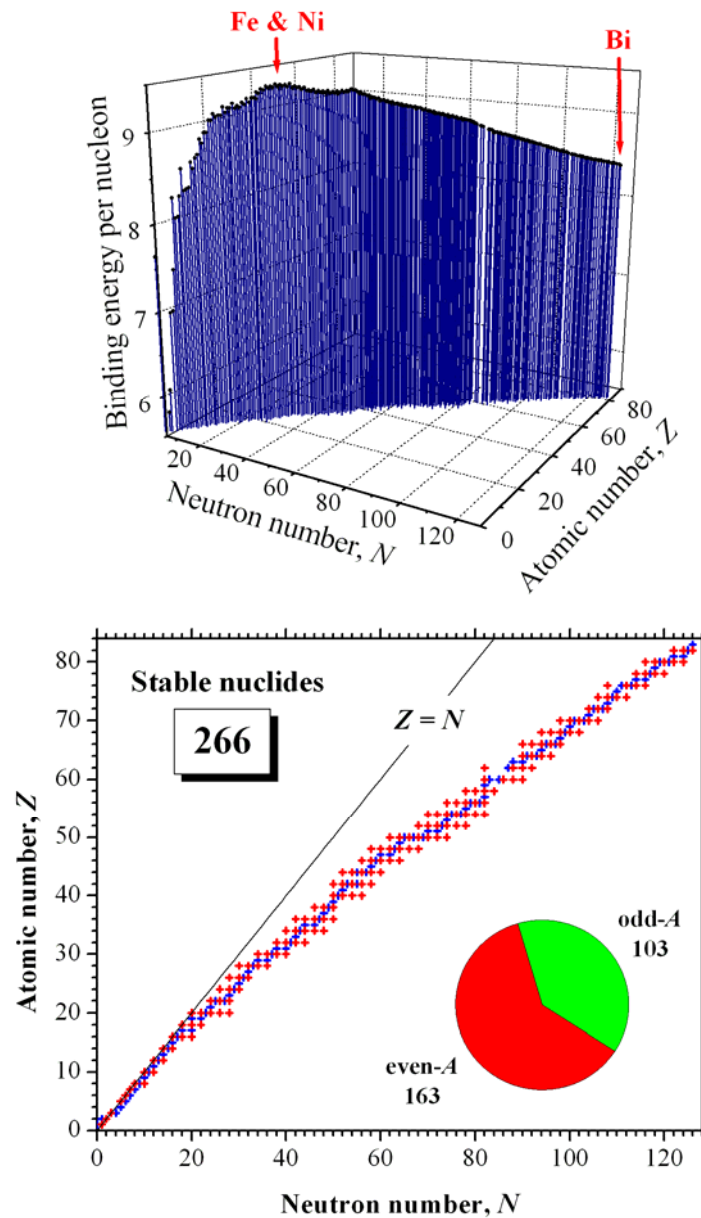


Figure 26: The upper panel shows the lateral view of the ‘ridge’ of the continent of stability whose map is presented by Figure 6. The average binding energy per nucleon (or rather its mass equivalent) is given in units of μ , i.e. approximately in MeV. The most stable elements ${}_{26}\text{Fe}$ and ${}_{28}\text{Ni}$, as well as the heaviest one (${}_{83}\text{Bi}$) are indicated by arrows. The bottom panel shows the points marked out by the drop lines on the horizontal plane of the 3D graph. It also represents the union of the four graphs in Figure 23. Even- A nuclides are shown in red, odd- A nuclides in blue in the plot. Note that the former are scattered around the latter that form quite a thin line. The line $Z = N$ is also plotted to show that the ‘ridge’ of highest stability rather soon (i.e. somewhere between $Z = 10$ and 20) starts to bend away

towards $N > Z$ values so that the short-range nuclear forces can keep up with the long-range Coulomb repulsion as it gets increasingly stronger between the protons.

The volume energy gives an estimation of the binding energy of a drop of ‘nuclear liquid’ the constituent particles of which (the nucleons) are bonded to their direct neighbors only (which corresponds to the short range of nuclear force). If all such neighborhoods are alike (which also involves the charge independence of nuclear force), then, to a first approximation, the binding energy must be proportional to the number of particles, A :

$$E_V = a_V A. \quad (54)$$

The term is rightly called volume energy, because the mass number is indeed proportional to the volume of the nucleus V_N according to Equation (43). On the other hand, the fact that the above proportionality is supported by the resulted equation is also a proof of the short range of nuclear force. If, namely, each nucleon within the nucleus would (equally) feel the attractive presence of the rest of the nucleons ($A - 1$), there would be $A(A - 1)/2$ (equal) contributions to the volume energy¹⁵, which would result in an approximate proportionality to A^2 rather than to A .

However, the volume energy overestimates the binding energy, because we considered all neighborhoods equal although the nucleons on the surface of the nucleus have fewer neighbors to be bonded to. Therefore we have to subtract a term that is proportional to the surface area S_N of the nucleus. According to Equation (42) this surface term must have the following form:

$$E_S = a_S A^{2/3}. \quad (55)$$

Further subtraction is needed because of the Coulomb energy resulted from the repulsion between the protons enclosed in a sphere of radius R_N . This correction is proportional to the work needed to squeeze the electric charge Ze represented by the protons in the sphere, a value proportional to Z^2/R_N . Thus, considering Equation (41) we can write:

$$E_C = a_C \frac{Z^2}{A^{1/3}}. \quad (56)$$

The penalty for any deviation from the line $Z = N$ has been suggested to be:

$$E_A = a_A \frac{(N - Z)^2}{A} = a_A \frac{(A - 2Z)^2}{A} = a_A \frac{4Z^2 - 4AZ + A^2}{A}. \quad (57)$$

Note that light nuclei (small A) pay a relatively larger penalty for any deviation from symmetry than heavy nuclei do, which is in agreement with the initial trend $Z = N$. In other words: a low isobaric spin (isospin) is an advantage concerning the stability of the nucleus (see footnote 14).

The final term can increase, decrease or leave unchanged the sum of the previous terms according to the rules of the odd–even game of cards mentioned before:

$$E_p = \begin{cases} + a_p A^{-\alpha} & \text{for ee} \\ 0 & \text{for eo \& oe} \\ - a_p A^{-\alpha} & \text{for oo} \end{cases} \quad (58)$$

¹⁵ If we have A different points, we can draw $A(A-1)$ lines to connect them with each other, where each line would represent a tie among them giving a contribution to binding energy.

Various authors used different values for the power α to characterize the mass-number dependence of the above term for the even- A case: $\alpha = 1/3, 1/2, 3/4$, or 1 . Taking, e.g. $\alpha = 1$, Equations (53)–(58) yield the following formula for the *average binding energy per nucleon*:

$$\frac{B}{A} = a_v - \frac{a_s}{A^{1/3}} - a_c \frac{Z^2}{A^{4/3}} - a_A \left(4 \frac{Z^2}{A^2} - 4 \frac{Z}{A} + 1 \right) + \begin{cases} + a_p A^{-2} & \text{for ee} \\ 0 & \text{for eo \& oe} \\ - a_p A^{-2} & \text{for oo} \end{cases} \quad (59)$$

The first thing to be noticed is that if it were not for the last term, the plot of B/A vs. Z for any constant value of A (i.e. for any isobar) would be an upside down parabola with its tip showing up (because the single Z^2 term that remains after the parenthesis is eliminated has a negative sign).

Looking at the last term we can see that whenever A is an odd number, the sequence of the isobaric nuclides is like this: oe, eo, oe, eo, oe, ... In other words, the last term vanishes and the points follow a single parabola. Looking at the lower right panel in Figure 43 representing series of concrete isobars, we can indeed see a single parabola, however, it is upright. The difference is caused by Eq. (36) which shows that the B/A values discussed here and the mass excess Δ plotted there have opposite signs, and therefore their plots must be the flipped-over versions of each other. (See also Figure 10 showing both types of plots for the same series of isobaric nuclides in the even- A case discussed below.)

For even- A nuclides (ee or oo) the situation is slightly more complicated, because now there are two ‘parallel’ B/A parabolas one shifted up (ee), while the other down (oo) by the same energy value relative to the ‘neutral’ position with a total distance of $2 a_p A^{-2}$ between them [assuming $\alpha = 1$ in Eq. (58)]. If, instead of B/A , the mass is directly plotted against Z (this is what is called a mass parabola) then the main difference will be that the parabolas turn upwards and the e-e parabola representing higher stability will now be the lower one. In either case, the subsequent isobaric points (ee, oo, ee, oo, ee, ...) will be jumping from one parabola to the other as we can see in the schematic Figure 27 as well as in Figure 43 (even- A plots calculated from experimental values). The latter also shows the method of jumping: β -decay, an isobaric process, makes it possible to move along Z in either direction.

In order to better understand Figure 27, note the following:

- The vertical position of the two parabolas relative to each other (which depends on the gradient of the curves around the minimum) changes with the mass number.
- The symmetry axis of the parabolas crosses the Z axis at a random point (which means that the probability that the crossing point will exactly fall on a specific point pre-defined relative to two integers is 0). Therefore we can exclude with certainty that the minimum will be exactly at an integer or a half-integer value. (Thinking about it, the latter conclusion explains at once why there is only one stable nuclide if there is only one parabola as is the case with odd- A isobars!)
- One can conclude from Eq. (59) that the mass parabolas isobars with lower A are squeezed into each other to a greater extent.

The ‘one parabola for odd- A and two parabolas for even- A ’ rule explains also why the even- A points scatter up and down around the odd- A points in the main diagram of the lower panel in Figure 24. Indirectly (through plots like that in Figures 27 and 43) the same rule explains the scattering of the (red) even- A points around the more steady sequence of the (blue) odd- A

points on the lower panel in Figure 26.

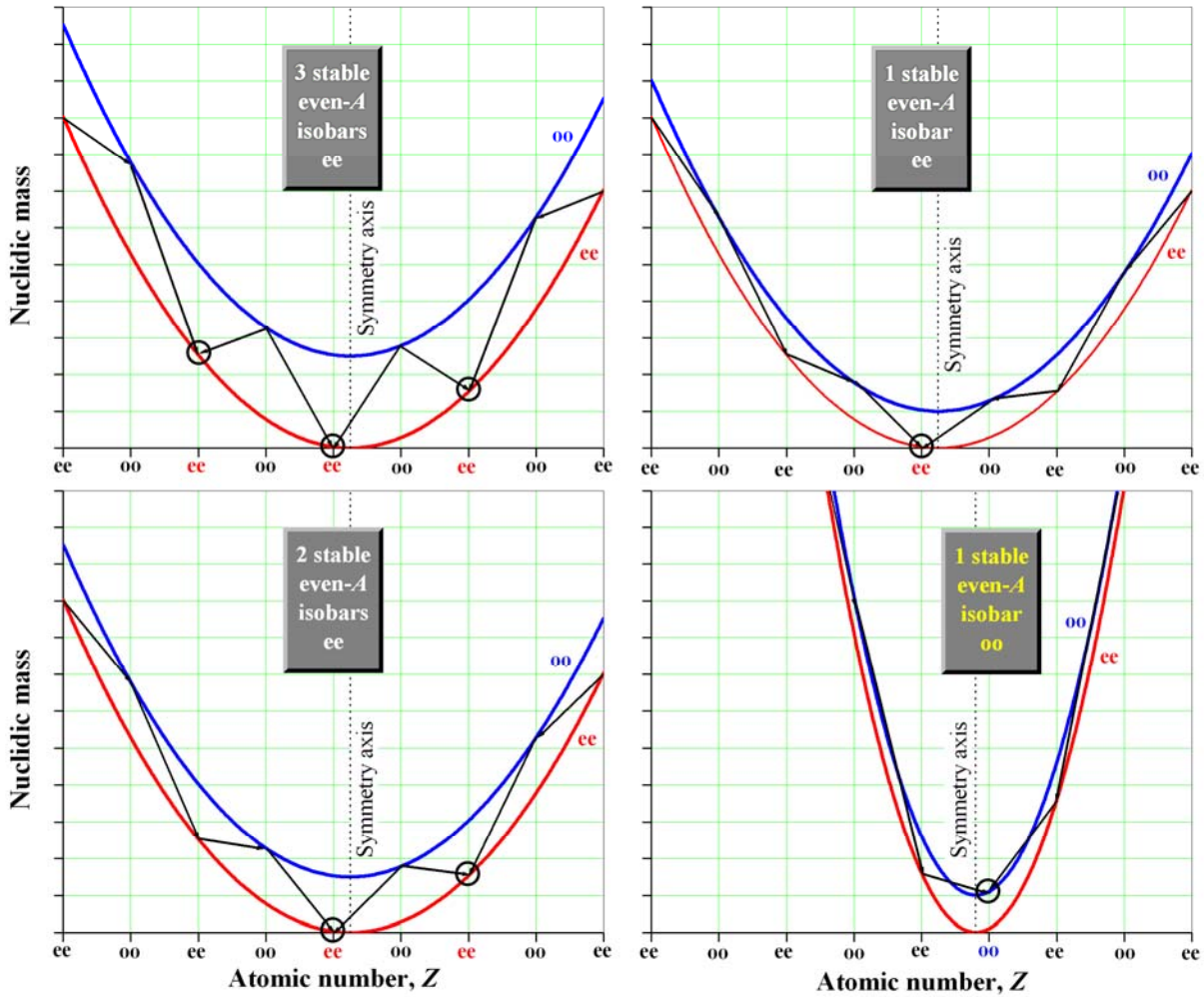


Figure 27: Schematic mass parabolas to explain why there can be 1, 2 or 3 stable isobaric nuclides for the even- A case (whereas in the odd- A case only 1 stable nuclide is possible). The three diagrams representing cases when the minimum is near to an even Z value speak for themselves. When the minimum is close to an odd Z , the situation is basically the same unless A that the parabolas are squeezed together too much. Then it can happen that the single minimum that can be actually reached falls on the upper o-o parabola. This only occurs in 4 cases. The experimental mass parabolas of one of these cases (^{14}N) are shown in Figure 44.

Figure 28 shows the plot of Eq. (59) for odd- A nuclides with set values $a_V = 14$ MeV, $a_S = 13$ MeV, $a_C = 0.6$ MeV, and $a_A = 19$ MeV. The $Z(A)$ function (which is also needed for the plot) was estimated by a polynomial fit of the odd- A points in Figure 26. As one can see, the Weizsäcker equation (53) gives a reasonably good explanation for the general shape of the plots in Figure 24, although the details including the magic numbers remain unexplained. The equation does not work well for light nuclei either, but the tendencies are clear: the surface contribution decreases with increasing A , whereas both the Coulomb and the asymmetry contributions increase.

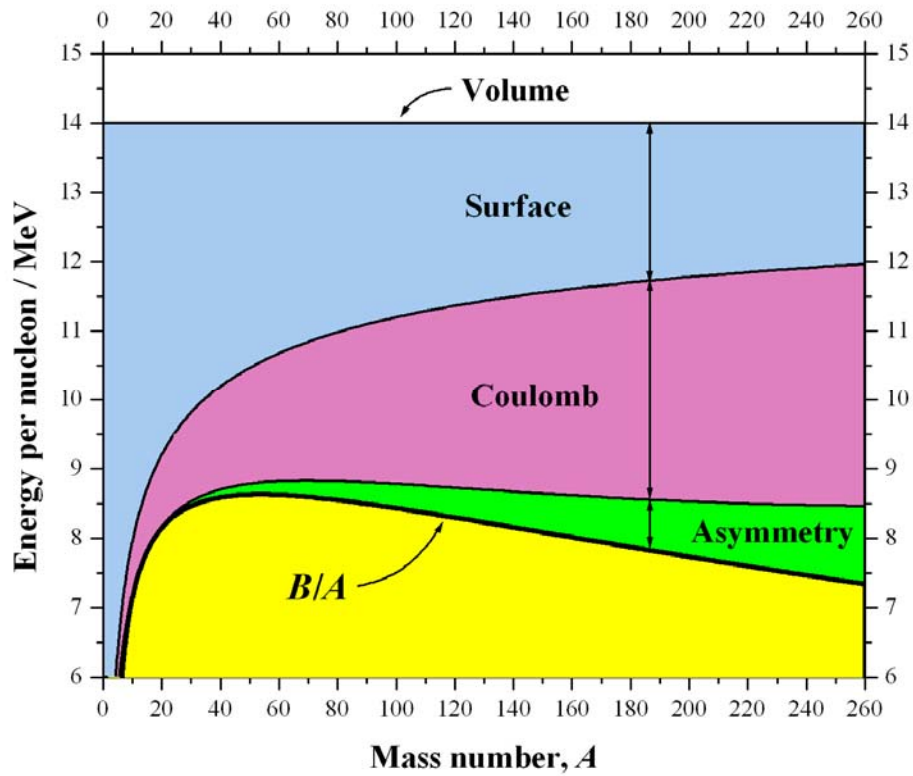


Figure 28: Average binding energy per nucleon for odd- A nuclides and the components of B/A calculated from Eq. (59) derived from the Weizsäcker equation (53).

7. Introduction to Nuclear Reactions

7.1. Types of Nuclear Reactions

Figure 29 illustrates the nuclear reaction $X(a,b)Y$, which is a short-hand notation for the process:



where ‘a’ is the *bombarding particle/photon (projectile)*, ‘X’ is a placeholder for the chemical symbol representing the *target nucleus/atom*, ‘Y’ (not to be mixed up with the concrete chemical symbol of the element yttrium) is a placeholder for the chemical symbol representing the nucleus/atom of the element created in the reaction, and ‘b’ stands for the particle(s) leaving the nucleus.

Such a reaction may proceed directly or through the formation of an intermediate stage called a *compound nucleus*.

Direct reactions only involve a few particles. Reaction times ($\sim 10^{-22}$ s) are of the same order that is needed for a projectile to ‘fly through’ the target nucleus. Typically there is an angular correlation between the direction of the projectile and the directions of the formed products (in the center-of-mass frame too). In other words, the ‘system’ in a sense keeps the memory of its past.

Compound-nucleus reactions take about a million times longer ($\sim 10^{-16}$ s) to be completed than the ‘fly-through time’, which leaves plenty of time for the system to forget about its past. Therefore—if looked at in a center-of-mass frame—the products fly in random directions relative to the original direction of the entering projectile. Therefore the angular correlation typical of direct reactions is missing, which does not mean that there is no angular correlation between the products themselves, because the system is subject to momentum conservation.

The symbols ‘a’ and ‘b’ often denote *photon* (γ), *neutron* (n), *proton* (p, i.e. ${}^1\text{H}^+$), *deuteron* (d, i.e. ${}^2\text{H}^+$), *triton* (t, i.e. ${}^3\text{H}^+$), *helion* (h, i.e. ${}^3\text{He}^{2+}$) or *alpha particle* (α , i.e. ${}^4\text{He}^{2+}$).

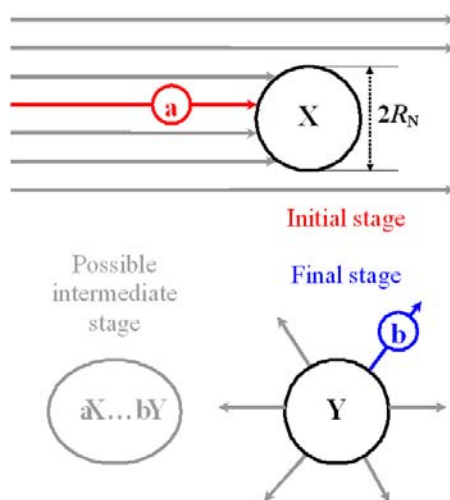


Figure 29: Naïve representation of the nuclear reaction $X(a,b)Y$. Large spheres represent nuclei, small ones are particles. The possible intermediate can be a ‘compound nucleus’, the amalgamation of the interacting particles, that exists long enough to forget its past, so that the particle ‘b’ is emitted in any

direction with equal probability. In ‘direct reactions’ where this stage is skipped, the memory of the past is not lost and the likelihood of particle emission is not isotropic anymore. (R_N is the nuclear radius.)

The symbols $X(a,a)X$ and $X(a,a')^*X$ denote *elastic* and *inelastic scattering*, respectively. In the latter case an excited-state nucleus (*X) is left behind.

If more than one particle is emitted, the shorthand-notation is $X(a,bc)Y$, $X(a,bb)Y \equiv X(a,2b)Y$, etc., where the ejected particles are listed after the comma in the parentheses.

If the product is helium or other light element whose nucleus has a separate symbol (e.g., α), then there are alternative notations, e.g., $X(a,b)^4\text{He} \equiv X(a,b\alpha)$. Note that in this case Y is missing after the end parenthesis.

For [neutron-induced fission](#) there is a special symbol (n,f) meaning:



where Y indicates *fission fragments* (FFs). If $\nu > 1$, then under appropriate conditions chain reaction may evolve. Such a (controlled) chain reaction is the basis of the nuclear energy production using ^{235}U as a fuel. It is interesting to note that L. Szilard applied for a patent on the possibility of nuclear chain reaction as early as 1934, i.e. half a decade before O. Hahn et al. discovered the fission of uranium.

Table 8 shows some examples of nuclear reactions using nuclidic notation. Apart from the classification given in the first column, some of the examples also represent a different classification, according to which reactions may belong to one of the following types: *capture*, *stripping*, *pick-up*, *fission*, and *fusion*. (Stripping and pick-up involve [particle transfer](#) between the projectile and the target.) There is also a group of reactions called [spallation](#). The latter is induced by very energetic projectiles (e.g. cosmic radiation or laser-generated protons) which may break off several small pieces from the target nucleus in direct interaction after which further low-energy particles may ‘evaporate’ which take away the excess ‘heat’ of the nucleus left behind. For instance, cosmogenic ^{10}Be is continuously produced in the upper atmosphere by the spallation of nitrogen and oxygen bombarded by cosmic-ray protons.

Table 8: Examples of nuclear reactions. The reaction is given in both ‘long-hand’ and ‘short-hand’ version provided that the latter is used at all.

Symbol	Example	Characterization
(α ,p)	${}^4_2\text{He} + {}^{14}_7\text{N} \rightarrow {}^{17}_8\text{O} + {}^1_1\text{H}$ ${}^{14}_7\text{N}(\alpha, p){}^{17}_8\text{O}$	This nuclear reaction was observed by Rutherford in 1919 while irradiating nitrogen with alpha particles. It is not only the first artificial nuclear reaction, but also considered as the experimental proof that the proton, the nucleus of the lightest nuclide ${}^1_1\text{H}$, is the constituent of atomic nuclei in general, giving them positive electric charge.
(α ,n)	${}^4_2\text{He} + {}^9_4\text{Be} \rightarrow {}^{12}_6\text{C} + {}^1_0\text{n}$ ${}^9_4\text{Be}(\alpha, n){}^{12}_6\text{C}$	This nuclear reaction was studied by Chadwick in 1932 by irradiating beryllium with alpha particles. He proved that the neutral radiation emitted consisted of massive particles rather than γ photons. Thus he discovered the neutron as the second constituent of atomic nuclei besides the proton.
(γ ,n)	$\gamma + {}^2_1\text{H} \rightarrow {}^1_1\text{H} + {}^1_0\text{n}$ ${}^2_1\text{H}(\gamma, n){}^1_1\text{H}$	High-energy gamma photons can directly knock out a neutron from the nucleus. Deuterium, one of the few stable nuclides formed shortly after the Big Bang , is sensitive to this type of reaction.

(p,γ)	${}^1_1\text{H} + {}^7_3\text{Li} \rightarrow {}^8_4\text{Be} + \gamma$ ${}^7_3\text{Li}(p, \gamma){}^8_4\text{Be}$	The (radiative) capture of a proton is only one type of <i>capture reactions</i> when the bombarding particle is swallowed by the target nucleus (and only a gamma photon is emitted). <i>Neutron capture</i> (n,γ), e.g., is an important reaction in neutron activation analysis (NAA).
(d,h)	${}^2_1\text{H} + {}^{59}_{27}\text{Co} \rightarrow {}^{58}_{26}\text{Fe} + {}^3_2\text{He}$ ${}^{59}_{27}\text{Co}(d, h){}^{58}_{26}\text{Fe}$	This reaction of the deuteron d (${}^2\text{H}^+$ ion) is an example of <i>pick-up reactions</i> , when the bombarding particle takes away a nucleon (a proton this time) from the nucleus and leaves the scene as a heavier particle (helion, h, this time, i.e. a ${}^3\text{He}^{2+}$ ion).
(d,n)	${}^2_1\text{H} + {}^3_1\text{H} \rightarrow {}^4_2\text{He} + {}^1_0\text{n}$ ${}^3_1\text{H}(d, n){}^4_2\text{He}$	This highly exoergic <i>fusion reaction</i> ($Q = 14.1$ MeV) is the most promising option to fuel the <i>fusion reactors</i> of the future. It also exemplifies <i>stripping reactions</i> when a part (a proton this time) is stripped off from the projectile (a deuteron) to be swallowed by the nucleus, while the rest (the neutron) breaks away.
(n,nt)	${}^1_0\text{n} + {}^7_3\text{Li} \rightarrow {}^4_2\text{He} + {}^3_1\text{H} + {}^1_0\text{n}$ ${}^7_3\text{Li}(n, nt){}^4_2\text{He}$	This process can be also important for future energy production, because it can supply the above fusion reaction with tritium by making use of the neutrons produced (t is for triton, ${}^3\text{H}^+$).
(n,p)	${}^1_0\text{n} + {}^{14}_7\text{N} \rightarrow {}^{14}_6\text{C} + {}^1_1\text{H}$ ${}^{14}_7\text{N}(n, p){}^{14}_6\text{C}$	This reaction takes place in the upper atmosphere. It continuously re-produces ‘radiocarbon’ ${}^{14}\text{C}$, the spring that keeps running the clock of one of the most important methods of radiometric dating.
(n,f)	${}^1_0\text{n} + {}^{235}_{92}\text{U} \rightarrow {}^{140}_{56}\text{B} + {}^{94}_{36}\text{Kr} + 2 {}^1_0\text{n}$	<i>Induced fission</i> (f, IF) of ${}^{235}\text{U}$ produces more neutrons than it consumes, which makes it possible to maintain a <i>chain reaction</i> for controlled energy production in fission reactors. The nucleus usually splits asymmetrically to two parts, called fission fragments. These (and the secondary fission products formed from them somewhat later) have a large variety of composition, so the shown fission is only one example of the many possibilities.

7.2. Reactions Induced by Neutrons and Positive Ions

7.2.1. Geometrical Cross Section of the Nucleus

As we have seen in the section 5.1 the atomic nucleus can be pictured as a more or less solid sphere. To a first approximation, the *nuclear radius* (R_N) only depends on the mass number A :

$$R_N \approx r_0 A^{1/3}, \quad (62)$$

where the proportionality constant r_0 is about 1.3 fm.

This means that the *cross-sectional area of the nucleus* called *geometrical cross section* (σ_G) is:

$$\sigma_G = R_N^2 \pi \approx \pi r_0^2 A^{2/3}. \quad (63)$$

Taking ${}^{81}\text{Br}$ (one of the natural isotopes of bromine) as an example of medium-size nuclei, the above formula yields 99.4 fm^2 , a value close to 100 fm^2 . The area this large is called *barn* (b):

$$1 \text{ b} = 100 \text{ fm}^2 = 10^{-28} \text{ m}^2, \quad (64)$$

which, therefore, is a convenient unit for specifying the geometrical cross section of nuclei. Note that the cross-sectional area of the bromine atom itself (having an atomic radius $1.15 \text{ \AA} = 1.15 \times 10^5 \text{ fm}$) is $4.15 \times 10^8 \text{ b}$, i.e. almost half a billion times larger than that of its nucleus.

7.2.2. The Nucleus as Felt by a Neutron and a Proton

Before proceeding any further let us have a look again at Figure 17 with its lower panels showing the possible potential energy of a neutron and a proton approaching towards a nucleus.

There are two types of force acting between the nucleons that build up a nucleus or get close enough to it:

- nuclear force (the attractive residual of the strong/color force acting between the quarks which build up the individual nucleons)
- Coulomb force (repulsive electric force between the protons due to their positive charge).

Both types of nucleons are ‘sensitive’ to the nuclear force, which attracts them equally.

Nuclear force, although very strong if the nucleons are close enough, has a very short range. With extreme simplification, nuclear force can be pictured as the adhesion between a stick tape and a piece of paper: no contact—no adhesion.

The repulsive Coulomb force acting between the (positive) proton and the (positive) nucleus, on the other hand, has an infinite range. Of course, there is no electric repulsion between the (electrically neutral) neutron and the nucleus. This means that at a large enough distance (which is just a little longer than the nuclear radius), the proton only feels the electric repulsive force of the nucleus, whereas the neutron feels nothing.

Getting very near to the nucleus (for which to happen the proton has to be an energetic projectile in order to overcome the Coulomb repulsion of the nucleus), the nucleons start to feel the attraction of the nuclear force. For the neutron this means that it ‘drops’ unhindered into the potential well of the nucleus. With the proton the situation is not that simple. At distances smaller than the size of an average nucleus, the nuclear force (residual strong force) is about 20 times stronger than the Coulomb force, and therefore nuclear force dominates over Coulomb force in the nucleus. As a result, the nucleus also acts as a potential well for the proton. This well is, however, less deep and it also has a ‘brim’ called Coulomb barrier at a distance where the nuclear force starts to conquer the Coulomb force. The proton must have at least as much energy as the height of the brim to get to the nucleus. Since the forces that are responsible for nuclear reactions are short-range forces, this means that the necessary condition for a reaction to happen is that the proton (or any other positive projectile) should have enough initial kinetic energy to overcome the Coulomb barrier.

Summary: The neutron, being a neutral particle, can approach the nucleus with as little energy as it wants. Even thermal neutrons have no problem with getting in close contact with the nucleus. The proton, on the other hand, being a positive particle, has to conquer the Coulomb barrier surrounding the nucleus which can take an initial kinetic energy in the order of a few MeV.

7.2.3. Reaction Cross Section Systematics

Using the naïve approach of nuclear reactions shown in Figure 29, the reaction rate R could be

given for a thin target as follows:

$$R = -\frac{dN_X}{dt} = \frac{dN_Y}{dt} = \phi_a S \frac{\sigma_G n_X V}{S} = \phi_a \sigma_G N_X, \quad (65)$$

provided that every collision between a projectile ‘a’ and the nucleus ‘X’ leads to reaction. In the above equation S is the irradiated area of the homogeneous target, $V = S l$ is the irradiated volume (l is the target thickness, cm), n_X is the *number density* of the target nuclei (number of nuclei per volume, cm^{-3}), N_X is the total number of target nuclei exposed to the homogeneous beam of particles (i.e., $N_X = n_X V$), and ϕ_a is the *particle flux* (number of particles per area per time, $\text{cm}^{-2} \text{s}^{-1}$) also called the *fluence rate*, and σ_G is the geometrical cross section of the target nucleus X.

Note that the fraction in Eq. (65) expresses the fraction of the total area S ‘blocked’ by target nuclei provided that they do not ‘hide’ behind each other. However, hiding of nuclei is very unlikely in thin targets, considering their tiny size relative to the atoms, even if the latter are sitting in a close-packed lattice—see the comment after Eq. (64). So the same fraction can also be considered as the geometrical probability that a single projectile aimed at the target will actually hit a nucleus, thus inducing a reaction.

Note also that in the final form of the above equation:

$$R = \phi_a \sigma N_X \quad (66)$$

the physical quantity σ (from which the subscript G has been removed for a reason which will be explained below) carries a probabilistic meaning, i.e. the larger it is, the likelier the reaction. Note that there is a more than just formal correspondence between Eqs. (75) and (66) inasmuch as $A \Leftrightarrow R$, $N \Leftrightarrow N_X$, and $\lambda \Leftrightarrow \phi_a \sigma$. (See also the legend of Figure 35.)

Now, if we put aside the naïve interpretation and try to re-interpret σ by measurement, we will find (see Figure 30) that the actual values of the probability factor σ —or *cross section* as is simply called—are a far cry from the actual geometrical cross section σ_G most of the time.

The qualitative interpretation of the energy dependence of the cross section of ion-induced reactions is straightforward, because no reaction can be expected if the ion is repelled by the nucleus before they could get in contact. The behavior of neutrons can only be explained by the *de Broglie wavelength* that all particles possess:

$$\lambda_{\text{dB}} = \frac{h}{p}, \quad (67)$$

where p is the momentum of the particle—neutron this time. Since slower neutrons have smaller momentum ($p = mu$ in the non-relativistic case), their wavelengths will be larger. This can be interpreted in the following naïve way. A neutron having a large de Broglie wavelength is ‘all over the place’ and therefore it ‘feels’ the presence of nuclei from a distance that is in inverse proportion to its speed u , thus multiplying its chances to induce nuclear reaction in one of them.

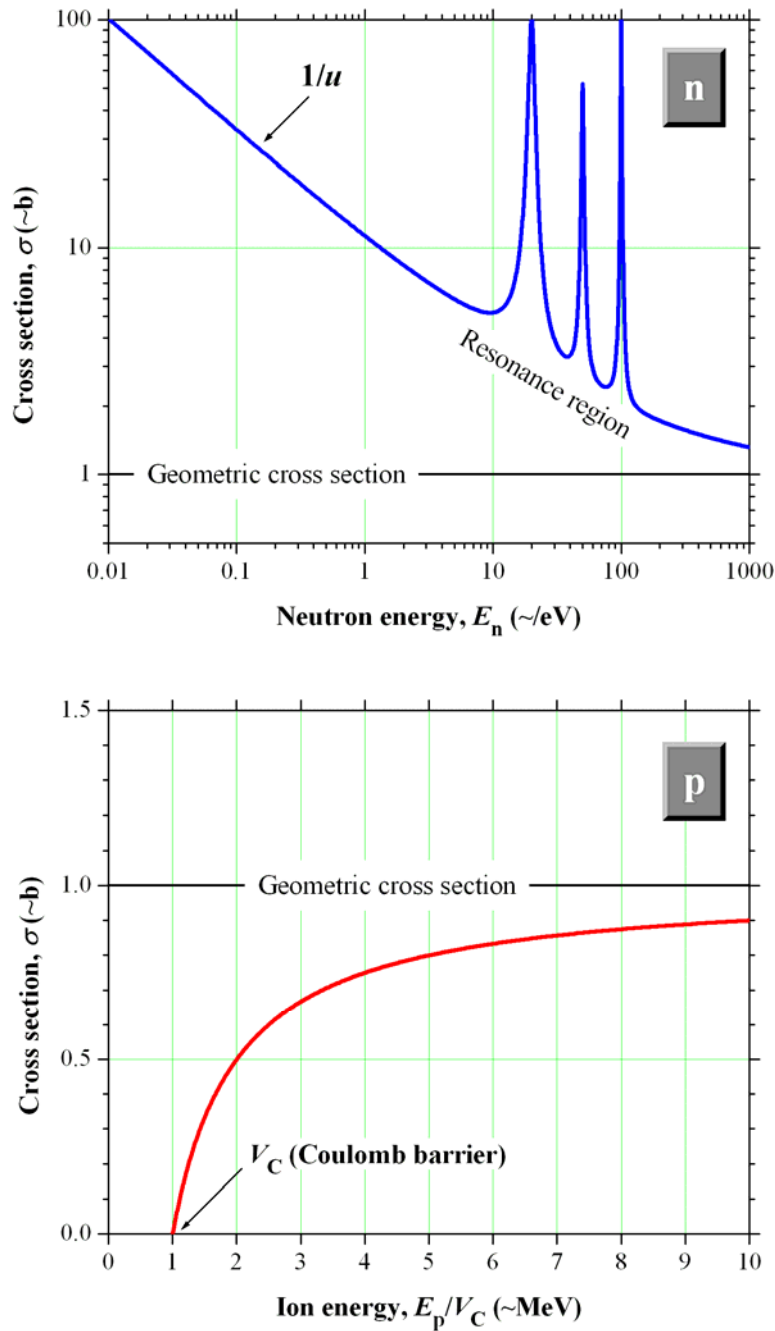


Figure 30: Schematic comparison of the cross sections of nuclear reactions induced by neutrons and charged nuclear particles exemplified by the proton. The asymptotic cross section for both types of particles is in the order of the geometrical cross section of the nucleus (~ 1 b). However, positive ions approach it from below, but neutrons (for which there is no Coulomb barrier to conquer) start from much higher values than the actual geometrical cross section due to quantum mechanical effects. (On the upper panel, u is the speed of the neutron.)

This would also explain the ‘one-over- u ’ dependence of the *excitation function* (as such curves are called) on the upper panel of Figure 30. (This dependence is often mentioned as the ‘one-over- v ’ rule, where v , of course, is a reference to the usual notation of the speed ‘ v ’. The letter ‘ v ’ however, written in italic, is very similar to the Greek letter ν , and therefore I prefer to use the symbol u instead.)

The *resonance peaks* on the excitation function are at energies which happen to match one of

the levels of the compound nucleus formed from the target nucleus and the neutron projectile. At resonance energies radiative neutron capture (n,γ) suddenly becomes much more probable than it would follow from the general trend. The shape of the resonance peaks (Breit–Wigner curves) is mathematically the same as that of the peaks of Mössbauer spectra (Lorentzian curve).

Cross sections of charged-particle reactions are usually measured in millibarns (mb) and level off at $\sim 1000 \text{ mb} = 1 \text{ b}$. The actual cross sections for neutrons, on the other hand, can be much higher than shown in Figure 30, exceeding even 10^4 b . For instance, the (n,γ) cross section of ^{113}Cd is $2.06 \times 10^4 \text{ b}$, much larger than the cross-sectional area of its nucleus, which is only $\sim 1.25 \text{ b}$. No wonder that cadmium is used in the control rods of nuclear reactors. The (n,γ) cross section of ^{157}Gd —also used for controlling reactors—is even higher: $2.54 \times 10^5 \text{ b}$, whereas the geometrical cross section of its nucleus is only $\sim 1.55 \text{ b}$. (In linear scale this means that the effective diameter of its nucleus is about 400 times larger than its actual size.) Apropos reactors, note that ^{135}Xe (causing ‘[Xe poisoning](#)’ in reactors), the decay product of ^{135}I , one of the heavy fragments of ^{235}U fission, has a cross section as large as $\sim 3 \times 10^6 \text{ b}$ for thermal neutrons.

Although γ -resonance fluorescence (serving as a basis for Mössbauer spectroscopy) is not considered a nuclear reaction, it can be formally written as $X(\gamma,\gamma)X$. In the case of ^{57}Fe , e.g., the 14.41 keV transition has a maximum cross section of $\sigma_0 = 2.56 \times 10^6 \text{ b}$. The actual geometrical cross section of its nucleus is only $\sim 0.8 \text{ b}$. Considering that the atomic radius of iron is 1.4 \AA , the cross-sectional area of an atom is $\sim 6.16 \times 10^8 \text{ b}$. That means that the nuclear cross section is almost half per cent ($\sim 0.4\%$) of the cross-sectional area of the atom. On linear scale the following ratios hold:

- (actual diameter of the nucleus) : (effective diameter of the nucleus) = 1 : 1790
- (effective diameter of the nucleus) : (diameter of the atom) = 1 : 15.5.

As we can see, nuclear cross sections can be very much larger than the nucleus, however, they are still much smaller than the atom itself.

8. Radioactivity-Related Concepts

8.1. Characterization of the Main Decay Modes and Radiations

Radioactive decay is a spontaneous process (see Figure 8) in which an *unstable* atomic nucleus transforms into one or more different nuclei, or to a lower energy level of the same nucleus.

The *radioactive isotopes* of an element—e.g. tritium, ^3H , the super-heavy isotope of hydrogen—are called *radioisotopes*. Radioactive nuclides in general are called *radionuclides*.

The decaying species is referred to as *parent* or *mother* and the product is called *daughter*. The general notation for the daughter nuclide is D, whereas that for the parent/mother is P (which is not to be mixed up with the chemical symbol of the element phosphorus).

In the process one or more charged (e.g. α , β) or neutral (n) particles and/or photons (γ) are also released from the nucleus making it possible to detect individual decay events ‘on-line’. Neutrinos (ν), however, that accompany all types of β decay, are notorious for their ‘ghost-like’ nature, avoiding detection (see Figure 31, the original of which is indirect proof of the existence of the electron antineutrino). This is so, because neutrinos have very little ‘inclination’ to interact with matter, which is the basis of all direct methods of particle detection. They are the most penetrating of all particles mentioned. So much so that the vast majority of the neutrinos coming from the Sun pass through the Earth as if it were nothing but empty space in spite of the fact that their flux at this distance is still $\Phi_\nu \approx 5 \times 10^{10} \text{ cm}^{-2} \text{ s}^{-1}$. (This means that about 200 trillion high-energy solar neutrinos ‘hit’ us every second without doing any harm to us.)

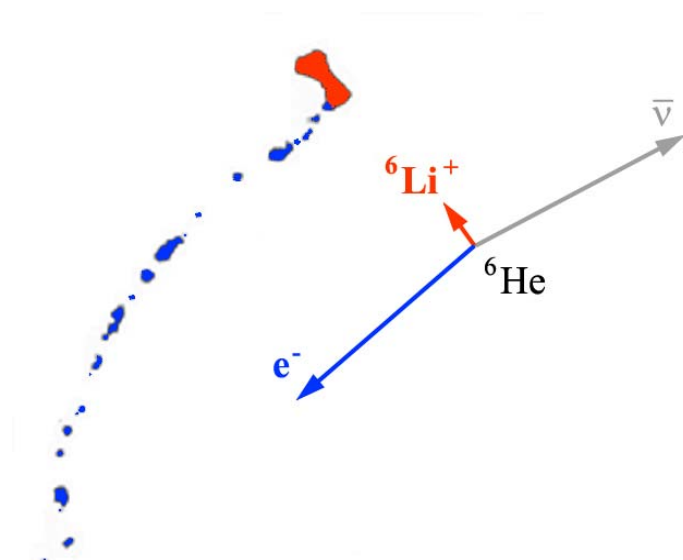


Figure 31: This graphically ‘processed’ version of a cloud-chamber picture¹⁶ (courtesy of J. Csikai, ATOMKI, Debrecen, Hungary) shows a decay event of ^6He β decaying to ^6Li . The recoil of ^6Li (short thick track of red color) is well observable due to its small nuclidic mass. The antineutrino plays ‘poltergeist’ (an expression borrowed from the title of Reines’s Nobel Lecture), i.e., its presence is

¹⁶ The original picture was published by J. Csikai and A. Szalay in 1957, a year after the direct observation of the ‘free neutrino’ that brought a [Nobel Prize](#) to F. Reines in 1995.

only revealed by the apparent lack of momentum conservation. (The ‘hand-drawn’ arrows represent the momentum vectors which are supposed to cancel each other.)

Apart from neutrinos, high-energy (i.e. ‘hard’) [γ-rays are the most penetrating](#) of the radiations, but a few centimeters of lead already absorb about 90% of 1 MeV photons.

Charged particles like α and β have *finite range* meaning that these particles can penetrate in matter only to a certain distance called *range* (R) that depends on the type and energy of radiation. For instance, the [range of typical \$\beta\$ radiation](#) is a few millimeters in water/living tissue, while [α particles](#) cannot even penetrate through the dead cells covering our skin. (Their range is just a few centimeters in air.)

The *energy spectrum* (energy distribution) of γ -rays is *discrete*, meaning that only certain energies are represented in it, each being connected with the transition between two well defined nuclear energy levels. The α particles originating from one particular ‘branch’ of α decay (see Figure 36) are also *monoenergetic*, and therefore α spectra are also discrete. On the other hand, the energy distribution of β particles is continuous between 0 and a certain maximum value E_β called *end-point energy* (see Figure 32).

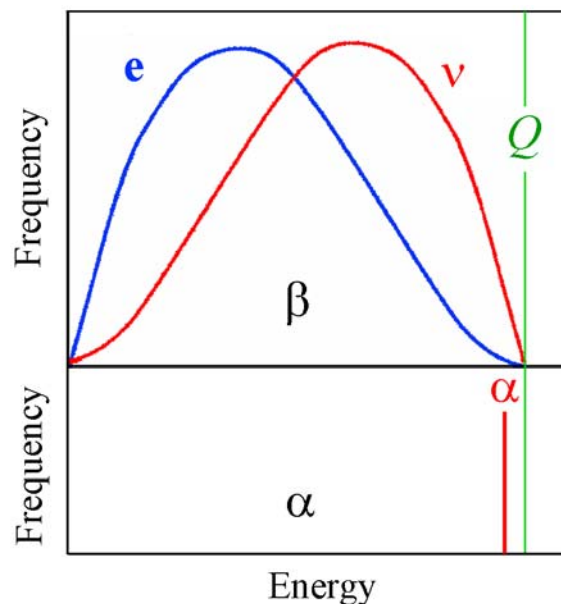


Figure 32: Schematic energy spectra of β and α decay. In β^\pm decay the energy distribution of the e^-/e^+ (e) is continuous (blue curve). For heavy atoms the recoil is negligible and therefore the upper limit of the electron/positron energy called end point energy (E_β) is practically equal to the Q -value (green vertical line). The neutrino spectrum (ν) is the mirror image of the electron spectrum (continuous red curve). In electron capture (EC) the whole Q -value (minus the recoil energy E_R of the daughter and the binding energy E_K of the captured electron) is carried away by a monoenergetic neutrino. In α decay the Q -value is divided between the recoiled daughter and the α particle, and therefore it has a monoenergetic (or at least discrete) energy spectrum with $E_\alpha = Q - E_R < Q$ (red vertical line).

The reason for the difference is this. With [α decay](#), the Q -value is divided between two particles only, i.e. between ${}^4\text{He}$ and the daughter ${}^{A-4}\text{D}$. (The γ emission—also called γ decay—which often follows α decay is disregarded here because it is a next step.) According to Eq. (130), energy and momentum conservation laws unambiguously set the ratio of kinetic energies thus gained to $E_R:E_\alpha = 4:(A-4)$, where E_R is the *recoil energy* of the daughter (Figure 32, lower spectrum). With [β± decay](#), on the other hand, where there are three particles to share the Q -value, conservation laws allow a continuity of possibilities (Figure 32, upper spectra).

For instance, the energy E_{e^-} of the electron can be as low as 0 (when Q_β is divided between the recoiled daughter and the antineutrino) or as high as $E_\beta = Q_\beta - E_R \approx Q_\beta$ (when the whole energy is divided between the electron and the daughter). Since every decay event is accompanied by the simultaneous emission of an electron with energy E_{e^-} ($0 \leq E_{e^-} \leq E_\beta$) and an antineutrino of complementary energy $E_\nu = E_\beta - E_{e^-}$, the energy distribution of the antineutrino is (1) also continuous and (2) identical with the mirror image of the energy spectrum of the electron. In electron capture (EC), however, there are only two particles—the recoiled daughter and the neutrino—to share the available part of the Q -value, and therefore the neutrino radiation is monoenergetic in this case, with an energy of $E_\nu = (Q_{EC} - E_R - E_K) \approx (Q_{EC} - E_K)$, where E_K is the binding energy of the electron that is usually captured from the K shell.

As a result of radioactive decay extranuclear particles/photons may also be emitted from the atom either as part of the decay process (e^- emission in internal conversion, IC) or as an aftereffect (*inner bremsstrahlung* in β decay in general and EC in particular; *characteristic X-rays* or *Auger electrons* emitted during the rearrangement of the orbital electrons after EC).

Some of the *decay modes* as well as the *emitted radiations* are summarized in Table 9. I have adopted the convention of denoting β^+ and/or EC together with the symbol ε (which is used by many authors as a synonym for EC). We will call β^- and ε together beta decay (β). Note that all three types of β decay are isobaric processes, leaving the mass number A constant.

Table 9: Examples of radioactive decay modes. The symbols P (parent) and D (daughter) stand here for nuclides, i.e. atoms, not nuclei. Charge balancing is based on the assumption that the number of orbital electrons is the same (Z) on both sides of the equations. Therefore a charged particle emitted by the nucleus leaves behind an ion of the opposite charge which is denoted by a right superscript. The less frequent and therefore more exotic decay modes—such as cluster decay, neutron decay, proton decay, double beta decay, beta-delayed neutron decay—mentioned or indicated in Figures 33 and 51 are explained in section 9.5.

Decay (symbol)	Equation balanced for charge	Characterization
alpha (α)	${}^A_Z\text{P}_N \rightarrow {}^{A-4}_{Z-2}\text{D}_{N-2}^{2-} + \alpha$	It decreases the Z to N ratio of proton-rich (mostly heavy) nuclei. The α particle taking away 2p and 2n from the nucleus is itself the nucleus of ordinary helium. In other words, it is a ${}^4_2\text{He}^{2+}$ ion.
beta minus (β^-)	${}^A_Z\text{P}_N \rightarrow {}^A_{Z+1}\text{D}_{N-1}^+ + \beta^- + \bar{\nu}$ ($n \rightarrow p + \beta^- + \bar{\nu}_e$) n: <u>free neutron</u> or a <u>neutron bound in a nucleus</u>	Also called negatron decay, it increases the Z to N ratio of proton-deficient nuclei. It involves the decay of a neutron to a proton, while two light particles leave the nucleus. The β^- particle emitted is an electron e^- , which can be easily detected. The other radiation particle is an (electron) antineutrino $\bar{\nu}$.
beta plus (β^+)	${}^A_Z\text{P}_N \rightarrow {}^A_{Z-1}\text{D}_{N+1}^- + \beta^+ + \nu$ ($p \rightarrow n + \beta^+ + \nu_e$) p: <u>proton bound in a nucleus</u>	Also called positron decay, it decreases the Z to N ratio of proton-rich nuclei. It involves the decay of a proton to a neutron, while two light particles are emitted by the nucleus. In contrast to the neutrino ν , the β^+ particle (which is a positron e^+) can be easily detected through the annihilation process $e^+ + e^- \rightarrow 2\gamma$, which produces two annihilation photons of 511 keV each leaving the scene in opposite directions (Figure 63).
electron capture (EC)	${}^A_Z\text{P}_N \rightarrow {}^A_{Z-1}\text{D}_{N+1} + \nu$ ($e^- + p \rightarrow n + \nu_e$) p: <u>proton bound in a nucleus</u>	This decay mode competes with β^+ decay. Rather than emitting a positron, the nucleus captures an orbital electron of the atom with the same result. Since K electrons are available in all atoms, the electron

		captured is not indicated explicitly on the left-hand side of the nuclidic equation. However, a neutral atom is formed. Inner bremsstrahlung caused by the acceleration of the electron while being captured and characteristic X-ray or Auger electron emission (that accompany the filling of the hole in the K shell of D) make this decay observable.
gamma emission (γ)	${}^A_Z\text{P}_N^* \rightarrow {}^A_Z\text{P}_N + \gamma$ ${}^A_m_Z\text{P}_N \rightarrow {}^A_Z\text{D}_N + \gamma$	Following α and β decay the nucleus may form in an excited state ($*$). The excited state can ‘decay’ to the ground state or a lower excited state (without changing either Z or N) by the emission of a gamma photon. The γ emission of a ‘long-lived’ excited state (m) is called isomeric transition (IT).
internal conversion (IC)	${}^A_Z\text{P}_N^* \rightarrow {}^A_Z\text{P}_N^+ + e^-$	This process competes with γ emission. The excitation energy of the nucleus is carried away by an orbital electron (most often a K electron) which is expelled from the atom, leaving behind an excited positive ion. (Note that the electron is missing from an inner shell.)
spontaneous fission (SF)	${}^A_Z\text{P}_N \rightarrow \text{D}_{\text{light}} + \text{D}_{\text{heavy}} + \nu n$	In this process that only occurs with the heaviest nuclides, the nucleus splits asymmetrically to two parts, called fission fragments, and a few neutrons are also released. The products have a large variety of compositions concentrated in a lower (light) and a higher range of A (heavy). For instance, $A_{\text{light}} \approx 85\text{--}105$ and $A_{\text{heavy}} \approx 130\text{--}150$ for the SF of ${}^{238}\text{U}$.

To give an example for the notation, let us consider the following *alpha decay* (balanced for charge):



In this decay ${}^{228}\text{Th}$ is the parent nuclide and ${}^{224}\text{Ra}$ is its daughter. So, by neglecting the gamma radiation accompanying the process, the general equation would be:



In the concrete process the nucleus emits an α particle to ease its relative neutron deficiency. It might seem puzzling that α decay can increase the neutron to proton ratio although it decreases both Z and N by the same amount. Later on, in connection with Figure 38, we will see the reason for this. The explanation is based on the fact that whenever α decay occurs, Z is actually almost always less than N . [See, e.g., the nuclide ${}_{90}\text{Th}_{138}$ in Eq. (68).]

Depending on which level of the daughter nucleus ${}^{224}\text{Ra}$ is directly produced (see the *decay scheme* in the upper panel of Figure 36), the decay event is followed by the emission of $n = 0, 1,$ or 2 gamma photons. The alpha particle (or the gamma photon) tells the detector that an atom has just disintegrated in the source. Some detecting systems can even measure the energy of the particle/photon and therefore it is also possible to find out which one of the possible transitions has occurred.

8.2. Radioactive Decay vs. Chemical and Nuclear Reactions

Partly because nuclear science has been dominated by physicists and not chemists, radioactive decay processes and nuclear reactions have always been treated separately. To a chemist such a rigid distinction may seem to be rather ‘unnatural’, because among chemical reactions unimolecular decomposition (the obvious analog of decay) is just a special type having first-

order kinetics as expressed by the equivalent of Eq. (75), which can be obtained by performing the substitutions $c \Leftrightarrow N$ and $k_{\text{uni}} \Leftrightarrow \lambda$ (where c is the concentration and k_{uni} is the rate coefficient). Even the half-life formula (74) works considering the correspondence $t_{1/2} \Leftrightarrow T_{1/2}$.

There is, however, a deep difference between first-order chemical reactions and ‘true’ radioactive decays, namely that k_{uni} depends on temperature due to thermal activation, whereas λ does not. This is why radioactive decay can only be a *spontaneous process per se*.

As regards radioactive decay, individual nuclei of one particular radionuclide live lonely and independent lives unaffected by their neighbors no matter how frequently or vehemently the atoms themselves bump into each other. The decay of nuclei is governed by the *laws of statistics* (more precisely: their life-time distribution is exponential giving the deeper explanation of the exponential decay law), provided that the decay is *energetically feasible* at all (spontaneous processes require that the total mass decrease) and not forbidden by any of the various *conservation laws of particle physics*.

Nuclear reactions, on the other hand, are in many respects similar to their chemical counterparts. First of all, as Eq. (60) shows, they involve real interactions of particles. This is revealed by the story that usually goes with similar equations: ‘Nucleus/nuclide ‘X’ (the target) is bombarded by particle ‘a’, as a result of which another nucleus/nuclide ‘Y’ is formed and a particle ‘b’ is emitted.’ The introductory part of the story can be alternatively this: ‘Nucleus/nuclide ‘X’ collides with particle ‘a’...’

Note that one type of beta-decay, *electron capture* (EC), is actually based on the interaction between an orbital electron and the nucleus which absorbs it with some probability. Since the probability of EC is proportional to the ‘availability’ of the electron in the nucleus, external conditions that have an effect on this (such as very high pressure or even the change of the chemical environment), also affect to some degree the decay constant. On the other hand, EC also possesses the characteristics of radioactive decay. Nuclei capable of ϵ decay are ‘sitting’ in the center of an atom, waiting for the electron to ‘come by’. This should happen eventually, as the probability density of s electrons has a maximum in the very center of the atom. The other criterion of decay—namely that it should be spontaneous—is also fulfilled, as no external ‘force’ is needed for the EC to occur.

Figure 33 compares the possible outcomes of some types of radioactive decay and nuclear reaction using the same segment of a nuclide chart.

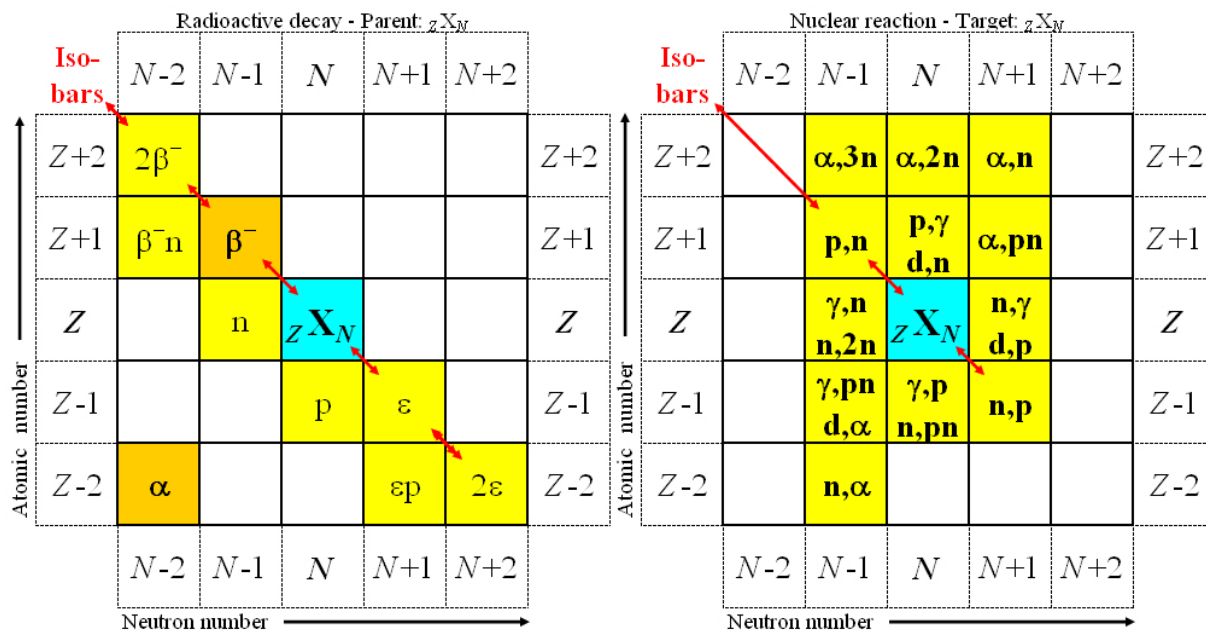


Figure 33: Representation of some possible modes of radioactive decay (left panel), a spontaneous process, and some nuclear reactions in the same range of cells of a schematic chart of nuclides. (For better legibility I have dropped the usual parentheses when denoting nuclear reactions on the right panel.) The cell of the initial nuclide is shaded turquoise. The yellowed cells specify nuclides produced by the indicated decay/reaction. The empty cells represent nuclides that cannot be produced by any of these processes. Horizontal rows of cells represent isotopes, vertical columns contain isotones. **Isobaric nuclides** are along slanting lines like the red arrows indicate. Note that the basic types of beta decay— β^- and ϵ (i.e. β^+ and EC)—are isobaric processes, i.e. they do not change the mass number. The cells of decays common in naturally occurring decay series (α and β^-) are shaded gold and the symbols are printed in bold.

8.3. Characterization of Radioactive Samples—Decay Rate and Count Rate

The *decay rate* in a given radioactive sample—i.e. the number of parent nuclei disintegrated within a short period of time divided by the length of that period—is called the *activity* (A) of that sample. In the simplest case of having one radionuclide that decays to a stable nuclide we can write:

$$A = -\frac{dN}{dt}, \tag{70}$$

where N is the number of the atoms/nuclei of the radionuclide at time t .

The SI unit of activity is the *becquerel* (Bq) meaning 1 decay/disintegration per 1 second (i.e. 1 dps):

$$1 \text{ Bq} = 1 \text{ s}^{-1}. \tag{71}$$

As mentioned before, the *curie* (Ci), the former unit of activity, is still used by many workers. It was originally defined as the activity of 1 g of pure ^{226}Ra ($\sim 3.66 \times 10^{10}$ dps). However, it was re-defined in 1950, to make it independent of the accuracy of activity measurements. The conversion is now exactly $1 \text{ Ci} = 3.7 \times 10^{10} \text{ Bq}$.

For various reasons it may be important how ‘concentrated’ the radioactivity is in a given sample. The most common quantities used for characterizing a sample from this aspect are

specific activity (the activity of the sample divided by the mass of the sample) and activity concentration (activity of the sample divided by the volume of the sample).

When *radioactive sources* are prepared (e.g., by nuclear reaction), the radionuclide produced in the target can be an isotope of an element that was not originally present in the sample. Such a nuclide preparation is per se *carrier-free*. If it is left as is or if it is dissolved without adding to it any *isotopic carrier* (i.e. a mixture of the *inactive isotopes* of the same element), the source or the sample is referred to as *no-carrier-added (n.c.a.)*. The term carrier-free is also used for any (not necessarily radioactive) nuclide preparation if other isotopes are absent. A substance added to the nuclide preparation is sometimes called *non-isotopic carrier* if it does not contain the element represented by the given nuclide.

The radioactivity of a given sample is often detected by counting the radiation particles (e.g. α , β , or γ) coming from the sample for a given period of time. The *count rate* or *counting rate* determined from such a measurement is given in cps (counts per second) etc. units. It is not appropriate to use Bq in this context, although the count rate R , in an ideal case, is proportional to the *absolute activity* (as activity is referred to in such cases to avoid misunderstanding):

$$R = \eta A, \quad (72)$$

where the number $\eta < 1$, called *detector efficiency*, can be thought of as the probability of observing a single decay event.

8.4. Half-Life, Mean Life, Decay Constant and the Exponential Law of Decay

Different radionuclides live for different lengths of time on an average. It is common with all types of radionuclides that starting from a large number N_0 of the nuclei/atoms of the same nuclide, their number will drop to half of the original number after a characteristic time called *half-life* $T_{1/2}$. After the next half-life their number will halve again, etc., and this half-life will remain the same after any number of halving. This property—which is related to the agelessness of radionuclides—is described by the following formula given in different forms by changing the base of the exponential function:

$$N = N_0 \left(\frac{1}{2}\right)^{\frac{t}{T_{1/2}}} = N_0 2^{-\frac{t}{T_{1/2}}} = N_0 \exp\left(-\frac{t}{\tau}\right) = N_0 \exp(-\lambda t). \quad (73)$$

All three parameters appearing in the above formulae—called the exponential law of decay—characterize equally well the decayability of a radionuclide. The half-life can be easily calculated from the *mean life* τ or the *decay constant* λ using the following relationship:

$$T_{1/2} = (\ln 2) \tau = \frac{\ln 2}{\lambda}. \quad (74)$$

The decay constant λ can be thought of as the probability that a given nucleus will decay in the next short period of time per the length of that time. Applying Eq. (70) to the exponential law (73), we find that the decay constant establishes proportionality between the decay rate (activity) and the number of parent nuclei that are still present:

$$A = -\frac{dN}{dt} = -N_0 \frac{d}{dt} \exp(-\lambda t) = \lambda N_0 \exp(-\lambda t) = \lambda N. \quad (75)$$

The mean life τ —as its name indicates—is the expected lifetime of a given radioactive atom

measured from any moment when its existence is considered as certainty. (Note that this awkward definition implies that radioactive atoms are ‘ageless’ however ‘mortal’ entities, whose future life expectancy is independent of their age.) The parameter τ also doubles as the standard deviation of the exponential lifetime distribution that ‘determines’ the fate of the atom in the future. For more information see the electronic version of Statistical Aspects of Nuclear Measurements ([StatNuclMeas e.pdf](#)) originally written for Kluwer as Chapter 7 in Vol. 1 of the Handbook of Nuclear Chemistry (<http://www.wkap.nl/prod/b/1-4020-1305-1>)¹⁸.

8.5. Decay Chain, Equilibrium, Branching, and Decay Schemes

Radioactive decay rarely leads to stability in a single step. So a series of subsequent decays occur forming a *decay chain* or *decay series*. If the activities of all the members of the series are equal to that of their (primary) parent, they are said to be in (*secular*) *equilibrium*. The kinetic conditions for equilibrium will be discussed later. However, the main point as regards secular equilibrium can be easily understood by the help of Figure 34, in which the proportionalities $A_k = \lambda_k N_k$ are based on Eq. (75).

To give an example for a decay chain, I should mention that ^{224}Ra , introduced in Eq. (68) as the daughter of ^{228}Th , is itself an α emitter thus doubling as the parent of ^{220}Rn , that particular isotope of the element radon which is called thoron in some fields (see also the legend of Figure 4). Actually all three of them are members of a long *decay chain* shown in the upper left panel of Figure 51:

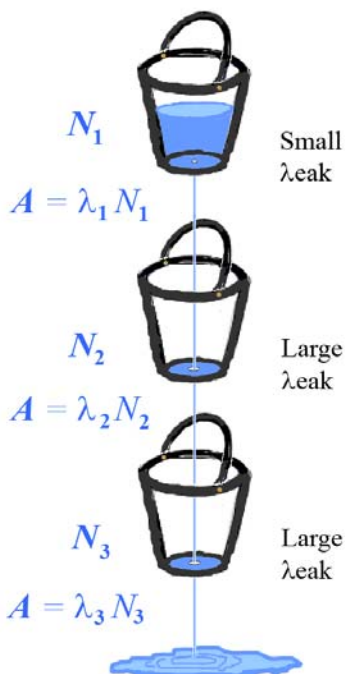


Figure 34: The ‘leaking bucket’ metaphor of secular equilibrium. If the uppermost bucket (primary parent) has the smallest leak (λ), then the water leaking out flows right through the rest of the buckets

¹⁷ A short condensation of it is also available in Hungarian ([Distributions H.pdf](#))

¹⁸ A short condensation of it is also available in Hungarian ([Distributions H.pdf](#))

underneath (daughters). Note that at equilibrium only the activities (flow rates) are equal but not the quantities of the individual members. The larger is λ , the smaller is N .

The decay schemes in Figure 36 demonstrate cases when there is more than one possibility for a radionuclide to decay. These alternative ways of decay are called *branches*. Thinking along the line presented by Figure 34, there is also an analogy between the activities A_k and the flow rates of water running through parallel leaks of different cross-sectional areas (λ_k) from the same bucket. Figure 35 makes it clear that the *branching ratios* can be expressed by the decay constants of the individual branches either as simple ratios of the partial decay constants λ_1, λ_2 , etc.:

$$A_1 : A_2 : \dots = \lambda_1 : \lambda_2 : \dots \quad (77)$$

or as fractions/percentages relative to the total $\lambda = \sum \lambda_k$.

The *yield of fission products* (Y_k , given as a fraction of the SF events when the k th fission product is formed) is a similar concept to the branching ratio. If N_k is the number of the atoms produced in the k th branch (which may or may not decay further, but which are considered stable for the present purpose), we can write:

$$A_1 : A_2 : \dots = N_1 : N_2 : \dots = \lambda_1 : \lambda_2 : \dots \quad (78)$$

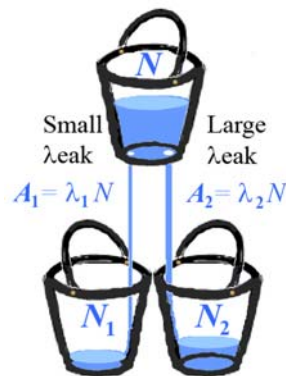


Figure 35: The ‘leaking bucket’ metaphor of branching decay. If the upper bucket (parent) has two leaks of different cross-sectional areas (λ_1 and λ_2), then both the flow rates (A_1 and A_2) of water and the contents (N_1 and N_2) of the buckets underneath (daughters) will be proportional to the cross sections of the leaks. The total flow rate ($A = A_1 + A_2$) will be determined by the total cross section ($\lambda = \lambda_1 + \lambda_2$) of the leaks, and the branching ratios (A_1/A and A_2/A) will be given by λ_1/λ and λ_2/λ . The phrasing of the metaphor also suggests an analogy between the partial decay constants (λ_1 and λ_2) of branching decay and the partial cross sections (σ_1 and σ_2) of different ‘channels’ of nuclear reactions.

Decay schemes are graphic representations of the possible outcomes of the decay of one or more nuclides. They may be quite intricate full of numerical data on level/transition energies, mean lives/half-lives and branching ratios. Those shown in Figure 36 are simplified for clarity’s sake. With simplified schemes like these it is customary to use slanting arrows to represent decays that change the atomic number. Arrows pointing to the left show that Z decreases (α, ϵ), those pointing to the right mean that Z increases (β^-). The different types of γ decay (e.g., γ emission and IC) are always represented by vertical arrows. The arrow of β^+ decay is only broken to call attention to the fact that this type of decay can only take place if Q_ϵ is large enough to cover the energy expense of producing an electron–positron pair which costs $2m_e c^2 = 1.022$ MeV.

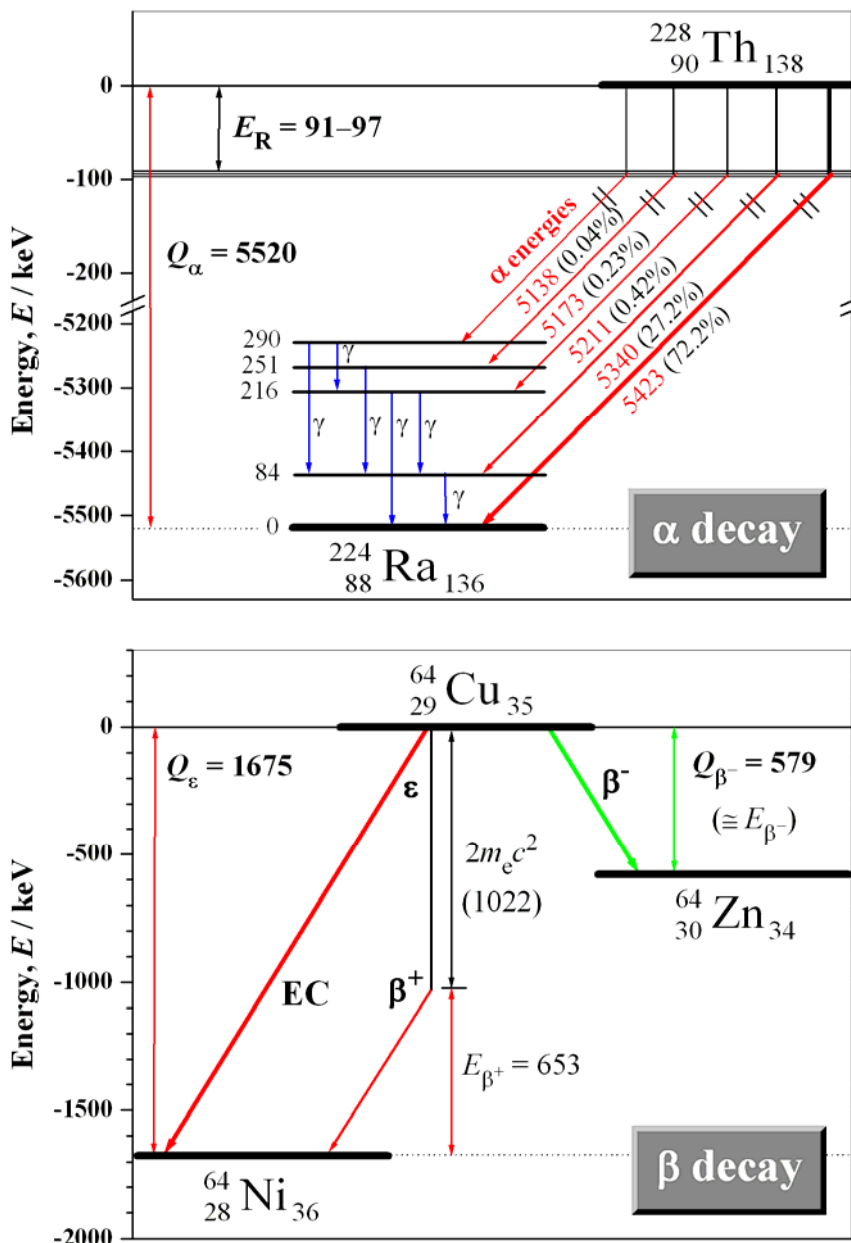


Figure 36: Decay schemes of alpha and beta decay. The numbers indicate energy in keV. The α decaying nuclide ^{228}Th on the upper panel is the second member of the $4n+0$ series (Figure 51). It is a typical example of its kind with the branching ratio (given as percentage) showing very strong dependence on the α energy E_α : the higher E_α , the ‘stronger’ the branch. (See the Geiger–Nuttall plot in Figure 19.) The level scheme of the daughter is by far not complete (see for detailed level schemes at <http://www.nndc.bnl.gov/chart>, *Chart of Nuclides database, National Nuclear Data Center*, where the information to this figure is extracted from). Only those levels are shown that are reached by the α decay of the parent. Note also that about 1.8% of the Q -value is deposited on the daughter as recoil energy E_R . (The higher E_α , the larger is E_R : hence the blurred appearance of the line from which the red slanting arrows start.) This small fraction still amounts to almost 100 keV, the equivalent of ~ 1 GK, which makes recoil atoms really ‘hot’. The β decaying ^{64}Cu is one of the 50 or so odd- Z -odd- N nuclides that decay both by β^- (39%) and by ϵ (61%). (See the spectra in Figure 58.) The ϵ branch is divided between β^+ (17.4%) and EC (43.6%).

8.6. Radionuclides on Earth

Some of the radionuclides shown by nuclide charts can be found on Earth under natural

conditions. These *naturally occurring radionuclides* belong to three classes.

Primordial radionuclides have long half-lives and therefore have survived the 4.5 billion or so years since the formation of Earth and the Solar System. There are about 26 such nuclides including the *primary parents* of the three naturally occurring decay series in Figure 51 (^{232}Th , ^{235}U , and ^{238}U), but so are ^{40}K ($T_{1/2} = 1.28 \text{ Ga}$) and ^{87}Rb ($T_{1/2} = 48 \text{ Ga}$) as well. (Note that in physical cosmology, the adjective primordial is used for stable nuclides formed in the very young universe, such as deuterium, ^2H , the heavy isotope of hydrogen.)

Secondary natural radionuclides (about 45) are the relatively short-lived members of the natural decay chains continuously re-produced by their primary parents. The isotopes of radon, e.g. (which receive much attention due to their environmental importance) are formed from the natural uranium and thorium content of rocks. Of the radon isotopes the following two are most common: ^{222}Rn (descendant of ^{238}U , the primary parent of the $4n+2$ series) and ^{220}Rn (descendant of ^{232}Th , the primary parent of the $4n+0$ series).

Induced natural radionuclides, also called *cosmogenic radionuclides*, (about 10) owe their existence to cosmic rays that continuously produce them from stable nuclides via nuclear reaction. Two of them—*radiocarbon* ^{14}C and *tritium* ^3H —are produced by the nuclear reactions $^{14}\text{N}(n,p)^{14}\text{C}$ and $^{14}\text{N}(n,t)^{12}\text{C}$, respectively (where t is triton, the nucleus of tritium).

The rest of the radionuclides on the nuclide chart (well over 2000 now) are all *artificially produced* including ^{22}Na , ^{60}Co , and ^{137}Cs .

9. Towards Greater Stability—Radioactive Decay

9.1. Radioactive Decay and the Chart of Nuclides

Figure 37 shows the Chart of Nuclides colored according to different levels of the average binding energy per nucleon thus presenting a contour map of the valley of stability. *Stable nuclides*, however, are found not only in the deepest part of the terrain (see the black ‘pit’ containing among others the iron and its neighbors), but almost all along the bottom of the valley up to its upper quarter as shown by the black cells in Figure 38.

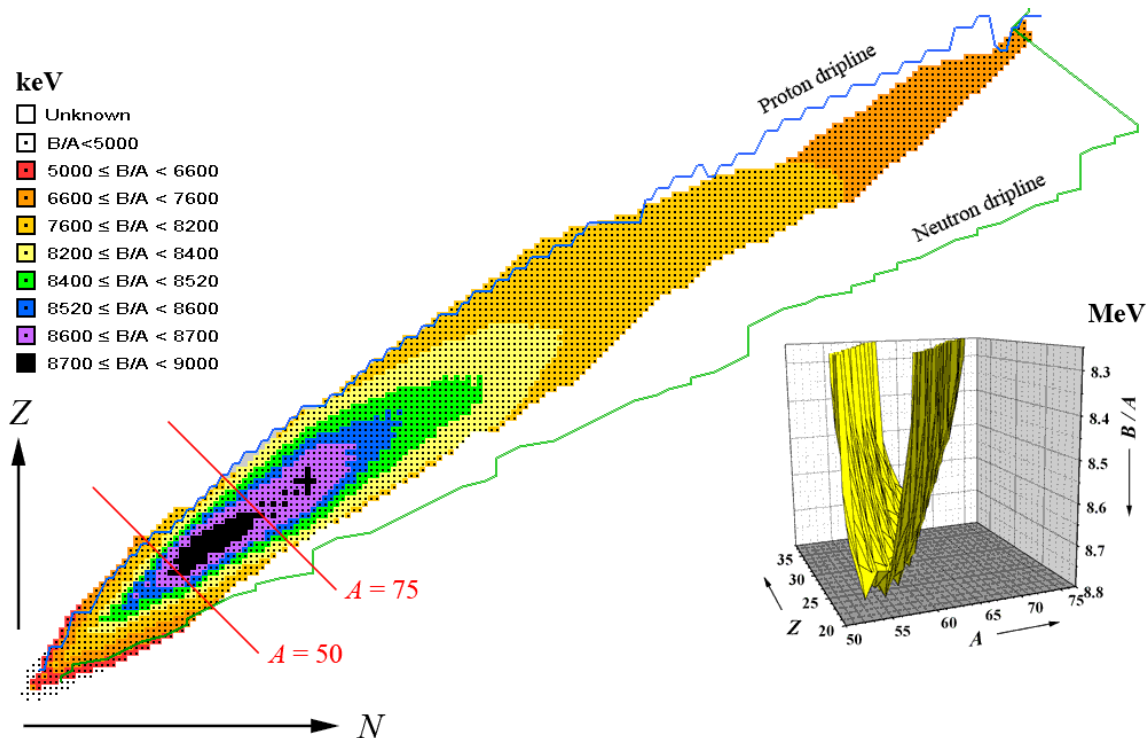


Figure 37: Chart of Nuclides colored according to different levels of the average binding energy per nucleon. The main figure was created by using *Nucleus-Win* http://amdc.in2p3.fr/web/nubdisp_en.html, a free software, produced by AMDC at CSNSM-Orsay. The driplines are results of theoretical calculations and indicate the estimated limits beyond which the captured proton or neutron ‘instantaneously’ evaporates again from the nucleus. The 3D inset in the lower right corner shows the section of the ‘valley of beta stability’ between the isobars for $A = 50$ and $A = 75$ that enclose the deepest part of the valley with nickel, iron and their neighbors. The basically parabolic cross section of the valley along the isobars has a more or less ragged appearance for any fixed value of A with the concrete shape depending on whether A is even or odd (Figures 43 and 44).

In 2006 the approximate number of stable elements was about 228. (A few decades before their number were still believed to be over 260, but about three dozen of those turned out to undergo very slow decay.) Starting from the light nuclides, the bottom of the valley slopes rather steeply down to the absolute minimum which is reached ^{62}Ni , which is followed by ^{58}Fe and then by ^{56}Fe in the contest for stability. (It is interesting to note that, in spite of this, the third of the contest is much more abundant than the winner two, because the production of ^{56}Fe —and of iron in general—is favored by the processes of nucleosynthesis. As a matter of fact, the isotopic abundance of the winner ^{62}Ni is rather low even among the rest of the isotopes of Ni as we can see in Figure 77.) Then the bottom of the valley gently slopes up

indicating less stability, until stability stops at Bi. Beyond Bi and up the parabolic walls of the valley we can only find radionuclides. The latter—depending on which side of the valley they occupy, what their ‘altitude’ is and how far along the valley they are situated—seek better stability by undergoing different modes of radioactive decay.

Figure 38 shows the Chart of Nuclides colored according to the most common decay modes.

The theoretical *driplines* mark the borders of the canyon of the stability on the plateau of absolute instability beyond which it is not feasible for a nucleon to join a nucleus.

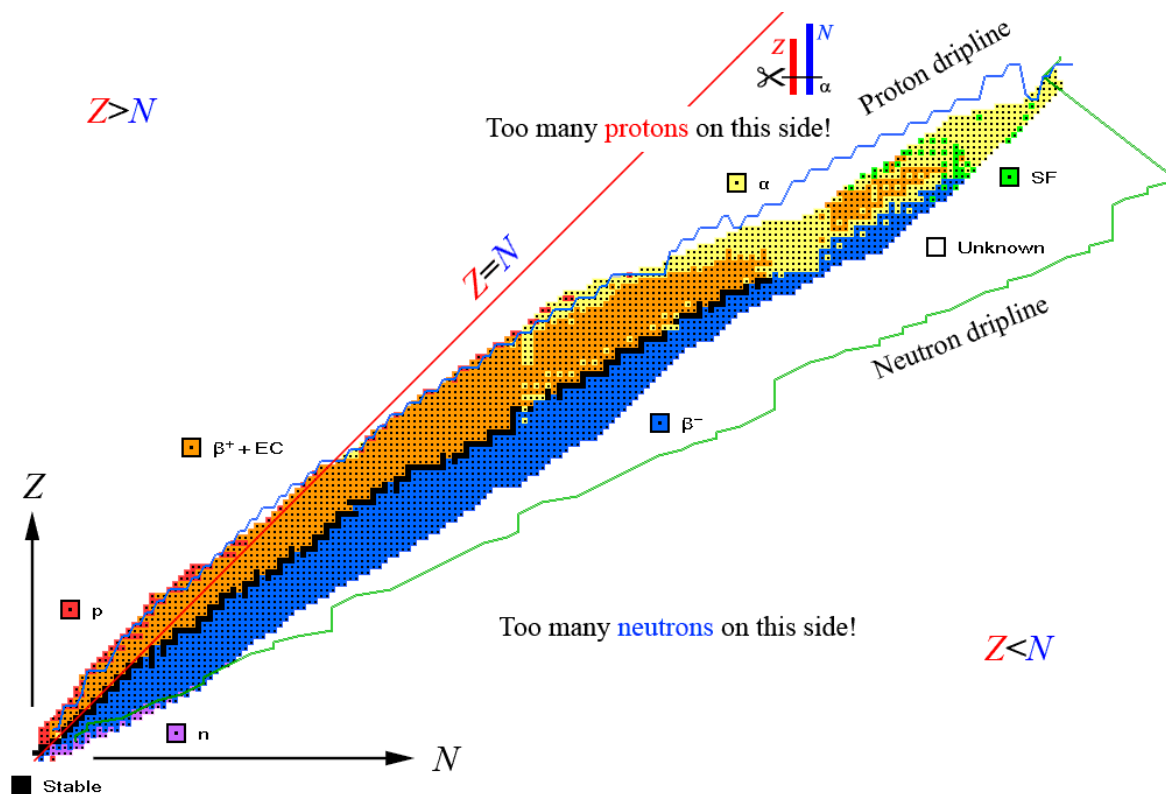


Figure 38: Chart of Nuclides colored according to decay mode (created by using *Nucleus-Win* http://amdc.in2p3.fr/web/nubdisp_en.html, a free software, produced by AMDC at CSNSM-Orsay). The details are explained in the text. The drawing with the scissors in the upper part of the figure (just below the line $Z = N$) helps to understand why α decay can decrease the relative number of protons in a neutron-deficient nucleus in spite of the fact that the α particle takes away protons and neutrons in equal number. Note that α decay only occurs below the line $Z = N$, where $Z < N$. This means that the neutron deficiency is only relative and not absolute. The rest is obvious from the diagram: cutting off equal lengths of two unequal sticks makes the shorter one (Z) relatively even shorter than the other (N).

The black zigzag in the bottom of the valley is occupied by stable nuclides for which the ratio Z to N is optimal. If it were only for thermodynamics, the only stable nuclide would be ^{62}Ni sitting at the deepest point of the valley. In that case the whole Universe would be a huge ball of nickel, so to say, but isn't. Fortunately for us carbon-based life forms, we live in a relatively young Universe still far from this kind of stability (see the dominance of the lightest elements H and He in Figure 22). Under normal terrestrial conditions motion along the bottom of the valley is frozen or very-very slow, but humankind has already reached a level of technical development which makes it possible for us to accelerate the motion down the valley (fission weapons and fission reactors) and up the valley (fusion bombs and—hopefully within a few decades—the fusion reactors of the future) in order to get energy by bringing nuclei closer to iron.

On the ‘northern’ slopes of the valley, where there is relative *neutron deficiency*, the dominant decay process is ϵ (β^+ and/or EC). Alpha decay only becomes dominant for $A>210$, but then, above $A=230$ and $Z=100$ it gets strong competition from spontaneous fission (SF).

Remembering that the Coulomb barrier of the nucleus is lower for protons than for α particles, it is puzzling that Nature has chosen such an awkward way like α decay to get rid of the relative proton excess of neutron-deficient nuclei. As a matter of fact, the straightforward solution, i.e. spontaneous (not β -delayed) proton emission was first observed as late as 1970 with a nuclear isomer. The first ground-state nucleus to undergo *proton decay* was only observed in 1981. The reason why α decay is preferred to p decay lies in the remarkably high stability of the doubly-magic ${}^4\text{He}$ nucleus (see Figure 24). This makes it energetically more feasible for the nucleus to emit a whole α particle than a single proton, except in the vicinity of the proton dripline. However, not only proton decay, but also *two-proton decay* has been observed in at least one ground-state nuclide (${}^{45}\text{Fe}$, 2002).

On the ‘southern’ slopes of the stability valley β^- decay dominates all the way down to the neutron dripline, however for very large A values it also gets competed both by α decay and SF. For instance, ${}^{238}\text{U}$, the primary parent of the $4n+2$ series is one of such nuclides (see Figure 39).

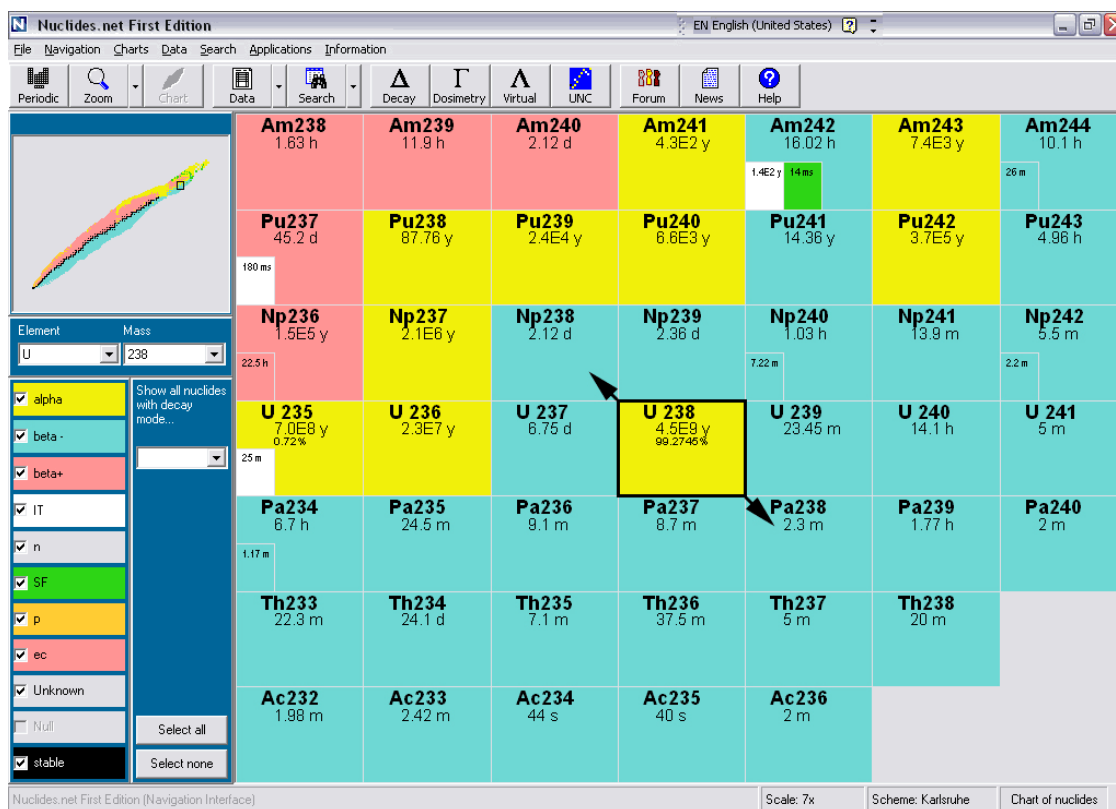


Figure 39: ${}^{238}\text{U}$, the heaviest of naturally occurring nuclides, is situated on the ‘southern’ side of the stability valley. This can be seen from the fact that both of its isobaric neighbors indicated by arrows are β^- decaying nuclides. Still, it undergoes α decay with a very weak branch of SF the possible products of which are shown in Figure 47. (The figure has been prepared from the screen picture of *Nuclides.net*.)

9.2. Investigation of the Spontaneity of Beta and Alpha Decay

As mentioned earlier, the Q -value is a physical quantity of energy dimension that can be used

for the characterization of processes like radioactive decay and nuclear reactions. To spare the reader the trouble of looking up the respective formulae I am citing the definition:

$$Q = \sum_A m c^2 - \sum_\Omega m c^2 = \sum_\Omega E_{\text{kin}} - \sum_A E_{\text{kin}} = \Delta E_{\text{kin}}, \quad (79)$$

where m stands for the (atomic or particle) masses and E_{kin} for the kinetic energies (in the general sense meaning that the whole $E_\gamma = h\nu$ energy of a photon is considered as kinetic energy), 'A' means the reactants and 'Ω' the products. Or, with more user-friendly notation, we can also write:

$$Q = \left(\sum_A m - \sum_\Omega m \right) \times 931.494 \frac{\text{MeV}}{\text{u}} = \left(\sum_A M - \sum_\Omega M \right) \times 931.494 \text{ MeV}, \quad (80)$$

where u is the unified atomic mass unit and M is the nuclidic mass or the particle mass in u as explained in connection with Eq. (17):

$$M = m / \text{u}. \quad (81)$$

Note that instead of Eq. (80) we could also have written:

$$Q = (-\Delta M)_{A \rightarrow \Omega} \times 931.494 \text{ MeV}, \quad (82)$$

since the 'mass change' of the process is $\Delta M \equiv \sum_\Omega M - \sum_A M$, i.e. the sum of mass of the products (Ω) minus that of the reactants (A).

As we already know, *spontaneous processes* are distinguished from all other processes in that they are to satisfy the condition:

$$Q > 0 \quad (83)$$

expressing that they need no 'external help' to undergo as is clear from the fact that they produce more energy than they consume. (Note that the total kinetic energy of the products is larger in this case than that of the reactants.)

We are going to check the decays mentioned in the title as regards the above criterion. We will see that there are considerable differences between the various types of β decay.

Beta minus decay, whose prototype (the decay of a free neutron) has been given as an example of spontaneous processes in Figure 8, is only one of the three basic types of beta decay. The equation of β⁻ decay for atoms is as follows:



The story that goes with the equation is this. 'A neutron in the nucleus of a *neutral atom* ${}_Z^A \text{X}_N$ undergoes beta minus decay and transforms to a proton while an electron and an antineutrino are emitted from the nucleus. Therefore the number of neutrons N decreases to $N-1$ and that of the protons Z increases to $Z+1$. Thus the total nucleon number $A = (N-1)+(Z+1) = N+Z$ remains constant indicating that β⁻ decay is an *isobaric process*. Since the number of orbital electrons also remains the same (i.e., Z), what is formed is a +1 isobaric ion of the next element on the periodic table. So we have an extra electron (i.e. the β⁻-particle) and a hole in one of the electronic shells of the atom. The hole and the free electron cancel each other, and we wind up with a neutral atom of ${}_{Z+1}^A \text{X}_{N-1}$ '.

As I have pointed out above, beta minus decay (as all basic types of beta decay) is an *isobaric*

process. The members of a sequence of such decays all remain on the same isobaric line characterized by A (see Figure 40). Note that if A is even (e.g. 118), then the subsequent $Z-N$ combinations will be alternatively ...ee, oo, ee, oo, ... (where e means even and o means odd). For an odd value of A (e.g. 119), the sequence will be ...eo, oe, eo, oe,

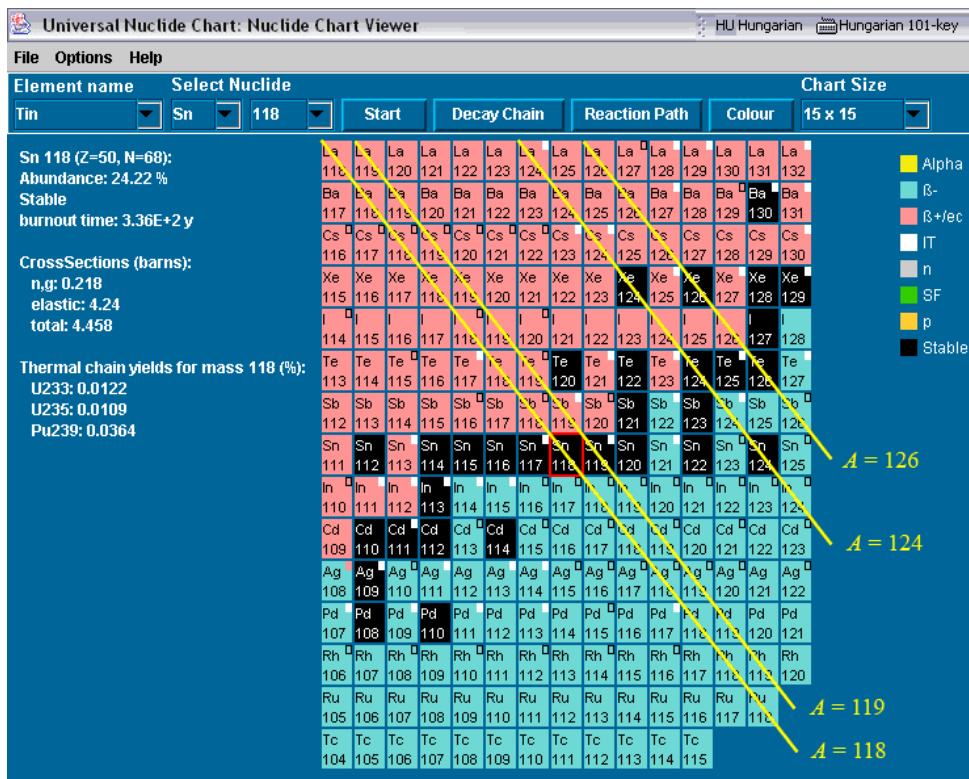
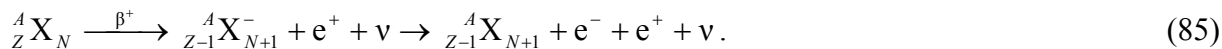


Figure 40: Screen picture of an electronic nuclide chart from the CD-ROM supplied with the book Radioactivity–Radionuclides–Radiation (*Universal Nuclide Chart, Copyright European Communities, 2005*). Black cells in this particular case indicate stable and primordial nuclides, colored cells radionuclides. Different cell colors indicate different types of radioactive decay as explained by the legend on the right. The yellow slanting lines drawn ‘by hand’ connect the isobaric nuclides shown in Figure 43.

The atomic equation of *beta plus decay* (when a *bound* proton spontaneously transforms to a *bound* neutron while a positron and a neutrino is emitted by the nucleus) is as follows:



Note that this time the process written for neutral atoms yields a negatron and a positron which do not cancel each other. As a matter of fact, when they annihilate with each other, the energy equivalent of two electron masses ($2m_e c^2 = 1022 \text{ keV}$) is released, which must be considered when writing up the energy balance of the transformation.

There is also a third basic type of β decay called *electron capture* (EC), which—similarly to β^+ decay—involves the conversion of one bound proton to a neutron. If it is not important to distinguish between the two competing processes (i.e., between β^+ and EC), then I will denote them by the Greek letter ε (which, by the way, is also used in the literature as an alternative notation for EC). Electron capture is not really a decay in the strict sense, because it is based on the interaction of the nucleus with an (atomic) electron (most likely a K electron, because 1s electrons have the highest probability density in the nucleus making them best candidates for being captured). The chances that an orbital electron will be available for the nucleus

whenever it ‘feels like’ to undergo EC increase with the atomic number Z for two reasons:

- The innermost part of the atomic shells (especially the K-shell) gets contracted as the nuclear charge increases.
- Large- Z nuclei tend to be heavier, which means they have larger volume because the nuclear volume is proportional to the mass number A according to Eq. (43).

Therefore EC alone (i.e. without competing β^+ decay) preferably occurs with heavy nuclei as shown in Figure 41.

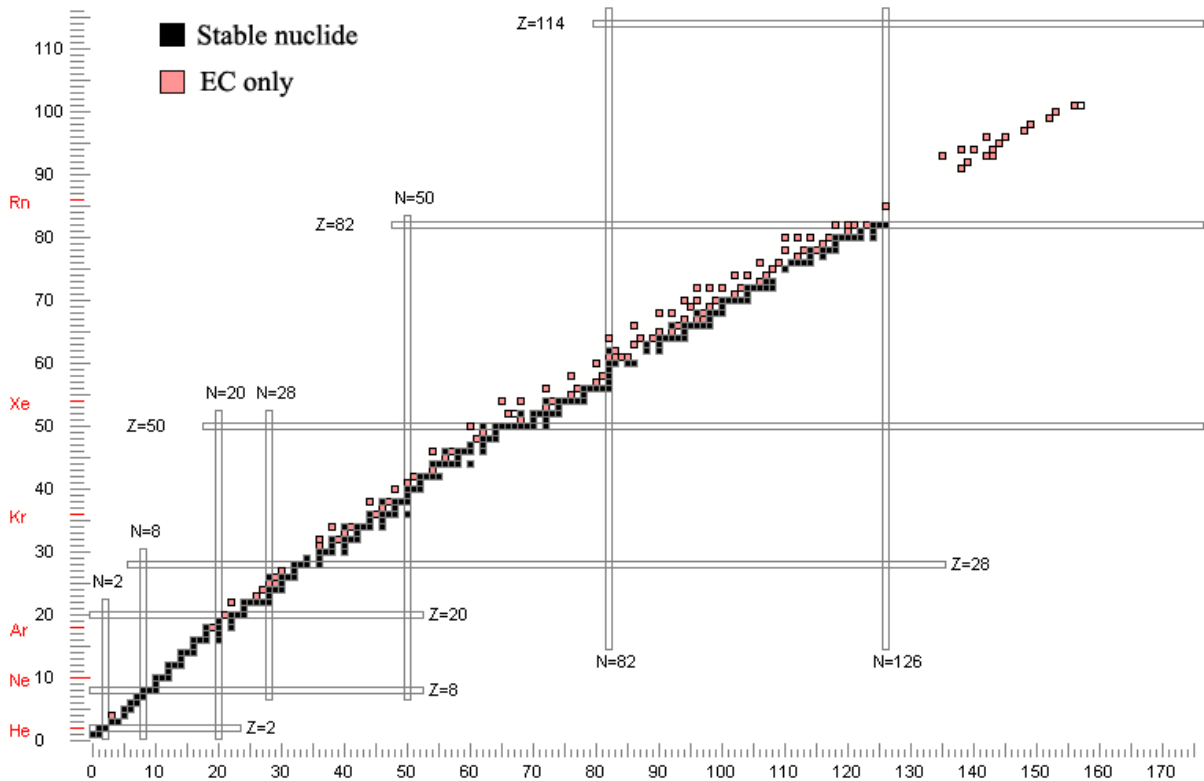


Figure 41: This figure has been prepared using the Nuclide Explorer function of *Nucleonica* (<http://www.nucleonica.net/>). Only two types of nuclides have been selected for displaying: stable ones and those decaying exclusively via EC. There is a clear preference for EC to occur with heavy nuclei which have much larger overlap with the wave function of orbital electrons especially from the 1s shell (K electrons).

The atomic equation of EC is as follows:



where $E_K > 0$ is the binding energy of a K electron, which will be released eventually as the orbital electrons find their places on the lowest-energy shells. As we see, this time the story (and the equation) is somewhat different, because the number of protons and that of the orbital electrons decrease simultaneously, and therefore a neutral atom transforms into another neutral one. However, the atom is formed in a highly excited state (hence the symbol *), because there is a hole in one of the inner shells (most often in the K shell as mentioned before).

Note that the sole purpose of the above stories is to help balancing the equations. The real stories are much more complicated, however, because the decay of the nucleus is an enormous

trauma in the life of the atom causing multiple ionization, etc. For instance, in the case of EC, [the hole in the inner shell gets filled](#) in a short time, and therefore the decay is accompanied with the emission of *characteristic X-rays* and/or *Auger electrons*. The electron, while being captured, is accelerated and therefore *inner bremsstrahlung* is also typical of this mode of decay. *Gamma radiation* is also common with all types of β decay, because the daughter nucleus is often ‘born’ in one of the possible excited states which usually lose the excess energy by gamma decay.

The general conditions for spontaneity phrased by Eqs. (80) and (83) can be applied to the special cases of beta decays as follows.

Neglecting the mass of the antineutrino in Eq. (84) (which can be done according to Figure 8 and Table 2) we can immediately write the condition of spontaneity for beta minus decay in terms of the difference between the atomic masses of the parent and daughter:

$$Q_{\beta^-} = (-\Delta M)_{\beta^-} \times 931.494 \text{ MeV} > 0, \quad (87)$$

where:

$$(-\Delta M)_{\beta^-} = {}^A_Z M - {}^A_{Z+1} M. \quad (88)$$

For the other two types of beta decay, the nuclidic-mass difference between parent and daughter is:

$$(-\Delta M)_{\epsilon} = {}^A_Z M - {}^A_{Z-1} M. \quad (89)$$

Let us introduce the following energy quantity related to the above mass difference:

$$Q_{\epsilon} = (-\Delta M)_{\epsilon} \times 931.494 \text{ MeV}. \quad (90)$$

Using the above notation we get from Eq. (85):

$$Q_{\beta^+} = Q_{\epsilon} - 2m_e c^2 = Q_{\epsilon} - 1022 \text{ keV} > 0,$$

which yields the following condition of spontaneity for beta plus decay:

$$Q_{\epsilon} > 1022 \text{ keV}. \quad (91)$$

For EC we get from Eq. (86):

$$Q_{\text{EC}} = Q_{\epsilon} - E_K > 0, \quad (92)$$

which yields the following condition of spontaneity for electron capture:

$$Q_{\epsilon} > E_K. \quad (93)$$

Comparing Eqs. (91) and (93) we can conclude that EC has less severe energetic conditions than β^+ decay, because E_K is only about 150 keV even for ${}_{102}\text{No}$. On the other hand, β^+ decay can become very fast if the 1022 keV threshold is considerably exceeded by the energy equivalent of the mass decrease. (See also Figure 42.)

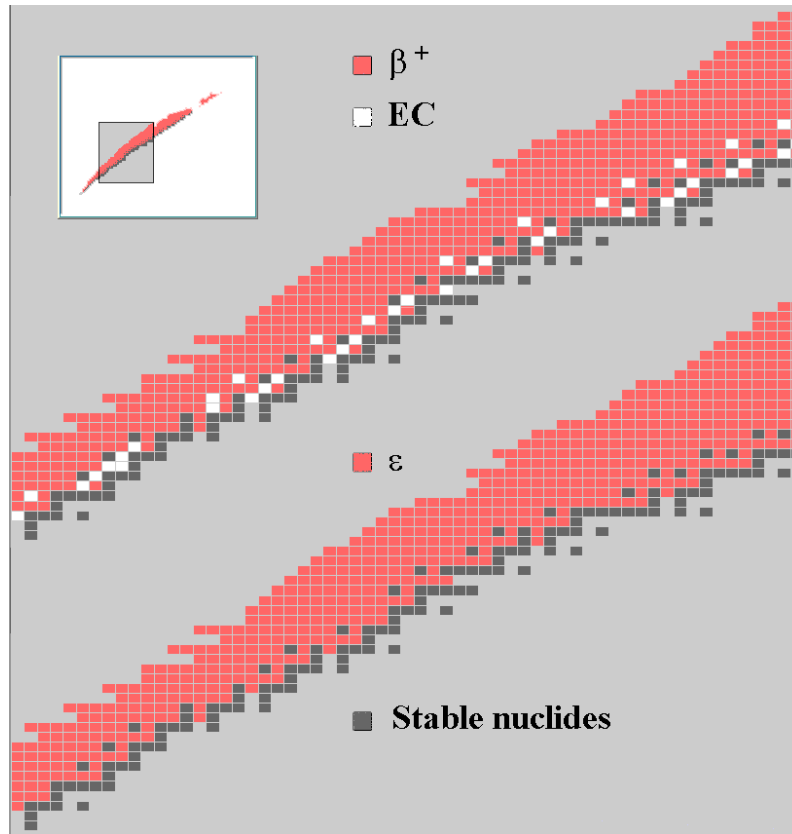


Figure 42: This figure has been prepared using screen pictures of the software *Nuclides.Net* whose database makes it possible to display the two types of ‘ ϵ decay’, i.e. beta plus decay (β^+) and electron capture (EC), separately. The inset shows which section of the Nuclide Chart is displayed by the major diagrams. In the upper diagram, only the cells of stable and the β^+ decaying nuclides have been colored. Nuclides indicated by the white cells can only decay by EC, because—being close to the bottom of the stability valley— β^+ decay is not always feasible. Note that the latter can only take place, if the mass decrease available to ϵ is at least $2 m_e$ (~ 1.02 MeV). However the mass parabolas that determine the profile of the valley are relatively flat at the minimum, which often makes impossible a mass change that large. (See Figures 43 and 37.)

In order to judge the stability of a nuclide against various types of beta decay, it is useful to plot isobaric data calculated for the *mass excess* Δ defined as

$${}^A_Z\Delta = ({}^A_ZM - A)u. \quad (94)$$

Note that for isobaric nuclides (see Figures 43 and 44) the mass excess gives the same plot as the atomic mass $m_a = M u$, except that the data-points/curves are shifted by a constant value $A u$ towards the origin. Figure 43 also helps to understand why exactly the black boxes are those in Figure 40 that contain the stable nuclides along the slanting isobaric lines that are drawn ‘by hand’ in the screen picture.

Mass parabolas—presented in Figure 43 as mass-excess vs. atomic-number plots for isobaric nuclides—are characteristically different for odd- A nuclides (lower right panel) and even- A nuclides (the rest of the panels). As follows from Eq. (59), odd- A isobaric nuclides are supposed to line up along a single parabola. On the other hand, even- A isobaric nuclides occupy two parabolas, because the parabola of odd- Z and odd- N (oo) combinations is shifted up towards less stability, whereas that of the even- Z and even- N (ee) combinations is shifted down towards higher stability.

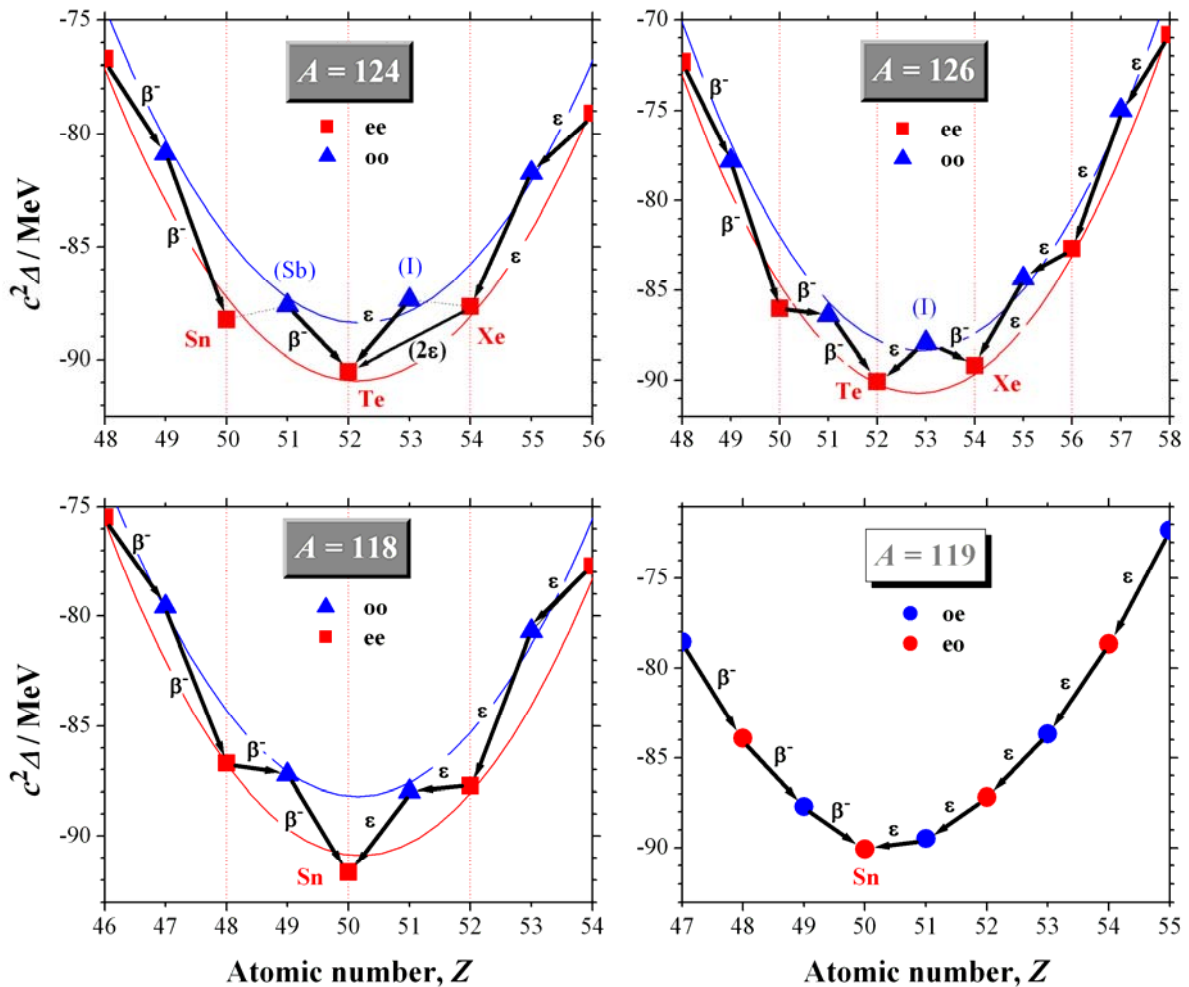


Figure 43: Mass parabolas for the isobaric nuclides connected by slanting lines in Figure 40 in the vicinity of highest stability (characterized by the minimum of mass). Note the striking difference between the only odd- A plot (lower right panel) and the rest of the plots representing even- A nuclides. See the text for further explanation.

The simplest types of β decay (i.e. ε and β^- decay) are spontaneous isobaric processes changing the atomic number by one unit at a time. Spontaneity demands that the rest energy (mass) should decrease in each step as indicated by the arrows in Figure 43 that represent experimentally observed decays. As a consequence of this, the number of beta-stable nuclides for any odd value of A can only be one. The only beta-stable nuclide can be either an even-odd one (such as in the above example of ^{119}Sn) or an odd-even one with equal probability (see the lower panels in Figure 23).

On the other hand, the number of beta-stable even- A isobars can be 1, 2 or even 3 (see the upper panels in Figure 23). Note that in the upper right panel of Figure 43 there is an unstable nuclide (^{126}I) that can reach stability both by β^- decay and by ε (see the decay scheme in Figure 45). Such an ‘odd’ behavior can only be observed with odd-odd (oo) nuclides (there are about fifty such cases altogether). Note that on the upper left panel, the nuclide ^{124}Xe is not absolutely stable. It decays to ^{124}Te very-very slowly (with a half life almost ten million times longer than the age of the Universe). The transformation is made possible by 2ε decay: a type of [double beta decay](#), when either two positrons are emitted or two electrons are captured with the simultaneous emission of two neutrinos. Note also that ^{124}Sb and ^{124}I do not show the peculiar behavior of ^{126}I , although both of their neighbors have lower mass as one can see

from the slant of the dotted lines connecting them. This shows that the spontaneity criterion $Q > 0$ (which is satisfied in both directions) is only a necessary however not sufficient condition for the decay to occur. This is especially conspicuous in the case of β decay, where there is no Coulomb barrier to overcome. However, the probability of the decay becomes small if the energy to be released is small (like in this case), and there are other factors too which can affect the decay rate.

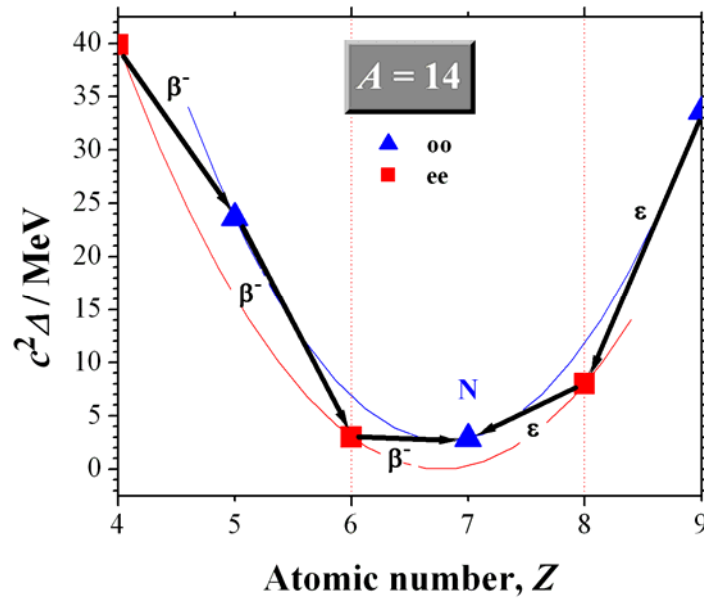
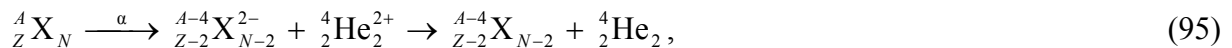


Figure 44: In only 4 out of the 163 stable even- A nuclides both Z and N are odd numbers (see the upper right panel in Figure 23). The above plot helps to understand the reasons. For light nuclei the mass parabolas are considerably steeper around the minimum than usual. Therefore, if the minimum happens to be near to an odd- Z value, then the neighboring even-even isobars may be shifted above the odd-odd one— ^{14}N this time—making it the most stable against all the ‘odds’.

The mass excess cannot be used directly to compare the relative stabilities of non-isobaric nuclides. However, the Q -value of any type of decay must be positive in order that it can occur. For instance, in the case of [alpha decay](#), when a $^4\text{He}^{2+}$ ion (i.e. an α particle) breaks free from the nucleus:



the necessary condition phrased in terms of the Q -value reads like this:

$$Q_\alpha = (-\Delta M)_\alpha \times 931.494 \text{ MeV} > 0, \quad (96)$$

where:

$$(-\Delta M)_\alpha = {}^A_Z M - {}^{A-4}_{Z-2} M - {}^4_2 M. \quad (97)$$

9.3. Gamma Decay

Alpha and beta decay etc. often leave behind an excited daughter nucleus (see, e.g. Figure 45). The excitation levels are discrete as follows from the shell model and can be quite complex. There are several ways for the excited nucleus to get rid of the excess energy.

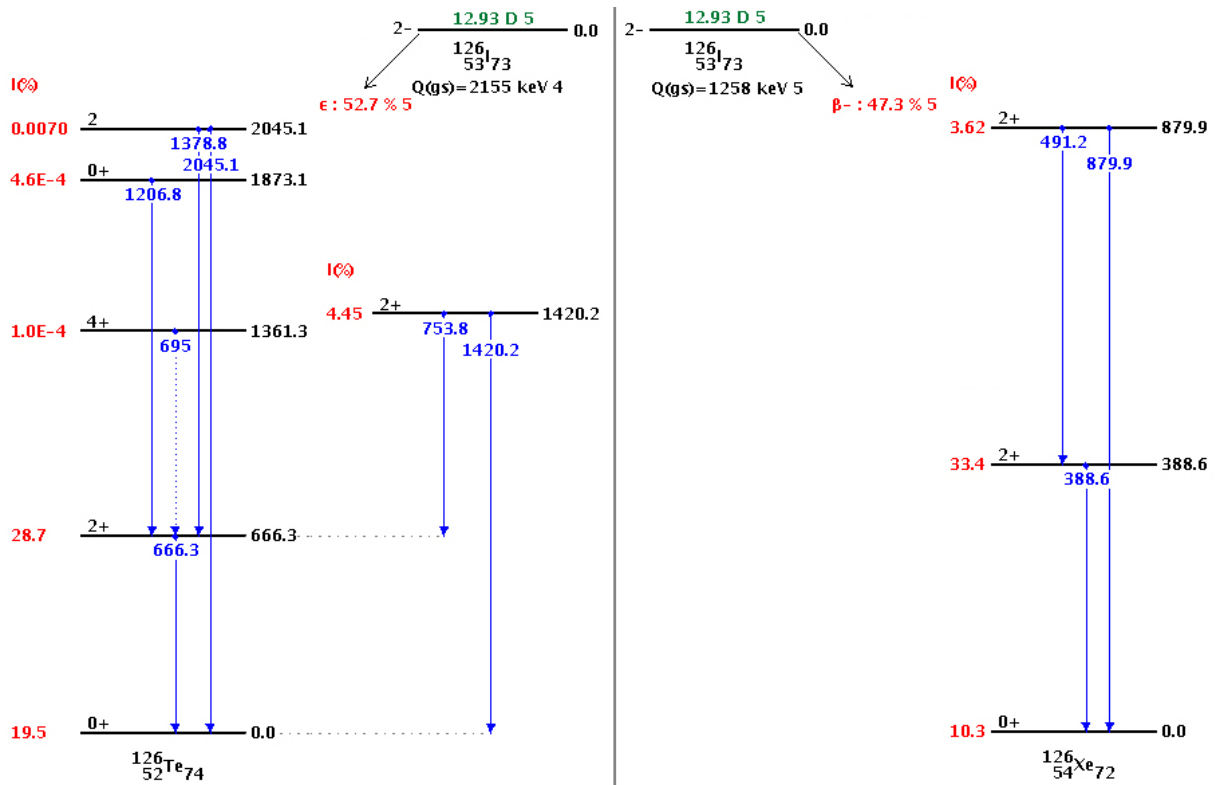


Figure 45: Decay scheme of ^{126}I undergoing both ϵ and β^- decay as seen on the upper right panel of Figure 43. (The half-life is shown in green.) The 52.7% contribution of the ϵ branch comes mainly from EC. β^- decay is only about 2/100 (1,01%) of the branch. Only those levels of the daughters are shown which are reached by the decay of the parent. $I(\%)$ indicates the percentage (red numbers) of all decay events landing at the given level. The blue numbers show the energy of the γ transition in keV, whereas the black ones the height of the level relative to the corresponding ground state (^{126}Te or ^{126}Xe). The symbols 2-, 0+ etc. indicate the nuclear spin and the parity of the state. (Information extracted from the Chart of Nuclides database, National Nuclear Data Center, <http://www.nndc.bnl.gov/chart>)¹⁹

The most common process is γ emission, when a γ photon takes away the energy difference between two nuclear levels. This is quite an analogous process to the characteristic X-ray emission or light emission of atoms.

The alternative process of γ emission is *internal conversion* (IC), when the energy difference between the nuclear levels is taken away by an orbital electron most probably from the K shell. Since the electron has to be released from the atom, its kinetic energy E_{e^-} will be accordingly lower than that of the photon:

$$E_{e^-} = E_{\gamma} - E_K, \quad (98)$$

where E_{γ} is the photon energy and E_K is the binding energy of the electron.

A less common alternative of γ emission is (*internal*) *pair production* (PP), when the excitation energy is converted to the mass and the kinetic energy of a positron–negatron pair. It is needless to say that PP can only take place if the energy is at least 1022 keV, the energy equivalent of $2m_e$. The frequency of PP events is still no more than $\sim 0.1\%$ of γ -events.

The above three processes are referred to as γ decay.

¹⁹ This database is one of those few places where the notation ϵ refers to the same thing as elsewhere in this text, i.e. β^+ decay and electron capture (EC) together, rather than EC alone.

Disregarding PP, the ratio of IC events to γ emission events is called the *conversion coefficient*, ranging from $\alpha = 0$ to infinity. The latter limit—meaning that γ emission is practically excluded—seems to be reached in certain cases. Internal conversion as the only way of de-excitation has been observed with nuclear isomers for which selection rules concerning multipolarity forbid the transition from the excited state to the ground state via photon emission. On the other hand, the way is open for internal conversion because K electrons, for instance, are always available with some probability in the nucleus ready to take away the excess energy of the latter. In general—owing to the similar probabilistic background—internal conversion as an alternative of γ emission prefers high- Z nuclides within the family of γ decays, same as electron capture (EC) as an alternative of beta plus decay within the family of β decays.

The name ‘internal conversion’, by the way, is a heritage from olden times when the phenomenon was thought of as a two-step process starting with the release of a γ photon which, however, gets converted to the kinetic energy of an orbital electron knocked out via photoelectric effect from the same atom. The fact that with some nuclides γ emission cannot be observed but conversion electrons get emitted disproves this model but the name stuck.

Sometimes, the excited state is relatively long-lived. As mentioned before, such states are called *nuclear isomers* or *metastable states* and are denoted ^{Am}X as opposed to other states (such as the ground state ^{Ag}X). The number of long-lived nuclear isomers culminates around magic values of N or Z . The half-life criterion for an excited-state nucleus to earn the status of a nuclear isomer (and thus to be considered an independent nuclide according to IUPAC) is creeping down with years. A couple of decades ago it was somewhere around 1 ms, now it is about 1 ns. (It also means that the number of atomic species considered as different nuclides has considerably increased during that period just because of this.)

Nuclear isomers normally reach a lower energy state by γ decay, which, in this particular case, is also referred to as *isomeric transition* (IT).

Nuclear isomers, however, can also choose other ways towards stability. Actually their discovery in 1921 was also connected with this type of behavior, namely, O. Hahn observed that ^{234}Pa (a β decaying isotope of protactinium) consists of two radioactive components with different half-lives (1.17 min and 6.7 h). The 1.17 min component turned out to be due to the β decay of the nuclear isomer ^{234m}Pa .

9.4. Fission

Spontaneous fission (SF) is the decay mode of the heaviest nuclei. Its Q -value is very high, on the order of 200 MeV, making SF decaying nuclei very powerful ‘time-bombs’—fortunately on the sub-microscopic scale.

SF is typically a binary process (although ternary fission also occurs with very low probability) meaning that the nucleus X scissions to two major parts called fission fragments F_1 and F_2 from which a couple of *prompt neutrons* evaporate within 1 fs or so. Thus the fission fragments transform to *primary fission products*²⁰ P_1 and P_2 :

²⁰ Note that there is no agreement in the literature in the use of the terms *fission fragment* and *primary fission product*. Some authors even consider the terms *fission fragment* and *fission product* as synonyms. Some of the latest literature uses the expression *fission fragments before and after neutron evaporation*. Anyway, I will use the terms in the sense that all *fission fragments* are *fission products*, but only a certain type of *fission products* are *fission fragments*.

$$X \rightarrow F_1 + F_2 \rightarrow P_1 + P_2 + \nu n. \tag{99}$$

The primary products of SF (just like those of induced fission IF) have unequal masses with a wide (and typically) bimodal mass distribution. Thus the following example of the SF of ^{252}Cf shows just one (and not the most frequent) combination of the large variety of primary products:



Note that the neutron numbers of the stable strontium isotopes are $N = 46 \dots 50$ and those of neodymium are $N = 82 \dots 88$. Therefore, the above example demonstrates that the primary decay products (in spite of the evaporation of prompt neutrons) are in the ‘southern’ neutron-rich side of the stability valley (see figure 46) and therefore they start a series of β^- decays leading down to the bottom of the valley.

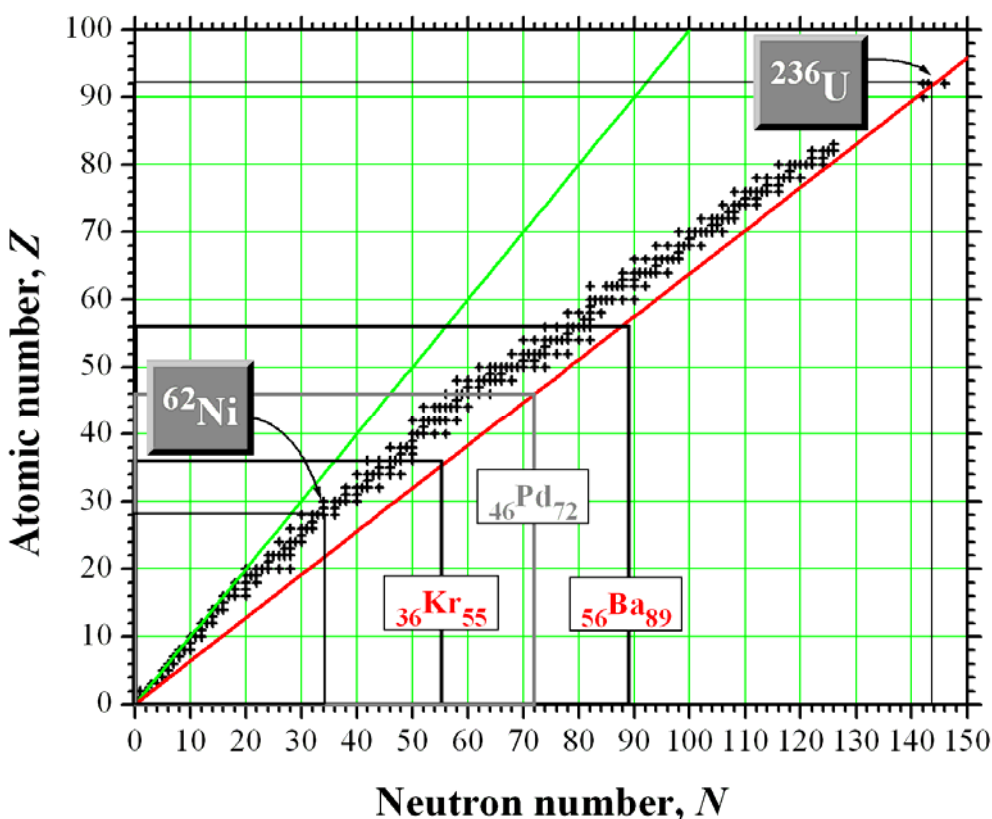


Figure 46: Nuclide map showing stable and primordial nuclides only to explain the beta activity of fission fragments. Since the valley of stability is bending away from the green line representing $Z = N$, the proton to neutron ratio of a fissile heavy nucleus is characterized by a less steep line similar to the red one ($Z \approx 0.64 N$), which crosses the ‘southern’ neutron-rich side of the valley. If the ^{236}U nucleus (taken only as an example²¹) were split symmetrically, then (disregarding prompt neutrons) two ^{118}Pd nuclei would be formed. We can easily check in a [nuclide chart](#) that the heaviest stable isotope of palladium, ^{110}Pd , is kind of an island of stability itself, surrounded by β^- decaying nuclides. It is true that most heavy nuclei split asymmetrically, but both fission fragments—like krypton (^{91}Kr) and barium (^{145}Ba) in the case indicated—fall to the same side of the valley. Note that even the lighter fragment is beyond the deepest point of the valley occupied by ^{62}Ni (see Figure 37).

Such a series is referred to as a *mass chain*, because—with β^- decay being an isobaric

²¹ ^{236}U is not a primordial nuclide. It is formed from ^{235}U as a result of the neutron capture leading eventually to fission.

process—all the members have the same mass number A as the primary product (if processes like β^-n —producing delayed neutrons—are disregarded which lead out from the isobaric chain). All decay products of the primary fission product are referred to as *fission products*. The term fission product also refers to the primary fission products and the fission fragments.

The distributions of fission products are characterized by various types of fission yields s of which two will be explained here and represented in the case of the SF of ^{238}U (see Figure 47).

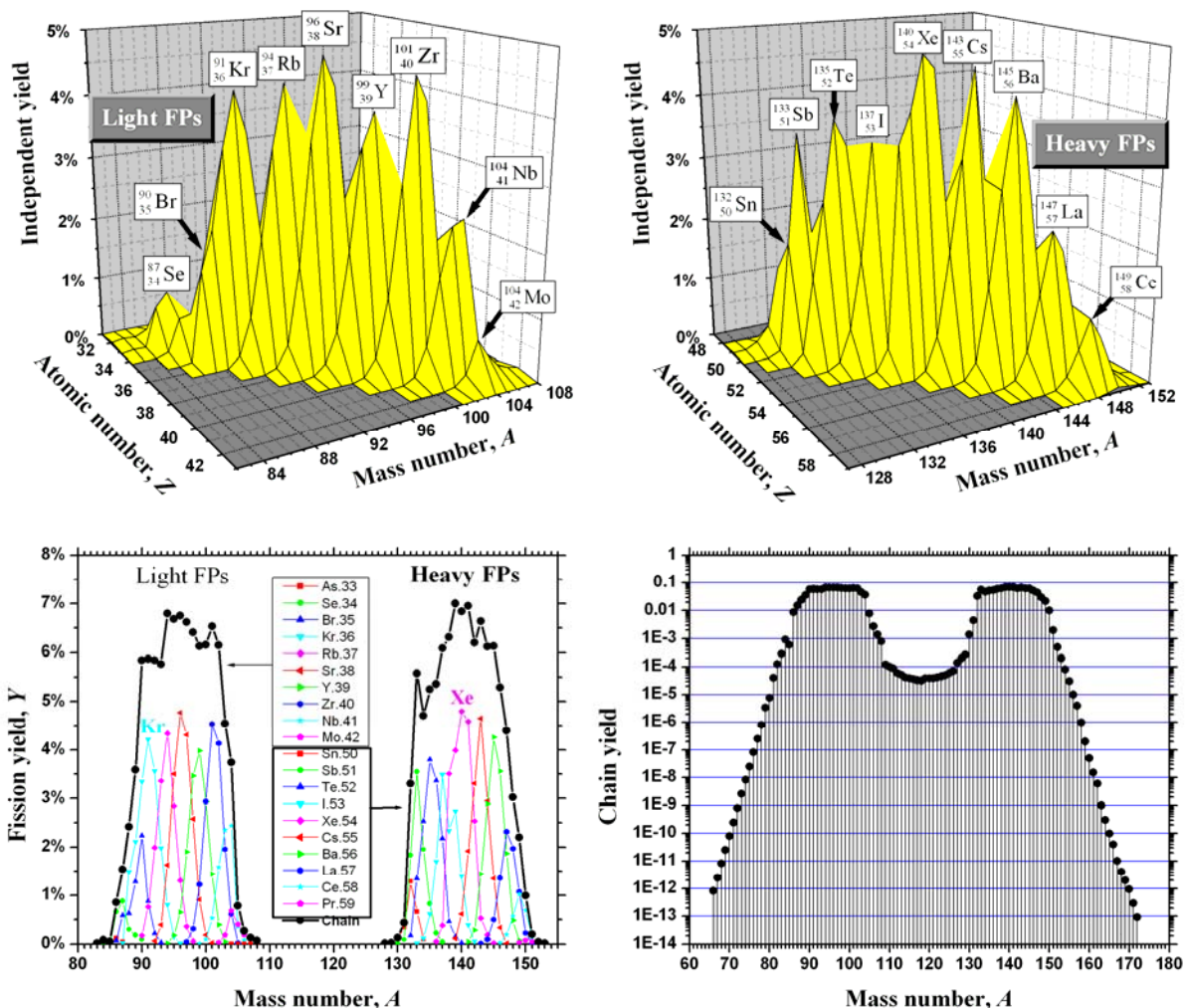


Figure 47: Independent fission yields (upper panels and the color graphs in the lower left panel) as well as chain yields (lower panels) for the SF of ^{238}U . The semi-logarithmic plot of the lower right panel shows a large variety of fission products, although the major products form two rather distinct peaks according to the linear plots. (Elements of $Z = 43\text{--}49$ are practically missing.) Note that both the light FPs and the heavy FPs contain a major noble gas component (Kr and Xe). Each colored curve in the lower left panel connects the independent yields of the isotopes of an element. The black envelop is the chain yield obtained by adding up the ordinates of the colored curves. (The data for the figures have been extracted from *Nuclides.net*.)

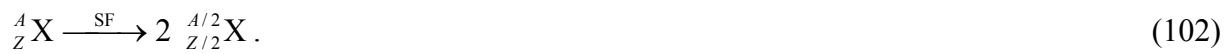
The *independent fission yield* (Y_{indep}) refers to individual nuclides ^A_ZX that are the primary products of SF. It gives the fraction of fission events leading to the formation of a given nuclide as a primary product. Since two nuclides are produced in each asymmetric SF event, adding up Y_{indep} values for all primary products (i.e. for all combinations of Z and A) gives a sum close to 2 instead of just 1. The Y_{indep} values are actually the density values of a 2D distribution (normalized to 2) over the Z - A plane (see the upper panels in Figure 47). The

values for a given Z show the relative contribution of the isotopes of the element Z to the primary products of the SF.

The *chain yield* (Y_{chain}) refers to the total of isobaric nuclides produced as a consequence of the SF (and the subsequent β^- decays). It gives the fraction of fission events leading to the formation of isobaric nuclides with a given A . It is a 1D distribution of A and can be regarded as the marginal distribution of $Y_{\text{indep}}(Z, A)$ obtained by adding up all values of Y_{indep} belonging to different Z s for a given A :

$$Y_{\text{chain}}(A) = \sum_Z Y_{\text{indep}}(Z, A). \quad (101)$$

The Weizsäcker equation (53) can also give an explanation for the instability of large- Z nuclei against spontaneous fission SF. For simplicity's sake let us consider that the nucleus splits in two equal parts (actually asymmetric fission is favored with the simultaneous emission of a few neutrons):



This can only happen if the binding energy per nucleon is larger for the *fission fragment* ${}^{A/2}_{Z/2}\text{X}$ than for the parent nuclide ${}^A_Z\text{X}$. Neglecting the pairing energy term in Eq. (59), we can easily get a minimum condition for the *fissility parameter* Z^2/A :

$$\frac{Z^2}{A} > \varphi \propto \frac{a_s}{a_c}. \quad (103)$$

The value actually obtained for the lower boundary ($\varphi = 15.2$) is obviously too low. It would namely predict fissility for ${}_{36}\text{Kr}$, one of the common lower-mass [fission products](#) of the [neutron-induced asymmetric fission of \${}^{235}\text{U}\$](#) (see Figure 46). Further-developed liquid drop models, considering among others that the skin of the nucleus (see Figure 13) is somewhat diffuse, set the value of φ somewhere between 40 and 50. Note, however, that for ${}^{238}\text{U}$, undergoing very slow SF, the fissility parameter is $92^2/238 = 35.6$, which means, that this parameter should be used carefully before arriving to premature conclusions. On the other hand, the parameters a_s and a_c appearing in Eq. (103) make it clear that the surface tension tries to keep the fissioning nucleus together, whereas the Coulomb repulsion tries to split it. The problem is the general tendency observed in Figure 28, namely, that the contribution of surface energy (providing surface tension) gradually decreases (at least relatively), while that of the Coulomb term increases. Therefore, if the fissility parameter exceeds the value of ~ 48 , then the initially spherical nucleus becomes unprotected from elongation and splits apart spontaneously without any Coulomb barrier (see Figure 48).

Strangely enough, it is the larger binding energy due to pairing that makes heavy odd- N nuclei more vulnerable to neutron-induced fission. This is also the reason why ${}^{235}\text{U}$ (${}_{92}\text{U}_{143}$) is fissioned by thermal (i.e. low-energy/low-speed) neutrons whereas ${}^{238}\text{U}$ (${}_{92}\text{U}_{146}$) is not. In the first case (when neutron capture causes an odd- $N \rightarrow$ even- N change to occur), the binding energy excess gained by the daughter ${}^*\text{U}-236$ (6.3 MeV) is much larger due to the pairing term than in the second case (when an even- $N \rightarrow$ odd- N change occurs) resulting in the formation of ${}^*\text{U}-239$ (4.8 MeV). This means that ${}^*\text{U}-236$ possesses large enough excitation energy to fission, even if the kinetic energy of the captured neutron was negligibly small. ${}^*\text{U}-239$, on the other hand, can only fission if the kinetic energy of the captured neutron was large enough to considerably increase the excitation energy. Besides, due to the $\sigma \propto 1/u$ rule of neutron

capture, the neutron-induced fission of U-235 is not only energetically more feasible than that of U-238, but also a more likely process provided that the high-energy fission neutrons that maintain the chain reaction are slowed down to thermal energy (and low speed u) by a suitable moderator material.

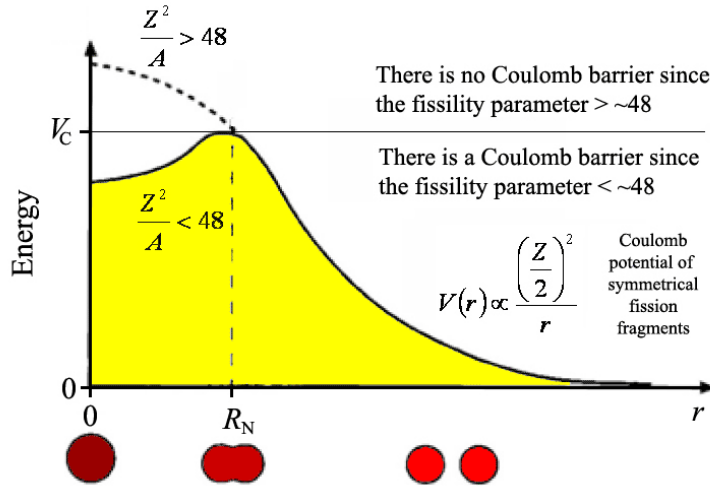


Figure 48: The sufficient condition for SF to occur is that the fissility parameter be greater than about 48. In this case, namely, the energy of a spherical nucleus continuously decreases as its oblate distortion increases. This kind of distortion eventually leads to the scissioning of the nucleus. The horizontal axis shows the distance r of the centers of mass of the fission fragments (FFs) moving away from each other.

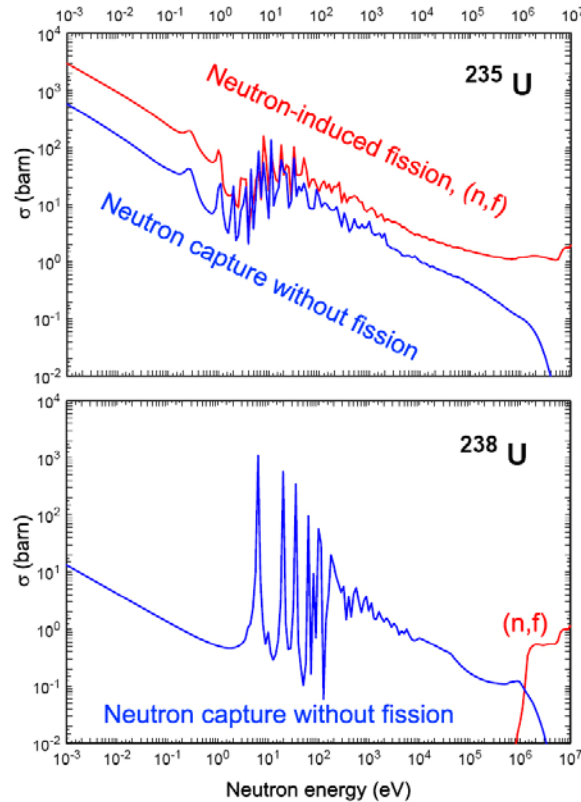


Figure 49: Comparison of the cross sections of neutron-induced fission (n,f) and neutron capture as a function of neutron energy for the most common natural isotopes of uranium.

9.5. Exotic and Rare Decay Modes

Apart from the decay modes discussed before there are more exotic ways for the nucleus to transform into a more stable one. They are usually very slow or rare processes.

One type of them, called *double beta decay*— 2β ($\beta\beta$) or 2ε ($\varepsilon\varepsilon$)—, has already been mentioned before. This type of decay helps to make the shortcut in one single step between ^{124}Xe and ^{124}Te (see the upper left panel of Figure 43) which is energetically impossible via two subsequent β decays because the ‘intermediate’ ^{124}I has higher rest energy (mass) than ^{124}Xe . The process in which two antineutrinos are also released ($2\nu\beta\beta$) was first observed with ^{82}Se in 1987. The *neutrinoless* process has not yet been discovered as of 2008, although it is searched for with great effort.

There are also other types of special β decay called *beta-delayed particle emission*. These types of decay occur when the daughter nucleus is born in a highly excited state following β decay and it gets rid of the extra energy not via γ decay, but by ejecting one or more nucleons or an α particle. On the proton-rich side of the stability valley, e.g., the emission of a proton following ε has been observed (εp). On the neutron-rich side, the release of one or two neutrons is possible following β^- decay ($\beta^- n$, $\beta^- nn$). The emission of alpha particles has also been observed for some nuclei in all types of β decay ($\beta\alpha$). For a few nuclei, even fission can take place following ε . In spite of their relative rarity, one of them, *beta-delayed neutron emission* ($\beta^- n$) also has practical importance being responsible for delayed neutron emission in nuclear reactors, one of the key elements of reactor control.

There is also a very interesting type of beta minus decay called *bound-beta decay* β_b . This type of decay proves that the stability of the neutron is not the exclusive business of the nucleus but of the atom as a whole (see Figure 50). It also shows that the calculation of the binding energy from the nuclidic masses (in order to judge the stability of the nucleus) is probably the correct thing to do and not just an unavoidable compromise chosen because nuclear masses are not known accurately enough. To keep the story short, stable nuclides like ^{163}Dy (for which β_b decay was first observed) may become unstable when they get completely stripped of their electrons. As a matter of fact, the half-life of $^{163}\text{Dy}^{66+}$ ions—i.e. bare ^{163}Dy nuclei—turned out to be a mere 50 days, whereas neutral dysprosium is absolutely stable. In a way β_b decay can also be considered as a reversed EC, because the electron emitted by the nucleus gets immediately captured by one of the empty shells of the atom:



However, the term **inverse β decay** is reserved for special types of neutrino reactions, not for spontaneous processes. Such a process was used by [F. Reines](#) and C.L. Cowan in 1956 to prove the existence of electron antineutrino by [direct detection](#):



where the proton p is not bound in a heavier nucleus, but the nucleus of ^1H hydrogen, the constituent of ordinary water H_2O .

Later, in 1967, [R. Davis Jr.](#) used another type of inverse β decay to discover the [solar neutrino problem](#), which means that fewer (electron) neutrinos seemed to be produced by the Sun than expected. This process can really be considered as a reversed EC:

$$\nu + {}^{37}_{17}\text{Cl}_{20} \rightarrow {}^{37}_{18}\text{Ar}_{19} + e^{-} . \quad (106)$$

More recent experiments performed at [SNO](#) (*Sudbury Neutrino Observatory*) detect electron neutrinos by using heavy water as a target:

$$\nu + d \rightarrow 2p + e^{-} , \quad (107)$$

where the deuteron d is the nucleus of the deuterium ${}^2\text{H}$.

The discovery of various types of *cluster decay* (heavy-ion emission) is ‘esthetically’ satisfying because it shows that there is no absolute gap between α emission and fission. Cluster decay opens a parallel channel in some α emitters situated in the boundary region between α decay and SF. Due to the much higher Coulomb barrier, however, the α branch of the decay is typically billions or trillions faster than the parallel cluster emission branch. A few examples for this type of decay (${}^{14}\text{C}$, ${}^{24}\text{Ne}$, ${}^{26}\text{Ne}$, and ${}^{28}\text{Mg}$ emission) have also been discovered in members of the major decay series shown in Figure 51.

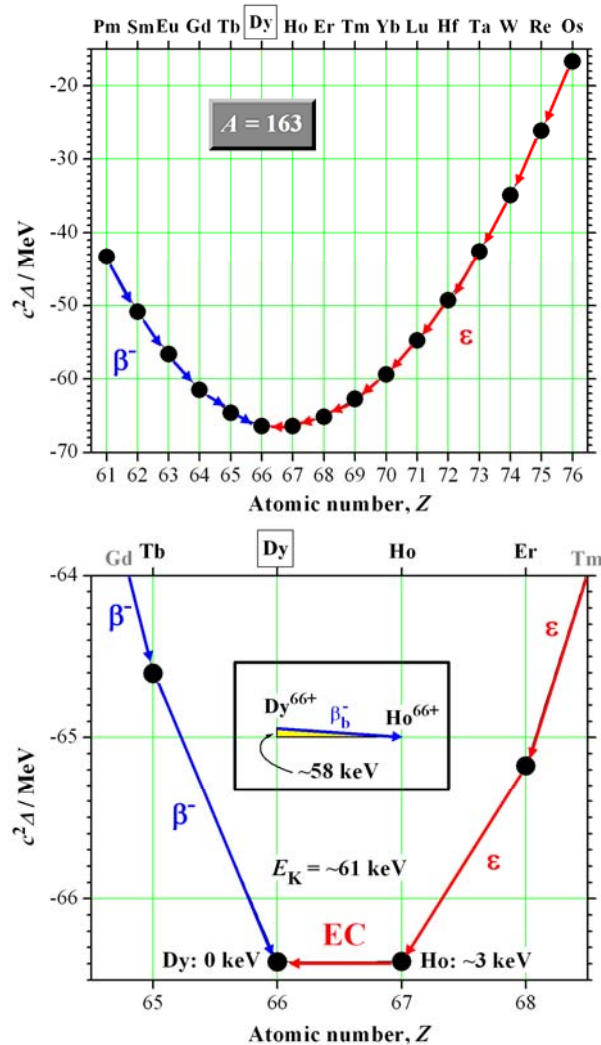


Figure 50: Typical odd- A mass parabola for the isobaric nuclides of ${}^{163}\text{Dy}$ (upper panel). The lower panel shows the tip region of the parabola. Note that the rest energy (mass) of the unstable ${}^{163}\text{Ho}$ atom ($T_{1/2} = 4570$ a) is only ~ 3 keV higher than that of the stable ${}^{163}\text{Dy}$ atom. (This tiny difference only makes EC possible. For β^+ decay to occur at least $2m_e c^2 \approx 1.02$ MeV of mass difference is needed, which is about the same as the distance between the horizontal grid lines on the lower panel.) This 3 keV is also characteristic of the mass difference between the nuclear masses. On the other hand, the

binding energy of the K-shell (~ 61 keV in ${}_{67}\text{Ho}^{66+}$) is much larger. Therefore a bare ${}^{163}\text{Dy}^{66+}$ nucleus can undergo β_b decay, because about $61 \text{ keV} - 3 \text{ keV} = \sim 58 \text{ keV}$ energy is released while the Dy decays and the newborn electron is captured by the empty K shell of Ho. The slope of the blue arrow representing β_b decay in the inset is about in proportion with the rest of the arrows in the same panel.

10. Kinetics of Radioactive Decay and Activation

10.1. Radioactive Decay and Growth

As we can see in Figure 51, what we call the four major decay series are actually networks of simple decay processes. These series, also called decay chains, are basically composed of (successive and branching) steps of α and β^- decay. This explains why there are exactly four such series. Since α decay changes the mass number always by (-4), and β^- decay leaves it unchanged, the mass numbers of the members of any one series give the same residue (i.e. 0, 1, 2, or 3) on division by 4, staying in the same residue class modulo 4 as their primary parent.

Note that in the $4n+2$ series about 70 ppm of the ${}^{210}\text{Tl}$ nuclei suffer β^-n decay²² to ${}^{209}\text{Pb}$, the last but one member of the $4n+1$ series that β decays to stable ${}^{209}\text{Bi}$. In the strict sense, therefore, the four series are not quite independent but interlaced via rare processes such as this.

Different types of *cluster decay* (when a light nucleus heavier than He^{2+} is ejected from the decaying nucleus) make shortcuts (${}^{20}\text{O}$, ${}^{24}\text{Ne}$, and ${}^{28}\text{Mg}$) within a series and partly open channels between them (${}^{14}\text{C}$). These, however, are very rare types of decay that are only indicated in Figure 51 to make the picture complete.

The directed graph representing such a network is built up from the following three types of units:

(1) A *single decay* or a linear sequence of decay steps that form a ‘real’ *decay series*:



where the ellipsis ... in parentheses means that the unit can be part of a longer chain, and λ_1 above the arrow is the decay constant of X_1 decaying to X_2 .

(2) *Diverging branches*:



where λ_1 and λ_2 are the *partial decay constants* of X decaying to Y_1 and Y_2 , respectively. For the overall decay process of X we have $\lambda = \lambda_1 + \lambda_2$. The *branching ratios* mentioned already in connection with Figure 36 are λ_1/λ and λ_2/λ , respectively.

(3) *Converging branches*:



The solution of the differential equation systems describing such decay networks has been

²² β^-n -delayed neutron emission, i.e., beta decay followed by neutron emission.

known for almost a century. There are even user-friendly computer programs which calculate the time dependence of the numbers of atoms and the activities for the parent and its various daughters and other ‘descendants’ displaying the results in various forms (see e.g. Figure 52).

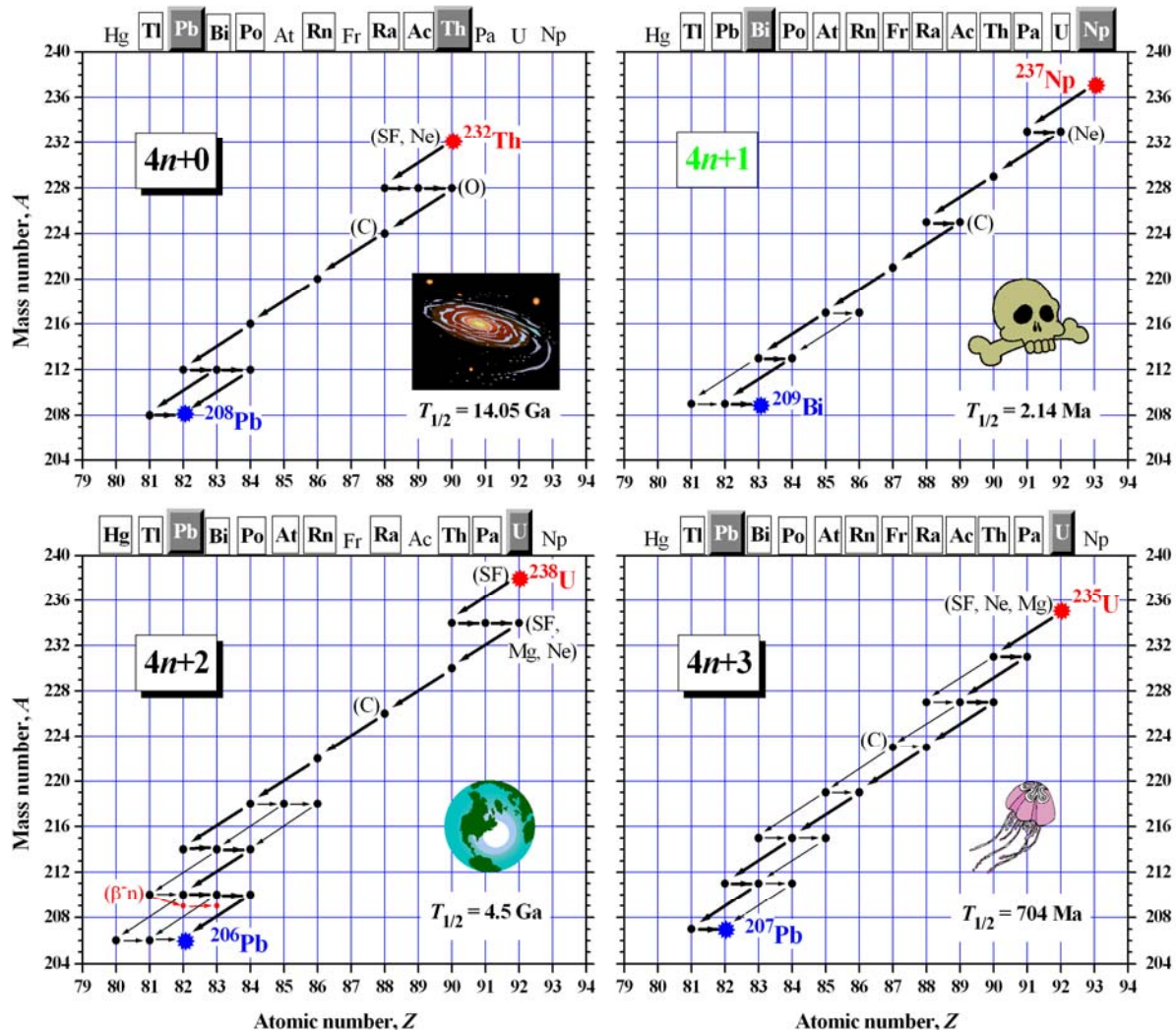


Figure 51: There are four major decay series that start from the most stable nuclides in the vicinity of uranium. The series stop at the uppermost end of absolute stability at ${}_{82}\text{Pb}$ or ${}_{83}\text{Bi}$. The insets are to visualize the half-lives of the primary parents. The number of ${}^{232}\text{Th}$ atoms has halved only once since the Universe was born. The half-life of ${}^{238}\text{U}$ is just about equal to the age of the Earth and therefore half of this nuclide is still around. The number of ${}^{235}\text{U}$ atoms halved once since the late [Proterozoic Period](#). Those present have survived 6 to 7 halving periods since the Earth was formed from the debris of a supernova. No wonder that there is much less ${}^{235}\text{U}$ now²³ than ${}^{238}\text{U}$. Finally, the half-life of ${}^{237}\text{Np}$ is commensurable with the age of the genus *Homo* that includes us and our closest but extinct relatives. This series has become extinct over a period of more than 2000 half-lives that have elapsed since the formation of Earth. The remaining three are referred to as [naturally occurring decay series](#).

²³ Some 1,7 Ga ago there was a lot more U-235 around than there is now as is proven by the remains of an [ancient natural nuclear reactor](#) found at Oklo, Gabon, in 1972. Its operation was based on the fortunate coincidence of certain geological conditions as well as on the fact that no enrichment was necessary at that time.. It is interesting to note that P.K. Kuroda figured out the possibility and the ‘design’ of such reactors as early as 1956.



Figure 52: The decay series of ^{238}U simulated by an applet from the CD-ROM supplied with the book Radioactivity–Radionuclides–Radiation (*Universal Nuclide Chart, Copyright European Communities, 2005*). [The applet](#) and the whole UNC is also part of the software package *Nuclides.net*.

We restrict our attention to the following two-step series, a special case of Eq. (108):



The differential equations describing the above decay chain are as follows:

$$\frac{dN_1}{dt} = -\lambda_1 N_1, \quad (112)$$

$$\frac{dN_2}{dt} = \lambda_1 N_1 - \lambda_2 N_2. \quad (113)$$

Note that in the latter case the negative of the derivative is not equal to the activity A_2 of the nuclide X_2 as one might erroneously assume from Eq. (75). Actually, the correct interpretation of the term ‘activity’ (**activity is decay rate** and not just the changing rate of the number of radioactive atoms) tells us that $A_2 = \lambda_2 N_2$ and, similarly, $A_1 = \lambda_1 N_1$.

The solutions for the initial condition $N_2(0) = 0$ are:

$$N_1(t) = N_1(0) \exp(-\lambda_1 t), \quad (114)$$

$$N_2(t) = \frac{\lambda_1}{\lambda_2 - \lambda_1} N_1(0) [\exp(-\lambda_1 t) - \exp(-\lambda_2 t)]. \quad (115)$$

Due to proportionality between the number of atoms and activity we can also write the result in the following form by multiplying the above equations with λ_1 and λ_2 , respectively:

$$A_1(t) = A_1(0) \exp(-\lambda_1 t), \quad (116)$$

$$A_2(t) = \frac{\lambda_2}{\lambda_2 - \lambda_1} A_1(0) [\exp(-\lambda_1 t) - \exp(-\lambda_2 t)]. \quad (117)$$

The latter equation can be used to explain the difference between *transient equilibrium*,

secular equilibrium (see Figure 34) and *non-equilibrium* between parent (X_1) and daughter (X_2).

Note that because the exponential function is very sensitive to the magnitude of the exponent, if $\lambda_2 > \lambda_1$, then, after some time, the second exponential function in the bracket will become negligible in comparison with the first one. Therefore we can write after about 5-10 half-lives of X_2 :

$$A_2(t) = \frac{\lambda_2}{\lambda_2 - \lambda_1} A_1(0) \exp(-\lambda_1 t) = \frac{\lambda_2}{\lambda_2 - \lambda_1} A_1(t), \quad (118)$$

which expresses proportionality between the activities of the parent and daughter. This is what is called *radioactive equilibrium* in general. The activity curve is usually represented as a semi-logarithmic plot [e.g. $\ln(A/Bq)$ vs. t]. Taking the logarithm (to any base) of the above proportionality we get:

$$\log[A_2(t)/Bq] - \log[A_1(t)/Bq] = \log\left(\frac{\lambda_2}{\lambda_2 - \lambda_1}\right) = \text{constant}, \quad (119)$$

which makes equilibrium conspicuous on semi-logarithmic plots, because the activity curves of the respective nuclides run ‘parallel’ in this case, i.e. they keep the same vertical distance. The activities themselves change with the time, of course,—hence the name *transient equilibrium*.

There is a special case of equilibrium (actually an extreme limit), called *secular equilibrium*, when $\lambda_2 \gg \lambda_1$. Now we can also neglect λ_1 in the denominator in Eq. (118):

$$A_2(t) = A_1(t), \quad (120)$$

i.e., the proportionality becomes equality. Using a normal time scale, the slow decay is not reflected by the decrease of the activities—the straight lines of the activities in the semi-logarithmic plot are apparently horizontal, concealing the transient nature of the equilibrium—which explains the use of the adjective ‘secular’ (meaning ‘continuing through long ages’) in this case.

If $\lambda_2 < \lambda_1$, then there is *no equilibrium* at any time, but after a while, the parent completely disappears.

Independently of whether there can be equilibrium or not, the activity A_2 of the daughter passes through a maximum at the time:

$$t_{\max A_2} = \frac{\ln \frac{\lambda_2}{\lambda_1}}{\lambda_2 - \lambda_1}, \quad (121)$$

as we can ascertain by the derivation of Eq. (118). Note that because the activity and the number of atoms are proportional to each other, the above equation also determines the time when the number of daughter atoms reaches its maximum.

Figure 53 shows the results of the activity calculation for a three-step series for all possible permutations of 1 unit, 3 units, and 9 units assigned to the mean life $\tau = 1/\lambda$. Complete lack of equilibrium can only be observed in the upper left panel where the mean lives monotonically increase in the series. Even more interesting is the conclusion that can be drawn from the bottom panels. If the primary parent of a series is longer-lived than any of its daughters, then,

after a while, equilibrium will set in along the whole series, no matter how the mean lives of the daughters are related to each other. This conclusion can be generalized for any number of steps.

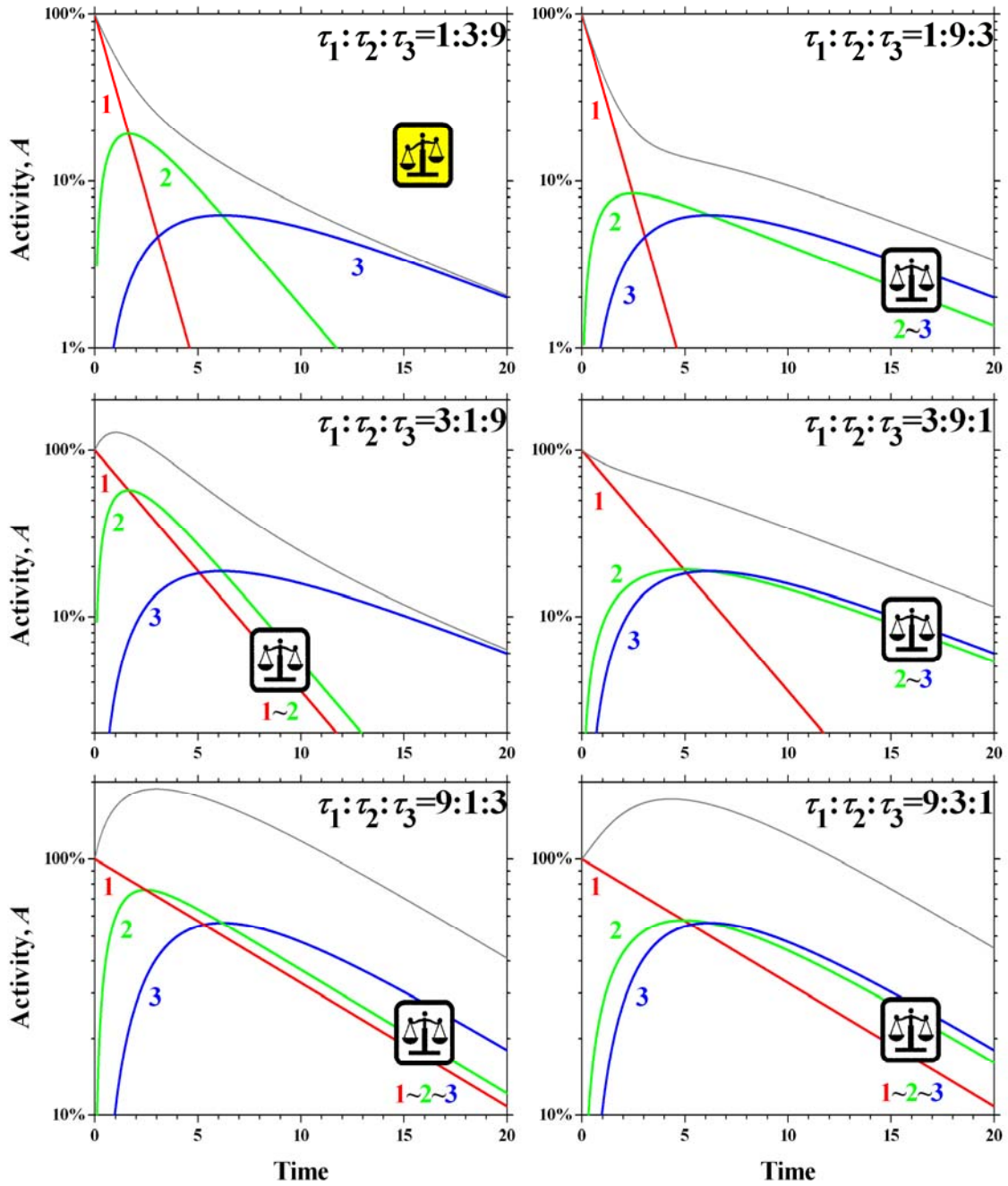


Figure 53: Activities of the members of a 3-member decay series calculated for the case when the initial number of atoms is set to zero except for the first member. The symbol ‘~’ indicates equilibrium between some of the members identified by numbers 1, 2, and 3. (Equilibrium is revealed by parallel lines in semi-logarithmic plot, a characteristic of proportionality.) The balanced scales show that whenever a parent is longer-lived than its daughter, (transient) equilibrium sets in rather soon. Note that the activities of the daughters (2, 3) invariably go through a maximum. Surprising as it may seem, the total activity (drawn by a thin gray line) also has a maximum whenever equilibrium is possible between the primary parent (1) and its immediate daughter (2). (The time parameter τ_{\min} means the shortest of the mean lives τ_1 , τ_2 and τ_3 .)

10.2. Decay Following Activation

A special case of successive processes is that when the parent (X_1) is stable, but it is induced to transformation by nuclear reaction, the product of which (X_2) is radioactive. For instance, in the case of neutron activation—using the correspondence $\lambda \Leftrightarrow \phi\sigma$ —Eq. (111) can be rewritten as:



where ϕ is the neutron flux (neutrons $\text{cm}^{-2} \text{s}^{-1}$) and σ_1 is the cross section of, say, neutron capture in NAA:



Of course, it can also be related to a natural process such as the production of cosmogenic ^{14}C via the reaction



Instead of dealing with the general case—which yields the same results as Eq. (111) except that the substitutions $\lambda_1 \Leftrightarrow \phi\sigma_1$ and $A_1 \Leftrightarrow \phi\sigma_1 N_1$ have to be carried out in the respective equations, e.g.:

$$t_{\max A_2} = \frac{\ln \frac{\lambda_2}{\phi\sigma_1}}{\lambda_2 - \phi\sigma_1}, \quad (125)$$

we will assume that N_1 remains practically constant during irradiation. This means that only a tiny fraction of X_1 will be activated.

Now we only need the equivalent of Eq. (113):

$$\frac{dN_2}{dt} = \phi\sigma_1 N_1 - \lambda_2 N_2, \quad (126)$$

from which we get:

$$A_2 = \lambda_2 N_2 = \phi\sigma_1 N_1 [1 - \exp(-\lambda_2 t)] \xrightarrow{t \rightarrow \infty} \phi\sigma_1 N_1. \quad (127)$$

We can see from the above equation that for constant time of activation, the activity of the product will be proportional to N_1 , offering a simple method for the quantitative analysis of the nuclide X_1 by NAA. Note that the same is true for the asymptotic limit of the activity (see Figure 54). The latter fact is used, e.g., in the case of *radiocarbon dating*, when the time (Δt) elapsed since the death of an organism is eventually determined from the following type of equation:

$$N_2(\Delta t) = \frac{\phi\sigma_1 N_1}{\lambda_2} \exp(-\lambda_2 \Delta t), \quad (128)$$

where the subscript 1 stands for ^{14}N , and 2 for ^{14}C .

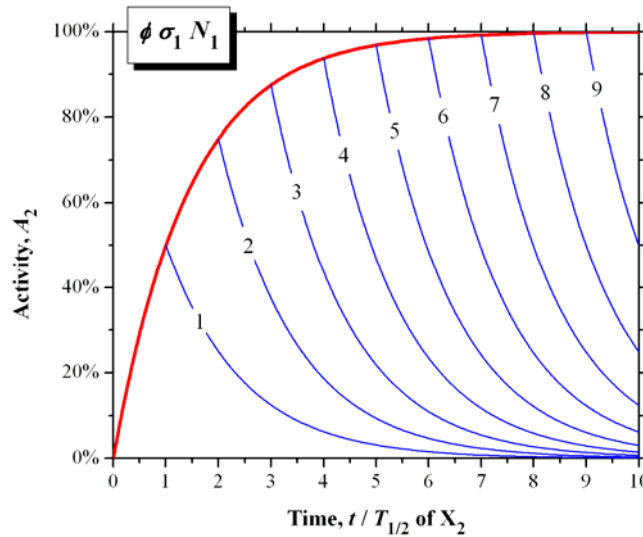


Figure 54: The change of activity of the product during and after activation. The time unit on the horizontal axis is the half-life of the product. The thick red curve represents activation, while the blue curves represent ‘cooling’, i.e. the activity of the product, when the activation is interrupted after 1, 2, 3, etc. half-life units. It is obvious that after 3-4 half-life units, further increasing the duration of activation is of little use, because the 100% value ($\phi \sigma_1 N_1$) can only be reached asymptotically.

10.3. Parallel Decay Processes

In this case there is no ‘genetic’ relationship between two or more radionuclides decaying in parallel. This can be the case, e.g., after neutron activation of a specimen containing several nuclides which were activated.

Taking the simplest case, when there are only two radionuclides present in the source both of which decay to stable nuclides in one single step, we have a linear combination of two exponential curves as shown by Figure 55 in semi logarithmic plot. We can see that the slow and steady wins the race.

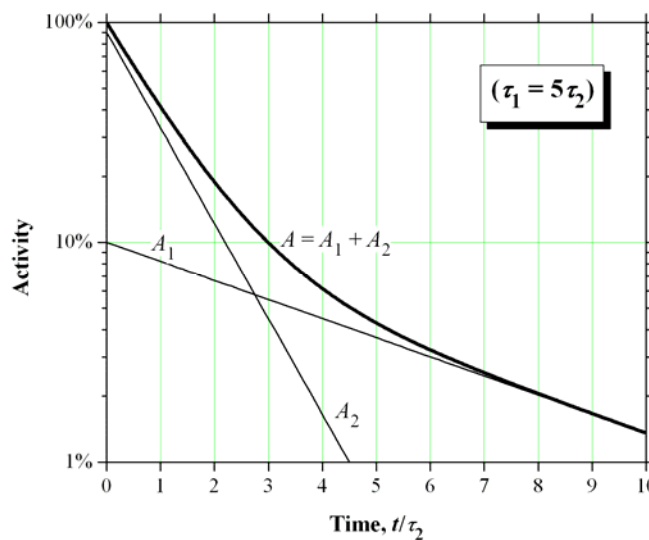


Figure 55: The activity of a source containing the mixture of two radionuclides having no genetic relationship. We can see that nuclide 1, due to its longer mean life, will survive nuclide 2, although its initial activity at $t = 0$ is much lower.

11. Aftereffects of Radioactive Decay and Nuclear Reactions

Radioactive decay brings about either inevitably or with some probability changes in the state of the daughter atom or leads to the emission of extranuclear radiation coming from that atom. These aftereffects depend on the type and the Q -value of the decay process.

11.1. Recoil

Maybe the most trivial aftereffect of radioactive decay or nuclear reaction is the *recoil* of the ‘daughter’ atom as a result of the emission of the radiation ‘particle’. As a simple example we take the following one-particle emission model:



where P is the **p**arent (at rest), R is the **r**ecoiled daughter nuclide, r is the **r**adiation particle emitted, and Q is the decay energy (Q -value) divided between R and r as kinetic energy according to the ‘rules’ of energy and momentum conservation. The radiation particle can be an α particle (α decay), a β^\pm particle (β^\pm decay events when the neutrino’s share of energy is negligible), γ photon (γ decay), or ν (EC, when only neutrinos are emitted from the nucleus), etc.

Figure 56 shows the recoil energy gained by an extremely light daughter atom (nuclidic mass $M = 4$) and a heavy one ($M = 240$) as a function of the kinetic energy of the radiation particle for one-particle emission. (The relativistic calculations are given in chapter 17.)

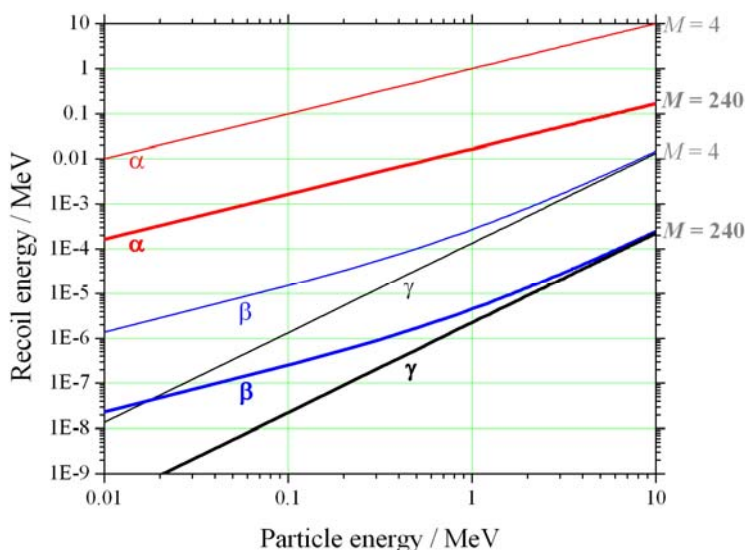


Figure 56: Recoil energy of the daughter atom as a function of the kinetic energy of the radiation particle (α , β , and γ) for one-particle emission. The curves have been calculated for two extreme cases, i.e., for a very light daughter with nuclidic mass $M = 4$ (thin lines), and a heavy one with $M = 240$ (thick lines).

As a general tendency we can notice that the lighter the recoil atom, the larger is the recoil energy (see also the legend of Figure 31). Also, heavier radiation particles have a larger recoiling effect.

Note that that the log–log plots of α particles and γ photons are straight lines with slopes 1 and 2, respectively. This is the reflection of straight proportionality in the first case and quadratic relationship in the second between recoil energy and particle energy as shown by Eqs. (130)

and (132), respectively.

Note also that initially (i.e. for low particle energies) the log–log plots of β particles are also linear running parallel with those of the heavy α particles. This means that the recoil energies left behind by them are (although not equal but at least) in straight proportion for any given (low) particle energy. Then, as the energy (and thus the speed) of the β particles increases, they gradually become ‘relativistic’ and their curve asymptotically approaches the steeper curve of γ radiation. In other words, very fast electrons behave kind of ‘photon-like’.

Neutrino emission curves would practically match γ curves because of the neutrino’s negligible mass.

The recoiling effect changes in the following order for low-energy radiation particles: $\alpha \gg \beta > \gamma = \nu$. For high energies we have: $\alpha \gg \beta \geq \gamma = \nu$.

It would have been hard for me at this point not to include Figure 57, which sheds light on the relativistic background of the curves seen in Figure 56. For better comparison the same colors are use in both figures.

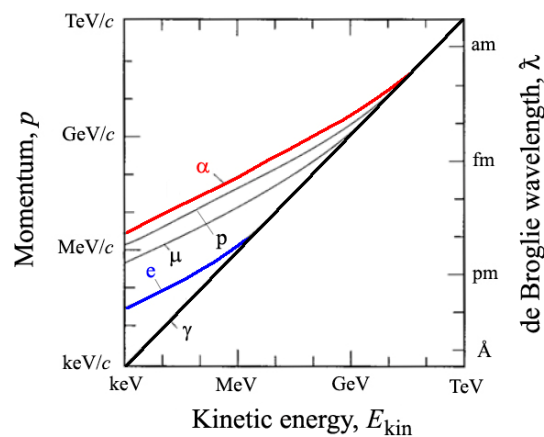


Figure 57: Particles, depending on their mass, sooner or later start to behave ‘photon-like’ as their kinetic energy increases [see Eq. (176)] The similarity is expressed as proportionality between momentum and kinetic energy, a characteristic of photons ($p_\gamma = E_\gamma/c$). For massive particles—at least for low energies (i.e. at non-relativistic speeds)—it is the square of the momentum that is proportional to the kinetic energy ($p^2 = 2 m E_{\text{kin}}$) and not the momentum itself. The vertical axis on the right shows the reduced de Broglie wavelength $\lambda_{\text{dB}}/(2\pi)$ changing in inverse proportion with the momentum. Note that the upper part of the horizontal axis covers much higher energies than that of Figure 56.

Let us now return to the discussion of Figure 56.

As regards α decay, only the thick curve is really important in the figure, because this decay mode predominantly occurs with heavy nuclides. The energy range of α particles is concentrated to the upper third of the logarithmic scale of the abscissa. Typical α energies, namely, are between 4–6 MeV, and the total variation is between 1.8 MeV (^{144}Nd) and 11.7 MeV ($^{212\text{m}}\text{Po}$), which is slightly above the range shown in the figure. The typical recoil energy is about 0.1 MeV (100 keV), which is quite considerable as revealed by its molar energy (10 GJ mol^{-1}) and temperature (1 GK) equivalents calculated from Eqs. (7) and (8), respectively. So daughter nuclides of α decay are rightly referred to as ‘hot atoms’.

Since α particles are too heavy to behave relativistically in this energy range, we can use the nonrelativistic recoil formula (200) for them:

$$E_R = \frac{m_r}{m_R} E_r. \quad (130)$$

As we can see, the total energy released in the decay ($Q = E_R + E_r$) is divided between the recoil atom and the radiation particle in inverse proportion to their respective masses m_R and m_r .

One can easily derive from Eq. (130) (or directly from momentum conservation) that in the non-relativistic case the speeds (u) will also be in inverse proportion to the masses (provided that the parent atom was originally at rest or the center of mass frame is used):

$$u_R = \frac{m_r}{m_R} u_r. \quad (131)$$

Formula (130) can also be used to judge the recoil energy of [fission fragments](#) directly produced in the scission phase of spontaneous fission. In the case of the SF of ^{238}U , for instance, the total energy released is enormous, being about 200 MeV, 80% of which (~ 160 MeV) is shared by the lighter (r, $A \approx 95$) and the heavier fission fragment (R, $A \approx 140$). According to Eq. (130), this means that the fragments possess recoil energies in the order of 65-95 MeV, which is way out of the range of Fig. 56.

With β decay, the so-called *end-point energies* or *maximum energies* denoted by E_β or E_{\max} (see Figure 58) cover the range of 17-18 keV (^3H and ^{210}Pb) through 14 MeV (^8B), i.e., practically the whole range shown in the abscissa of Figure 56. However, the typical energies are a little below the typical α energies, somewhere between a few hundred keV and a few MeV. Because of this, the nonrelativistic recoil formula (130) gives but a rough estimation for β decay. Beta decay occurs anywhere along the chart of nuclides, and therefore both β^- and β^+ curves are equally important in Figure 56.

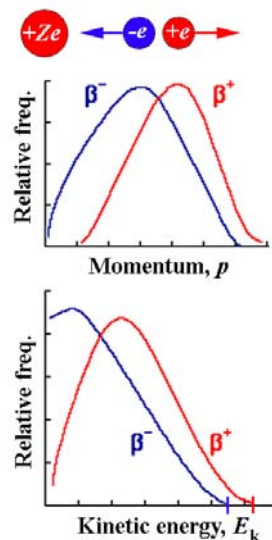


Figure 58: Schematic momentum and energy spectra of β^- and β^+ particles (after C.N. Booth, <http://www.shef.ac.uk/physics/teaching/phy303/phy303-4.html>). The spectra represent ^{64}Cu undergoing both β^- and β^+ decay (see the decay scheme on the lower panel in Figure 36) with similar E_β values (end-point energies) marked by vertical bars. This is a fortunate coincidence making easier to notice the difference between e^- and e^+ emission, namely, that Coulomb attraction of the nucleus decelerates electrons whereas Coulomb repulsion accelerates positrons. Therefore the energy and momentum spectra of β^- and β^+ particles are characteristically different at low energies. Also, the average β^- energy

is only about 1/3 of the end-point energy E_{β^-} (the highest possible kinetic energy of electrons being limited by Q_{β^-}), whereas the average β^+ energy is relatively higher (40% of E_{β^+} or so).

In the case of γ emission, the recoil energy of the atom (and thus its share from $Q = E_R + E_\gamma$) is rather small, but according to Eq. (202) it depends more sensitively on energy than the recoil caused by ‘corpuscular’ radiations:

$$E_R = \frac{E_\gamma^2}{2m_R c^2} \approx \frac{(E_\gamma / \text{keV})^2}{1863 M_R} \text{ eV}, \quad (132)$$

where $M_R = m_R/u$ is the nuclidic mass of the recoil atom.

For instance, in the case of the 14.41 keV gamma transition of the first excited state of ^{57}Fe (the most often used tracer nuclide in Mössbauer spectroscopy) the recoil energy calculated from the above formula is only ~ 0.002 eV, which is lower than kT at room temperature. However this transition produces extremely ‘soft’ γ -rays. (Note that the characteristic X-rays of Pb are between 72-87 keV, showing that the photons of ‘hard’ X-rays can have higher energies than soft γ -rays.) On the other hand, this tiny recoil energy would make Mössbauer spectroscopy of iron impossible, if ^{57}Fe were not ‘frozen’ into the lattice of a crystal grain which, as a whole, can absorb the energy of recoil with some probability. From the viewpoint of the ^{57}Fe atom this means recoilless/phononless emission without appreciable decrease of the gamma energy relative to the Q -value of the transition. This is what is called the Mössbauer effect, the physical basis of Mössbauer spectroscopy.

The above formula can also be used, e.g., for radiative neutron capture, if the kinetic energy of the neutrons is negligible. For instance, in the $^{127}\text{I}(n,\gamma)^{128}\text{I}$ reaction induced by ~ 0.025 eV thermal neutrons a variety of γ photons are produced. Although the most common energy is $E_\gamma = 133.61$ keV, even ~ 1 MeV photons are emitted with some probability. The recoil energy calculated for the latter value is ~ 4 eV, which is twice the 2 eV energy of the C-I bond in $\text{CH}_3\text{CH}_2\text{I}$. This explains the *Szilárd–Chalmers process* first observed with this compound under the same conditions. The effect means that the recoil energy tears off the daughter nuclide ^{128}I from the chemical bond as proven by the fact that it can be extracted with water (which does not mix with ethyl iodide). ^{128}I can be easily detected in the aqueous phase due to its β activity ($T_{1/2} = 25$ min).

To judge the importance of recoil in nuclear reactions in general (i.e. when the energy of the reacting projectile cannot be neglected), consider the simple process:



in which r is the reacting projectile, T is the target nucleus (considered at rest in the laboratory system) and R is the resulted nucleus (actually the equivalent of the possible intermediate stage in Figure 29). With this notation we find from energy and momentum conservation that the reinterpreted version of Eq. (130) remains valid, i.e. the recoil energy of the resulted nucleus is:

$$E_R = \frac{m_r}{m_R} E_r. \quad (134)$$

The above equation gives the physical basis of the *recoil separation* of higher transuranium elements produced by heavy ions as projectiles.

11.2. Inner Bremsstrahlung, X-Rays and Auger Effect

In order to explain what inner bremsstrahlung is, I must first introduce bremsstrahlung, one of the typical interactions of energetic β particles with matter.

Bremsstrahlung—German for ‘slowing-down radiation’—is a type of [electromagnetic radiation](#) (like characteristic X-rays, γ -rays or visible light) emitted when charged particles are accelerated, e.g. in the Coulomb field of a nucleus or in a synchrotron. Note that ‘slowing-down’ also means acceleration—only negative in sign. The sign, however, is unimportant with the radiant power being proportional to the square of the acceleration: $\Phi_e \propto a^2$.

Bremsstrahlung is only significant in the case of the lightest charged particles, i.e. with e^- and e^+ . Its energy distribution is continuous between zero and the kinetic energy of the accelerating particle that supplies the radiation with energy. The upper limit is reached in the rare event when the total kinetic energy of the particle is spent on the production of one single photon. For high-energy electrons therefore, the high-energy part of bremsstrahlung falls in the range of what is called X-rays. (For this reason it is often referred to in Hungarian as ‘fékezési röntgensugárzás’, meaning ‘slowing-down X-rays’—a term not used in English.)

Inner bremsstrahlung occurs, e.g., when the bremsstrahlung is produced in the daughter atom of a β^-/β^+ decaying parent as a result of the e^-/e^+ being decelerated/accelerated by the Coulomb field of the very nucleus that is left behind (see also the legend of Figure 58). Electron capture is also accompanied with bremsstrahlung, because of the captured electron. In this case the radiation energy decreases the energy available for the neutrino.

Characteristic X-rays originate from L→K etc. high-energy electronic transitions, and therefore their energy is indeed characteristic of the chemical element in which the transition takes place. Since the orbital electron captured in EC most of the time originates from the K shell, characteristic X-rays are always to be expected in this case.

Auger²⁴ effect is a competitive process with X-ray etc. emission, when the energy difference between two atomic shells (which is released while an outer electron jumps in a lower lying electron hole) is carried away by an outer orbital electron rather than by an electromagnetic quantum. While the electron hole is gradually moving to outer shells from the K or the L shell (Figure 59), an *Auger cascade* can evolve leading to the formation of a multiply ionized atom and a number of *Auger electrons*.

²⁴ The effect is named after French physicist Pierre Victor Auger (pronounce: au like o in over, g like s in measure, er like ay in say).

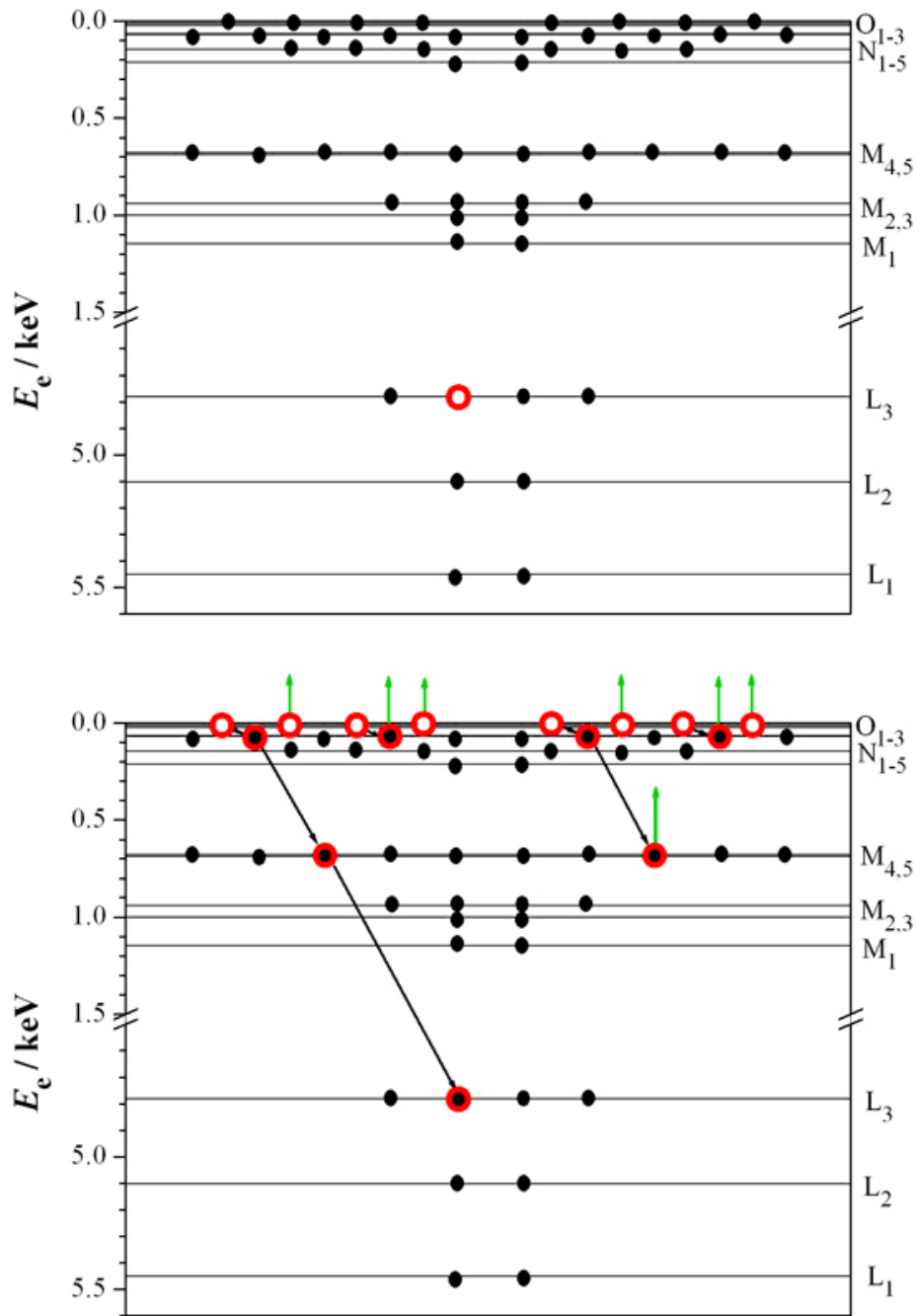


Figure 59: Auger cascade in ${}_{54}\text{Xe}^+$ starting from one electron hole in the L shell (upper panel) and ending up with a Xe^{8+} ion with its O shell completely stripped of electrons (lower panel). Each slanting (black) arrow represents an inner hole being filled with an outer electron leaving behind an outer hole.

The energy released is spent on breaking loose an orbital electron called an Auger electron (see the vertical green arrows) and providing it with kinetic energy. The hole left behind by the Auger electron can be filled in a similar fashion, thus the number of holes (ideally) doubles in each stage of the cascade as the holes move from one shell to the next until they reach the valence shell (which is the O shell this time). It follows from the mechanism that the energy spectrum of the Auger electrons, similarly to X-rays, will be characteristic of the chemical element because both are determined by the binding energies (E_e) of the electrons concerned.

12. Interaction of Nuclear Radiations with Matter

This chapter will concentrate on the interactions of nuclear radiations that are directly produced by the most common types of radioactive decay (i.e., α , β , and γ). Concerning the interactions of neutrons only their slowing-down process will be discussed which has an effect on their reaction cross section and thus on the operation of nuclear reactors.

When nuclear radiations, neutrons, accelerated heavy ions or cosmic rays pass through matter they interact with its constituents. The matter (which will be often referred to as the *absorber*) can be an experimental sample, a shielding built to protect workers from radiation, construction materials of a nuclear reactor, the sensitive part of a radiation detector, or a living tissue exposed to outer or inner radiation. The various topics that are directly based on the interactions discussed in this chapter are as follows:

- detection of nuclear radiations
- radiation chemistry
- radiation biology
- radiation protection
- radiation therapy

As a result of radiation–matter interactions—depending on the type and the initial energy of the radiation as well as the properties of the interacting material—both the radiation and the matter suffer changes.

As regards the radiation, its constituents may eventually give away their (kinetic) energy either in a single interaction (predominantly photons) or in a sequence of interactions (predominantly electrons, positive ions and neutrons) and stop in the absorber. The *penetrating power* depends a lot on the type of the radiations even if the energy of the radiation particles/photons is the same. (Of course, when comparing electromagnetic radiations—X-rays, bremsstrahlung, and γ -rays—with each other, the photon energy is an unambiguous characteristic; the same as the interactions of α particles originating from different decays only depend on their energy if the absorber is the same.)

As regards the absorber material, it absorbs a huge amount of energy (at least in chemical terms) from each radiation particle that is stopped by it. (Remember that the chemical activation energy is only ~ 1 eV, whereas the particle energies considered in this chapter are usually between ~ 10 keV and ~ 10 MeV that are typical of radiation particles produced by radioactive decay and its aftereffects, which means a factor of 10 000 to 10 000 000 in energy.)

In the case of *directly ionizing radiations* (consisting of charged particles such as α and β) there are two important microscopic quantities given by the same mathematical formula:

$$\text{LET} = -\frac{dE}{dx} = S, \quad (135)$$

where dE is the change of the energy of the ‘average’ particle while slowing in the absorber material over a short linear distance dx .

The LET-value, the accepted abbreviation of what is called the *linear energy transfer*, describes the slowing process of the ionizing particle from the viewpoint of the absorber such as a living tissue. As such it is used for the characterization of different radiations.

This interpretation of the quantity dE/dx (called in old literature as ‘*specific energy loss*’²⁵) is very important in dosimetry that will be introduced in the next section. A larger LET-value, namely, means that the energy of the given type of particle is deposited over a shorter distance, i.e. in a smaller volume/mass. Remember the painful effect when a magnifying glass concentrates the energy of warming sunlight to a small area on our skin (an experiment probably most of us tried out as a child). It needs no further explanation that (for any given energy) radiations with higher LET-values (e.g. α) do more harm in the living tissue (if the energy is fully absorbed) than low-LET radiations (e.g. β).

As the energy transferred to the tissue is spent on ionization, larger LET-value means more ion-electron pairs per unit distance. On the microscopic scale this translates to problems ranging from ‘some of the cells have to cope with an ion-electron pair suddenly popped up in them’ (low LET-value) to ‘a lot of neighbor cells should cope (but cannot) with lots of ion-electron pairs suddenly flooding them’ (very large LET values).

On the other hand, it must also be clear, that high-LET radiations (α) have shorter *range*, R , (see Figure 61) than low-LET ones (β) because they stop within a shorter distance on average. This leads us to another interpretation of the quantity dE/dx .

The symbol S , standing for (*linear*) *stopping power*, considers the slowing process from the viewpoint of the particle. As such it is used for the characterization of different absorber materials. The higher the stopping power, the more effective the given material is when used as a shielding against the radiation. The stopping power is often expressed in terms of surface density d (also referred to as ‘mass thickness; unit: mass per area) rather than in terms of linear distance x . In that case it is sometimes called *mass stopping power*:

$$S = -\frac{dE}{dd}. \quad (136)$$

The sections following the next one will describe the radiation-matter interactions for different types of radiations from the microscopic point of view.

12.1. Dosimetric Concepts

When radiation interacts with matter, the macroscopic consequences on the latter (e.g. on a living tissue) depend not only on the total amount of radiation energy absorbed, but also on its specific value as expressed by the *absorbed dose*, one of the most important quantities of *physical dosimetry*:

$$D = \frac{E}{m}, \quad (137)$$

where m is the mass of the material in which the radiation energy E has been absorbed. The SI unit of the absorbed dose is called *gray* ($1 \text{ Gy} = 1 \text{ J kg}^{-1}$) named after the British physicist Louis Harold [Gray](#) (1905-1965) who did pioneering work in radiobiology.

As regards, e.g., biological effects, the reparatory mechanisms of cells need to cope with the damage caused by the radiation, and therefore the *dose rate*:

²⁵ The name is not conforming with the [recommendations of IUPAC](#) and IUPAP, because the adjective ‘specific’ is supposed to refer to a quantity divided by mass.

$$\dot{D} = \frac{dD}{dt} \quad (138)$$

is also an important physical *dosimetric quantity*.

As different radiations have different LET values, the actual harm caused by them cannot be characterized by the absorbed dose alone even if the dose rate is kept constant. Neither are the tissues equally sensitive to radiations. The quantities of *biological dosimetry* try to take care of these differences from the viewpoint of *radiation protection*.

The quantity that was created to make the effects of different radiations on a given tissue/organ comparable as regards harmful effects is related to the equivalent dose (H_T), which has its own unit sievert ($1 \text{ Sv} = 1 \text{ J kg}^{-1}$) named after the Swedish medical physicist Rolf Maximilian [Sievert](#) (1896-1966) who was renowned expert of the biological effects of radiation.

The *equivalent dose* acquired by tissue/organ T due to radiation R is defined as follows:

$$H_{T,R} = w_R \times D_{T,R}, \quad (139)$$

where $D_{T,R}$ is the dose absorbed by tissue/organ T from radiation R, and w_R is the radiation weighting factor.

It is w_R what actually makes the radiations comparable. In a way X-rays, γ , and β radiations are used kind of a standard by assigning the value $w_R = 1$ to them. To more dangerous radiations higher weighting factors are assigned, i.e., $w_R = 2-3$ for thermal neutrons, $w_R = 10$ for fast neutrons and protons, and $w_R = 20$ for α particles. As we see, w_R is considered a pure number, but actually is a conversion factor having the unit Sv Gy^{-1} . Note that the radiation weighting factors (unlike atomic fractions or percentages) are not normalized, just rather arbitrary values.

The calculation of the equivalent dose for a tissue (H_T) is, however, straightforward:

$$H_T = \sum_R H_{T,R}, \quad (140)$$

where the summation goes for all radiations hitting the given tissue/organ.

The quantity that was created to make the sensitivities of different tissues/organs towards radiations comparable as regards harmful effects is related to the effective dose (E), whose unit is also sievert ($1 \text{ Sv} = 1 \text{ J kg}^{-1}$) just like in the case of the equivalent dose H_T .

The *effective dose* acquired by the whole body is defined as follows:

$$E = \sum_T (w_T \times H_T), \quad (141)$$

where w_T is the *tissue weighting factor*.

It is w_T what actually makes the tissues/organs comparable. Unlike radiation weighting factors, tissue weighting factors are normalized, i.e. they add up to 1 for the whole body:

$$\sum_T w_T = 1. \quad (142)$$

As we see, w_T is considered a pure number, and really it is. The highest value ($w_T = 0.2$, i.e. 20% of the whole body) is assigned to the gonads. The next five (with $w_T = 0.12$ each) most sensitive are: red bone marrow, colon, lung, and stomach. Then follow: bladder, breast, liver,

esophagus, and thyroid ($w_T = 0.05$ each). The row is closed by skin and bone surface ($w_T = 0.01$ both). The remaining ($w_T = 0.05$) covers the rest of the body.

Beside those mentioned above there are several more dosimetric quantities defined (exposure dose, kerma, etc.), and a lot of outdated units exist parallel with the SI units (roentgen, rad, rem, etc.). However these are out of the scope of the present chapter.

12.2. Interactions of Alpha Radiation (Heavy Ions)

Imagine a high-energy α particle (a prototype of energetic heavy ions) passing through some substance. Its trajectory goes right through a cloud formed by a swarming multitude of light charged particles called electrons among which tiny but massive charge centers called atomic nuclei show up occasionally along the track. Chances of hitting such a nucleus either by ‘premature’ electromagnetic collision (note that the repulsive Coulomb field acts between them like an elastic type of bumper) or by ‘physical contact’ are rather small but not negligible. The odds of the first type of collision leading to [large-angle scattering of the \$\alpha\$ particle in a thin foil](#) of gold or platinum are about 1:8000. This rare event, however, helped Rutherford to discover the atomic nucleus in 1911. The second type of collision is equally rare, however when it happens, it can lead to nuclear reaction such as the process $^{14}\text{N}(\alpha, p)^{17}\text{O}$ observed also by Rutherford in 1919 (Table 8).

Nevertheless, the characteristic interaction of an α particle with matter is not a single collision/reaction with one of the nuclei but a series of inelastic electromagnetic collisions with lots of electrons, as a result of which the α particle gradually slows down, then starts to pick up an electron or two which may get ‘scrubbed off’ again, but eventually stops winding up as a neutral He atom.

In the slowing-down process the α particle loses its energy in chunks of ~ 100 - 200 eV on average, each chunk carried away by an electromagnetically ‘knocked’ (or rather ‘yanked’) electron of the substance. These primary electrons are sometimes referred to as δ electrons with the Greek letter reminding of the fact that such electrons are energetic enough to cause further ionization/excitation in the substance. Note that to produce an electron-ion pair costs ~ 30 eV in a gas and ~ 3 eV in a semiconductor. This means that most ionizations/excitations are produced by the slowing δ electrons and not by the α particle itself.

It is important to stress that the collisions between the α particle and the electrons are electromagnetic in nature. In other words, the α particle cannot be pictured as a simple cannon ball that knocks electrons away with brute force. In a way, the opposite is true, as follows from the LET formula ([Bethe–Bloch formula](#)) valid for heavy ions slowed by an absorber consisting of a pure element:

$$-\frac{dE}{dx} \propto \left(\frac{z^2}{u^2} \right)_{\text{ion}} (nZ)_{\text{abs}} \propto \left(\frac{m z^2}{E_{\text{kin}}} \right)_{\text{ion}} (nZ)_{\text{abs}}, \quad (143)$$

where the quantities in the first parentheses are characteristic of the ion (z is the charge number, u is the speed, m is the mass, and E_{kin} is the kinetic energy in the non-relativistic limit) and those in the second parentheses describe the absorber (n is the number density of atoms, Z is the atomic number of the element). Note that the product $(nZ)_{\text{abs}}$ is actually the concentration of the ‘electron soup’ (more exactly: the number density of electrons) in the absorber.

Looking at the first parentheses we can see that at first, when the ions still have high speed (and therefore high energy—relativistic or not) they ionize less atoms per length unit, than later, when they get slower. This is reflected by the initial part of the *Bragg curve* shown in Figure 60. (Note that electrons, however light, also have some inertia and those farther from the trajectory of the ion can hardly feel the Coulomb attraction before the ion has disappeared in the ‘distance’.)

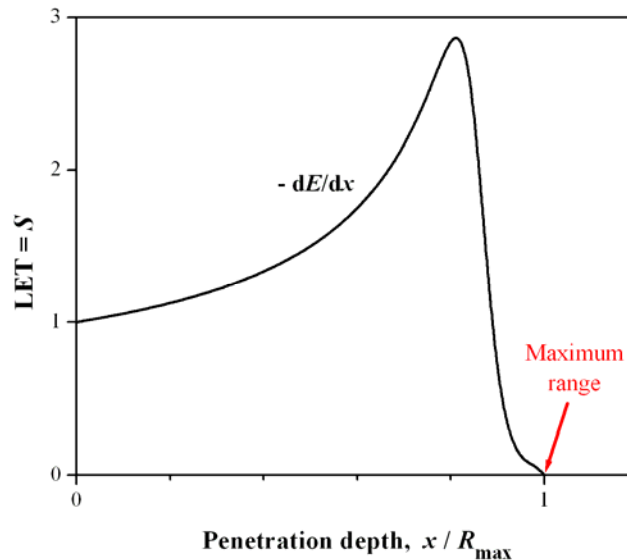


Figure 60: Schematic Bragg curve showing the linear energy transfer of (monoenergetic) α particles—the representatives of heavy positive ions—as the function of their penetration depth in an absorber. Contrary to expectations, the ‘ionizing power’ of the particles entering the absorber ($x = 0$) is lower than towards the end of their journey, just before they get stopped by the absorber. The curve breaks down as the slowed ions start to pick up electrons to become neutral He atoms at the end of the thermalization process. The sharp maximum of the curve is used in radiotherapy to ‘burn’ tumors covered by a layer of healthy tissue by the aid of accelerated ions without doing more harm than absolutely necessary.

As the ions approach the end of their journey (which is normally less than the *maximum range* R_{\max} also shown in Figure 61) and thus their energy approaches zero, Eq. (143) apparently fails as it predicts infinitely high LET value, which is clearly nonsense, and is also in contradiction with the Bragg curve. The contradiction can be reconciled by considering that the average charge of the ions gradually decreases and finally drops to zero as the slowed-down ions pick up electrons from the absorber.

Note that according to the non-relativistic limit of Eq. (143), the heavier the ion, the larger is the LET value, and therefore the shorter is the range of the ion, because it loses its energy in a shorter distance due to ionization. This partly explains why the recoil tracks of fission fragments are of microscopic size although they are very energetic particles.

The range R of heavy ions is approximately proportional to the b th power of their initial kinetic energy:

$$R \approx \{E_0\}^b, \quad (144)$$

where b is ~ 1.75 for α particles and other not too heavy ions that keep their original charge along most of their range, and ~ 0.5 for FPs whose average charge decreases gradually as they slow down. This means that the range of FPs is actually proportional to their initial speed

$(R \propto u_0)$.

The energy dependence of R and the shape of the Bragg curve can be used in radiotherapy for fine-tuning the ‘burning’ depth of the accelerated ions in applications indicated in the legend of Figure 60. Equation (144) is also an ancient tool for the energy calibration of α particles using the length of [tracks](#) left behind, e.g., in [nuclear emulsions](#).

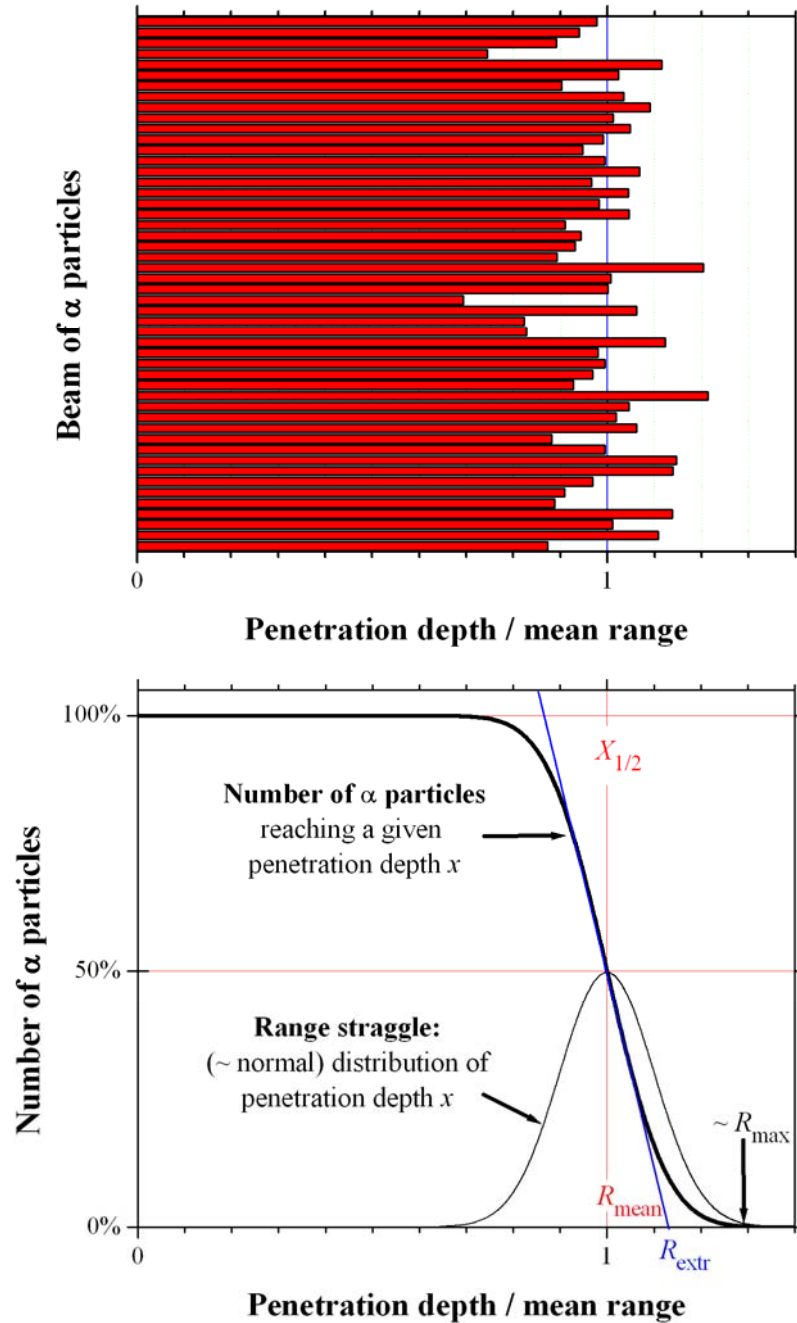


Figure 61: Absorption of α particles in matter. The mean range R_{mean} is about equal to the half-thickness $X_{1/2}$, i.e. the penetration depth x , where 50% of the radiation gets absorbed. The range R is usually identified either with R_{mean} or with the extrapolated range R_{extr} , because the maximum range R_{max} at which all α particles are absorbed cannot be measured accurately. The straggling is caused by stochastic effects, namely, the concrete ranges of individual α particles (upper panel) are not quite the same even if they have exactly the same initial energy.

12.3. Interactions of Beta Radiation (Light Ionizing Particles)

With regards to radiation–matter interactions at high particle energies, the main difference between heavy positive ions and electrons is not that they are oppositely charged—as a matter of fact the interactions of positrons will also be treated here—but because of the mass difference itself. First of all, fast electrons (and positrons) belong to the same weight-class as the orbital electrons in the absorber which slow them via inelastic collisions. Because of this, multiple large-angle scattering on (nuclei and) electrons is the rule rather than the exception. As a result, electrons travel in the absorber in a rather erratic way, and following a zigzag path they often exit the absorber on the same side they entered (Figure 62, upper panel). *Beta back-scattering* as this inelastic phenomenon is called can be used for analytical purposes because the back-scattered fraction (*albedo*) depends on the atomic number of the substance. Beta particles also have a continuous energy distribution (Figure 32) as opposed to alpha particles which are basically monoenergetic or at least their energy spectrum has but a few discrete lines (see also the upper panel in Figure 36). As a result, the absorption curve of β particles is much different from that of the α particles (Figure 61). It follows an almost exponential curve (Figure 62, lower panel), however, without the ‘tail’ spreading to infinity. Their range is usually characterized by the extrapolated range R_{extr} or by the half-thickness $X_{1/2}$, which, however, is not analogous to that of photons discussed later, neither is equal to the mean range as in the case of α radiation. Because of the ‘quasi-exponential’ attenuation of the β beam (or Auger electrons), the term effective attenuation length (EAL) is also used meaning the thickness of absorber at which the beam intensity drops to $1/e$ of the initial value. (See also the mean free path of photons.)

Because electrons are easily deflected, the acceleration (deceleration) and the bremsstrahlung caused by this may have considerable contribution to their LET-value/stopping power:

$$-\frac{dE}{dx} = \left(-\frac{dE}{dx}\right)_{\text{ionization}} + \left(-\frac{dE}{dx}\right)_{\text{bremsstrahlung}}, \quad (145)$$

where the ionization term is the analogue of the stopping power formula of heavy ions shown by Eq. (143), except that some consequences of the lightness of the colliding electrons have to be taken into consideration (e.g. that they tend to behave relativistically). The second term becomes important here because the probability of photon emission (or, more exactly, the radiant power) is inverse proportional to the square of the mass of the accelerating particle ($\propto m^{-2}$). This makes the contribution of *bremsstrahlung* ~ 54 million times higher with β radiation than with α radiation under similar conditions. The ratio of the above two terms depends on the energy and the atomic number of the absorber:

$$\left(-\frac{dE}{dx}\right)_{\text{ionization}} : \left(-\frac{dE}{dx}\right)_{\text{bremsstrahlung}} \approx 1 : \frac{E}{800 \text{ MeV}} Z. \quad (146)$$

Thus, above ~ 10 MeV of electron energy, bremsstrahlung becomes the dominating of the two terms for absorbers made from heavy elements such as ${}_{82}\text{Pb}$. This explains why *synchrotron radiation* (which is also high-energy bremsstrahlung) is produced by accelerating electrons and not protons, for instance.

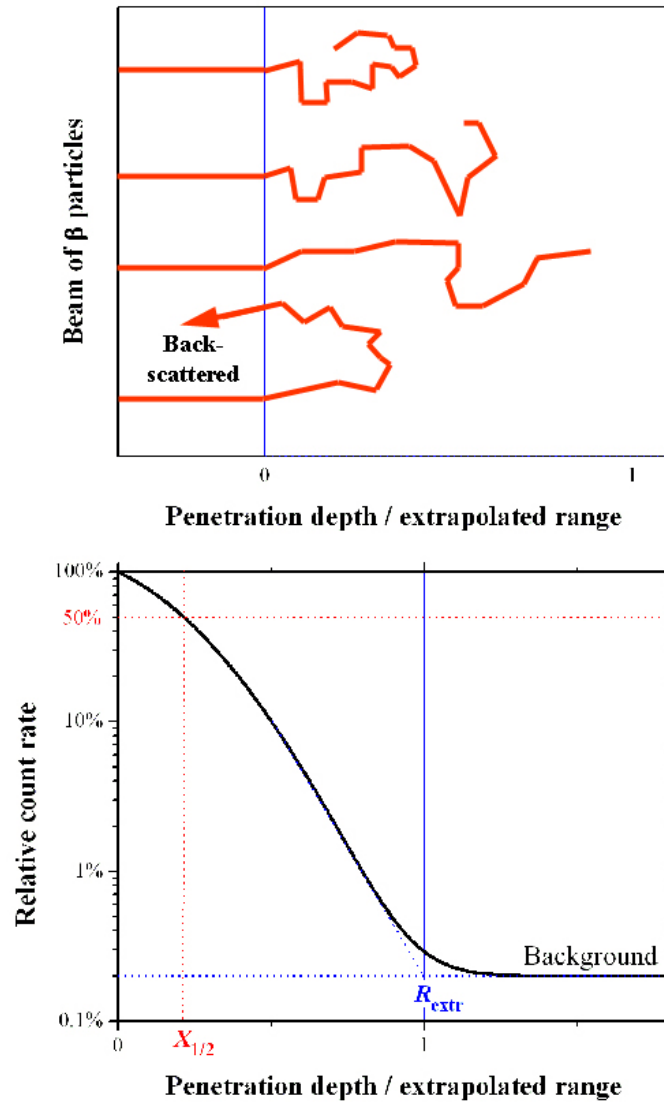


Figure 62: Absorption of β particles in matter. The range R is usually identified with the extrapolated range R_{extr} . The half-thickness $X_{1/2}$ also characterizes penetrating power. The straggling of β particles is much broader because multiple scattering (upper panel) leading sometimes to back-scattering typical of them. They are not monoenergetic either, and therefore the absorption curve (lower panel) is approximately exponential (note that the vertical axis has logarithmic scale). The background can be caused by γ photons which are also detected by the β counter.

As mentioned above, the interactions of high-energy positrons are not much different from electrons of the same energy except that they lose their energy somewhat faster. The real difference between them becomes observable when they get thermalized. A slow positron spends, namely, long enough time in the vicinity of an electron (its antiparticle) either to form together a short-lived hydrogen-atom like bound system called *positronium* (Ps):



or they can undergo *free annihilation* right away (Figure 63), most often producing two ~ 511 keV *annihilation photons* which leave the scene in opposite directions because of momentum conservation:



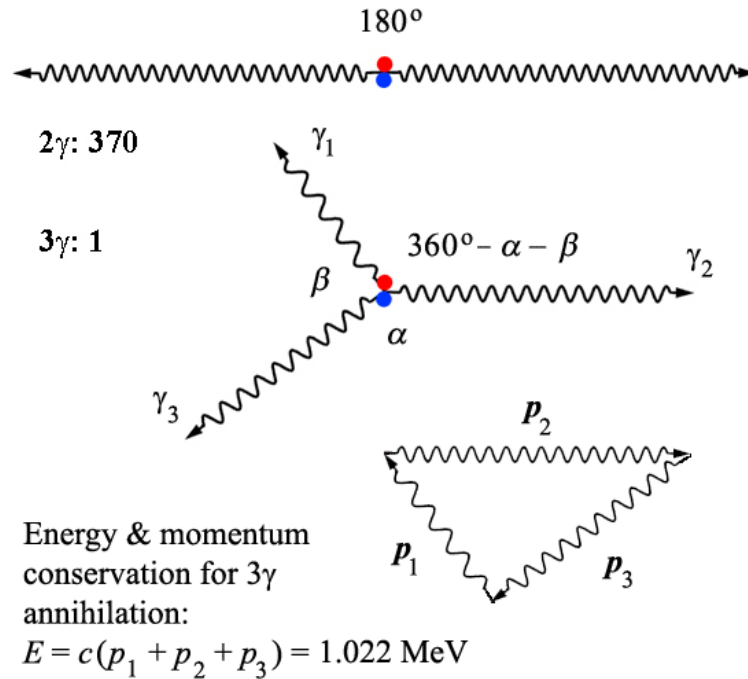


Figure 63: Free annihilation of a positron–electron pair. The most probable process is [2γ annihilation](#) (upper diagram) representing more than 99.7% of free annihilation events. Each annihilation photon carries away the rest energy $m_e c^2 = 511 \text{ keV}$ of one annihilating particle. The next most frequent event is 3γ annihilation (middle diagram), when the co-planar photons have an infinite number of different possibilities of how to share the total rest energy $2m_e c^2 = 1022 \text{ keV}$ while satisfying momentum conservation (lower diagram). [While representing photons, the lengths of the wavy arrows and the frequencies of the sine waves were drawn to be proportional both to the momentum and the energy carried by them. Thus momentum conservation is reflected by the fact that the three momentum vectors form a closed triangle (the momentum of the electron–positron pair is namely neglected). Energy conservation is translated to the language of geometry like this. Consider the infinite set of similar triangles and select that particular one whose perimeter equals E/c , where $E = 1.022 \text{ MeV}$.]

Note that annihilation photons differ from ‘regular’ γ photons (originating from nuclear transition), namely, their energy is not that well-defined. This is so because the positrons annihilate before they are fully stopped and their kinetic energy adds to the rest energy $2m_e c^2 = 1022 \text{ keV}$ which is divided between the photons.

Positrons are formed as two ‘variants’ in the proportion 1 to 3. The first variant is para positronium (p-Ps: 1 part) in which the spins of the positron and the electron have opposite directions ($\uparrow\downarrow$). This means that in the ground state (when the orbital momentum is 0) the total angular momentum is 0. This is a singlet state, which can ‘show itself’ only in a single way when placed, e.g., in a magnetic field. The second one is ortho positronium (o-Ps: 3 parts) in which the spins of the positron and the electron are parallel ($\uparrow\uparrow$) and therefore the observable value (projection) of the total angular momentum in the ground state is 1 (\hbar). This is a triplet state, which can behave in three different ways in a magnetic field, namely the projection of the angular momentum can be +1, 0 or –1 relative to the direction determined by the magnetic flux density \mathbf{B} . These directions represent different energies due to the magnetic moment that goes with the angular momentum. (Note that the magnetic needle cannot be indifferent either to its own direction relative to the magnetic field. Otherwise, namely, it could not be a useful part of a compass.) For those being averse to quantum mechanics, the exact ratio of formation 1:3 must be an important indication that some of its concepts are of great relevance to reality. In the given case, e.g., the triplet must be considered as an assembly of three independent

entities per se because the 1:3 ratio of formation does not depend at all on the presence of a magnetic field.

There are two remarkable differences between the singlet p-Ps having parity (+1) and the triplet o-Ps with parity (-1):

1. The mean life of p-Ps is about 0.1 ns, while o-Ps lives as ‘long’ as 140 ns.
2. The p-Ps can only annihilate to an even number of photons typically undergoing 2γ annihilation similarly to the upper diagram in Figure 63)
3. The o-Ps can only annihilate to an odd number of photons with the typical process being 3γ annihilation like in the middle diagram in Figure 63. The angular distribution is reflected by Figures 64-65 calculated from Eq. (149).

Difference 2-3 follows from the conservation of *parity*. Parity is *multiplicative quantity* (as opposed to *additive quantities* such as electric charge, momentum or baryon number etc. that are also conserved). Considering that the parity of photons is (-1), then for 2γ annihilation the parity of the photons formed is $(-1)\times(-1) = (+1)$, which equals the parity of p-Ps. In 3γ annihilation the parity of the photons is $(-1)^3 = (-1)$, which is equal to the parity of o-Ps.

According to [You et al.](#) the angular distribution of 3γ annihilation is described by the following symmetric formula:

$$P(\alpha, \beta, \gamma) = \left[(1 - \cos \alpha)^2 + (1 - \cos \beta)^2 + (1 - \cos \gamma)^2 \right] \frac{\sin \alpha \cdot \sin \beta \cdot \sin \gamma}{(\sin \alpha + \sin \beta + \sin \gamma)^3}, \quad (149)$$

in which P is the probability; the angles α and β are explained by the middle diagram in Figure 63; and γ is the third angle ($360^\circ - \alpha - \beta$) there.

The above formula is interesting not only from the viewpoint of positron annihilation, but also because it shows why it is so important to define exactly what ‘experiment’ is related to the given distribution. (See, e.g., [Bertrand’s paradox](#).) Figure 64 shows the original function (149) in two types of presentation, whereas Figure 65 shows that symmetric case, when $\alpha = \beta$ and $\gamma = 2\theta$.

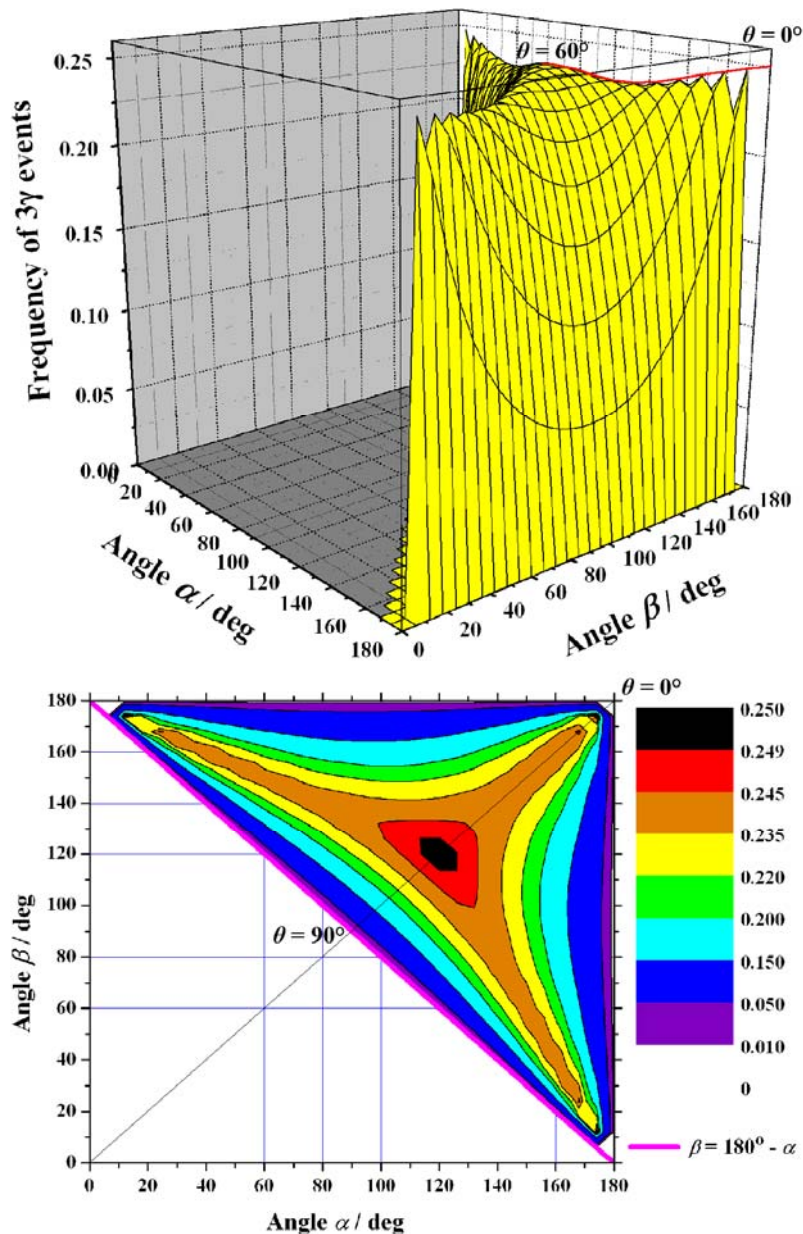


Figure 64: Angular distribution of photons formed via the 3 γ annihilation of o-Ps calculated from Eq. (149). The o-Ps ($\uparrow\uparrow$) can only decay by 3 γ annihilation. A possible geometry for the annihilation is shown in the middle diagram in Figure 63 also indicating the angles α and β . (For the explanation of the angle θ see Figure 65.). The upper panel of the figure shows a 3D presentation of the angular distribution, whereas the lower one is the contour map of the same distribution. Note that in the lower left \blacktriangle of the contour map the conditions of momentum and energy conservation (explained in the legend of Figure 63) cannot be satisfied at all and therefore it is a white area of the map. It is clear from the map that symmetric decay (black spot on the map), when three ~ 341 keV photons leave the scene at 120° , is rather frequent. However, the events when two photons go nearly (but not exactly) parallel and the third one goes in the opposite direction keeping the momentum in balance seem to be also common (see the tips of the triangular ‘pirate hat’). In contrast to Figure 65, this distribution belongs to an experiment in which the radiation source is surrounded by a spherically arranged array of detectors detecting all coplanar 3 γ events. What if we select a certain direction pointing to one of the detectors, restricting our attention only to 3 γ events at which the selected detector also gives a signal?

Would that change the distribution? What if we only select a plane that contains the source and consider only 3 γ signals from detectors crossed by the plane? What if we make both restrictions?

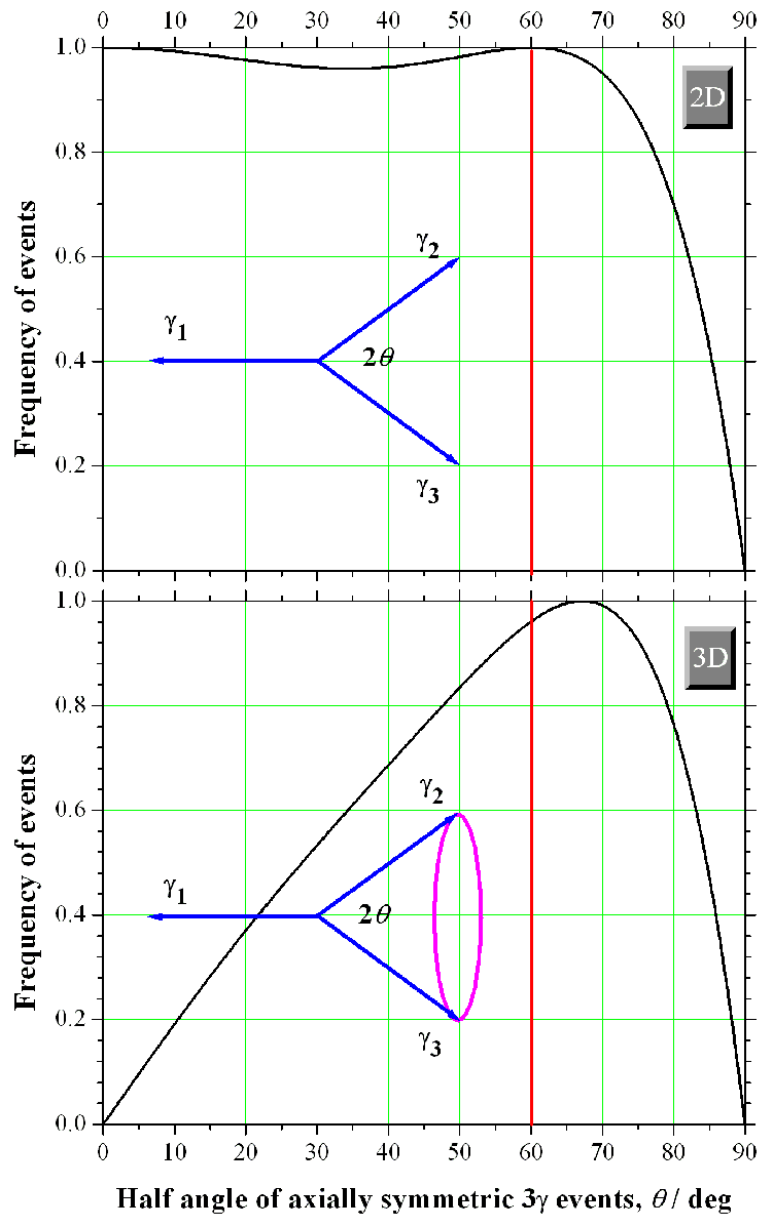


Figure 65: The upper panel has been prepared after [You et al.](#), who studied the 3γ annihilation of o-Ps at the symmetric geometry indicated by the inset using three detectors. (γ_i s are unit vectors showing the directions of the photons/detectors.) One should imagine the graph standing straight in the symmetry plane of the ‘three-cornered hat’ in the lower panel of Figure 64 in such a way that $\theta = 0^\circ$ corresponds to the upper right corner of the square, while $\theta = 90^\circ$ to its center. In that position the curve nicely fits the contour of the 3D presentation on the upper panel of Figure 64 along the diagonal plane perpendicular to the direction of looking (see the red line). The authors have found experimentally a good agreement with the shown theoretical graph, whose maximum is at $\theta = 60^\circ$ (which represents a totally symmetrical 3γ event with $\alpha = \beta = 2\theta = 120^\circ$ between the γ quanta). The lower panel is to indicate that the spatial frequencies would be different. Due to the cylindrical symmetry around the axis γ_1 , namely, the frequency of events with a given angle θ will be proportional to the circumference of the **magenta circle**, which must be taken into consideration by a factor of $\sin \theta$. As we see, the maximum of the curve thus obtained is a bit off from maximum symmetry. Also, the $\theta = 0^\circ$ corner of the pirate hat represents a low-probability event in space. In contrast to Figure 64, these distributions belong to experiments in which one of the detectors surrounding the radiation source is fixed (the detector pointed at by vector γ_1) and only those coplanar 3γ events are considered at which that particular detector gave a signal and, moreover, the sites of the other two detectors are symmetrical to the γ_1 axis. In the upper panel even the plane of the detectors is fixed.

Another important consequence of the lightness of β particles in general follows from the fact that they are much faster at any given energy than heavy ones (such as α particles). As a matter of fact, β particles move so fast that they tend to be ‘relativistic’ as demonstrated by Figure 66.

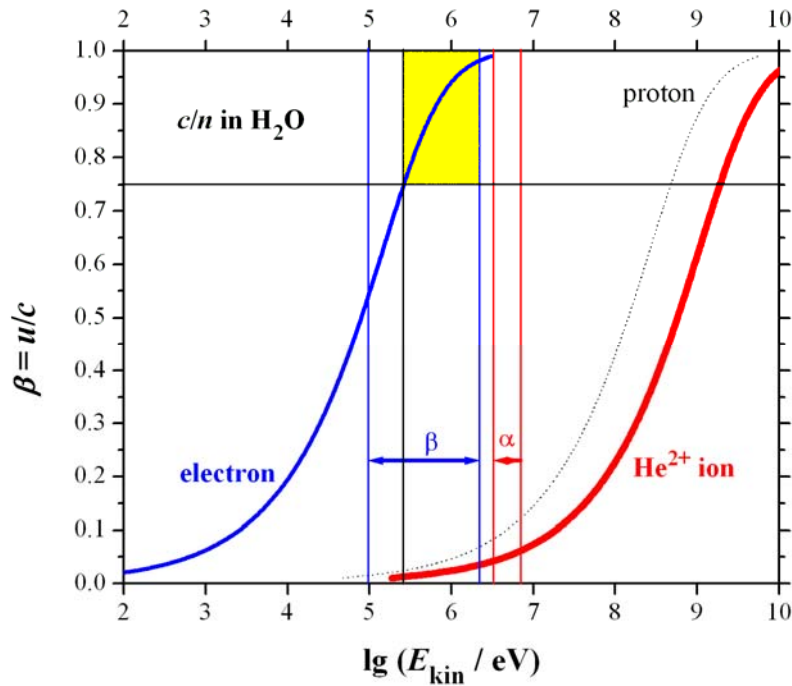


Figure 66: Speed vs. kinetic energy plot for particles with different masses. On the logarithmic energy axis 3 is for 1 keV, 6 is for 1 MeV, and 9 is for 1 GeV. The vertical axis (β) measures the particle speed u relative to the speed of light c in empty space. The typical energy ranges for β and α particles produced by natural radioactivity are indicated by horizontal arrows. Light particles, like electrons from the β decay, can easily have enough kinetic energy (see the shaded rectangle) to move faster than visible light propagates in a condensed phase such as water. Heavier particles, like He^{2+} ions, can only become relativistic (under terrestrial conditions) when accelerated artificially to several GeV. The horizontal line at $\beta = 0.75$ determines the threshold energy for different particles below which they remain undetected by a Cherenkov counter.

The yellowed energy/speed range in Figure 66 is of particular importance, because when the speed u of a particle exceeds the speed of light in a substance such as water (c_w):

$$u > c_w = \frac{c}{n_w}, \quad (150)$$

(where $n_w \approx 1.333$ is the index of refraction of water at $\lambda = 589$ nm) the particle becomes the source of visible light called *Cherenkov radiation*. Since visible-light photons carry little energy, the contribution of Cherenkov radiation to Eq. (145) is negligible. It is important, however, for particle detection because:

- it only occurs above the *threshold energy* at which condition (150) is fulfilled;
- its direction is correlated with the direction of motion of the particle.

The latter feature is caused by the fact that Cherenkov radiation can be interpreted as an electromagnetic kind of [shock wave](#). Shock waves can be observed when power-boats (faster than the propagation rate of waves) plough through still water. The straight wavefront starting at both sides of the prow enclose an angle 2δ which gets smaller as the boat gets faster. The shock wave itself moves away from the track of the boat at right angles to the line of the

wavefront, and therefore its propagation direction is determined by the complementary angle ε of the angle δ as seen in Figure 67. Note that ε ($= 90^\circ - \delta$) gets larger as the boat gets faster.

The relationship between the propagation direction of Cherenkov radiation and the speed of the particle is given by the following formula:

$$\cos \varepsilon = \frac{c}{u n_w}, \quad (151)$$

which only gives reasonable result if condition (150) is fulfilled.

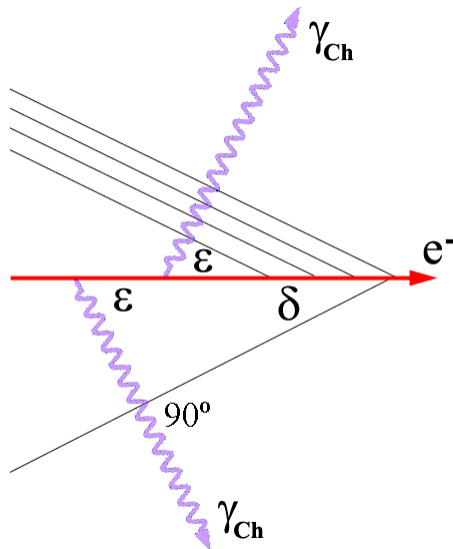


Figure 67: Beta particles (moving in a condensed phase such as liquid water) with energies higher than a few hundred keV are sources of visible light called Cherenkov radiation. The direction of the [bluish light](#) (γ_{Ch}) depends on the velocity of the electron as explained in the text. There is only one conical wavefront moving together with the electron. The parallel gray lines above the horizontal red arrow (representing the track of the electron) are only drawn to show the past positions of the wavefront thus indicating the actual direction of propagation of the wave. Note that the maximum of the angle ε in water is $\sim 41.4^\circ$. The angle shown in the figure ($\sim 64^\circ$) could however be measured in diamond having higher index of refraction.

The directional correlation of Cherenkov radiation and its conical propagation was used by Japanese scientists, to provide convincing proof of the solar origin of some of the neutrino radiation on Earth. The neutrino detector called [Super-Kamiokande](#) is a huge water container (filled with $50\,000\text{ m}^3$ of H_2O), surrounded by a multitude of light sensors (more than 11 thousand photomultiplier tubes—PMTs—of 50 cm diameter). Some of the neutrinos—in a similar way like photons in the Compton effect (see the next section)—undergo elastic collision with an electron, which gains enormous energy/velocity in the process, thus becoming the source of Cherenkov radiation.

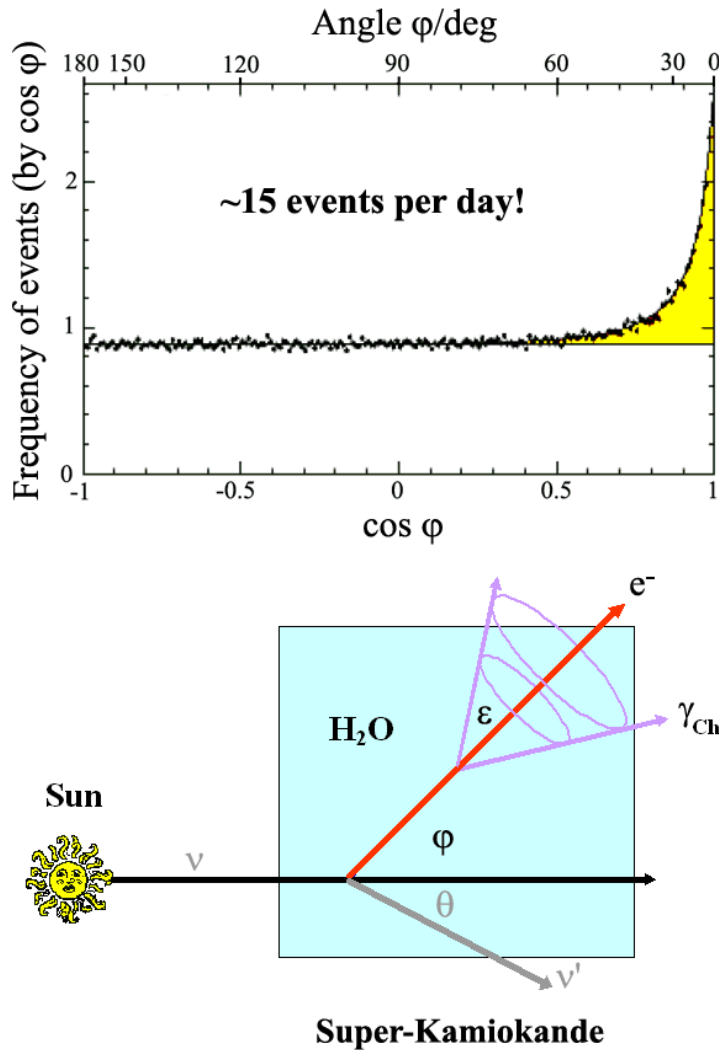


Figure 68: Between 1996-2001, by using the neutrino detector Super-Kamiokande 22 400 neutrino events were detected and analyzed according to the angle φ enclosed by the direction of the Sun and that of the motion of electrons knocked out by neutrinos. The electrons themselves were detected by the Cherenkov radiation produced by them. The upper panel shows the distribution of $\cos \varphi$, but for convenience's sake I marked a few φ values as well. The histogram gives convincing evidence of the origin of the yellow-filled peak at $\varphi = 0^\circ$. These electrons moving away from Sun must have been released by solar neutrinos. The lower panel shows the scattering of a solar neutrino on an electron.

The process follows the general scheme of the Compton scattering of photons, but in this case the angle φ is measured (which characterizes the initial direction of the electron) rather than θ . The directional angle φ can be measured, because the Cherenkov photons (γ_{Ch}) created by the electron activate only photoelectric multiplier tubes that are aligned along a ring (see Figure 69) out of the total 11 146 of PMTs watching 40% of the container surface. (after Masayuki Nakahata http://www.aapps.org/archive/bulletin/vol13/13_4/13_4_p07p12.pdf).

By making use of the propagation characteristic of the radiation, the computer processing the detector signals is able to filter out from the background 15(!) events a day that are related to electrons knocked by neutrinos. It can also figure out the energy/speed of the electron as well as its location and direction of propagation. The latter is characterized by the angle φ in Figure 68. From Eq. (189) one can easily see, why exactly the distribution of the $\cos \varphi$ values is given on the upper panel instead of the angle φ directly. The same equation also shows that for higher-energy electrons the angle φ gets smaller. Looking at the upper panel, therefore, we can conclude that the electrons are predominantly forward-scattered with rather high energy. This

also means that the scattering geometry on the lower panel bay far not typical, because the angle φ on the histogram is less than 30° in most of the cases.

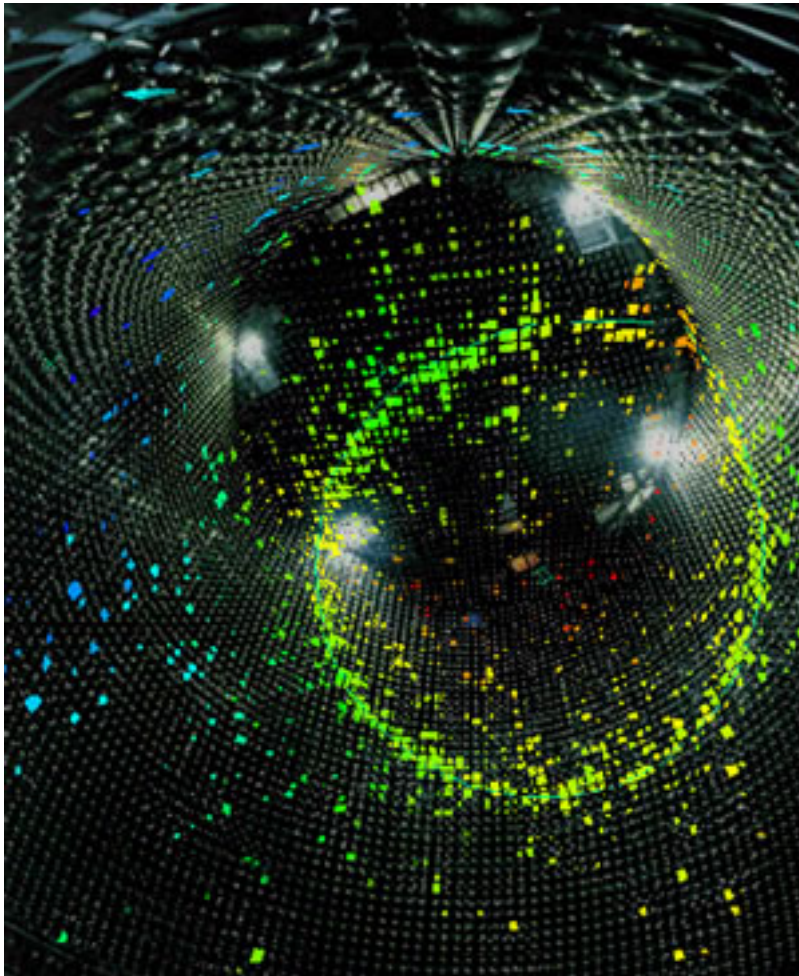


Figure 69: A neutrino event captured by the neutrino detector Super-Kamiokande. The mosaic is formed by a tremendous number of PMTs. Those in green color show the conical cross section of Cherenkov radiation on the surface. From the shape of this ring one can locate the axis of the cone along which the electron started its journey in the water after having been knocked by the neutrino. The size of the ring and the opening angle of the cone reveals where the apex of the cone is. The latter is pointing directly at the site of the neutrino event. (Source: <http://www.lbl.gov/Science-Articles/Archive/sabl/2006/Jan/04-TEV-pt2.html>).

12.4. Interactions of Gamma Radiation (High-Energy Photons)

The most important interactions of X-rays and γ -rays with matter are Compton scattering, photoelectric effect and [pair production](#) (Figure 70).

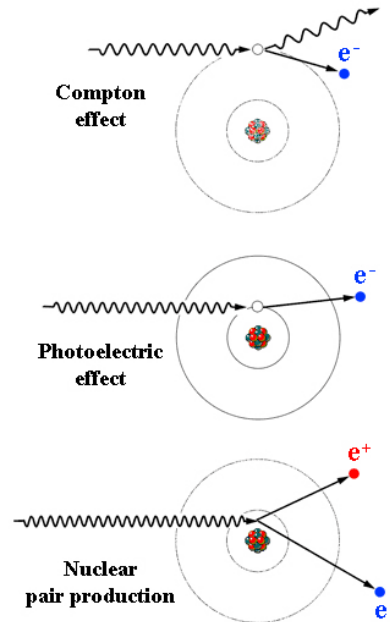


Figure 70: Schematic representation of the major interactions of high-energy photons with matter. In [Compton scattering](#) the binding energy of the (valence) electron is negligible compared to that of the photon, and therefore their ‘collision’ is basically elastic (i.e. quasi elastic). [Photoelectric effect](#) is an inelastic process. If energetically possible, a strongly bound K electron is knocked out while the atom is also ‘yanked’ thus absorbing the excess momentum of the photon which stops to exist. [Nuclear pair production](#) takes place in the Coulomb field of the nucleus. The high-energy photon ($E_\gamma > 2m_e c^2 = 1022 \text{ keV}$) disappears and a positron–electron pair pop up instead. The nucleus is a ‘silent partner’ in the process taking away the excess momentum of the ‘deceased’ photon.

Compton scattering (also called *Compton effect*) is the (quasi) elastic scattering of a photon γ (with energy $h\nu$ and momentum $h\nu/c$) on a free electron initially at rest (Figure 71). As a result of the collision the electron gets moving (with kinetic energy E_e and momentum p_e). As a result, the photon (γ') is deflected by an angle θ relative to the original direction and both its energy ($h\nu'$) and momentum ($h\nu'/c$) will be less due to energy and momentum conservation.

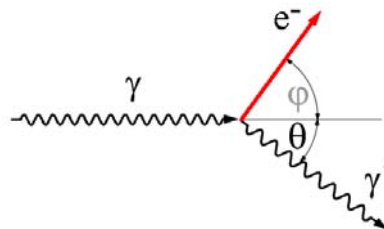


Figure 71: Compton scattering is an elastic (actually: quasi elastic) collision of a photon with a (quasi) free electron. The lengths of the arrows are proportional to the conserving momenta. The frequencies of the sine waves pictured are also proportional to the energies of the photons (as well as to their momenta because $p_\gamma = E_\gamma/c = h\nu/c$ for photons).

At the scattering geometry shown in Figure 71 (which is just an example chosen from an infinite number of different possibilities), the ratio of the momenta is:

$$\frac{h\nu}{c} : \frac{h\nu'}{c} : p_{e^-} = 5 : 4 : 3. \quad (152)$$

Energy conservation in this particular case demands that for the energies we have

$$h\nu : h\nu' : E_{e^-} = 5 : 4 : 1, \quad (153)$$

because $5 = 4 + 1$.

This simple example makes it clear that energy and momentum conservation involving both photons and ‘massive’ particles is a delicate business because the energy to momentum ratio is different for photons and other particles (with mass) except when the latter are extremely relativistic and start to behave ‘photon-like’ (see Figure 57). It also helps to understand, why photoelectric effect (see further below) is impossible to occur with a free electron and why its probability increases with the binding energy of the electron up to the limit where it is still energetically possible to tear off the electron from binding.

Figure 72 shows some important features of the Compton effect with 511 keV annihilation photons taken as an example. As we can see on the upper panel of the figure, the scattering angle θ of the photon (Figure 71) also determines the energy (as well as the direction φ) of the Compton electron. Compton electrons have a continuous energy distribution (see the lower panel of Figure 72). The energy distribution of Compton-scattered photons is also continuous and it is easily obtained by flipping the distribution of the electrons around the vertical line drawn at half of the initial energy of the photon (i.e. at 255.5 keV this time).

Compton electrons get the maximum energy when the photons are back-scattered at 180° (upper panel in Figure 72). However, as we can see from Eq. (187), the photon cannot lose its total energy in this (quasi) elastic interaction. Therefore a minimum of energy (namely, that corresponding to the angle $\theta = 180^\circ$) is conserved, no matter what the scattering geometry is:

$$E_{\gamma'} = \frac{E_{\gamma}}{1 + \frac{E_{\gamma}}{m_e c^2} (1 - \cos\theta)} \geq (E_{\gamma'})_{\min} = \frac{E_{\gamma}}{1 + \frac{2E_{\gamma}}{m_e c^2}} = \frac{E_{\gamma}}{1 + \frac{E_{\gamma}}{255.5 \text{ keV}}} > 0, \quad (154)$$

which, in the given case ($E_{\gamma} = 511 \text{ keV}$), guarantees *at least* an energy of $E_{\gamma'} = 511/3 \text{ keV} \approx 170 \text{ keV}$ for the scattered photon.

Since the minimum energy of the scattered photon and the maximum energy of the Compton electron add up to the energy of the original photon we can write:

$$(E_{e, \text{kin}})_{\max} = E_{\gamma} - (E_{\gamma'})_{\min} = \frac{E_{\gamma}}{1 + \frac{m_e c^2}{2E_{\gamma}}} = \frac{E_{\gamma}}{1 + \frac{255.5 \text{ keV}}{E_{\gamma}}} < E_{\gamma}, \quad (155)$$

which, in the given case ($E_{\gamma} = 511 \text{ keV}$), guarantees *at most* an energy of $E_{e, \text{kin}} = 511/1.5 \text{ keV} \approx 341 \text{ keV}$ for the kicked electron.

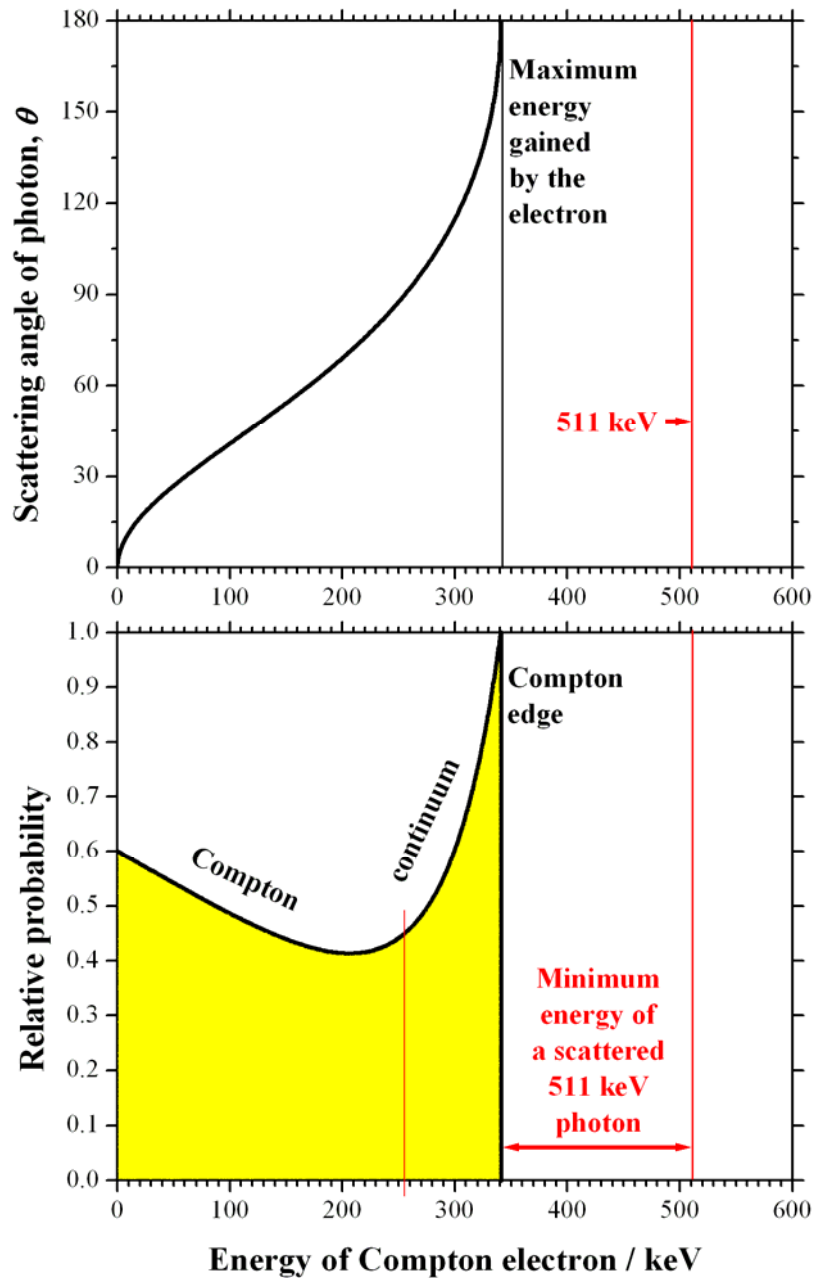


Figure 72: Characteristics of Compton effect with 511 keV annihilation photons taken as an example. The scattering angle θ determines the energy of the Compton electron (upper panel). The Compton electrons have a continuous energy distribution (lower panel). The energy distribution of Compton-scattered photons is also continuous and can be obtained from that of the electrons by flipping it around the vertical axis drawn at 511/2 keV (see Figure 73).

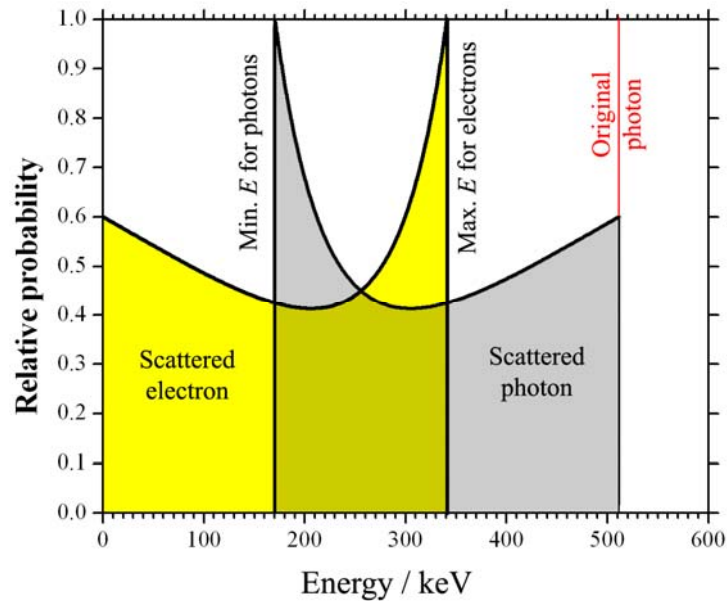


Figure 73: Characteristic energy distributions of Compton scattered annihilation photons and knocked Compton electrons. The two distributions are mirror images of each other, because two particles divide the original energy of the photon (511 keV in the present case) between themselves. Therefore different types of particles whose energies are complementary relative to the original energy must be equal in number.

In the inelastic *photoelectric effect*, on the other hand, the whole 511 keV would be spent on releasing a lower-lying orbital electron—most probably a K electron—and providing it with kinetic energy. The kinetic energy of the *photoelectron* will then be equal to the difference of the photon energy and the binding energy of the orbital the electron is knocked out from. The photon ceases to exist as a result of the photoelectric effect. The inner electron hole in the atom will be filled by an outer orbital electron followed by X-ray emission and/or Auger effect.

The story of the photoelectric effect may have sounded like it was about a bilateral transaction between the photon and the electron. However the atom from which the electron is torn off also plays an important role, namely, it is needed for the energy and momentum conservation to be fulfilled. When the photon ‘hits’ the electron, the atom itself gets more involved in the process if the binding energy of the electron is higher. (Or, using a metaphor: when picking apples from a tree, ripe apples come off quite easily without quivering a leaf, while unripe ones clinging with their stems pull the whole branch before they release it. The first case is analogous to Compton effect, while the second to the photoelectric effect.) The involvement of the atom can be seen by having a closer look at the K-edge in Figure 74.

The interpretation of the K-edge is as follows. For high-energy photons all 82 electrons of ^{82}Pb are (in principle) available for photoelectric effect. However, as soon as the photon energy decreases below 88 keV (~ 0.09 MeV), which is the binding energy on the K shell of lead, the two K electrons are not available anymore for photoelectric effect. The fact that the probability drops dramatically at this point (to $\sim 10\%$) shows that the possible contribution of the K electrons to photoelectric effect is much higher ($\sim 90\%$) than expected from their relative number ($2/82 \approx 2.4\%$). At still lower energies there are several more (but less sharp) edges (L-edges etc) that are out of the scale of Figure 74. The very existence of such edges proves that the chances for photoelectric effect are the better the stronger is the bond between the electron and the atom. (Provided, of course, that the photon energy is enough to break the bond.)

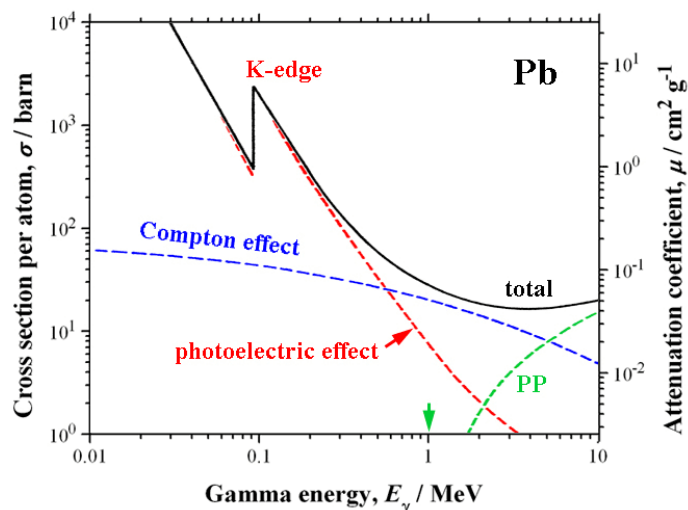


Figure 74: Cross sections and mass attenuation coefficients for the three major interactions of photons in ${}_{82}\text{Pb}$ as the function of the photon energy. For high- Z elements like lead, the dominant interaction at low energies is photoelectric effect, while Compton effect is relatively unimportant. (For low- Z elements Compton effect dominates over photoelectric effect in this energy range.) The overall tendency of both interactions is decreasing; however the probability of photoelectric effect decreases faster and therefore around 1 MeV Compton effect takes over. Slightly above 1 MeV (indicated by the green arrow) pair production (PP) aided by nuclei begins and gradually becomes the dominant interaction at higher energies. The K-edge on the curve of the photoelectric effect is explained in the text.

Pair production (PP) is the ‘transformation’ of a high-energy photon (i.e. ‘pure energy’) to a particle–antiparticle pair consisting of an electron e^- and a positron e^+ (in this particular case). The ‘silent partner’ helping energy and momentum to be conserved is usually a nucleus, but in the schematic example shown in Figure 75 it is an orbital electron knocked out from an atom. Nuclear (i.e. nucleus-aided) PP occurs above ~ 1.022 MeV representing the rest energy of two electrons ($2m_e c^2$) as seen in Figure 74. Since the nucleus is heavy, it needs to take up very little energy to absorb the excess momentum of the photon. Therefore its recoil is too small to make it visible on photographs like the original of Figure 75. The threshold energy of electron-aided PP ($4m_e c^2 = 2.044$ MeV) is twice as high as that of the nucleus-aided process, because the knocked-out electron is light and therefore it has to acquire considerable kinetic energy to be able to carry away enough momentum. Without an accessory like that (e.g. in a vacuum void even of electromagnetic field) pair production would be impossible. (Think about the limiting case of nuclear PP, when the energy $h\nu$ of the photon is just about enough for the positron and electron to pop up from ‘nothing’. They have practically neither kinetic energy nor momentum. Thus, the momentum $h\nu/c$ of the photon has to be taken by a third mass: a nucleus in this case, which is heavy enough to do this ‘favor’ for a negligible price paid in energy.)

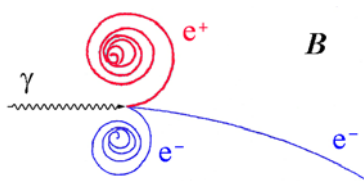


Figure 75: Schematic bubble chamber photograph of electron-aided pair production (PP) taken in a magnetic field. The induction vector \mathbf{B} is perpendicular to the plane of the picture pointing away from the observer. The energy of the photon (leaving no track in the chamber) is much higher than the

combined rest energies of the electron–positron pair ($2m_e c^2 = 1.022 \text{ MeV}$). In a magnetic field the tracks of oppositely charged particles curl in opposite directions around the field lines. The slower is the particle, the tighter the curl. The tracks of the pair resemble the spiral springs of a clock, showing that the electron and the positron are gradually slowed down by the substance in the chamber. The fast electron with the almost straight track is an orbital electron of an atom carrying away the excess momentum of the photon which ceases to exist after the interaction. (Graphics prepared *after the original* from Lawrence Livermore National Laboratory, <http://www.llnl.gov/>.)

As a result of the interactions of γ - and X-rays with matter, high-energy electrons (photoelectric effect and Compton effect) or positrons (PP) may form. These secondary particles interact with matter similarly to β radiation (see the previous subsection).

The absorption of a beam of monoenergetic (or ‘monochromatic’) photons follows an exponential law that is similar to the Beer–Lambert law known from chemistry:

$$I = I_0 \exp(-\mu x), \quad (156)$$

where I is the intensity of X- or γ -radiation that has passed through an absorber layer whose absorption properties are characterized by μ and thickness by x , and I_0 is the initial intensity of the beam entering the absorber. The quantity μ is the *mass attenuation coefficient* (unit: $\text{cm}^2 \text{ g}^{-1}$ as seen on the right vertical axis of Figure 74) and x is the *surface density* of the absorber (unit: g cm^{-2}). The quantities μ and x can also be interpreted as the *linear attenuation coefficient* (unit: cm^{-1}) and the *linear distance* (unit: cm). The respective quantities are connected through the (mass) density ρ (unit: g cm^{-3}): $\mu_{\text{lin}} = \rho \mu_{\text{mass}}$ and $\rho x_{\text{lin}} = x_{\text{mass}}$.

Note that the absorption equation (156) is mathematically equivalent to the exponential law of decay (73) with the following correspondences: $I \Leftrightarrow N$, $I_0 \Leftrightarrow N_0$, $\mu \Leftrightarrow \lambda$, and $x \Leftrightarrow t$.

The reasons for the equivalence are as follows:

- The *agelessness* of radioactive atoms causing exponential distribution of the lifetimes translates to *indefatigability* of the photons meaning that they—in contrast to directly ionizing particles—are not losing energy in a continuous way as they penetrate the absorber. Therefore, at any point of their ‘trajectory’, they have the same chance to get to a given distance without any interaction as if they had just started their journey. This means that the distribution of the distances ending with interaction has to be exponential.
- Interacting photons are absorbed or cleared away from the beam via scattering. In any way they are lost as regards detection. Therefore the exponential law also holds for the number of photons detected as the function of the absorber thickness.

It follows from the exponential absorption law that photons cannot have a ‘range’ in the same sense as ionizing particles do. They, namely, can penetrate any thickness with some probability. The parameter δ , which could be called the mean range by the correspondence ($\delta = 1/\mu \Leftrightarrow \tau = 1/\lambda$), is actually called the *mean free path*. Instead of half-life $T_{1/2}$ we have now *half-thickness* $X_{1/2}$ meaning an absorber thickness halving the intensity of the beam. The next half-thickness halves the intensity again and so on.

Besides the exponential rule of light absorption, the indefatigability of photons—in a different sense—is an everyday experience. This is what makes it possible for us to see stars light years away with naked eyes. The increasing redshift of spectrum lines with increasing distance—the only observation that could be interpreted as a proof of fatigue (note that redshift means lower frequency, i.e. lower energy)—is however attributed to the *Doppler effect* caused by the [Hubble expansion](#) of the Universe.

12.5. Interactions of Neutrons

The most important interactions of neutrons are based on their electric neutrality and their sensitivity to the nuclear force (residual color force, see also the section 4.1). Therefore they practically do not ionize the matter but can induce various nuclear reactions as we have seen in chapter 7 (see Table 8 and Figure 33). Neutron capture and neutron activation in general serve as a basis for NAA, an important analytical application. Another important type of neutron reaction—neutron-induced fission—is the basis of nuclear energy production.

Here only the slowing process will be discussed, because of the importance of thermal neutrons in different applications including the fission of ^{235}U , the most common fuel of nuclear reactors. (See also the upper panel of Figure 30.)

Out of the two possible slowing mechanisms that do not consume neutrons—elastic collision $X(n,n)X$ and inelastic collision $X(n,n')^*X$ on the nuclei X of the *moderator* material—elastic collision is the more effective and the more desirable.

The elastic collision can be pictured as the random (i.e. not necessarily head-on) collision of two elastic balls, one with ‘mass’ 1 (neutron) and another with ‘mass’ A (X), where A is the mass number of X .

If the neutron of initial energy E_0 collides with a nucleus at rest, its energy E after the elastic collision will be limited by the following inequality:

$$\alpha \equiv \left(\frac{A-1}{A+1} \right)^2 \leq \frac{E}{E_0} < 1, \quad (157)$$

where the lower limit α corresponds to head-on collision and the upper one to the ‘just-missed-it’ event.

The lower limit α is 0%, 11%, and 72% for ^1H , ^2H , and ^{12}C , respectively, and approaches 100% as the mass number increases. No wonder that ordinary water—basically pure $^1\text{H}_2\text{O}$ —is used as moderator in many nuclear reactors. In the case of ^1H , namely, the neutron can lose its whole kinetic energy even in one single head-on collision with a proton. Most of the time, however, several random collisions are needed for the neutron to slow down to a given lower energy, e.g. to thermal energy kT .

The *lethargy* (u) is a quantity often used instead of the energy E to characterize neutrons slowed from an initial energy E_0 :

$$u = \ln \left(\frac{E_0}{E} \right). \quad (158)$$

Note that the name of this quantity is really appropriate, because slowing ($E < E_0$) means that the neutrons become more ‘lethargic’, i.e. their lethargy increases²⁶. The value of E_0 is usually taken as the energy of fission neutrons (1-2 MeV). The thermal energy kT at room temperature corresponds then to $u \approx 18$.

The *lethargy gain* while the neutron gets slowed down from energy E_{high} to energy E_{low} is:

²⁶ Note that the relation between lethargy and energy is very much similar to the relation between pH and hydronium-ion concentration. Both are logarithmic and both are inverse relationships in the sense that whenever the lethargy/pH increases, the energy/hydronium-ion concentration decreases, and vice versa.

$$\Delta u = u_{\text{low}} - u_{\text{high}} = \ln\left(\frac{E_0}{E_{\text{low}}}\right) - \ln\left(\frac{E_0}{E_{\text{high}}}\right) = \ln\left(\frac{E_{\text{high}}}{E_{\text{low}}}\right). \quad (159)$$

The mean lethargy gain ξ in a single collision turns out to be independent of the initial energy:

$$\xi = 1 + \frac{\alpha}{1-\alpha} \ln \alpha. \quad (160)$$

Thus the average number ν of collisions that are needed to reach a given lethargy gain Δu is:

$$\nu = \frac{\Delta u}{\xi}. \quad (161)$$

This result translates to:

$$\nu = \frac{18}{\xi} \quad (162)$$

when fission neutrons are thermalized.

The value of ξ is 1 for ^1H , 0.725 for ^2H , and 0.158 for ^{12}C . Thus the average numbers of collisions to reach thermalization are 18, 25, and 114, respectively.

13. Nucleosynthesis

13.1. Chemical Puzzle—Binding Energies vs. Abundances of Elements and Isotopes

It has been mentioned before that we live in a relatively young Universe, where there is plenty of hydrogen to fuel stars, factories of heavier elements. The present state of affairs in the Solar System is documented by Figure 76 showing the atomic abundances of different isobars in a semi-logarithmic plot.

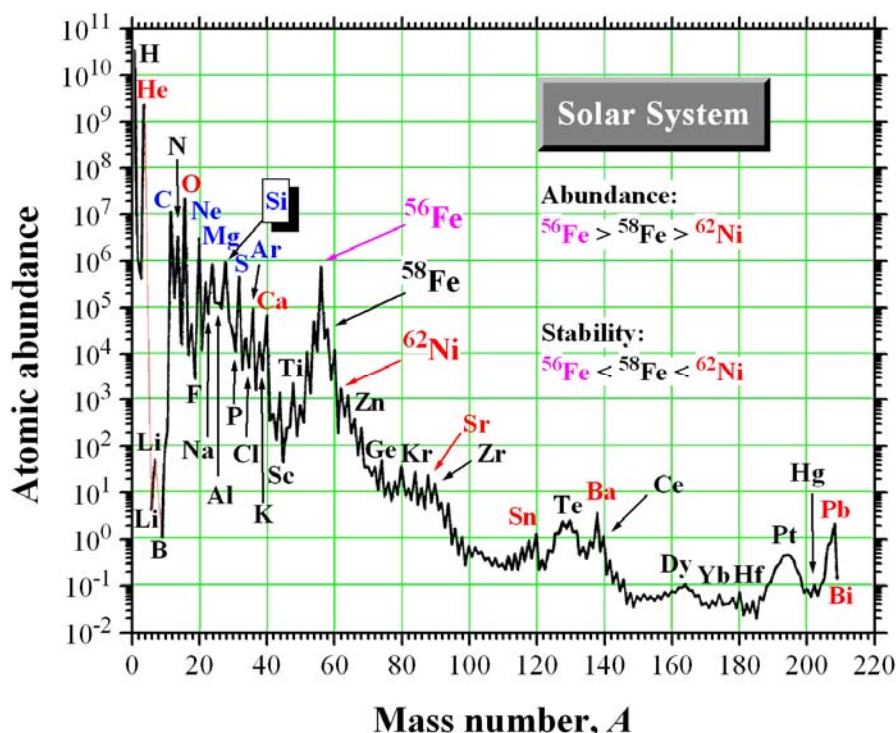


Figure 76: Abundances of stable isobars in the Solar System. Red color indicates magic nuclides/elements, blue color shows α nuclides (unless they are also magic). The nuclear composition of the latter is given by $Z = N = 2n$ ($n = 1, 2, 3, \dots$). The most abundant of the three most stable nuclides (^{62}Ni , ^{58}Fe , and ^{56}Fe) is colored magenta. Note that ^{56}Fe is almost as common as silicon ^{28}Si , which is used as a reference (10^6 Si atoms). The thin red lines connecting the data points ^4He – ^6Li and ^7Li – ^9B are to call attention to the fact that there is no stable nuclide for $A = 5$ and 8 (see Figure 25). The elemental abundances in the SS are shown in Figure 22.

Note that the number of atoms of the third most abundant element, oxygen, the only stable isobar for $A = 16$, is a mere $\sim 0.1\%$ of hydrogen atoms, represented by its most abundant isotope ^1H . Iron, one of the most stable elements as regards the average binding energy per nucleon, and a common element on Earth, is much less abundant in the Solar System than helium (less than 0.1% of ^4He atoms). Helium however is a very rare element on Earth due to its lightness and because it only occurs in elementary state, forming monatomic gas. This, namely, makes it easy for He atoms to gain the escape velocity from thermal motion which enables them to break free from the gravity of our planet.

According to Figure 76, the three most stable nuclides in the Universe (^{62}Ni , ^{58}Fe , and ^{56}Fe) show opposite trends as regards stability and abundance. This is a telltale sign that stability

alone does not explain the elemental composition of the Universe because kinetics and mechanisms of processes are just as important questions for nucleosynthesis.

Figure 77 contains another important clue as regards the possible role of kinetics and mechanisms in nucleosynthesis. Apparently ^{62}Ni , the most stable of all nuclides, is not even the most abundant stable isotope of nickel. As a matter of fact, its contribution to nickel is just a few percent, whereas the least stable isotope ^{58}Ni makes up almost 70% of this element.

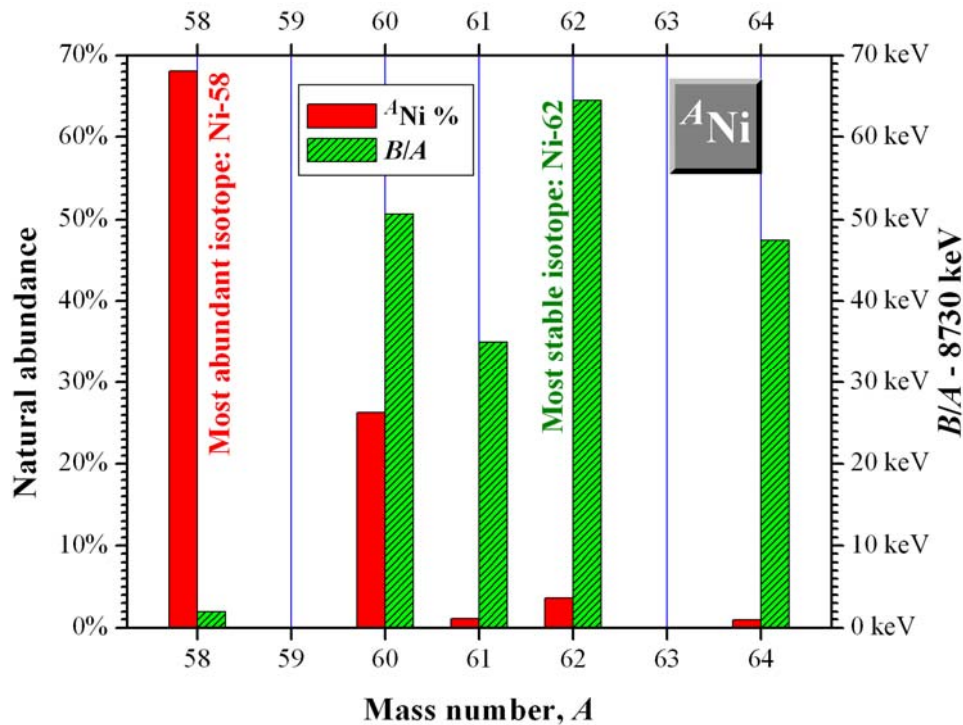


Figure 77: Comparison of natural abundances (red columns) and per nucleon binding energies (green columns) for stable isotopes of nickel. Contrary to (possible) expectations, natural abundances of stable isotopes are in no correlation with the B/A values, a clue indicating that stability is just one of the factors that determine the nuclidic composition of matter around us.

13.2. Nucleosynthetic processes and related concepts

This section draws heavily from the following website:

<http://nedwww.ipac.caltech.edu/level5/Glossary/frames.html>

3 α process: Also called the **triple- α process**, this is the initial step of **helium burning** sometimes referred to as *the* helium burning. In this exothermic nuclear reaction, helium is transformed into carbon ($3\ ^4\text{He} \rightarrow\ ^{12}\text{C} + 7,27\ \text{MeV}$). The process actually follows a two-step mechanism with the processes $2\ ^4\text{He} \rightarrow\ ^8\text{Be}$ and $^8\text{Be} +\ ^4\text{He} \rightarrow\ ^{12}\text{C}$ quickly following each other. This is the dominant process fueling red giants. As the hydrogen is exhausted in the core of a star, hydrogen burning cannot produce sufficient energy to withstand gravitation. Consequently, the core shrinks, which causes the temperature and the density to increase to about $2 \times 10^8\ \text{K}$ and $10^5\ \text{g cm}^{-3}$, respectively. Under such conditions three α particles can fuse to form an excited nucleus of ^{12}C , which occasionally decays into a stable ^{12}C nucleus. The overall process can be looked upon as an equilibrium between three ^4He nuclei and the excited $^{12*}\text{C}$ nucleus, with occasional irreversible leakage out of the equilibrium into the ground state of ^{12}C ($^{12*}\text{C} \rightarrow\ ^{12}\text{C} + 7,65\ \text{MeV}$) either by γ -ray cascade or internal pair production. Further capture of ^4He nuclei by ^{12}C nuclei produces ^{16}O and ^{20}Ne . Helium burning virtually stops at

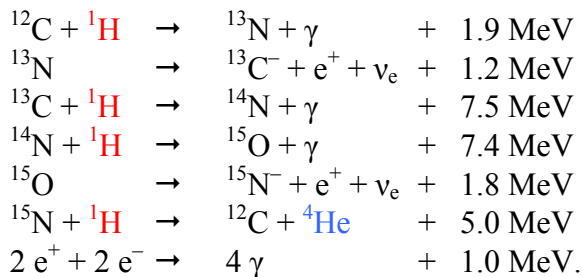
this point, but formation of ^{24}Mg has also been reported.

4N nuclei: Also called **α nuclei**. 4N nuclei are built from equal *and* even numbers of neutrons and protons. Their composition is therefore the multiple of the nucleon composition of an α particle which contains four nucleons (N) in the form of two protons (p) and two neutrons (n). 4N nuclei are formed in supernova envelopes at temperatures of at least 2×10^9 K and are very stable. (See the peaks in the inset of the lower panel in Figure 24.) The term is sometimes used in the sense even-even nuclei.

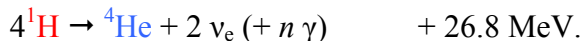
α - β - γ theory: Explanation of the *big-bang theory* in terms of nuclear physics, proposed by Ralph **Alpher**, Hans **Bethe** and George **Gamow**. To include Bethe as an author in the 1948 [\$\alpha\beta\gamma\$ paper](#) was actually meant as a pun by Gamow.

Carbon burning: The stage in the life cycle of some stars (after or towards the end of helium burning) when carbon is fused to produce heavier elements like oxygen, neon, sodium, and magnesium. [Carbon burning](#) eventually occurs in all stars with more than eight Solar masses (but it cannot occur below $\sim 4 M_{\odot}$).

CNO-I cycle: It is one of the **CNO** mechanisms (also called **carbon cycle**, **CN cycle**, or [Bethe–Weizsäcker cycle](#)) by which a star can produce energy by converting hydrogen into helium (besides the proton-proton chain fueling the Sun). (In the Sun, CNO cycles are responsible for less than 2% of the total ^4He production.) The CNO-I cycle consists of a series of nuclear reactions $^{12}\text{C}(p, \gamma)^{13}\text{N}(p, \gamma)^{14}\text{O}(\beta^+ \nu_e)^{14}\text{N}(p, \gamma)^{15}\text{O}(\beta^+ \nu_e)^{15}\text{N}(p, \alpha)^{12}\text{C}$ (see Figure 78), in which carbon, nitrogen, and oxygen serve as catalysts in the conversion. (Actually, the carbon, nitrogen, and oxygen can be pictured as the same nucleus going through a number of transformations in an endless cycle.) This cycle powers main-sequence stars with more than ~ 1.5 solar masses (M_{\odot}) as well as giants and supergiants of all masses. The cycle can only take place if the necessary carbon nuclei are present, and it requires higher temperatures (15–20 MK) and is far more temperature-dependent ($E \propto T^{15}$) than the proton-proton chain ($E \propto T^4$). The first step is the fusion of carbon and hydrogen nuclei. Using nuclidic notation and Q -values rounded to one decimal we have:



The net result is the same as for the p-p process or any other process converting hydrogen to helium:



The Q -values given for the β^+ steps are actually end-point energies, i.e., E_{β} values shown in Figure 32. (Q -values given in data bases, e.g. for [N-13](#), are higher than the end-point energy of the β^+ spectrum, because they are ground state to ground state values representing the difference between the rest energies of parent and daughter leaving the rest energies of radiation particles disregarded.) However, the positrons annihilate with available electrons to photons in a very short time. Annihilation photons thus formed (similarly to the gamma-photons produced in the other steps) have no chance to escape from the Sun. So their energy gets degraded and distributed among the particles in the core. That is why they are shown in

parentheses in the net equation. Neutrinos are a different matter. Most of them escape from the star carrying away, on an average, 1.7 MeV of the ~ 26.8 MeV released.

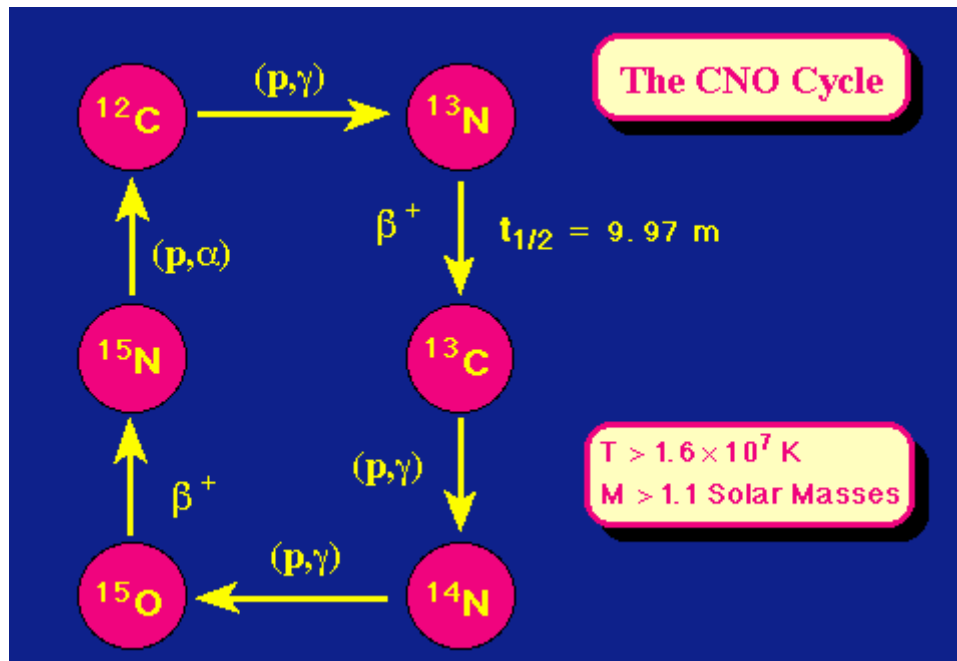


Figure 78: The CNO-I cycle is a major carbon-catalyzed mechanism of hydrogen burning in stars that are heavier and hotter than the Sun. As the Sun is not a first generation star (and therefore contains some carbon as well as other heavier elements), the CNO cycle is a weak competitor of the p-p chain but its contribution to helium production is less than 2%. Courtesy of Rick Firestone (<http://csep10.phys.utk.edu/astr162/lect/energy/cno.html>).

CNO-II cycle: (Also called **CNO bi-cycle** :-) It is similar to the CNO-I cycle, except that it consists of the steps $^{15}\text{N}(p, \gamma)^{16}\text{O}(p, \gamma)^{17}\text{F}(\beta^+ \nu_e)^{17}\text{O}(p, \alpha)^{14}\text{N}(p, \gamma)^{15}\text{O}(\beta^+ \nu_e)^{15}\text{N}$. The process depends on the presence of fluorine as a catalyst. For main-sequence stars greater than a few Solar masses (M_{\odot}), hydrogen burning by the CNO-II cycle is the main source of energy.

Explosive nucleosynthesis: Also called [supernova nucleosynthesis](#). It is the collective name of nucleosynthetic processes which occur in supernovae. These explosive processes produce the nuclei from neon up to and including the r -process nuclei. Explosive carbon burning produces nuclei from neon to silicon. Explosive oxygen burning produces nuclei from silicon to calcium. Explosive silicon burning produces the iron peak nuclei.

Helium burning: The stage when a star fuses helium into carbon (and oxygen). Stars with more than half a solar mass (M_{\odot}) eventually burn helium.

Helium flash: It means runaway helium burning under [degenerate conditions](#). The helium flash occurs in the hydrogen-exhausted core of a star in the red-giant phase of evolution. When, due to gravitational pressure, the degenerate core heats up to about 10^8 K, the helium nuclei start to undergo thermonuclear reactions. Once the helium burning has started, the temperature increases rapidly, and the extreme sensitivity of the nuclear reaction rate to temperature causes the helium-burning process to accelerate. This in turn raises the temperature, which further accelerates the helium burning, until a point is reached where the thermal pressure expands the core and thus removes the degeneracy and limits the flash. The helium flash can only occur when the helium core is less than about $2 M_{\odot}$ and thus it is restricted to low-mass stars.

Hydrogen burning: The fusion of hydrogen into helium. This is the process by which all [main-sequence stars](#) generate energy. Every star with more than 0.08 solar masses burns hydrogen.

Iron peak: A maximum on the element-abundance curve near mass number $A = 56$ (see Figure 76). It consists of the following elements: vanadium, chromium, manganese, iron, cobalt, nickel.

Oxygen burning: The stage when a star fuses oxygen into silicon and sulfur. It occurs only in stars with over eight Solar masses.

Primordial nucleosynthesis: The creation of elements during the first three minutes after the Big Bang. According to standard theory, primordial nucleosynthesis produced only five nuclides, all lightweight: hydrogen-1, hydrogen-2 (or deuterium), helium-3, helium-4, and lithium-7.

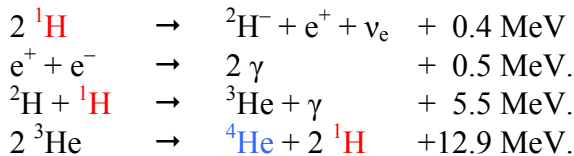
Proton-proton chain: (p-p chain) A series of thermonuclear reactions in which hydrogen nuclei are transformed into helium nuclei. The temperature and density required are about 10^7 K and 100 g cm^{-3} . It is the main source of energy in the Sun, where 10^{38} of these reactions occur every second. This nuclear sequence is also typical of all other main-sequence stars with less than 1.5 Solar masses. Hotter/heavier stars mainly burn hydrogen to helium by means of the CNO cycle. All parts of this reaction have been observed in the laboratory, except for the first step ${}^1\text{H}(p, \beta^+ \nu){}^2\text{H}$, which occurs only a few times in 10^{12} collisions of protons. The p-p chain divides into three main branches:

pp I: ${}^1\text{H}(p, \beta^+ \nu_e){}^2\text{H}(p, \gamma){}^3\text{He}({}^3\text{He}, 2p){}^4\text{He}$.

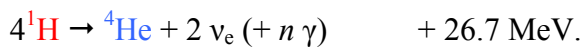
pp II: ${}^1\text{H}(p, \beta^+ \nu_e){}^2\text{H}(p, \gamma){}^3\text{He}({}^4\text{He}, \gamma){}^7\text{Be}(\beta^+ \nu_e){}^7\text{Li}(p, \alpha){}^4\text{He}$.

pp III: ${}^1\text{H}(p, \beta^+ \nu_e){}^2\text{H}(p, \gamma){}^3\text{He}({}^4\text{He}, \gamma){}^7\text{Be}(p, \gamma){}^8\text{B}(\beta^+ \nu){}^8\text{Be} \rightarrow 2 {}^4\text{He}$.

In the Sun the branch pp I is common (see Figure 79):



The net result is the same as for the CNO process or any other process converting hydrogen to helium (the apparent difference in the Q -value comes from rounding error):



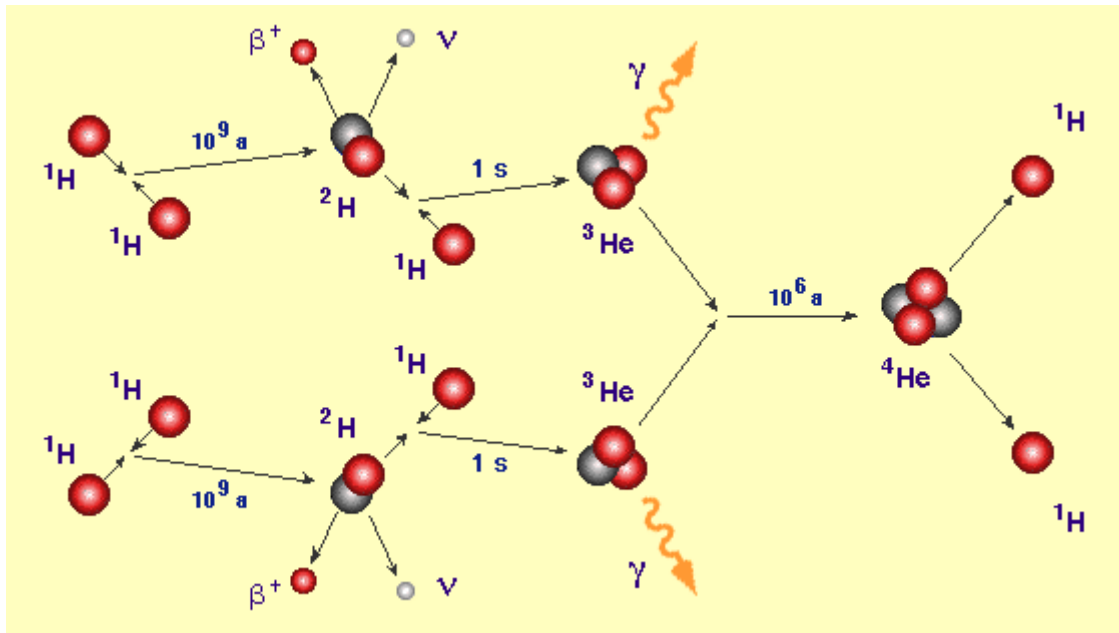


Figure 79: The pp I chain is the typical mechanism of hydrogen burning in main sequence stars with similar properties to those of the Sun. The rate determining step is the first one leading to the formation of ^2H deuterium. The processes pp II and pp III start at increasingly higher temperatures than that characteristic of the Sun's core. Courtesy of Rick Firestone (<http://csep10.phys.utk.edu/astr162/lect/energy/ppchain.html>).

***r*-process:** The rapid capture of neutrons. The nucleus absorbs abundant neutrons in rapid succession, so that regions of great nuclear instability are bridged in the chart of nuclides. The model accounts for the existence of all elements heavier than bismuth (up to $A \approx 298$) as well as the neutron-rich nuclides beyond iron. The *r*-process is based on the release of great numbers of neutrons in a very short time (less than 100 seconds). The source for such a large flux of neutrons is a supernova, at the boundary between the collapsing neutron star and the ejected material. However, other proposed sources have included such things as supernova shocks and black-hole-neutron-star collisions. The heavier *r*-process elements are synthesized at a temperature of about 10^9 K and an assumed neutron density of 10^{20} - 10^{30} per cm^3 . The *r*-process is terminated by neutron-induced fission. The existence of ^{244}Pu ($T_{1/2} = 82$ Ma) in the early solar system shows that at least one *r*-process event had occurred in the Galaxy just before the formation of the solar system.

***s*-process:** A slow neutron capture process in which heavy, stable, neutron-rich nuclei are synthesized from iron-peak elements by successive captures of free neutrons in a weak neutron flux, so there is time for β decay before another neutron is captured. (The average time between captures is about 10-100 years.) This slow but steady process of nucleosynthesis is assumed to take place during the red-giant phase of stellar evolution (after the core's He content got exhausted) at densities up to 10^5 g cm^{-3} and temperatures of about 3×10^8 K (neutron densities assumed are 10^{10} cm^{-3}). The *s*-process slowly builds stable nuclear species up to $A = 208$. It ends there, because any further capture of neutrons leads immediately to α -decay leading to the production of lead or thallium. The *s*-process probably occurs in stars where $M < 9 M_{\odot}$.

Silicon burning: At the end of the life for a high-mass star, silicon burning ignites creating iron and other elements of similar mass, before the star turns to a supernova.

Appendix

14. Special Relativity Aside—Summary of Equations and Notations

Relativity is thought to belong to the realm of science fiction by most people. However, the use of relativistic formulae is unavoidable if the particle speed u gets high enough. And this is so whenever β decay comes into the picture. Relativistic effects must also be considered when designing particle accelerators, particularly synchrotrons in which the electrons move practically at the speed of light.

As regards the following equations I have adopted the interpretation that particles have a unique [mass](#) m (also called intrinsic mass, invariant mass, proper mass, or, in older literature, ‘rest mass’) that determines their rest energy E_0 :

$$E_0 = m c^2. \quad (163)$$

For the total energy E and the momentum \mathbf{p} we have:

$$E^2 = m^2 c^4 + p^2 c^2, \quad (164)$$

$$\mathbf{p} = \frac{E}{c^2} \mathbf{u}, \quad (165)$$

where \mathbf{u} is the velocity²⁷ of the particle and c is the speed of light in empty space.

The explicit formulae for the total energy and the momentum are as follows:

$$E = \gamma m c^2, \quad (166)$$

$$\mathbf{p} = \gamma m \mathbf{u}, \quad (167)$$

where

$$\gamma = \frac{1}{\sqrt{1 - \beta^2}}, \quad (168)$$

$$\beta = \frac{\mathbf{u}}{c}. \quad (169)$$

(Note that in older literature the quantity γm is referred to as ‘relativistic mass’ also known as ‘apparent mass’, which increases with the particle speed u .)

The total energy can also be expressed as the sum of the rest energy E_0 and the kinetic energy E_{kin} :

$$E = E_0 + E_{\text{kin}} = m c^2 + E_{\text{kin}}. \quad (170)$$

The kinetic energy can also be given as a power series of u^2/c^2 :

²⁷ Note that the vector quantity \mathbf{u} that describes both the speed of motion (u) and its direction is called velocity. Therefore in ‘physics English’ the words *speed* and *velocity* are not synonymous.

$$E_{\text{kin}} = m c^2 \left[\frac{1}{2} \left(\frac{u^2}{c^2} \right) + \frac{3}{8} \left(\frac{u^2}{c^2} \right)^2 + \dots \right]. \quad (171)$$

Note that the above series only delivers the non-relativistic kinetic-energy formula if $u \ll c$. In that case, namely, all terms can be neglected in comparison with the first one, which yields $m u^2/2$ as expected.

15. Massless Particles—Cases of Extremely Relativistic Behavior

For massless particles, such as the photon γ , $m = 0$.

Therefore it follows from Eq. (164) that

$$p_\gamma = \frac{E_\gamma}{c}. \quad (172)$$

As a consequence of this and Eq. (165), such particles can only move (in a vacuum) with the speed of light c :

$$u_\gamma = c. \quad (173)$$

It also follows from Eq. (170) that the total energy E_γ comes from motion, i.e., it is of the kinetic type. (Nobody has ever seen a photon at rest.)

Note that the above two equations are approximately fulfilled whenever the share of the rest energy is negligible part of the total energy even if the particle is not massless. If, namely

$$E_0^2 = m^2 c^4 \ll m^2 c^4 + p^2 c^2 = E^2, \quad (174)$$

then:

$$E^2 \approx p^2 c^2, \quad (175)$$

and therefore

$$p \approx \frac{E}{c}, \quad (176)$$

In other words, the total energy (which practically consists of nothing but kinetic energy) will become proportional to the momentum as shown by Figure 57, and the particle moves with the speed of light:

$$u \approx c. \quad (177)$$

In this sense therefore such particles behave kind of ‘photon-like’.

16. Scattering of ‘photon-like’ particles on free ‘massive’ particles

The left drawing in Figure 80 tells the story of Compton scattering cartoon-wisely. The story is detailed in connection with the radiation–matter interactions (see Figure 71). The right drawing is more important at this moment anyway, showing the momentum conservation in a form that also applies, e.g., to electron scattering experiments performed to measure the size of atomic nuclei which use extremely fast electrons.

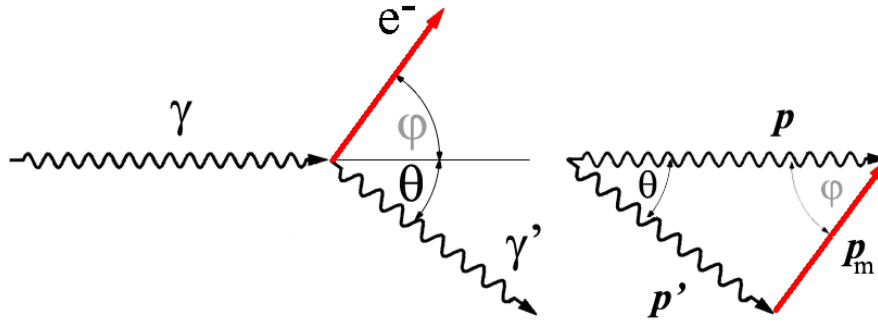


Figure 80: The left drawing shows Compton scattering, i.e. the scattering of a massless photon on a more massive particle, namely, a free electron. Compton effect serves as an example of a more general story, which is about the scattering of a light particle behaving ‘photon-like’ (e.g. an extremely fast electron or a neutrino) on a free massive particle initially at rest (e.g. a nucleus or an electron). To treat these cases together, the labeling of the right drawing (showing momentum conservation) does not contain direct reference to the photon (γ). Only the sine waves (representing the momentum vectors) are the same as a reminder that the particles behave ‘photon-like’, which, however, in this case has nothing to do with the wave nature of the particles. The label p_m at the solid red arrow represents the momentum vector of the massive scatterer particle. The angle θ is emphasized on the diagram, but φ would be just as good as far as geometry is concerned. The reason for the choice is simple: in general, it is much more difficult to measure the direction of motion of the massive particle. Unless the scattered particle is a neutrino, as in the case of the Super-Kamiokande detector shown in Figure 68, which was used to determine the angle φ of the electrons kicked by solar neutrinos.

The phenomena mentioned in the title will be treated together. Therefore Eqs. (172) and (176) will be rewritten as follows:

$$p \cong \frac{E}{c}, \quad (178)$$

where the relation ‘ \cong ’ means ‘=’ in the case of photon scattering (Compton effect) and ‘ \approx ’ in the case of high-energy electron scattering on nuclei.

The square of the moment of the massive particle can be readily expressed using the law of cosines (see the *momentum conservation* diagram on the right panel in Figure 80). Using also Eq. (178) we get:

$$p_m^2 = p^2 + p'^2 - 2 p p' \cos \theta \cong \frac{E^2}{c^2} + \frac{E'^2}{c^2} - 2 \frac{E E'}{c^2} \cos \theta. \quad (179)$$

Using Eq. (164), we can write for the total energy of the massive particle after scattering:

$$E_m^2 = m_m^2 c^4 + p_m^2 c^2. \quad (180)$$

Substituting Eq. (179) we have:

$$E_m^2 \cong m_m^2 c^4 + E^2 + E'^2 - 2 E E' \cos \theta. \quad (181)$$

Energy conservation also must be fulfilled for the total energy. Since the massive particle was originally at rest and therefore its total energy consisted of rest energy $m_m c^2$, we can write:

$$E + m_m c^2 = E' + E_m. \quad (182)$$

After rearranging and raising to the second power:

$$E_m^2 = m_m^2 c^4 + E^2 + E'^2 - 2(E E' - E m_m c^2 + E' m_m c^2). \quad (183)$$

Comparing the right sides of Eqs. (181) and (183) we can see that the three first terms cancel. After rearrangement and reduction, as well as division by $E E' m_m c^2$ we get:

$$\frac{1}{E'} - \frac{1}{E} \cong \frac{1 - \cos \theta}{m_m c^2}, \quad (184)$$

from which the energy of the scattered particle can be easily expressed as:

$$E' \cong \frac{E}{1 + \frac{E}{m_m c^2} (1 - \cos \theta)}. \quad (185)$$

As regards Compton scattering, the energy of the photon scattered by the electron is given by the following formula:

$$E_\gamma' = \frac{E_\gamma}{1 + \frac{E_\gamma}{m_e c^2} (1 - \cos \theta)}. \quad (186)$$

One can easily ascertain that E_γ' monotonically decreases, while θ increases from 0° to 180° .

- It is little surprise that the case ‘it-has-almost-missed-it’ ($\theta = 0^\circ$) is characterized by $E_\gamma' = E_\gamma$.
- It is more interesting that the scattered photon cannot get rid of its whole energy even at back-scattering geometry ($\theta = 180^\circ$) at which the energy loss is maximal. In other words, $E_\gamma' > 0$, because

$$E_\gamma' = \frac{E_\gamma}{1 + \frac{E_\gamma}{511 \text{ keV}} (1 - \cos \theta)} \geq \frac{E_\gamma}{1 + \frac{E_\gamma}{511 \text{ keV}} (1 - \cos 180^\circ)} = \frac{E_\gamma}{1 + \frac{E_\gamma}{255,5 \text{ keV}}} > 0. \quad (187)$$

This also means that photoelectric effect (as a result of which the whole energy of a photon is transferred to a bound electron and therefore the photon ceases to exist) cannot be considered as a limiting case of Compton effect.

The formula giving the energy of a high-speed electron scattered on a nucleus:

$$E_e' \approx \frac{E_e}{1 + \frac{E_e}{m_{\text{mag}} c^2} (1 - \cos \theta)} \approx \frac{E_e}{1 + \frac{E_e}{M \times 931 \text{ MeV}} (1 - \cos \theta)}, \quad (188)$$

where M is the nuclidic mass defined by Eq. (9).

And finally, without going into details, I give the formula found in the [literature](#) that connects the kinetic energy $E_{e, \text{kin}}$ of an electron—see Eq. (170)—kicked by a neutrino of energy E_ν with the angle φ characterizing the direction of motion of the electron:

$$\cos \varphi = \frac{1 + \frac{m_e c^2}{E_\nu}}{\sqrt{1 + \frac{2 m_e c^2}{E_{e, \text{kin}}}}}. \quad (189)$$

As we can verify, the larger the kinetic energy of the electron in a given neutrino scattering event, the smaller is the angle φ and, consequently, the more accurately matches the direction of motion of the electron the original direction of the neutrino. (See Figure 68.)

17. Calculation of Recoil Energy

Consider the binary decay

$$P \rightarrow R + r + Q, \quad (190)$$

where R is the recoil atom (daughter) and r is the radiation particle emitted.

The following notation will be used.

The total energies of R and r will be denoted by $E(R)$ and $E(r)$, respectively.

The kinetic energies of the respective particles will be denoted by E_R and E_r .

If the kinetic energy of the parent P is negligible, then the Q -value of the decay will appear as the kinetic energy of the recoil atom R and the radiation particle r:

$$Q = E_R + E_r. \quad (191)$$

It follows from Eq. (164) that

$$p_R^2 c^2 = E^2(R) - m_R^2 c^4, \quad (192)$$

$$p_r^2 c^2 = E^2(r) - m_r^2 c^4. \quad (193)$$

In the most general case we can set the right-hand sides of the above equations equal because of momentum conservation ($\mathbf{p}_R = -\mathbf{p}_r$):

$$E^2(R) - m_R^2 c^4 = E^2(r) - m_r^2 c^4. \quad (194)$$

Substituting the appropriate forms of Eq. (170) we get:

$$(m_R c^2 + E_R)^2 - m_R^2 c^4 = (m_r c^2 + E_r)^2 - m_r^2 c^4. \quad (195)$$

After rearrangement we get the following quadratic equation for E_R :

$$E_R^2 + 2 m_R c^2 E_R - (E_r^2 + 2 m_r c^2 E_r) = 0, \quad (196)$$

which yields the following equation for the recoil energy:

$$E_R = \sqrt{m_R^2 c^4 + E_r^2 + 2 m_r c^2 E_r} - m_R c^2. \quad (197)$$

Besides the above equation which is accurate, it is also worth deriving an approximate formula for the same process. If we can be sure that the recoil atom is not relativistic, then we can make use of momentum conservation and directly write:

$$E_R = \frac{p_R^2}{2m_R} = \frac{p_r^2}{2m_R}. \quad (198)$$

Expressing p_r using Eqs. (170) and (193) yields:

$$E_R = \frac{m_r}{m_R} E_r + \frac{E_r^2}{2 m_R c^2}. \quad (199)$$

If E_r is small, then the first term dominates over the second. In that case the Q -value will be divided in inverse proportion to the masses:

$$E_R \approx \frac{m_r}{m_R} E_r. \quad (200)$$

If E_r is large, then the first term can be neglected. This can happen with light particles like electrons at energies near to 10 MeV already:

$$E_R \approx \frac{E_r^2}{2 m_R c^2}. \quad (201)$$

For massless particles, like photons, the first term is zero for any value of energy:

$$E_R = \frac{E_\gamma^2}{2 m_R c^2}. \quad (202)$$

18. Half-Life from Level Width

Nuclear databases sometimes give the estimated half-lives of very *short-lived* radionuclides in the energy unit eV. This can be done because the so-called *time–energy uncertainty* formula²⁸ establishes relationship between the mean life of a decaying state and the energy uncertainty of that level as characterized by the *level width* Γ :

$$\tau \times \Gamma = \frac{h}{2\pi} = \hbar, \quad (203)$$

where Γ is the FWHM (full width at half the maximum) of the bell-shaped energy distribution and h is the *Planck constant* (Table 1).

The correspondence between half-lives in femtoseconds (1 fs = 10^{-15} s) and level widths in electron volts can be given as follows:

$$T_{1/2} / \text{fs} \Leftrightarrow \frac{0.456}{\Gamma / \text{eV}}. \quad (204)$$

For instance, the above formula yields 0.08 fs for the half-life of ${}^8\text{Be}$ (a nuclide of cosmological importance²⁹) from its level width of 5.6 eV found at the website <http://www.nndc.bnl.gov/chart/>.

²⁸ If you read Hungarian, you may want to download my paper on this topic ([Heisenberg.pdf](#)).

²⁹ The nucleus of ${}^8\text{Be}$ falls apart to two α particles as soon as it gets formed by the collision of two α particles in heavy stars fueled by ‘helium burning’. Therefore nucleosynthesis in these stars can only start with the very rare [3 \$\alpha\$ process](#), which produces ${}^{12}\text{C}$ directly, skipping the unstable ${}^8\text{Be}$.

Suggested Reading

Bibliographic items written in Hungarian are typed in bold style. The rest are in English.

Alfassi Z.B. (1994). *Chemical Analysis by Nuclear Methods*, 556 pp., John Wiley & Sons, Chichester
Besides containing 15 special chapters on the various methods discussed by experts, the book also contains a 120-page introductory part on radiation–matter interactions, instrumentation, radiation sources and radiation protection.

Bódizs D. (2006). *Atommagsugárzások mérés technikái*, 271 old., Typotex, Budapest

A címe tökéletesen tükrözi a könyv tartalmát. A detektorok ismertetésén túl kitér az elektronikus jelfeldolgozásra, és ismerteti néhány spektroszkópiai módszert is. Bódizs Dénes a BME tanreaktorának munkatársa, s ő vezette be hagyományosan a Magkémiai laborot végző ELTE-s vegyészhallgatókat a neutronaktivációs mérés rejtelmeibe.

Bröcker B. (1995). *SH atlasz – Atomfizika*, 256 old., Springer-Verlag, Budapest

Igen jó ábrákkal illusztrált könyv, melynek képleteivel óvatosan kell bánni, mert igen sok félregépelést tartalmaznak.

Choppin G., Liljenzin J.-O., Rydberg J. (2002). *Radiochemistry and Nuclear Chemistry*, 3rd ed., 720 pp., Butterworth-Heinemann (Reed Elsevier), Woburn

The revised edition of one of the classics of RC&NC. A very good book.

Cohen E.R., Giacomo P. (1987). Symbols, units, nomenclature and fundamental constants in physics. *Physica A*, **146A**, 1-68

The 1987 revision of the IUPAP recommendations filed as Document I.U.P.A.P.-25 (SUNAMCO 87-1). It is also the last revision as of 2007.

Cunningham J.G. (1964). *Introduction to the Atomic Nucleus*, 220 pp., Elsevier Publishing Company, Amsterdam.

It delivers what its title promises. A very well written and didactic introduction to everything important up to (but not including) the quark hypothesis that was just born when the book got published. It is still very much worth reading.

Ehmann W.D., Vance D.E. (1991). *Radiochemistry and Nuclear Methods of Analysis*, 531 pp., John Wiley & Sons, N. York

A rather popular introduction to the field of RC&NC.

Eisenbund L., Garvey G.T., Wigner E.P. (1967). *General Principles of Nuclear Structure*, in *Handbook of Physics* (Eds. Condon E.U. and Odishaw H.) Mc Graw–Hill Book Co., New York

Eisenbund L., Garvey G.T., Wigner E.P. (1969). *Az atommag szerkezete*, 144 old., Akadémiai Könyvkiadó, Budapest

A könyv angol eredetije 1967-ben jelent meg. Ennek ellenére a kvarkokról nem esik még szó a könyvben. A magyar kiadáshoz a harmadik szerző, Wigner Jenő írt előszót „magyar születésű”-nek vallva magát, de az aláírás E.P. Wigner. A könyvet Györgyi Géza fordította, aki maga is szerepel ezen a listán szerzőként.

Friedlander G., Kennedy J.W., Macias E.S., Miller J.M. (1981). *Nuclear and Radiochemistry*, 3rd ed., 684 pp., John Wiley & Sons, New York

One of the classics of RC&NC. A very good book.

Györgyi G. (1961). *Elméleti magfizika*, 432 old., Akadémiai Könyvkiadó, Budapest

A maga nemében nagyon jó könyv, tele kvantummechanikával. Maga Wigner Jenő is így jellemezte 1969-ben: „Elméleti magfizikája még korántsem avult el és emlékezem, milyen jó benyomást tett rám, amikor olvastam”.

Haïssinsky M. (1963). *A magkémia és alkalmazásai*, 782 old., Akadémiai Kiadó, Budapest

A szerző, Moïse Haïssinsky, Marie Curie és Irène Joliot-Curie munkatársa volt, majd az Institute du Radium igazgatója lett. Háttérét (radiokémia) figyelembe véve különösen érdekes, hogy ennek a könyvnek, mely az akkori RK&MK egészét átfogta, éppen ezt a címet adta. Ő is azok közé tartozott tehát, akik ennek az egész széles területnek a megjelölésére a magkémia (*chimie nucléaire*) elnevezést szorgalmazták.

Hraskó P. (2002). *Relativitáselmélet*. 435 old., Typotex, Budapest

Hraskó Péter a BME mérnökfizikus hallgatóinak szánta ezt a könyvet, mely a speciális és az általános relativitáselméletet egyaránt tárgyalja. Idézet a könyv 111. oldaláról: „Ebben a könyvben a tömeg és az energia olyan fogalmával dolgozunk, amely nem fér össze az ekvivalenciájukkal: egy test tömege arányos a nyugvó testben tárolt energiával, de nem mindenfajta energiához tartozik tömeg. Az mc^2 szorzatot nyugalmi energiának fogjuk nevezni, de a nyugalmi tömeg elnevezést és a mozgási tömeg fogalmát nem fogjuk használni.”

Jánossy L. (1963). *Atommaglexikon*, 453 old. + 32 képd., Akadémiai Kiadó, Budapest

A Jánossy Lajos akadémikus által főszerkesztett mű kiváló forrásként használható a korabeli ismeretek magyar nevezéktana és definíciói tekintetében.

Kiss D., Horváth Á., Kiss Á. (1998). *Kísérleti atomfizika*, 472 old., ELTE Eötvös Kiadó, Budapest

Az élvezetes stílusban megírt könyv jó bevezetést ad a magfizikába (ezen belül olyan instrumentális területekre is, mint a detektorok, gyorsítók és a reaktorok), valamint a részecskefizikába. Horváth Ákos és Kiss Ádám jelenleg (2007) az ELTE Atomfizikai Tanszékének munkatársa, ill. tanszékvezetője. A 2001-ben elhunyt Kiss Dezső akadémikus 1989-92 között első külföldi főigazgatója volt a dubnai Egyesített Atommagkutató Intézetnek (Joint Institute for Nuclear Research, JINR).

Kiss D., Kajcsos Zs. (1984). *Nukleáris technika*, 467 old., Tankönyvkiadó, Budapest

Nagyon jó bevezető mű a címében jelzett területre. Elsősorban a részecske-detektálás, a különböző nukleáris spektroszkópiai módszerek, a gyorsítók, valamint a reaktorok világába vezet be, de a fizikai alapokat is tárgyalja, ezért egy fajta kísérleti mag-, ill. részecskefizika könyvnek is tekinthető. Kiss Dezső szerzői hitele az előző könyv leírásából érzékelhető. Kajcsos Zsolt fizikus (KFKI) főleg pozitronannihilációs spektroszkópusként szerzett nevet magának, de készített olyan berendezést is, amellyel ún. időfüggő Mössbauer-spektroszkópiát lehet végezni.

Kiss I., Vértes A. (1979). *Magkémia*, 476 old., Akadémiai Kiadó, Budapest

A mű átfogja az RK&MK egészét. Hosszú évek óta egyik, ha nem a fő meghatározója, ill. alapműve a magyar nyelvű szakirodalomnak ezen a téren. Vértes Attila Széchenyi-díjas akadémikus az ELTE Magkémiai Tanszékének megalapítója, majd hosszú időn keresztül tanszékvezetője volt. A Kossuth-díjas Kiss István a KFKI Kémiai Főosztályának vezetője, s a könyv megírása tájt az International Atomic Energy Agency (IAEA, Nemzetközi Atomenergia Ügynökség) bécsi központjának osztályvezetője volt.

Knoll G.F. (2000). *Radiation Detection and Measurement*, 3rd ed., 802 pp., John Wiley & Sons, New York

[Besides obvious topics promised by the title, the book contains introductory chapters on radiation sources, radiation–matter interactions and statistical aspects of nuclear measurements.

Leo W.R. (1994). *Techniques for Nuclear and Particle Physics Experiments: A How-to Approach*, 2nd revised ed., 378 pp., Springer-Verlag, New York

Besides detection of radiations, the book contains a strong introduction to radiation–matter interactions and statistical aspects. A very good book.

Lieser K.H. (2001). *Nuclear and Radiochemistry: Fundamentals and Applications*, 2nd revised ed., 462 pp., WILEY-VCH Verlag GmbH, Weinheim

A comprehensive book on RC&NC with rich variety of applications.

Loveland W.D., Morrissey D., Seaborg G.T. (2006). *Modern Nuclear Chemistry*, 671 pp., John Wiley & Sons, Hoboken

A curiosity of a book whose 3rd author (deceased in 1999) was not only eye witness of the discovery of several artificial elements, but also took part in the discovery of nine out of them.

Mackintosh R., Al-Khalili J., Jonson B., Peña T. (2001). *Nucleus—A Trip into the Heart of Matter*, 143 pp., Canopus Publishing Limited, Bristol

Simple and enjoyable text supported by great illustrations. The book is both easy to understand and fun to read even for high-school students. The topics discussed connect the micro world of subatomic particles with the whole of the Universe.

Mackintosh R., Al-Khalili J., Jonson B., Peña T. (2003). *Az atommag – Utazás az anyag szívébe*, 143 old., Akadémiai Könyvkiadó, Budapest

A remek illusztrációkkal támogatott egyszerű szöveg középiskolások számára is könnyen érthetővé és vonzóvá teszi a tárgyalt fogalmakat és gondolatokat. A könyv témája a mikrovilágtól az univerzumig ível.

Magill J. (2003). *Nuclides.net—An Integrated Environment for Computations on Radionuclides and their Radiation*, 271 pp., Springer, Berlin Heidelberg

It contains a CD-ROM with a powerful program doing just what the book's subtitle promises. The user gets access to a web server to perform calculations via the internet. Besides giving advice on the use of the program, the book also contains lots of case studies on various topics. The software itself is a real treasure both for the presentation of nuclide data and for visualizing radioactive decay series 'in action' as well as doing decay and dose calculations. A new edition of Nuclides.net—NUCLEONICA—became available in 2007 (for more information see www.nucleonica.net).

Magill J., Galy J. (2005). *Radioactivity · Radionuclides · Radiation*, 259 pp., Springer, Berlin Heidelberg

This great little book provides a well structured introduction to nuclear science with several applications—some written as separate chapters. It also contains a CD-ROM of the Universal Nuclide Chart—an 'electronic' chart of the nuclides.

Magill J., Pfennig G., Galy J. (2006). *Karlsruher Nuklidkarte*, 7th Edition, European Commission, Forschungszentrum Karlsruhe

The Joint Research Centre published this particular edition to coincide with the 50th anniversary of the

Forschungszentrum Karlsruhe. It contains data on 2962 experimentally observed ground-state nuclides and 692 nuclear isomers. New and updated decay data are given on 618 nuclides not found in the previous 6th edition published in 1998. The fold-out chart comes with a 44 pp. booklet in English, but the main features of the nuclide chart are also explained in Chinese, French, German, Russian and Spanish.

Muhin K.N. (1985). *Kísérleti magfizika*, 762 old., Tankönyvkiadó, Budapest

Vegyészek számára is érthető mélységben tárgyalja a nukleáris tudományok (így a magkémia) közös fizikai alapjait.

Nagy L.Gy. (1983). *Radiokémia és izotóptechnika*, 563 old., Tankönyvkiadó, Budapest

Nagy Lajos György néhai műegyetemi professzor könyve átfogja az RK&MK egészét. Sokáig tankönyvként szolgált a BME-n és más magyar egyetemeken.

Okun L.B. (1989). The concept of mass. *Physics Today*, June 1989, 31-36.

An interpretation of special relativity formulae containing momentum, energy and speed/velocity in terms of unique mass/rest energy and total energy rather than rest mass and moving mass. It is an enlightening paper worth reading both by laypersons and physicists.

Vértes A., Kiss I. (1987). *Nuclear Chemistry*, 619 pp., Elsevier Scientific Publishing Company, Amsterdam

A comprehensive book on RC&NC used as textbook all over the world.

Vértes A., Nagy S., Klencsár Z. (Eds) (2003). *Handbook of Nuclear Chemistry*, 2444 pp. in 5 volumes, Kluwer Academic Publishers (Springer), Dodrecht

A comprehensive handbook covering almost the whole of RC&NC written by an international team of 78 experts.

Vértes A., Nagy S., Süvegh K. (Eds) (1998). *Nuclear Methods in Mineralogy and Geology—Techniques and Applications*, 558 pp., Plenum Press (Springer), New York

A monograph in ten chapters written by an international team of 20 experts. The first chapter (pp. 1-113) by Nagy S., Süvegh K. and Vértes A. gives a general introduction to the field of RC&NC.

[Yao W.-M. et al.](#), J. Phys. G 33, 1 (2006)

An annual review of particle physics data by international experts. It can be found at the site

<http://pdg.lbl.gov/>.

Internet Sources

The list below mostly contains entries with free links to nuclear data sources.

Databases. <http://www.nndc.bnl.gov/databases/databases.html>. List of Nuclear Structure and Decay Databases, Nuclear Reaction Databases, and Bibliography Databases with short descriptions to the individual references.

Interactive Chart of Nuclides & Nudat 2. <http://www.nndc.bnl.gov/chart/> & <http://www.nndc.bnl.gov/nudat2/>. Access to a multitude of nuclear data offered in the form of a nuclide chart.

Nuclear Wallet Cards 2005. 7th Edition. <http://www.nndc.bnl.gov/wallet/wc7.html>. Access to some data of the isotopes of elements offered in the form of a periodic table.

Wapedia—Category: Nuclear chemistry. http://wapedia.mobi/en/Category:Nuclear_chemistry.

Glossary

For a comprehensive list of ‘semi-official’ nuclear terms, visit the website (<http://tinyurl.com/yxz2ml>) of the cross-referenced ‘IUPAC Glossary of terms for Radiochemistry and Nuclear Techniques’. [The Alphabetical index of the IUPAC Gold Book (<http://goldbook.iupac.org/index-alpha.html>) also contains lots of nuclear terms together with ‘official’ definitions.] Another free on-line nuclear glossary, ‘The Language of the Nucleus’, is found at <http://www.nuclearglossary.com/>. The ‘Glossary of Nuclear Science Terms’ (<http://www.lbl.gov/abc/Glossary.html>) is maintained by Lawrence Berkeley Laboratory. A good glossary on nuclear-reactor and regulation related terms is found at <http://www.nrc.gov/reading-rm/basic-ref/glossary.html> compiled by the US Nuclear Regulatory Commission. The ‘Glossary of Fusion Terms’ is also worth visiting at <http://www.fusion.org.uk/info/glossary.htm> for those interested in the terminology of thermonuclear fusion research, in particular magnetic confinement fusion. Further nuclear glossaries are listed at the website <http://www.trex-center.org/glossary.asp> under the title ‘Atomic and Nuclear Terms’ provided by Transportation Resource Exchange Center (T-REX). The most spectacular of these is the animated Glossary of Nuclear Science Terms at <http://ie.lbl.gov/education/glossary/glossaryf.htm>.

albedo: The fraction of particles (electrons, neutrons) ‘reflected’ from the surface (actually back-scattered from) a material.

background: Radiation/counting from any source that is not meant to be measured such as cosmic radiation or radiation from shielding, contamination, etc.

cosmic radiation: Mostly corpuscular radiation coming from outer space. 99% of the primary particles are protons and α particles. Their number ratio is about 7:1. Some of them are very-very energetic starting an avalanche of reactions when hitting nuclei in the air.

EC: Electron capture.

EFG: Electric field gradient.

FFs: Fission fragments: the primary products of fission formed directly in the scissioning phase together with a few prompt neutrons.

FP: Fission product.

FPS: Fission products.

fusion: (1) In nuclear science fusion means a nuclear reaction when lighter nuclei join to form a heavier nucleus.

(2) In chemistry fusion means melting, i.e. when a solid becomes a liquid.

IC: Internal conversion.

IF: (1) Induced fission. The notation ‘f’ is also used. (2) [Impact factor](#). It is considered as a measure of the importance of a given science journal. The IF of the journal in the year n is defined as the average number of citations per article in n to all articles published in the journal during the previous two-year period, i.e. in $(n-2)$ and $(n-1)$. If every article was cited once on an average, then $IF = 1$ for that year.

IT: Isomeric transition.

IUPAC: International Union of Pure and Applied Chemistry.

IUPAP: International Union of Pure and Applied Physics.

moderator: A material containing light atoms whose nuclei can effectively slow down neutrons by scattering them. The moderator should have low probability for neutron capture.

MRI: Magnetic resonance imaging.

NMR: Nuclear magnetic resonance.

nuclear emulsion: Used to prepare a special type of photographic plate. When wetted with a radionuclide solution, the latter diffuses into the light-sensitive layer and the tracks of α particles etc. left behind can be studied by a microscope after the plate has been developed.

nuclear force: An attractive type of force acting between nucleons. In older literature it was used as the synonym of strong force. Nowadays it is considered as the residuum of the ‘real’ strong/color force acting between quarks.

nuclidic mass: The atomic mass of a nuclide in unified atomic mass units (u).

number density: The number of specified atoms/particles in a given volume divided by that volume. It is usually denoted by n , and its value is normally given in cm^{-3} .

PP: Pair production, meaning the formation of a particle–antiparticle pair e.g. from a high-energy photon. Most often it means the formation of an electron–positron pair.

primordial nuclides: (1) Long-lived radionuclides that survived the 4.5 billion years since the Solar System exists. (2) A few (stable) nuclides formed in the early universe.

QCD: Quantum chromodynamics.

SF: Spontaneous fission.

SM: The Standard Model of particles and interactions.

SUNAMCO: Commission on Symbols, Unit, Nomenclature, Fundamental Constants and Atomic Masses (IUPAP).

XRFS: X-ray fluorescence spectroscopy.

ϵ : Beta plus (β^+) decay and electron capture (EC) together.

γ : (1) Notation of a photon in general. (2) A gamma photon produced by γ decay. The γ -rays consist of gamma photons.

Index

Page numbers in **bold** refer to figures. Those in *italics* are references to tables.

- 2**
- 2ε decay, 89
- 3**
- 3α process, 137
3γ annihilation of Ps, **122**
- 4**
- 4N nuclei, 138
- A**
- absolute activity, 76
absorbed dose (*D*), 113
absorber, 115
absorption of monoenergetic photons, 133
absorption of α particles in matter, **117**
absorption of β particles in matter, **119**
abundances of elements in the Solar System, **52**
abundances of isobars in the Solar System, **136**
activity, 10
activity (*A*), 75
activity concentration, 76
activity of the mixture of two radionuclides, **105**
activity of the product of activation, **105**
additive quantities, 121
aftereffects, 106
agelessness of radioactive atoms, 77, 133
alpha decay, 72, 90
alpha decay, condition of spontaneity, 90
alpha decay, explanation of, **73**
alpha nuclides, 55
alpha particle, 72
alpha particle (α), 63
alpha particles, absorption of, **117**
alpha spectrum of α decay, **71**
angstrom (Å), 21
angular distribution of 3γ annihilation of Ps, **122**
annihilation, 32
annihilation photons, 119
anticolors and colors, **37**
antineutrino, 33
antiparticles, 32
artificially produced radionuclides, 80
asymmetry term, 57
atomic mass constant (*m_u*), 22
atomic number, *Z*, 15
atomic weight. See relative atomic mass
attenuation coefficient, 133
attenuation coefficients for interactions of photons, **132**
Auger cascade, **111**
- Auger effect, 110
Auger electrons, emission after EC, 87
average binding energy per nucleon, **56, 58, 81**
average binding energy per nucleon (*B/A*), 26
average binding energy per nucleon for ⁸Be, **57**
Avogadro number (*N_A*), 21
- B**
- barn (b), 21, 65
baryon number, 32
baryon number conservation and proton stability, 36
baryon number, conservation of, 25
baryons, 35
becquerel (Bq), 10, 21, 75
Becquerel, Antoine Henri, 7
Beer–Lambert law, 133
beta back-scattering, 118
beta decay, conditions for spontaneity, 87
beta decay, inverse, 97
beta minus (β⁻) decay, 72
beta minus decay, 84
beta minus decay, condition of spontaneity, 87
beta particles, absorption of, **119**
beta plus (β⁺) decay, 72
beta plus *and* EC, ε decay, **88**
beta plus *and/or* EC together – ε, 72
beta plus decay, 85
beta plus decay, condition of spontaneity, 87
beta-delayed neutron decay, 72
beta-delayed neutron emission (β⁻n), 97
beta-delayed particle emission, 97
Bethe–Bloch formula, 115
Bethe–Weizsäcker cycle, 138
binary fission, 92
binding energy from Weizsäcker equation, **62**
binding energy of the atom (*E_a*), 25
binding energy of the electrons (*E_{Zc}*), 25
binding energy of the nucleus (*E_N*), 25
binding energy per nucleon, **56, 81**
binding energy per nucleon (*B/A*), **28**
binding energy per nucleon for ⁸Be, **57**
binding energy per nucleon, average (*B/A*), 26
biological dosimetry, 114
Bohr magneton (*μ_B*), 46
Boltzmann constant (*k*), 21
bombarding particle/photon, 63
Bose–Einstein statistics, 32
bosons, 32, 34
bound-beta decay (β_b), 97
Bragg curve, **116**
Bragg curve in radiotherapy, 117
branching decay, ‘leaking bucket’ metaphor of, **78**
branching ratios, 78, 99

Breit–Wigner curve, 69
 bremsstrahlung, 110
 bremsstrahlung, inner, 110

C

canyon of stability, 82
 capture reaction, 64
 capture reactions, 65
 carbon burning, 138
 carbon cycle, 138
 carrier, 76
 carrier-free, 76
 carriers of fundamental forces, 35
 Chadwick, James, 14
 chain reaction, 65
 chain yields, **94, 95**
 change of flavor, 33
 characteristic X-rays, 110
 characteristic X-rays, emission after EC, 87
 charge density in the nucleus, **38**
 charge number, 15
 charged particles in magnetic field, **133**
 charges, generalized, 32
 chart of nuclides, with binding energies, **81**
 chart of nuclides, with decay modes, **82**
 chemical symbol, general placeholder for, 17
 Cherenkov radiation, 124, **125**
 Chernobyl accident, 10
 classification of stable nuclides, **53**
 cluster decay, 72, 98, 99
 CN cycle, 138
 CNO-I cycle, 138, **139**
 CNO-II cycle, 139
 color charge, 36, 37
 colors and anticolors, **37**
 compound nucleus, 63
 compound-nucleus reactions, 63
 Compton electrons, energy distribution of, **130, 131**
 Compton photons, energy distribution of, **131**
 Compton scattering, **128, 144**
 Compton scattering, photon energy after, 145
 condition for spontaneity, 25
 confinement of quarks, 34, 37
 conservation of additive quantities, 121
 conservation of multiplicative quantities, 121
 continent of stability, **16, 58**
 converging branches, 99
 conversion coefficient, 92
 cooling after activation, 105
 cosmogenic ^{10}Be , 64
 cosmogenic ^{14}C , 104
 cosmogenic radionuclides, 80
 Coulomb barrier, **44, 66**
 Coulomb force, 31, 66
 Coulomb force (electric force), 42
 Coulomb term, 57
 count rate, 76
 counting rate. See count rate
 coupling, spin–orbit, 49
 cross section (σ) of nuclear reactions, 67

cross sections – neutrons vs. protons, **68**
 cross sections for different interactions of photons, **132**
 curie (Ci), 10, 21, 75
 Curie, Marie, 9
 curium, Cm, 10

D

dalton (Da), 22
 daughter, 70
 Davis Jr., Raymond, 10
 day (d), 21
 de Broglie wave length, reduced, **107**
 de Broglie wavelength, 67
 decay after activation, 104
 decay chain, 77
 decay constant (λ), 76
 decay rate, 10, 75
 decay scheme of ^{126}I , **91**
 decay schemes, 78
 decay schemes of alpha and beta decay, **79**
 decay series, 77. See decay chain
 decay series of ^{238}U , simulated, **101**
 decay series, naturally occurring, **100**
 delayed neutron emission, in nuclear reactors, 97
 detector efficiency, 76
 deuterium, 17
 deuteron (d), 63
 Dirac constant (\hbar), 21, 32
 direct reactions, 63, 64
 directly ionizing radiations, 112
 discovery of radioactivity, 7
 discovery of X-rays, 9
 disintegration rate, 10
 dispersion force, 31
 diverging branches, 99
 Doppler effect, 133
 dose rate, 113
 dosimetric concepts, 113
 dosimetric quantities, 114
 double beta decay, 72, 89
 double beta decay (2β , 2ε), 97
 doubly magic nuclei, 47
 driplines, 82

E

EC and beta plus, ε decay, **88**
 EC and/or β^+ together – ε , 72
 EC on the Nuclide Chart, **86**
 effective attenuation length (EAL), 118
 effective dose (E), 114
 Einstein, Albert, 7
 elastic collision of neutrons, 134
 electric field gradient (EFG), 41
 electric quadrupole moment, 41
 electron capture (EC), 72, 85
 electron capture, condition of spontaneity, 87
 electron mass (m_e), 21
 electron spectrum of β decay, **71**

electron volt (eV), 21
 electron volt (eV), definition of, 20
 electron volt, temperature equivalent of, 20
 electron, specific charge of, 9
 elementary bosons, 34, 35
 elementary charge (e), 21
 elementary fermions, 32
 elementary particles, 32
 ellipticity of nuclei and planets, **42**
 ellipticity, ϵ , 41
 end point energy (E_β), **71**
 end-point energy (E_β), 108
 energy and mass, 21
 energy and momentum spectra of β particles, **108**
 energy and temperature, 20, 21
 epsilon (ϵ) – EC and/or β^+ together, 72
 equivalent dose ($H_{T,R}$), 114
 escape velocity of He atoms, 51
 excitation function, 68
 explosive nucleosynthesis, 139
 exponential law of decay, 76
 extrapolated range (R_{extr}) of α particles, **117**
 extrapolated range (R_{extr}) of β particles, **119**

F

Fermi–Dirac statistics, 32
 fermions, 32
 fermions, elementary, 32
 Finnegans Wake, 34
 fissility parameter, 95
 fission, 64
 fission fragment (FF), 64
 fission fragments, 92
 fission fragments, β activity of, **93**
 fission product, 94
 fission products, primary, 92
 fission yield, 94
 fission yields, independent, **94**
 flavor, change of, 33
 fluence rate, 67
 free annihilation, 119
 free annihilation of a positron–electron pair, **120**
 free neutron, instability of, 36
 fundamental forces, 35
 fundamental particles, 32
 fusion, 64, 65
 fusion reaction, 65
 fusion, magnetic confinement, 151
 fusion, thermonuclear, 151
 FWHM (full width at half the maximum), 147

G

gamma decay, 91
 gamma emission, 91
 gamma radiation after beta decay, 87
 gamma-resonance fluorescence, 69
 gauge bosons, 34, 35
 Geiger–Nuttal plot, **45**
 Geiger–Nuttal rule, 44

generalized charges, 32
 geometrical cross section, 65
 gigaelectron volt (GeV), 21
 gravitational force, 35
 gray (Gy), 113
 Gray, Louis Harold, 113

H

half-life ($T_{1/2}$), 76
 half-life from level width, 147
 half-thickness ($X_{1/2}$) for photons, 133
 half-thickness ($X_{1/2}$) for α particles, **117**
 half-thickness ($X_{1/2}$) for β particles, **119**
 halo nuclei, 39
 halo nucleus ^{11}Li , **39**
 handedness, 33
 head-on collision, 134
 heavy-ion emission, 98
 helicity, 33
 helion (h), 63
 helium burning, 139
 helium flash, 139
 Hevesy, George (György), 13
 history of RC&NC, 7
 Hubble expansion of the Universe, 133
 Hund's rule, 48
 hydrogen burning, 140
 hydrogen, isotopes of, 17
 hyperfine splitting of nuclear levels, 41

I

impact factors (IF) of periodicals, 10
 inactive isotopes, 76
 indefatigability of photons, 133
 independent fission yields, **94**
 induced fission (f, IF), 65
 induced natural radionuclides, 80
 inner bremsstrahlung, 110
 inner bremsstrahlung, emission after EC, 87
 interaction of nuclear radiations with matter, 112
 interactions of neutrons, 134
 interactions of α radiation, 115
 interactions of β radiation, 118
 interactions of γ radiation, 128
 internal conversion (IC), 73, 91
 internal pair production (PP), 91, 137
 intrinsic magnetic moments, *46*
 inverse β decay, 97
 iron peak, 140
 Icsu. *See* Molnár, István
 isobar, 15
 isobar abundances in the Solar System, **136**
 isobaric chain, 94
 isobaric nuclides, **85**, *See* isobars
 isobaric process, 85
 isobars of ^{62}Ni , **28**
 isomeric transition (IT), 73, 92
 isospin (T), 54
 isotope, 15

isotonic nuclides. *See* isotones
 isotope, 15
 isotope effects, 13
 isotope enrichment, 13
 isotope separation, 13
 isotopic abundance, 23
 isotopic carrier, 76
 isotopic chemistry, 6
 isotopic nuclides. *See* isotopes
 isotopy, concept of, 13
 IUPAC Gold Book, 6, 151

J

j - j coupling, 49
 Joyce, James, 34

K

K-edge, 132
 K-edge, interpretation of, 131
 Kelvin-Thomson model. *See* plum pudding model
 kinetics of decay and activation, 99
 Kohman, Truman P., 14

L

lepton number, 32
 lepton number, conservation of, 25
 leptons, 33
 LET formula for electrons, 118
 LET formula for heavy ions, 115
 lethargy (u), 134
 lethargy gain, 134
 LET-value, 112
 level width (Γ), 147
 light year, 21
 linear attenuation coefficient, 133
 linear energy transfer. *See* LET-value
 linear stopping power (S), 113
 liquid drop model, 40
 London force, 31
 Lorentzian curve, 69

M

Mach number, 7
 Mach, Ernst, 7
 Mach's Principle, 7
 magic nuclei, 16, 47
 magic numbers, 'Mendeleev-type', 47
 magic numbers, nuclear, 47
 magnetic (dipole) moment, 45
 magnetic confinement fusion, 151
 magnetic moments of particles, 46
 magnetic properties, macroscopic, 47
 magneton, Bohr (μ_B), 46
 magneton, nuclear (μ_N), 46
 marginal distribution, 95
 mass attenuation coefficient, 133
 mass chain, 93
 mass defect, 28

mass deficit, 28
 mass excess (Δ), 27
 mass number, 39
 mass number, A , 15
 mass of a single atom (m_a), 23
 mass of a single nucleus (m_N), 15
 mass parabola, 98
 mass parabolas, 28, 89, 90
 mass parabolas, schematic, for even- A nuclides, 61
 mass stopping power (S), 113
 maximum activity of the daughter, 102
 maximum energy of β particles. *See* end-point energy
 maximum range (R_{\max}), 116
 maximum range (R_{\max}) of α particles, 117
 mean free path of photons, 133
 mean lethargy gain (ζ), 135
 mean life (τ), 76
 mesons, 35
 metastable states, 92
 moderator material, 134
 Molnár, István, 14
 momentum and energy spectra of β particles, 108
 momentum conservation in pair production (PP), 132
 momentum conservation in photoelectric effect, 131
 momentum vs. energy for particles, 107
 Mössbauer effect, 109
 Mössbauer spectroscopy, 6, 69, 109
 mother. *See* parent
 MRI, 6
 multiplicative quantities, 121

N

NAA, 134
 naturally occurring decay series, 100
 naturally occurring radionuclides, 80
 negatron, 32
 negatron decay. *See* beta minus decay
 neutrino, 33
 neutrino mass (m_ν), 21
 neutrino oscillation, 33
 neutrino passing kinetic energy to electron, 146
 neutrino spectrum of β decay, 71
 neutrino, direct detection of, 97
 neutrino, indirect detection of, 70
 neutron (n), 63
 neutron activation, 134
 neutron activation analysis (NAA), 65
 neutron capture, 134
 neutron capture (n, γ), 65
 neutron decay, 72
 neutron deficiency, 83
 neutron mass (m_n), 21
 neutron number, N , 15
 neutron separation energy (S_n), 29, 30
 neutron stars, 39
 neutron, discovery of, 14
 neutron, internal structure of, 46
 neutron, β^- decay of, 19, 24

neutron-induced fission, 134
 neutron-induced fission (n,f), 64
 neutron-induced fission in uranium, **96**
 neutrons, elastic collision of, 134
 neutrons, interactions of, 134
 Ni isotopes, B/A values of, **137**
 Ni isotopes, natural abundances of, **137**
 NMR, 6
 no equilibrium, 102
 Nobel prize \statistics\, **8**
 Nobel Prize \statistics\, 10
 Nobel Prizes in nuclear science, **8**
 no-carrier-added (n.c.a.), 76
 non-equilibrium, 102
 non-isotopic carrier, 76
 nuclear atom model, 9
 nuclear chemistry, 6
 nuclear emulsion, 117
 nuclear force, 31, 34, 35, 42, 66
 nuclear isomer, 16
 nuclear isomers, 92
 nuclear magic numbers, **16**, 47
 nuclear magneton (μ_N), 46
 nuclear mass (m_N), 15
 nuclear potential curves for subatomic particles, **43**
 nuclear radius formula, 38
 nuclear reaction $X(a,b)Y$, 63
 nuclear reaction $X(a,b)Y$, scheme of, **63**
 nuclear reactions, examples of, 64
 nuclear reactor, ancient natural in Oklo, **100**
 nuclear shell model, 47
 nuclear spin, 40
 nuclei, doubly magic, 47
 nuclei, magic, 47
 nucleon number. See mass number
 nucleon number, conservation of in radioactive decay, 25
 nucleons, 35
 nucleons (N), 14
 nucleons, anomalous magnetic moments of, 46
 nucleons, pairing off of, 48
 nucleosynthesis, explosive, 139
 nucleosynthesis, primordial, 140
 nucleus, charge density in, **38**
 nucleus, discovery of, 9
 nucleus, electric quadrupole moment of, 41
 nucleus, isospin projection of (T_z), 54
 nucleus, mass density of, 39
 nucleus, mass of, 39
 nucleus, radius of, 38
 nucleus, shape of, **41**
 nucleus, shell model of, 47
 nucleus, skin of, 38
 nucleus, skin thickness of, 38
 nucleus, surface area of, 39
 nucleus, volume of, 39
 nuclide, 15
 Nuclide Chart showing EC, **86**
 nuclide charts and nuclear isomers, 17
 nuclide charts, isotopes, isotones and isobars on, **18**

nuclidic mass, 22, 84
 nuclidic mass of the neutron, 23
 nuclidic notation, 17
 nuclidic notation of n, e and ν , 18
 number density, 67

O

oblate, 41
 Oklo, ancient natural nuclear reactor, **100**
 one-over-vee rule, 68
 orbital angular quantum number (l), 49
 oxygen burning, 140

P

pair production (PP), electron-aided, 132
 pair production (PP), internal, 91, 137
 pair production (PP), momentum conservation in, 132
 pair production (PP), nuclear, **128**, 132
 pair production (PP), nucleus-aided, **128**, 132
 pairing off of nucleons, 48
 pairing term, 58
 parallel decay, 105
 parent, 70
 parity, 40
 parity conservation, violation of in weak interaction, 41
 parity, conservation in Ps annihilation, 121
 parsec (pc), 21
 partial decay constants, 99
 Particle Data Group, 32
 particle flux, 67
 particle-transfer reaction, 64
 Pauli exclusion principle, 32, 36
 penetrating power, 112
 photoelectric effect, **128**
 photoelectric effect, momentum conservation in, 131
 photoelectron, 131
 photon (γ), 63
 physical constants, values of, 21
 physical dosimetry, 113
 pick-up reaction, 64, 65
 Planck constant (h), 21, 32
 Planck constant, reduced (\hbar), 21, 32
 plateau of absolute instability, 82
 plum pudding model, 9
 polonium, discovery of, 9
 positron, 32
 positron decay. See beta plus decay
 positron–electron pair, free annihilation of, **120**
 positronium Ps, 119
 positronium, 3γ annihilation of, **123**
 positronium, ortho (o-Ps), 120
 positronium, para (p-Ps), 120
 power, radiant, 118
 p-p chain, 140
 pp I chain, 140, **141**
 pp II chain, 140

pp III chain, 140
 primary fission products, 92
 primordial nucleosynthesis, 140
 primordial radionuclides, 80
 principal quantum number (n), 49
 prolate, 41
 prompt neutrons, 92
 protium, 17
 proton (p), 63
 proton decay, 72, 83
 proton emission, 83
 proton mass (m_p), 21
 proton number. See atomic number
 proton separation energy (S_p), 29, **30**
 proton stability and baryon number conservation, 36
 proton-antiproton collider, 32
 proton-proton chain, 140

Q

QCD, 37
 quadrupole moment formula, 41
 quantum chromodynamics, **37**
 quarks, 34
 quarks, electric charge of, 34
 Q -value, **24**, 83
 Q -value of a process, 24

R

radial quantum number (ν), 49
 radiant power, 118
 radiation chemistry, 6
 radiation exposure to photons, 10
 radiation protection, 114
 radiation weighting factor (w_R), 114
 radiation-matter interactions, 112
 radiative capture, 65
 radioactive decay modes, 72
 radioactive decay vs. chemical reactions, 73
 radioactive decay vs. nuclear reactions, **75**
 radioactive equilibrium, condition for, 102
 radioactive isotopes, 70
 radioactive nuclides, 70
 radioactive sources, production of, 76
 radioactive tracer technique, inventing of, 13
 radioactivity, discovery of, 7
 radiocarbon ^{14}C , 80
 radiocarbon dating, 104
 radiochemistry, 6
 radioisotopes. See radioactive isotopes
 radionuclides. See radioactive nuclides
 radionuclides, artificially produced, 80
 radionuclides, cosmogenic, 80
 radionuclides, induced natural, 80
 radionuclides, naturally occurring, 80
 radionuclides, primordial, 80
 radionuclides, secondary natural, 80
 radium, discovery of, 9
 radon as isotope name, Rn-222, **13**

range (R), 71
 range (R) of heavy ions vs. energy, 116
 RC&NC, 6
 reaction rate (R), 66
 reactor control, 97
 recoil energy (E_R), **71**
 recoil energy of the daughter atom, **106**
 recoil energy of γ emission, 109
 recoil formula, nonrelativistic, 107
 recoil of ^6Li caused by antineutrino, **70**
 recoil of fission fragments, 108
 recoil of the daughter atom, 106
 recoil separation of transuranium elements, 109
 reduced de Broglie wave length, **107**
 reduced Planck constant (\hbar), 32
 relative atomic mass (A_r), 23
 residual strong force, 34
 resonance peaks, 68
 rest energy (E_0), 22
 roentgen (R), 10
 roentgenium, Rg, 10
 roentgen-rays. See X-rays
 Röntgen, Wilhelm Conrad, 9
 Röntgen-rays. See X-rays
 r -process, 141
 rutherford (obsolete activity unit), 10
 Rutherford, Ernest, 9
 rutherfordium, Rf, 10

S

scattered electron, energy of, 145
 scattering, 64
 secondary natural radionuclides, 80
 secular equilibrium, 102
 secular equilibrium, 'leaking bucket' metaphor of, **77**
 secular equilibrium, condition for, 102
 Segrè plot, **18**
 separation energy, 29
 shell model, **48**
 shell model of the nucleus, 47
 sievert (Sv), 114
 Sievert, Rolf Maximilian, 114
 silicon burning, 141
 single decay, 99
 skin of the nucleus, 38
 skin thickness of nucleus, 38
 Skłodowska, Maria. See Curie, Marie
 Soddy, Frederick, 9
 solar neutrino problem, 97
 solar neutrino problem, discovery of, 10
 Solar System, isobar abundances in, **136**
 spallation, 64
 specific activity, 76
 specific charge, 9
 specific energy loss, 113
 speed of light in empty space (c), 21
 speed vs. kinetic energy for particles, **124**
 spin quantum number, 32
 spin-orbit coupling, 49

spontaneous fission (SF), 73, 92
 spontaneous fission, sufficient condition for, **96**
 spontaneous processes, criteria for, 84
 s-process, 141
 stable isotopes, number of, **50**
 stable nuclides, classification of, **53**
 standard atomic weight, 23
 Standard Model, 31
 Standard Model (SM), 14
 Standard Model Chart, 32
 stellar nucleosynthesis, 55
 stopping power (S), 113
 straggling of α particles, **117**
 straggling of β particles, **119**
 stripping reaction, 64, 65
 subatomic particle, 32
 supernova nucleosynthesis, 139
 surface density, 133
 surface term, 57
 Szilárd–Chalmers process, 109

T

target nucleus/atom, 63
 temperature equivalent of 1 eV, 20
 ternary fission, 92
 Tevatron, 32
 thermalization of radiation particles, 20
 thermonuclear fusion, 151
 Thomson, Joseph John, 9
 Thomson, Sir William. *See* Kelvin, Lord
 thoron as isotope name, Rn-220, **13**
 three-gamma annihilation, **120**
 three-gamma annihilation, angular distribution of, **123**
 three-member series, **103**
 tissue weighting factor (w_T), 114
 tracer technique, inventing of, 13
 transient equilibrium, 101
 triple alpha process, 55
 triple-alpha (3α) process, 147
 triple- α process, 137
 tritium, 17
 tritium ^3H , 80
 triton (t), 63

tunneling, 44
 tunneling of α particles, **44**
 two-gamma annihilation, **120**
 two-proton decay, 83
 two-step series, 101

U

U-238 in the stability valley, **83**
 unified atomic mass unit ($u \approx \text{amu}$, a.m.u.), 21
 units, 21
 uranium, neutron-induced fission in, **96**

V

valley of beta stability, **81**
 volume term, 57

W

Wapstra, Aaldert H., 20
 weak force, 35
 Weizsäcker equation, 57
 Woods–Saxon potential, 43

X

xenon poisoning, 69
 X-ray photography, 9
 X-rays, characteristic, 110
 X-rays, discovery of, 9
 XRFS, 6

Y

year (a), 21
 yield of fission products, 78

A

α nuclei, 138
 $\alpha\beta\gamma$ paper, 138
 α – β – γ theory, 138

B

β particles, momentum and energy spectra, **108**